2013

DISTRIBUTION AND IMPACTS OF PETROLEUM HYDROCARBONS IN LOUISIANA TIDAL MARSH SEDIMENTS FOLLOWING THE DEEPWATER HORIZON OIL SPILL

Rachel S. Hatch
University of Kentucky, rhatch86@gmail.com

STUDENT AGREEMENT:

I represent that my thesis or dissertation and abstract are my original work. Proper attribution has been given to all outside sources. I understand that I am solely responsible for obtaining any needed copyright permissions. I have obtained and attached hereto needed written permission statements(s) from the owner(s) of each third-party copyrighted matter to be included in my work, allowing electronic distribution (if such use is not permitted by the fair use doctrine).

I hereby grant to The University of Kentucky and its agents the non-exclusive license to archive and make accessible my work in whole or in part in all forms of media, now or hereafter known. I agree that the document mentioned above may be made available immediately for worldwide access unless a preapproved embargo applies.

I retain all other ownership rights to the copyright of my work. I also retain the right to use in future works (such as articles or books) all or part of my work. I understand that I am free to register the copyright to my work.

REVIEW, APPROVAL AND ACCEPTANCE

The document mentioned above has been reviewed and accepted by the student's advisor, on behalf of the advisory committee, and by the Director of Graduate Studies (DGS), on behalf of the program; we verify that this is the final, approved version of the student's dissertation including all changes required by the advisory committee. The undersigned agree to abide by the statements above.

Rachel S. Hatch, Student

Dr. Kevin M. Yeager, Major Professor

Dr. Edward W. Woolery, Director of Graduate Studies

DISTRIBUTION AND IMPACTS OF PETROLEUM HYDROCARBONS IN LOUISIANA TIDAL MARSH SEDIMENTS FOLLOWING THE DEEPWATER HORIZON OIL SPILL

THESIS

A thesis submitted in partial fulfillment of the requirements for the degree of Master of Science in the College of Arts and Sciences at the University of Kentucky

By

Rachel Sarah Hatch
Lexington, Kentucky

Director:
Dr. Kevin M. Yeager, Associate Professor of Earth and Environmental Sciences
Lexington, Kentucky

2013

ABSTRACT OF THESIS

DISTRIBUTION AND IMPACTS OF PETROLEUM HYDROCARBONS IN LOUISIANA TIDAL MARSH SEDIMENTS FOLLOWING THE DEEPWATER HORIZON OIL SPILL

Following the 2010 Deepwater Horizon (DWH) spill, sediment cores were analyzed from marshes at various levels of oiling to determine how deeply oil penetrated sediment in these marsh environments, and if at these sites it had quantifiably affected benthic ecosystems. Minimum mixing depths were determined from penetration of the lithogenic radionuclide ^{234}Th, which ranged from 0.25 to 4.5 cm. Sediment accumulation rates were determined using ^{210}Pb, with verification from ^{137}Cs in selected cores. Lead-210 profiles revealed long-term (decadal) mixing. Bay Jimmy, Louisiana was significantly affected by the DWH oil spill, as indicated by total polycyclic aromatic hydrocarbon concentrations of up to 21,913 ppb. This is far above the level at which adverse biological effects occur (4,022 ppb). Benthic foraminifera responded to the heavy oiling by decreases to standing stock and depth of habitation relative to unoiled sites, as well as exhibiting deformities. These data clearly show that oil can be quickly mixed into salt marsh sediments, with demonstrable impacts on indigenous benthos. Further, radioisotope inventories indicated that most of the sampled sites are in a net erosional state. Should marshes containing trapped DWH oil be submerged by rising sea level, there is a great potential for the remobilization of oil.

KEYWORDS: Deepwater Horizon; wetlands; radiogenic isotope geochemistry; petroleum hydrocarbons; benthic processes.

Multimedia Elements Used: JPEG (.jpg), PDF (.pdf), PNG (.png)

Rachel Sarah Hatch

Date

DISTRIBUTION AND IMPACTS OF PETROLEUM HYDROCARBONS IN LOUISIANA TIDAL MARSH SEDIMENTS FOLLOWING THE DEEPWATER HORIZON OIL SPILL

By

Rachel Sarah Hatch

Kevin M. Yeager
Director of Thesis

Edward W. Woolery
Director of Graduate Studies

Date

ACKNOWLEDGEMENTS

This thesis benefitted from the knowledge, direction, and support of many people. First, my Thesis Director, Kevin Yeager, not only provided me with financial support and the analytical tools to complete this thesis, but also the encouragement (and occasional provocation) that is necessary to keep a graduate student on track. Next, I wish to thank the rest of the Thesis Committee: Dave Moecher, Daehyun Kim, and Charlotte Brunner. Each individual both guided and challenged me, and advocated for my success along the way. I also thank past and present members of the Sedimentary, Environmental, and Radiochemical Research Laboratory for their input: Kim Schindler, Phillip Wolfe, Stephen Prosser, Olivia Woodruff, Michelle Johnston, Zachary Moore and Alyssa Eliopoulos, as well as members of the field crew who collected the samples used in this thesis work: Kim Schindler, Zheng Zhen Zhou, Nathan Couey, Shiva Shivarudrappa, Joel Loeffler, Jeremy Prouhet, Alyssa Jung, Carlo Fortner, Logan Dedeaux, Gopal Bera, Jennifer Brizzolara, Christopher Rom, DongJoo Joung, and Kevin Martin.

In addition to the technical and instrumental assistance above, I received equally important assistance from family and friends. In particular, my brother, Nicholas Hatch, was always willing to serve as a sounding board for my experiences and questions, as well as comic relief when it was needed most.

Last, but not least, funding provided by the National Science Foundation, NOAA's Northern Gulf Institute, Gulf Coast Association of Geological Societies, Geological Society of America, and the University of Kentucky Department of Earth and Environmental Sciences' Brown-McFarlan Fund and Pioneer Natural Resources Fellowship is graciously acknowledged.

TABLE OF CONTENTS

LIST OF TABLES

LIST OF FIGURES

CHAPTER ONE: INTRODUCTION

1.1 Event Background

On April 20, 2010, an explosion occurred on the Deepwater Horizon (DWH) drilling rig, causing oil to begin flowing out of the Macondo wellhead, located approximately 1,500 meters below on the seafloor. By the time the leak was capped nearly three months later on July 15, 2010, an estimated 4.9 million barrels (205.8 million U.S. gallons) of oil had leaked into the Gulf of Mexico (GOMx) (FRTG, 2011). By August 2010, oil landings had been reported along the Louisiana, Mississippi, Alabama and Florida coastlines, resulting in hydrocarbons being introduced to the sediments in these areas (Rosenbauer et al., 2010) (Figure 1.1).

1.2 Marshes: Background and Importance

Tidal salt or brackish marshes are coastal wetlands that are regularly flooded by tides. Tidal marshes along the northern GOMx serve many important ecological functions, including providing a habitat for numerous species of fish, birds and invertebrates (DeLaune et al., 1979), slowing shoreline erosion (Möller et al., 1999), filtering and absorbing excess nutrients and pollutants (Valiela et al., 2004), and sequestering carbon (Chmura et al., 2003). They also offer human and commercial benefits by acting as a buffer zone from hurricanes (Costanza et al., 2008) and providing economic stimulus from recreational services (Batker et al., 2010). The coastal plains of Mississippi and Louisiana are dissected by river drainage systems, including the Mississippi and Pearl Rivers, and over time the sediment deposits from these rivers have constructed coastal marsh habitats. There are nearly one million acres of saline and brackish marshland bordering the Mississippi and Louisiana coastlines (Batker et al.,

2010), sustaining high concentrations of plant and animal life. The commercial fishing industry harvests more than 1 billion pounds of seafood from the GOMx each year (NOAA, 2010a), and it is estimated that 90% of that catch spawns or lives at some point in their lives in coastal salt marshes (NOAA, 2010b).

Tidal marshes are valuable ecosystems, but their coastal locations make them susceptible to oil spills (Culbertson et al., 2008). Oil spilled into the ocean is easily transported via tidal currents and wind-produced transient currents to the shore and incorporated into sediments (Means and McMillin, 1993). Although some studies have found that marshes bordering the northern GOMx may have high natural recovery potential post-oiling (DeLaune and Wright, 2011), they are also considered to be the shoreline type most capable of long-term oil preservation. Peacock et al. (2005) and Reddy et al. (2002) found that, in spite of erosion and microbial degradation, it is typical for oil residues to persist in the fine-grained sediments of a salt marsh for decades or longer after a spill. These studies concerned the 1969 *Florida* barge oil spill near Wild Harbor, Massachusetts. While this bay-enclosed, Northern Atlantic salt marsh is not completely analogous to the salt marshes of the northern GOMx, these studies are important because they provide a rare set of data on the long-term fate and effects of petroleum hydrocarbons in these environments.

1.3 Research Goals

This thesis originally proposed to test two key hypotheses:

H_1: Salt marsh sediments of Dry Bread Island and Bay Jimmy, Louisiana were significantly impacted by the DWH oil spill, as indicated by total polycyclic aromatic

hydrocarbon (TPAH) concentrations well above what is considered the upper limit background for these areas (1.5 μg g^{-1}) (Iqbal et al., 2007).

H_2: These moderately to heavily DWH-oiled marsh sediments would be discernible from pristine to lightly DWH-oiled marsh sediments by exhibiting (a) high concentrations of sedimentary organic carbon (SOC), (b) shallower bioturbation depths, and (c) low abundance and depth of habitation of benthic meiofauna, as indicated by foraminifera.

To test the above hypotheses, the following variables were quantified: (1) total petroleum hydrocarbon (TPH) and TPAH concentrations for selected marsh sediments; (2) sediment grain size and physical properties; (3) SOC concentrations; (4) sediment accumulation rates; (5) bioturbation depths; and (6) changes to benthic meiofauna communities. These objectives were meant to allow for determining how deeply oil from the DWH spill had penetrated sediment in these marsh environments, and if at these sites it had quantifiably affected benthic ecosystems. The significance of each of these variables is explained in the remaining sections of this chapter.

1.4 Petroleum Hydrocarbons

Petroleum hydrocarbons are organic compounds that represent the main constituents of crude oil. Petroleum hydrocarbons include such chemical compounds as benzene, toluene and naphthalene. PAHs are one class of petroleum hydrocarbon, and have a molecular structure that includes two or more fused benzene rings. Petrogenic PAHs are formed from the breakdown of organic material and are associated with fossil fuels. Pyrogenic PAHs are associated with the incomplete combustion of organic fuels. It was expected that both types of PAHs would be seen in this study due to *in situ* burning

following the DWH spill (discussed in Chapter Four). Due to the variety of conditions in PAH formation, PAHs from these different sources yield different molecular distribution patterns. Petrogenic sources of hydrocarbons are reflected by the predominance of low molecular weight (LMW) PAHs, whereas pyrogenic sources are reflected by largely high molecular weight PAHs. On the basis of these differences, signature ratios of PAH components of the same molecular mass can be used to characterize source (Yunker et al., 1996; Yan et al., 2005). Reddy et al. (2011) determined that the oil of interest in this study, the Macondo-1 well oil (MC252), contains approximately 3.9% PAHs by weight.

The fate of PAHs following an oil spill is of particular interest because of their potential for bioaccumulation and toxicity to flora and fauna. The U.S. Department of Health and Human Services (DHHS) lists the following PAH compounds as being known animal carcinogens: benz[a]anthracene, benzo[b]fluoranthene, benzo[j]fluoranthene, benzo[k]fluoranthene, benzo[a]pyrene, dibenz[a.h]anthracene, and ideno[1,2,3-c,d]pyrene. Animal studies show that these PAHs can affect the hematopoietic (blood production), immune, reproductive, and neurologic systems and cause developmental defects (ATSDR, 1995). The U.S. Environmental Protection Agency (EPA) does not maintain a general toxicity level for total PAHs, but does assign maximum contaminant levels for drinking water for the seven carcinogenic PAH compounds as indicated by the DHHS. Table 1.1 summarizes the PAH compounds measured in this thesis, as well as their respective carcinogenicity classifications.

Based on a review of compiled biological and chemical data from marine and estuarine sediments, Long et al. (1995) reported that adverse biological effects occur at PAH concentrations higher than 4,022 ng g^{-1} (ppb). At present, NOAA uses this value as

an Effects Range-Low, or the level above which 10 percent of organisms show adverse effects to PAHs. Because of the highly adsorptive nature of organic-rich, fine-grained sediments found in marshes, PAHs can concentrate in these areas (Means and McMillin, 1993; Hartmann et al., 2004; Colombo et al., 2006). This means that organisms living in salt marshes may be subjected to higher levels of PAHs than those organisms residing in deeper water nearer to the initial site of the spill.

1.5 Sediment Physical Properties

It was expected that PAHs would rapidly associate with suspended and deposited organic sediment particles because of their nonpolar nature/limited water solubility (e.g., Mackay and Shiu, 1975; Smith, 2011). However, the presence of fine-grained sediments can also be important in the retention of oils in marsh sediments. For these reasons, it was important to determine the grain size profile for the uppermost portion of each core that could have been affected by oil.

Additionally, quantification of sediment sizes and textures can provide information on what benthic organisms are expected to live at each study location, which can then be compared in areas more or less contaminated with petroleum hydrocarbons. For example, a change in the major sediment grain size accumulating in the marsh changes the physical and chemical environment, strongly affecting distribution of foraminiferal assemblages (Murray, 2006).

1.6 Sedimentary Organic Carbon (SOC)

SOC includes particulate materials and compounds derived from plant and animals, and is a highly reactive sedimentary substrate. In the case of an oil spill where large amounts of organic contaminants are released into the environment, it is expected

that SOC will be affiliated with these contaminants (Polymenakou et al., 2006). This can be reflected in the sedimentary profile initially as an increase in SOC. However, because SOC is directly correlated with macrofaunal density, and the deposition of PAHs can perturb vegetation and benthic fauna (Burdige, 2007), SOC may later decline as the total biomass decreases (Hyland et al., 2005). Elemental analysis allows for the determination of SOC concentrations and inventories in sediments. It is then possible to combine these concentrations with sediment accumulation rates derived from ^{210}Pb and ^{137}Cs in order to make quantitative estimates of SOC flux over time.

1.7 Radiochemistry

The suite of radionuclides (^{234}Th, ^{7}Be, ^{210}Pb, ^{137}Cs) used in this study were chosen due to their range of half-lives, and their particle-reactive nature, which allows them to become concentrated in fine-grained, organic-rich sediments. Clays have high cation exchange capacity, and because these radioisotopes have higher adsorption energies than many other cations, they are preferentially adsorbed to clay-rich soils and sediments (Frere et al., 1963). Each radionuclide outlined below has a different chemistry, source, and half-life, allowing for the measurement of sediment accumulation rates and mixing depths using multiple radionuclide proxies, reducing possible errors from relying on only one method.

1.7.1 Lead-210

Lead-210 ($t_{1/2}$ = 22.4 years) is a continually produced, naturally occurring radionuclide. The atmospheric origin for ^{210}Pb is derived from the decay of ^{238}U to the noble gas ^{222}Rn at or near Earth's surface. Supported ^{210}Pb is produced through *in situ* decay of ^{222}Rn at depth in a soil or sediment. A portion of ^{222}Rn escapes to the

atmosphere, where it undergoes decay to ^{210}Pb, which is then supplied to Earth's surface by wet (precipitation) and dry (aerosols) deposition. This ^{210}Pb is then bound to organic and inorganic sediments and deposited, and is referred to as unsupported, or "excess" ^{210}Pb ($^{210}Pb_{xs}$). Lead-210 geochronology has been broadly applied to sediments in coastal settings, including wetland environments, over time scales of about a century (e.g., Smoak and Patchineelam, 1999; Mudd et al., 2009).

1.7.2 Cesium-137

Because of variability in sedimentary sections, independent tracers such as ^{137}Cs have been successfully used in conjunction with ^{210}Pb to corroborate calculations of sediment accumulation and chronology. Cesium-137 is a moderately long-lived ($t_{1/2}$ = 30.2 years) fission product radionuclide. In the 1940s, the United States and other countries began aboveground nuclear weapons testing, releasing fallout radionuclides including ^{137}Cs into the atmosphere. Cesium-137 first appeared in the atmosphere in significant quantity in 1953. After its release to the atmosphere, it is deposited on Earth's surface by wet and dry deposition and subsequently adsorbed onto sediments. Above-ground nuclear weapons testing peaked in 1963 before the Partial Test Ban Treaty was ratified, and both the first instance (~1953) and this 1963 peak of ^{137}Cs activity can be used to date sediment and derive a sediment accumulation rate (e.g., Santschi et al., 2001; Yeager et al., 2007). In a well-preserved sediment record, the shape of the ^{137}Cs activity concentration versus depth profile can be used to identify these two marker horizons (Williams and Hamilton, 1995). These stratigraphic variations in ^{137}Cs concentrations have been documented in various environments, including coastal marshes (e.g., DeLaune et al., 1978; Williams and Hamilton, 1995).

1.7.3 Thorium-234

Thorium-234 ($t_{1/2}$ = 24.1 days) has widely been used for the determination of mixing rates in marine sediment (e.g., Pope et al., 1996; Wheatcroft and Martin, 1996; Smoak and Patchineelam, 1999; Yeager et al., 2004). Thorium-234 is produced by the decay of ^{238}U (Figure 1.2), which is present in marine and brackish waters. Thorium and uranium reach secular equilibrium at shallow depths in the water column, and the thorium then binds strongly to organic and inorganic particulate matter, which can then be deposited. It is possible to then determine the sediment mixing depth by the maximum penetration depth of the excess ^{234}Th [$^{234}Th_{xs}$ = total ^{234}Th - ($^{234}Th_{supp}$ = ^{238}U)]. Thorium-234 is typically used as a tracer of biological mixing intensity because the rate of biological particle mixing generally exceeds that of sediment accumulation (Wheatcroft and Martin, 1996). Sediment profiles of $^{234}Th_{xs}$ activity concentration can be used to compute the particulate biodiffusion coefficient (D_b), which represents the intensity of bioturbation (Wheatcroft and Martin, 1996). Because of its short half-life (24.1 days), ^{234}Th is typically used to examine sedimentary processes that have occurred within the last ~100 days prior to sampling (Pope et al., 1996). This is useful in a study such as this, where resulting fluctuations in benthic populations and diversity may occur over very short timescales.

1.7.4 Beryllium-7

Beryllium-7 ($t_{1/2}$ = 53.5 days) is likewise a naturally occurring radionuclide, but it is cosmogenically produced in Earth's atmosphere by the interaction of oxygen and nitrogen with cosmic ray neutrons. About two-thirds of ^{7}Be is produced in the stratosphere, and the remaining one-third is produced in the troposphere (Lal and Peters,

1967). Because of the lengthy residence time (~ 1 year) of aerosol particles in the stratosphere, however, the main continuous flux of ^{7}Be to Earth's surface results from tropospheric precipitation (Sharma et al., 1987). Once on the Earth's surface, ^{7}Be is strongly adsorbed onto inorganic particles, such as clay minerals, but does not have much affinity for organic material (Bloom and Crecelius, 1983). The continuous fallout of ^{7}Be and its rapid decay in near-shore fine-grained sediments makes it a useful indicator of reworking in sediment deposited on time scales within several half-lives of measurement (~ 1 year) (Krishnaswami et al., 1980; Murray et al., 1992). Changes in bioturbation intensity (B_d) and bioturbation depths can be studied by determining the distribution of ^{7}Be in the sediment (e.g., Sharma et al., 1987; Yeager et al., 2004; Mudd et al., 2009).

1.8 Benthos

With respect to marine pollution concerns, the majority of the media's attention is often paid to large-bodied organisms such as birds and dolphins, whereas smaller-bodied organisms receive relatively little attention. This study focuses on benthic organisms having diameters approximately between 45 μm and 500 μm. Many tidal marshes are sites of high primary productivity, and the benthic organisms living on and in sediments play an important role in the productivity of the marsh. Certain organisms, such as polychaetes, constantly rework sediments as they burrow into them. These bioturbators circulate and remineralize organic matter and nutrients within sediments (Burns et al., 1993), as well as increase the oxygen content of sediments (Hippensteel, 2005). These processes are essential in supporting the nutrient demands of a healthy marsh ecosystem. Because bioturbation is a biological process, its extent is dependent on the environment and the diversity and density of indigenous species, and thus varies from low to high

marsh. Sharma et al. (1987) suggested that primary bioturbators, such as fiddler crabs, prefer the soft muddy sediments of the low marsh, where root densities are lowest. Hippensteel and Martin (1999) supported this theory by comparing depositional environments within marsh cores. They found that the highest mixing parameters were recorded in low marsh cores, whereas the lowest mixing parameter was recorded in a high marsh core.

Sediment mixing can also influence the transfer of particle-bound compounds (i.e., oil) and can destroy or distort the record of natural and/or anthropogenic processes. In this way, bioturbators play a role in the fate of organic contaminants; it is common for sediment mixing by bioturbators to allow for natural remediation of contaminants via enhanced microbial degradation at the sediment-water interface (Gardner et al., 1979) and where oxygenated water is pumped through burrows (Beeftink and Rozema, 1988).

Bioturbation depths determined from ^{7}Be and ^{234}Th can be correlated with changes in meiofauna. Meiofauna are represented in this study by benthic foraminifera, which have been used to infer the overall health of the benthos in connection with bioturbation data.

Changes to meiofaunal assemblages in terms of total abundance and number of species can occur when there is a buildup of pollutants over time, allowing for the monitoring of pollution by studying these faunal changes (Martin, 2000). Where there is no baseline study of the area prior to pollution, analysis of sediment cores extending into pre-pollution time periods can be invaluable, provided that early diagenesis has not biased the fossil assemblage through differential dissolution (Alve, 1995).

Foraminifera are a highly successful group of microorganisms that are ubiquitous in marine and brackish environments. Nearly all foraminifera possess a test (shell) of one or more chambers that surrounds the organism. The test is most commonly composed of secreted calcium carbonate ($CaCO_3$), but may also be organic (not mineralized), agglutinated (cemented sediment grains acquired from the environment), or, in rare cases, composed of opaline silica. Foraminifers grow by either periodically adding new chambers or increasing the size of a single chamber (Goldstein, 1999).

The vast majority of extant foraminifera are benthic, but there are 40-50 known planktonic species (Sen Gupta, 1999). Planktonic species are intolerant of brackish water, and have not been found in salinities below 30‰ (Arnold and Parker, 1999). As such, this study is focused on benthic species, which typically have limited mobility and are therefore directly influenced by any stresses introduced to the benthic environment (Bilyard, 1987). There are several other advantages to using benthic foraminifera: (1) they are abundant enough that they can be collected in statistically significant numbers; (2) their tests are often well preserved in the sediment column; and (3) their relatively short life spans (a few weeks up to five years) make their community structures susceptible to environmental changes (Yanko et al., 1999).

Foraminifera tend to develop malformed tests in stressed environments, making them useful as environmental quality indicators (Martínez-Colón et al., 2009). Changes in many factors can present as environmental stressors, though, such as temperature, pH, salinity, and turbidity. However, many studies have shown that, in otherwise healthy ecosystems, foraminiferal populations are predominantly controlled by food supply (e.g., Murray, 2001). In this case, the presence of oil can serve as an environmental stressor

because of its toxicity to plants that would become organic detritus, from which infaunal marsh foraminifera harvest bacteria for nutrition (Goldstein, 1999). Other studies have indicated that over-exposure to petroleum hydrocarbons directly affect the foraminifera. Morvan et al. (2004) performed both culture and *in situ* studies of foraminiferal assemblages in response to oil contamination following the 1999 *Erika* oil spill in intertidal zones off the Atlantic coast of France. The culture study showed that with increasing amounts of oil contamination, growth and reproduction events decreased dramatically and the incidence of morphological abnormalities increased.

Morphological abnormalities in benthic foraminifera have been used as proxies of the degree of environmental stress, such as that posed by oil (Yanko et al., 1998; Polovodova and Schönfeld, 2008). These abnormalities affect test development, resulting in features such as double apertures and twisted chambers (Yanko et al., 1999). In a comprehensive review of the effects of pollution on foraminifera, Alve (1995) provided several generalizations: (1) during their short lifespan, foraminifera respond quickly to natural and anthropogenic environmental changes; (2) tolerant or opportunistic species of foraminifera benefit from certain types of contamination and the resulting reduction in competition; and (3) decreased diversity can be found close to contaminant outfalls. Not only are meiofauna, such as benthic foraminifera, useful indicators of pollution, but they are also important sources of carbon to higher trophic levels. Thus, damage to meiofaunal diversity and overall population sizes could cause ecological ramifications farther up the food chain.

Changes of the benthos in near shore environments may be principally driven by fluctuations in organic matter input (Pearson and Rosenberg, 1978). The delivery of

petroleum hydrocarbons to an ecosystem results in organic enrichment. Organic matter is the food source for benthic fauna, but over-exposure to pollutants, such as petroleum hydrocarbons, can induce enhanced microbial respiration and result in hypoxia (Pearson and Rosenberg, 1978). As pollution increases, the total population size of foraminifera may increase due to rising numbers of tolerant species; however, overall species diversity falls. When hypertrophic conditions are reached, the number of foraminiferal tests peak. This is commonly followed by the development of an abiotic zone at the maxima of pollution (Alve, 1995). Pearson and Rosenberg (1978) determined that a similar pattern was apparent in the macrobenthos; as input of organic contaminants increase, diversity decreases to a few opportunistic species that develop large populations.

Table 1.1. Measured PAHs and their respective EPA classifications. A * indicates a compound that is considered to be a known animal carcinogen by the DHHS. A B2 classification is a probable human carcinogen, a C rating is a possible human carcinogen, and a D rating denotes that the compound is not classifiable.

Compound	EPA Carcinogenicity Classification	EPA Maximum Contaminant Level ($mg\ L^{-1}$)
Naphthalene	C	--
Biphenyl	D	--
Acenaphthylene	D	--
Acenaphthene	D	--
Fluorene	D	--
Phenanthrene	D	--
Anthracene	D	--
Dibenzothiophene	--	--
Fluoranthene	D	--
Pyrene	D	--
Benz(a)anthracene*	B2	0.0001
Chrysene	B2	0.0002
Benzo(b)fluoranthene*	B2	0.0002
Benzo(k)fluoranthene*	B2	0.0002
Benzo(e)pyrene	D	--
Benzo(a)pyrene*	B2	0.0002
Perylene	--	--
Indeno(1,2,3-c,d)pyrene*	B2	0.0004
Dibenz(a,h)anthracene*	B2	0.0003
Benzo(g,h,i)perylene	D	--

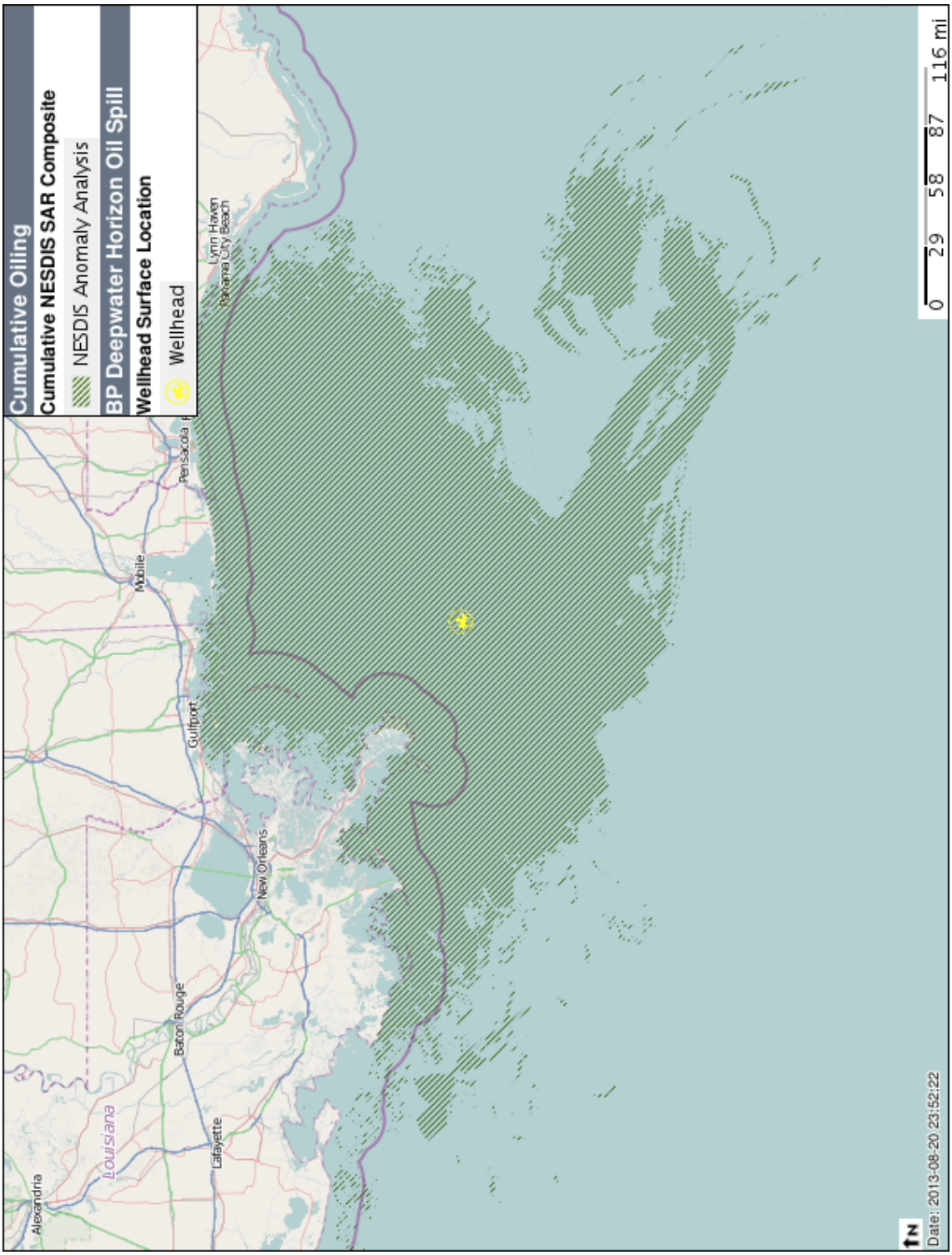

Figure 1.1. Location of the Macondo wellhead and composite spatial surface extent of the DWH oil spill in the Northern Gulf of Mexico (NOAA, 2013).

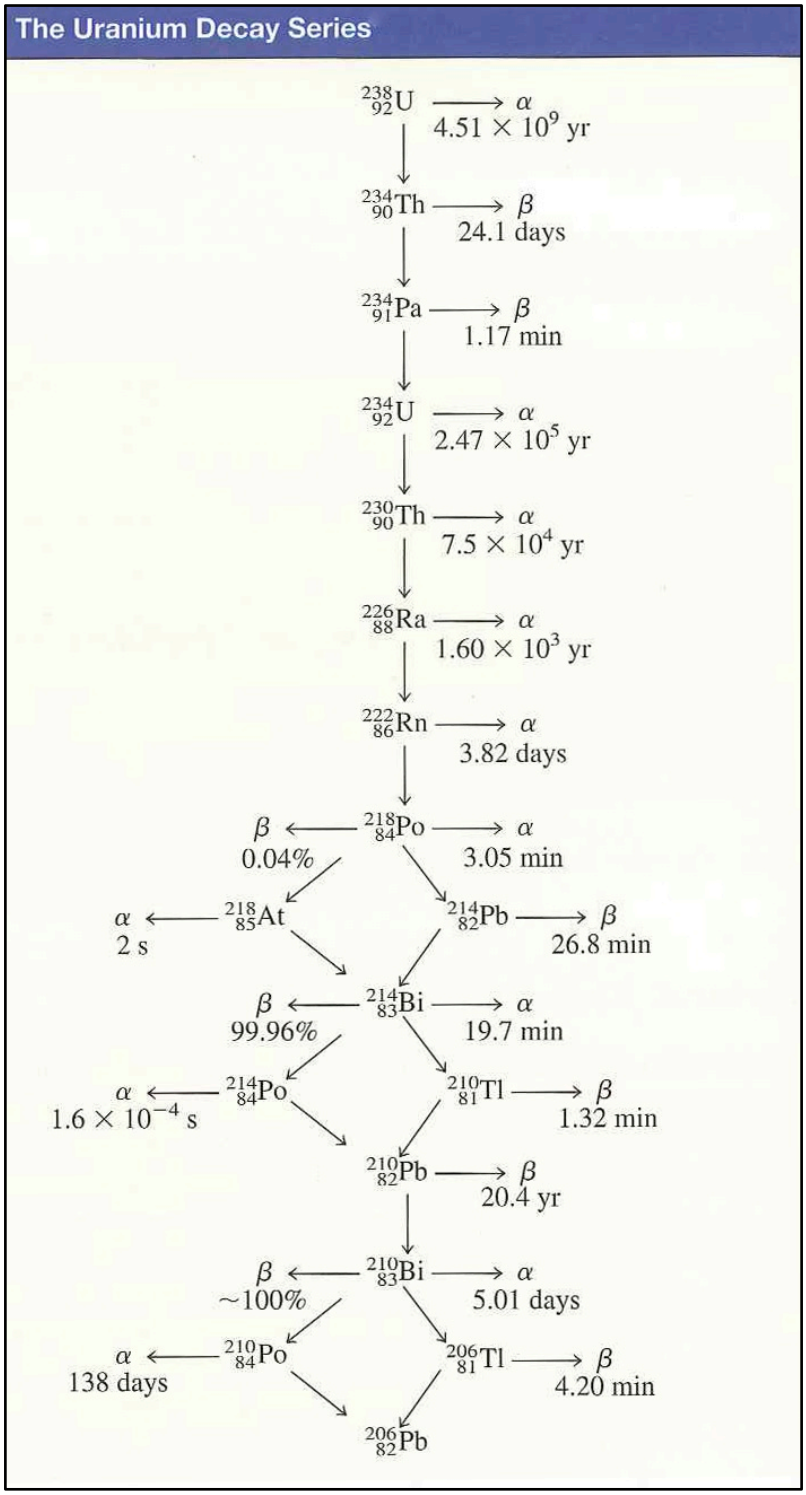

Figure 1.2. The ^{238}U decay series. Shows the half-life and types of radioactive decay of each isotope. From Chang, 2007.

CHAPTER TWO: METHODOLOGY

2.1 Geologic Setting and Study Area

The modern Mississippi Delta plain began to form during the Holocene, approximately 7,500 to 5,000 years ago (Coleman et al., 1998), and since that time has been shaped by episodes of building and abandonment of various delta lobes. The geomorphology of these abandoned lobes has been described by Fisk (1944), Kolb and Van Lopik (1958), Frazier (1967), and many others. The marsh deposits in the Mississippi River Delta are characterized by a sedimentary sequence consisting of shallow marine bay clays and marsh peats (Gosselink, 1984).

Following the DWH spill, five sampling locations were chosen based on data from NOAA's Environmental Response Management Application (ERMA), and included marsh islands and inlets in the northern GOMx that were expected to receive variable amounts of oil (Figure 2.1). The station names and their respective amount of expected oiling are as follows: Belle Fontaine, MS: little to no oiling; Rigolets, LA: moderate oiling; Keel Boat Pass, LA: moderate oiling; Dry Bread Island, LA: heavy oiling; and Bay Jimmy, LA: very heavy oiling (Table 2.1). Three of these five locations were chosen as a subset at the start of this project; however, it was later decided that a fourth station would be a beneficial addition. Thus, four of the original five stations will be discussed below (sans Belle Fontaine, MS).

2.2 Sampling Method

Sampling was completed in multiple stages, with samples taken approximately one year apart in 2010 and 2011; however, only the 2010 samples were analyzed for this thesis project. The exception is Bay Jimmy, which was sampled in 2011 and 2012, but

only the 2011 samples are used in this thesis. Replicate push cores of less than one meter in length were collected along transects at each station. Each core was assigned to a marsh environment based on changes in vegetation and relative elevation (Table 2.2, Figure 2.2). The "low" core was always taken within the subtidal zone of the marsh. This area is typically at nearly marine salinities and is characterized by little to no vegetation and a muddy facies, due to almost constant inundation by water. The "mid" and "high" cores were taken within the intertidal zone. The intertidal zone experiences daily inundation by tides, and is significantly influenced by local winds, storms, and tidal regime. The intertidal zone can have variable physical characteristics based on several factors, including duration of tidal submergence, wave and current energy, and the source of the sediment load (Frey and Basan, 1978). The intertidal zone can be broken into several marsh environments; here, we have sampled in the middle and high marshes. Thick plots of *Spartina alterniflora* are typical of the middle marsh. These grasses are excellent at capturing sediment and nutrients from the incoming tides. The high marsh is topographically higher, having less frequent inundation by tides, and therefore has increased contributions of plant detritus to sedimentary substrates (Williams and Hamilton, 1995).

Tidal ranges for marshes along the Louisiana coastline vary from approximately 0.3 to 0.5 m, although tides associated with storm fronts can push water up to elevations of 1 m or more above mean sea level (NOAA, 2009). These areas have a diurnal tidal cycle, meaning that they experience one high and one low tide per lunar day.

2.3 Thesis Sampling Sites

2.3.1 The Rigolets

This sampling site is abbreviated RIG for all labeling and identification purposes. A close-up image of the sampling sites is seen in Figure 2.3. RIG is located north of the present day Mississippi River Delta in a strait running between Lakes Pontchartrain and Borgne. This strait forms the boundary between New Orleans and St. Tammany Parishes. It is part of the Pontchartrain basin, the oldest drainage basin in the Mississippi River Delta Plain (Gosselink, 1984). 2,500 to 1,000 years ago, progradation of the St. Bernard Delta complex formed the south shore of Lake Pontchartrain and RIG (Kolb and Van Lopik, 1958). This area contains extensive marshes with well-developed salt and brackish zones. Additionally, it is generally a low energy environment, and because it is protected from the waters of the GOMx, it was expected to accumulate mainly fine-grained sediment.

The USGS monitors salinity in most marshes along the GOMx. Seasonal ranges for median daily salinity at RIG (USGS gauge 301001089442600) vary from approximately 3 to 6‰ in spring and increase to just over 10‰ in late summer (USGS, 2013). It is notable that salinity was atypically low (< 5‰) from June to September of 2010 due to controlled diversions of Mississippi River water intended to hold off surface oil from the spill (State of Louisiana, 2010). On the day of sampling, however, salinity appeared to be unaffected, as masured pore water salinities at the High and Mid sites were 12 and 6‰, respectively.

Definition of marsh position was based on changes in vegetation at all sites. A mudflat with submerged fringing *Spartina alterniflora* (smooth cordgrass) defined the

area where the Low core was taken at RIG. The area surrounding the Mid core was dominated by *Spartina alterniflora*. The High core was taken in an area containing *Spartina alterniflora*, *Spartina patens* (saltmarsh cordgrass) and *Distichlis spicata* (seashore saltgrass).

RIG was reported as heavily oiled in NOAA's Shoreline Cleanup Assessment Technique (SCAT) as of July 9, 2010. Even so, there were no site-specific Shoreline Treatment Recommendations (STRs) for this location. However, there was some shoreline cleanup treatment conducted early on under General STRs for the entire region. These treatment methods may have included use of sorbents, low pressure flushing, and skimmers and vacuums to remove oil near the marsh edge and in adjacent nearshore waters.

2.3.2 Keel Boat Pass Island

This sampling site is abbreviated KBP for all labeling and identification purposes. KBP is located north of the Mississippi River Delta in the Chandeleur Sound, part of the St. Bernard lobe of the Mississippi River Delta complex. The Chandeleur Sound is a shallow bay, with an average depth of 3 m, and is somewhat protected from GOMx waters by the Chandeleur Islands. This provides for a low energy environment, but less so than at an inlet site like RIG. KBP was expected to accumulate more sand than RIG due to its more open setting. KBP lies approximately 80 km east of New Orleans, LA. An image of the sampling sites is seen in Figure 2.4.

Seasonal ranges of salinity in the Chandeleur Sound (USGS gauge 07374526) are considered intermediate for this area, ranging from 5 to 9‰ in spring and increasing to 10

to 15‰ during summer (USGS, 2013). On the day of sampling, open water salinity was measured to be 13.4‰, with pore water salinity at the High site being 29‰.

An unvegetated mudflat defined the area where the Low core was taken at KBP. The Mid core was taken in an area dominated by *Spartina alterniflora* and *Salicornia bigelovii* (dwarf saltwort). The area surrounding the High core graded into *Spartina alterniflora* with *Salicornia bigelovii*, *Batis maritima* (turtleweed), and another herbaceous species.

Some of the heaviest oiling following the DWH spill was reported in NOAA's SCAT along portions of the KBP shoreline. However, these oiled areas were patchily distributed and not widespread. At the time of sampling, sorbent boom had been placed offshore but no oil was visible. While it was suspected that KBP might have been exposed to oil, measurements revealed that it in fact had the lowest surface sediment TPAH concentrations of any site considered herein. Therefore, it was chosen to be the "control" station for this study. However, as indicated in the results from foraminiferal data, even KBP does not adequately serve as a true control.

2.3.3 Dry Bread Island

This sampling site is abbreviated DBI for all labeling and identification purposes. Like KBP, DBI is located in the Chandeleur Sound, and is approximately 75 km east of New Orleans, LA. An image of the sampling sites is seen in Figure 2.5.

The typical salinities reported above for KBP also apply to DBI. DBI was sampled during the timeframe of controlled diversions of river water following the DWH spill. USGS gauge 07374526 recorded unusually low salinities from less than 1 to 7‰

during the period from July to late August, 2010. However, on the day of sampling open water salinity was measured to be 13.5‰ and pore water salinity was 16-17‰.

The contact between the subtidal and intertidal zones of the marsh was characterized by a large erosional marsh scarp (1 to 2 feet high) at this site. The Low core was taken within the unvegetated subtidal zone, and the Mid core was taken above the scarp in the intertidal zone. The Mid core was surrounded by *Spartina alterniflora*. The area around the High core was characterized by a change in vegetation to *Distichlis spicata* with some *Batis maritima*.

DBI was reported as heavily oiled in the SCAT. Oiling conditions were described as a 6 meter wide band of fresh oil and mousse covering 60% of the marsh vegetation (Zengel and Michel, 2013). Large patches of oil were indeed observed at the time of sampling for this project (Figure 2.6). Sorbent boom was placed just seaward of the marsh edge sometime after July, 2010 to prevent additional oil from reaching the marsh and to capture any oil released during cleaning. This sorbent boom was still present at the time of sampling. In addition, low pressure flushing was allowed as part of the site-specific STRs, and may have been carried out at this site (Figure 2.7).

2.3.4 Bay Jimmy

This sampling site is abbreviated BJ for all labeling and identification purposes. Bay Jimmy is a small body of water located approximately 60 km south of New Orleans, LA. An image of the sampling sites is seen in Figure 2.8. Bay Jimmy is part of upper Barataria Bay, a basin bounded on the east by a distributary ridge of the current Mississippi River channel.

Salinity in Barataria Bay (USGS gauge 07380251) is considered intermediate for this area, ranging from 5 to 15‰ in spring and increasing to 16‰ during late summer (USGS, 2013).

A largely non-vegetated mudflat defined the area where the Low core was taken. The area surrounding the Mid core was strongly dominated by *Spartina alterniflora*, with a trace of *Distichlis spicata* and *Batis maritima*. The High core was taken in an area dominated by *Spartina patens*, with some *Juncus roemerianus* (needle rush).

The SCAT indicated that locations in Barataria Bay (including Bay Jimmy) were heavily oiled. Zengel and Michel (2013) reported that initial oiling bands on the shoreline were typically 10 meters wide and covered more than 90% of the vegetation (Figure 2.9). They also reported heavily oiled wrack lines, heavily oiled vegetation mats, and thick (2-3 cm) layers of surface oil residue and mousse on the marsh substrate. They indicated that the mousse layer did not appear to be weathering where it was trapped below laid-over vegetation and wrack. Bay Jimmy and surrounding areas continue to be closed to commercial and recreational fishing due to the DWH spill through the 2013 fishing season (LDWF, 2013).

2.4 Laboratory Methods

All cores were refrigerated until analysis could begin. One core from each station was described, graphically logged and photographed prior to sectioning. Samples for determining bulk density were collected at 2 cm intervals and at obvious textural changes within each sediment core. Each bulk density sample was collected using a syringe of known volume, dried in an oven at 70° C, and re-weighed to obtain a bulk density value.

Cores to be used for radiochemistry and sedimentology were sectioned at 0.5 cm intervals over the first 3 cm, at 1 cm intervals thereafter to 30 cm, and at 2 cm intervals thereafter to the end of the core. Bulk sediment samples from each interval were dried in an oven at 70° C.

Cores to be used for organic geochemical analyses were sectioned using two different sampling schemes. RIG and KBP were sampled at 5 cm intervals for the entirety of the core. DBI and BJ were sampled at 1 cm intervals over the first 30 cm, and at 2 cm intervals thereafter to the end of the core. A subset of these samples was selected from the near surface of each core for determination of TPH and TPAH concentrations. These samples were kept refrigerated in amber vials until they were shipped to collaborators at the Geochemical and Environmental Research Group at Texas A&M University in College Station, Texas for analysis.

Grain size analysis was completed at each sectioning interval over the top 30 cm of each sediment core. In preparation for grain size determination, 1 to 3 grams of sediment was gently separated from the bulk sample, avoiding any large pieces of shelly material. A sodium hexametaphosphate solution was added to disperse sediment samples. If large quantities of organic material were visible, the sample was rinsed with distilled water over a No. 35 U.S. Standard Sieve (500 μm). The macro-organic matter collected on the sieve was dried and the weight recorded. For all samples, any remaining organic matter was destroyed by adding 30% H_2O_2 to the sample over heat to prevent the organic matter from acting as a binding agent (Day, 1965). The samples were inspected frequently while being heated, and an additional 10 mL of H_2O_2 or distilled water was alternately added whenever a sample came near dryness. When the samples were no

longer visibly reacting, they were removed from the hotplates. The samples were then rinsed into a centrifuge tube with distilled water and centrifuged with 0.5 M $MgCl_2$ until the supernatant was clear and the pH was near neutral. After decanting the supernatant, the remaining sediment was dried in an oven at 70° C. A Malvern Instruments Mastersizer S2000 particle size analyzer was then used to quantify the relative quantities of major mineral sediment size fractions including sand, silt and clay (*sensu* Wentworth). This instrument can accurately resolve particles from 0.02 μm to 2 mm in diameter.

Another portion of each sample was disaggregated with a mortar and pestle, and then ground in a Retsch RM-200 Mortar Miller. Again, samples with an abundance of macro-organic matter were sieved through a No. 35 U.S. Standard Sieve. Aliquots of the crushed sediment were used to determine: (1) carbonate percentages, (2) SOC concentrations, (3) activities of ^{234}Th, ^{7}Be and ^{137}Cs by gamma counting, and (4) activity of ^{210}Pb by alpha counting its granddaughter, ^{210}Po.

Determination of carbonate content in the samples was made using a weight-loss method modified from Molnia (1974). Samples of approximately 300 mg were weighed and subjected to a 10% solution of HCl to destroy any inorganic carbon. After sonicating and heating the solution, it was rinsed via vacuum-filtration through 0.4 μm membrane filters with distilled water. The remaining residue was dried at 70° C. The filter and insoluble sediment were then weighed again to calculate a carbonate percentage. From this, subsamples of 5 mg were placed into tin capsules for determination of SOC. These samples were analyzed using a Costech ECS 4010 Elemental Analyzer, which relies on thermal combustion to break the sample down into N_2 and CO_2 for detection (Yeager and Santschi, 2003; Yeager et al., 2004). To ensure data quality, 10% of the total number of

samples were analyzed in duplicate. In cases where the duplicate sample showed more than 15% deviation from the original sample, a triplicate sample was run. SOC concentrations were used to calculate an overall SOC inventory for each core as follows:

$$\sum_{0\text{-}30\text{cm}} [\text{interval thickness} \times (1 - \text{porosity} \times \text{grain density}) \times \text{SOC}]$$

In order to resolve ^{234}Th, ^{7}Be and ^{137}Cs profiles, high-resolution gamma spectrometry was used as described in Yeager et al. (2004). In summary, samples of 1 to 10 g were placed into plastic test tubes and sealed with epoxy. Silica gel was added to those samples that did not have equal geometries. After waiting 21 days for secular equilibrium to be reached between ^{226}Ra and ^{222}Rn (daughter isotopes of ^{234}Th), the samples were run on a Canberra DSA-1000 multi-channel analyzer mated to a GCW3023 HP-Ge well detector. Counts were repeated on a subset of representative samples six or more months after collection to determine $^{234}Th_{xs}$. This allowed all $^{234}Th_{xs}$ to decay and leave only that portion of the total ^{234}Th that is supported by direct decay of ^{238}U ($^{234}Th_{supp}$).

Sediment accumulation rates were determined where possible using ^{137}Cs by the following equation:

$$S = \frac{D_{pk}}{T}$$

where S is sediment accumulation, D_{pk} is the mass depth at which either the ^{137}Cs maximum occurs (1963) or the first incidence of ^{137}Cs can be determined (1953), and T is time (Yeager et al., 2007).

In order to determine ^{210}Pb activity, alpha spectrometry was used. Samples were spiked with a known amount of ^{209}Po tracer (Eckert & Ziegler Isotope Products, Catalog No. 7209) and completely digested over heat using concentrated acids (HF, HCl and

HNO_3). Ascorbic acid was then added to bind free Fe(III). Samples were plated by adding a silver disc to the solution, which provides a surface for the deposition of Polonium isotopes (Yeager et al., 2004). To ensure data quality, a blank sample was run with every set of ten samples. A Canberra Alpha Analyst Integrated Alpha Spectrometer, model 7200-12, was used to count the samples. The added ^{209}Po tracer, which does not occur in nature, is used as a reference point for determining the amount of ^{210}Po in the sample. It is assumed that ^{210}Po, an alpha emitter, is in secular equilibrium with ^{210}Pb.

There are several methods of reconstructing geochronology using ^{210}Pb. One method is to estimate age and/or average historical sedimentation rates by comparing the ^{210}Pb profile to atmospherically supported ^{210}Pb inventories (Noller, 2000). However, these inventory-based models assume a constant rate of sedimentation, which is not accurate for marsh settings that generally experience pulsed sedimentation. For the locations studied here, a more appropriate model is the Constant Rate of Supply (CRS) model, also known in the literature as the Constant Flux model (Noller, 2000). The CRS model assumes: (1) $^{210}Pb_{xs}$ is supplied to sediments at a constant rate over time, (2) the initial concentration within the sediment is variable, and (3) the rate of sediment deposition/accumulation is also variable (Goldberg, 1963). The activity of $^{210}Pb_{xs}$ (C_x) can be determined at any depth (x) using the law of radioactive decay:

$$C_x = C_0 e^{-\lambda t}$$

where λ is the decay constant for ^{210}Pb (0.031 yr^{-1}) and C_0 is the initial concentration of ^{210}Pb. Samples that provided a negative rate were considered extraneous and excluded from the remainder of the model. From the activity of $^{210}Pb_{xs}$, the age of a deposit at depth x can be determined from the following relation:

$$t = \frac{1}{\lambda} \ln\left(\frac{A_0}{A_x}\right)$$

where A_0 is the total $^{210}Pb_{xs}$ in the sediment column and A_x is the total $^{210}Pb_{xs}$ activity beneath depth x (Appleby and Oldfield, 1978). A sediment accumulation rate (S_a) for each depth interval can then be derived from the change in mass (ΔM) over change in time (Δt), as follows:

$$S_a = \frac{\Delta M}{\Delta t}$$

An averaged sediment accumulation rate may then be determined for an entire core.

Meiofauna samples were taken from push cores as well. Cores used for identifying and counting foraminifera were collected, sectioned, and analyzed by Dr. Charlotte Brunner and her research group at the University of Southern Mississippi. All of the data referenced in this thesis can be found in Brunner et al. (2013). The method can be summarized as follows. Cores were sectioned at 1 cm intervals to a depth of 10 cm within 24 hours of sampling. A buffered solution of 0.5 g rose Bengal per liter of seawater was mixed into each interval in order to stain and identify living or recently living specimens. The samples were then wet sieved on a 45-μm screen to capture both juvenile and adult foraminifera. The retained silt and sand-sized material was then refrigerated in alcohol to preserve the samples until they could be counted. At that time, the samples were split with a settling-type splitter into aliquots that could be conveniently viewed on a gridded Petri dish and inspected under an Olympus SZX12 dissecting microscope. All specimens from each aliquot were identified to species until approximately 300 total specimens were counted from each depth interval to determine species diversity and density, with deformed specimens being noted as well. The depth

of habitation (DOH) is defined as the depth at which 95% of stained specimens are accumulated, and the standing stock is calculated as the sum of densities from the surface to the depth of habitation.

Table 2.1. Summary of site-specific sampling information.

Sampling Site	Core Label	Latitude (degrees, minutes, seconds)	Longitude (degrees, minutes, seconds)	Collection date
Belle Fontaine	Low	30°21'12.80"N	88°45'14.11"W	5/13/10
	Mid	30°21'12.90"N	88°45'14.10"W	5/13/10
	High	30°21'13.00"N	88°45'14.10"W	5/13/10
Keel Boat Pass Island	Low	29°52'43.30"N	89°14'33.90"W	5/27/10
	Mid	29°52'43.40"N	89°14'34.40"W	5/27/10
	High	29°52'43.60"N	89°14'34.90"W	5/27/10
Rigolets	Low	30°09'52.20"N	89°40'5.70"W	8/1/10
	Mid	30°09'52.20"N	89°40'6.00"W	8/1/10
	High	30°09'52.00"N	89°40'6.10"W	8/1/10
Dry Bread Island	Low	29°50'32.00"N	89°18'14.00"W	8/4/10
	Mid	29°50'32.00"N	89°18'14.80"W	8/4/10
	High	29°50'32.10"N	89°18'14.90"W	8/4/10
Bay Jimmy	Low	29°26'35.70"N	89°53'59.00"W	6/4/11
	Mid	29°26'35.90"N	89°53'59.30"W	6/4/11
	High	29°26'36.10"N	89°53'59.50"W	6/4/11

Table 2.2. Marsh environment classifications for sampled cores.

Sampling Site	Core Label	Corresponding Environment
Keel Boat Pass Island	Low	Subtidal zone
	Mid	Middle marsh
	High	High marsh
Rigolets	Low	Subtidal zone
	Mid	(Lower) Middle marsh
	High	(Upper) Middle marsh
Dry Bread Island	Low	Subtidal zone
	Mid	Middle marsh
	High	High marsh
Bay Jimmy	Low	Subtidal zone
	Mid	Middle marsh
	High	High marsh

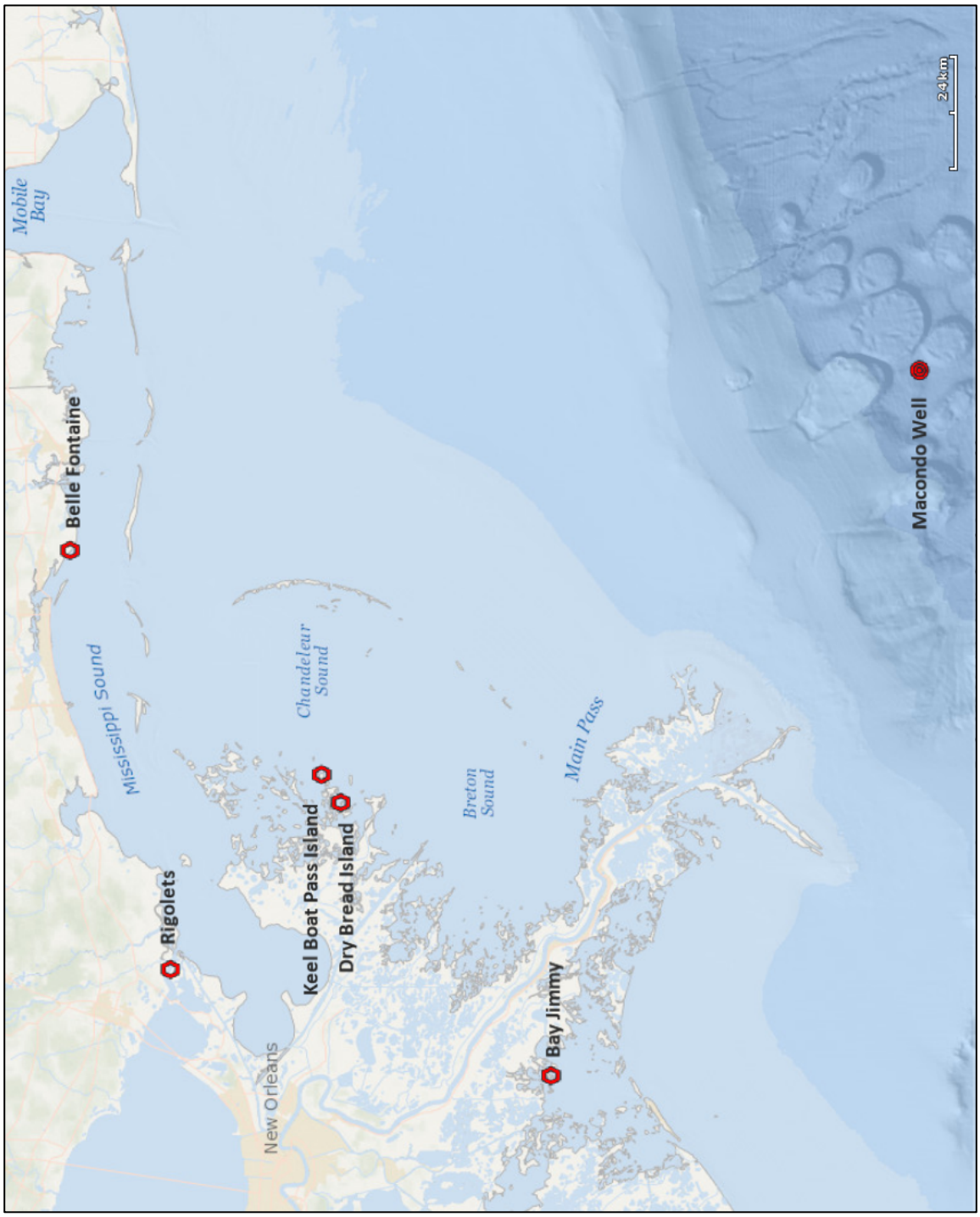

Figure 2.1. Map of all station locations and Macondo wellhead. Imagery courtesy of ESRI.

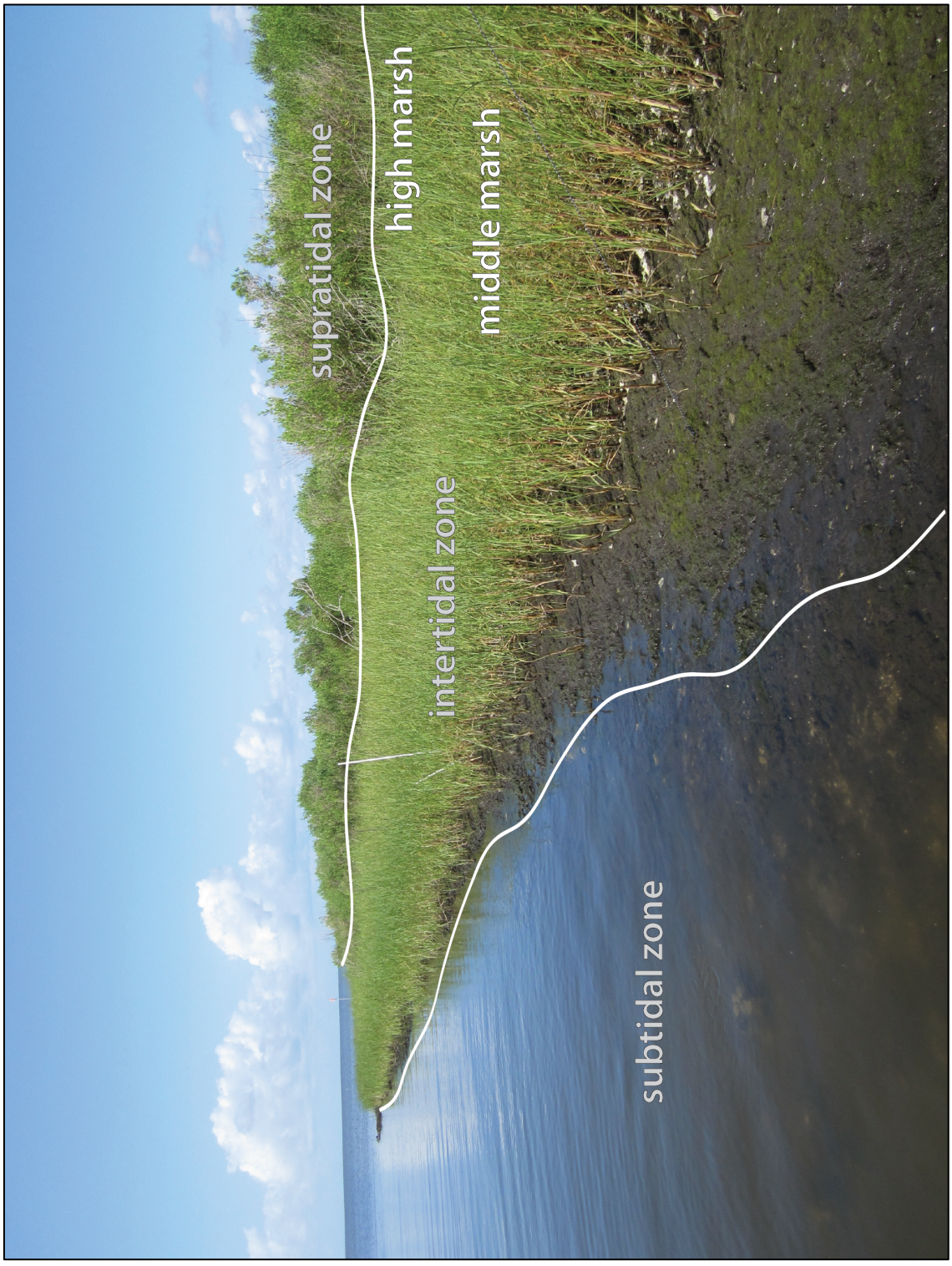

Figure 2.2. Photo illustrating marsh environments at Bay Jimmy.

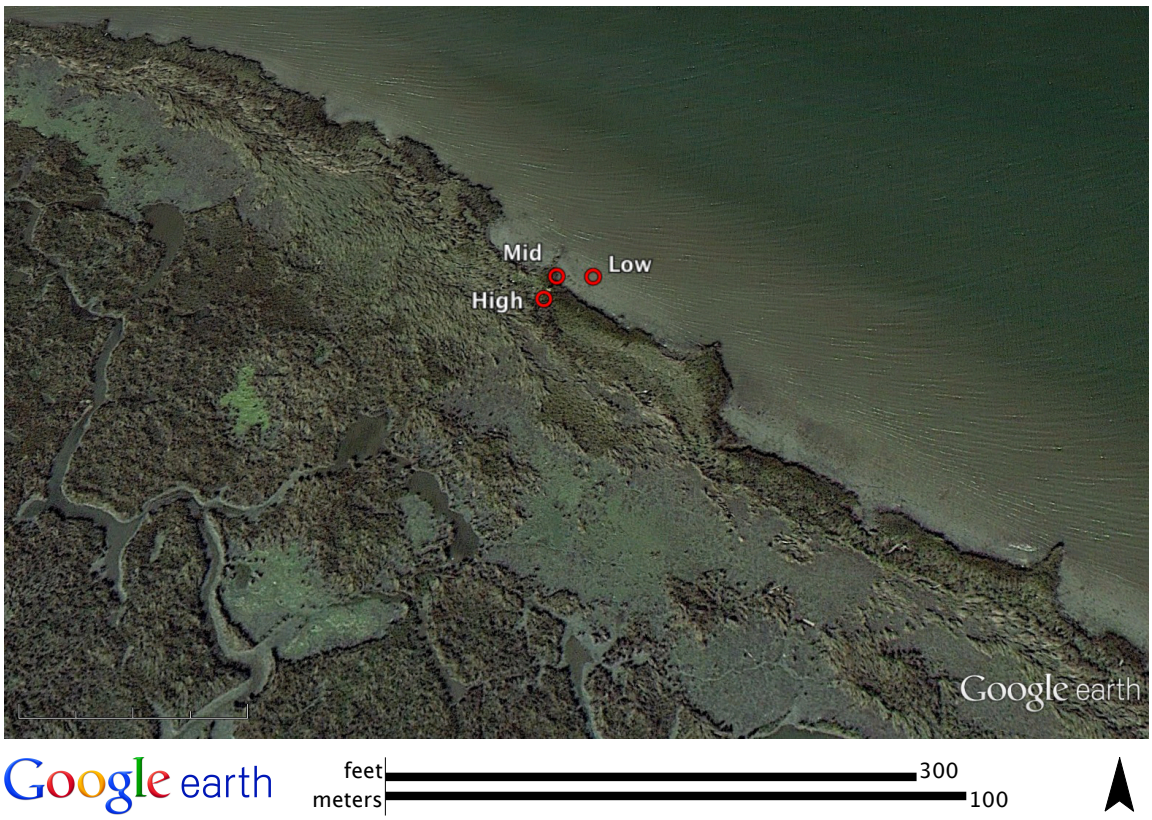

Figure 2.3. Image of Rigolets Pass, LA sampling locations. Imagery courtesy of Google Earth (2012).

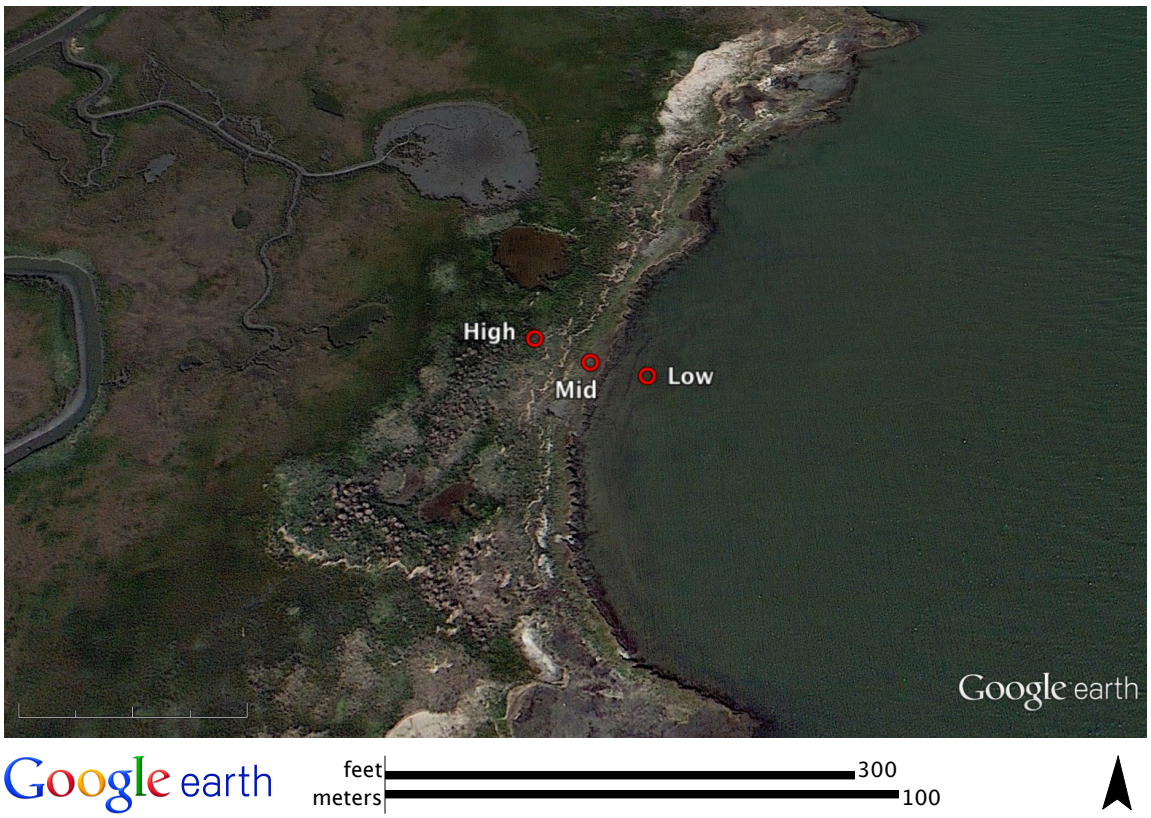

Figure 2.4. Image of Keel Boat Pass Island, LA sampling locations. Imagery courtesy of Google Earth (2012).

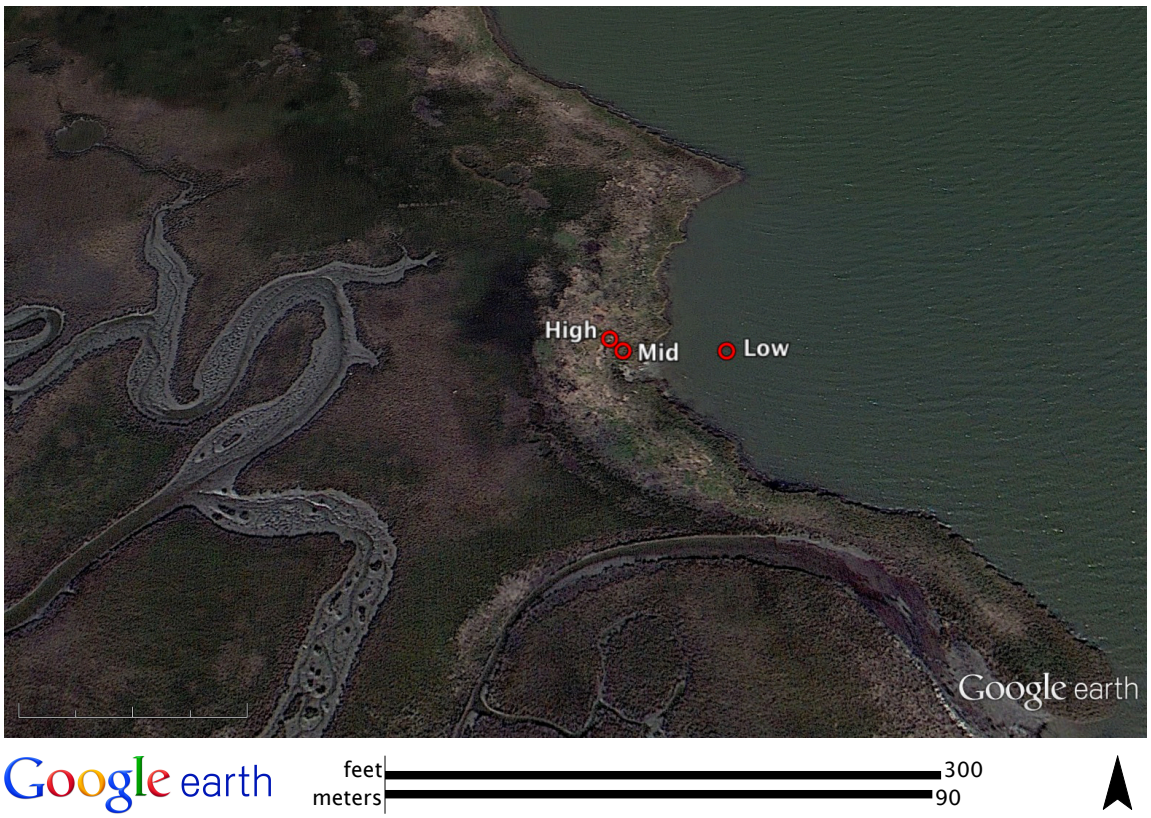

Figure 2.5. Image of Dry Bread Island, LA sampling locations. Imagery courtesy of Google Earth (2012).

Figure 2.6. Photograph of oil on dead patches of marsh grass (August 4, 2010). Photo credit: Dr. Charlotte Brunner.

Figure 2.7. Photograph of low pressure, high volume marsh flushing tested at Bay Jimmy, LA in September 2010. NOAA reports indicate that little to no oil was effectively mobilized from the sediment during demonstrations, and the flushing may have actually damaged the marsh by scouring sediments (Zengel and Michel, 2013). However, following vegetation cutting, this remediation method was approved for use at DBI and other sites.

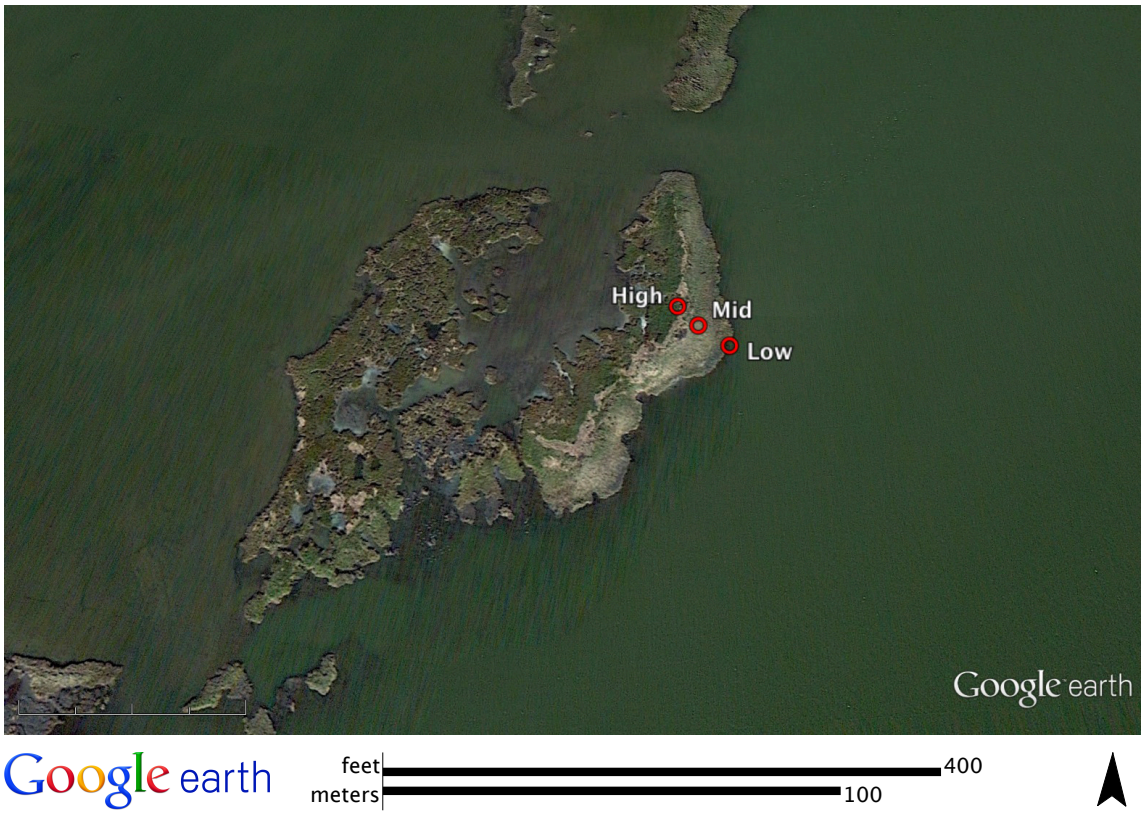

Figure 2.8. Image of Bay Jimmy, LA sampling locations. Imagery courtesy of Google Earth (2012).

Figure 2.9. Photograph of June 2010 initial oiling conditions at Bay Jimmy, LA. Photo credit: Zengel and Michel (2013).

CHAPTER THREE: RESULTS

Results are presented in the following order: sedimentology (grain size, stratigraphy, bulk density, SOC, carbonate); organic geochemistry (TPH/PAH); radiochemistry (^{210}Pb, ^{7}Be, ^{137}Cs, ^{234}Th); and micropaleontology (foraminifera). For each of these analyses, the order in which stations are discussed is as follows: RIG, KBP, DBI, and BJ.

3.1 Grain Size

Sediments from all sites were evaluated for grain size distribution to a depth of 30 cm. At RIG, all three coring sites were clearly dominated by silt (up to 89%). The percentage of clay was low (2 to 26%) both down-section and across-transect. The percentage of sand was variable, but remained relatively small (2 to 32%) at the Low and Mid sites, with higher percentages at the High site (6 to 57%) (Figure 3.1; see Appendix 3 for all data).

Because KBP demonstrated more variability upon visual inspection than the other stations, grain size was further analyzed from 30 to 50 cm in intervals of 2 cm. The clay content remained relatively small at the Low and Mid sites (1 to 10%), with slightly more variation at the High site (1 to 25%). Each core was dominated by alternating layers of silt and sand, which varied both across-transect and down-core.

DBI exhibited a general trend of coarsening with movement toward the High site. The Low site was dominated by silt (44 to 89%), while the High site was dominated by sand (41 to 90%). Similar to KBP, the clay content remained small for all cores (2 to 13%).

BJ was dominated by silt at all sites, with higher amounts of clay (3 to 43%), especially at the Mid site.

3.2 Stratigraphy

Where grain size data were available, percentages of sand, silt and clay were plotted on a Folk Ternary Diagram (Appendix 1) to give an average sediment size for the stratigraphic diagram. Below the depth of grain size characterization, the descriptions were based on visual interpretation of the core. Distance between cores was determined using the Haversine formula (Appendix 2). No elevation data were collected, so all cores begin at a zero depth.

As seen in the stratigraphic diagram for RIG (Figure 3.2), all sites contained organic matter and plant debris, although with decreasing prevalence down-core.

At KBP, all sites contained organic matter and plant debris (Figure 3.2). The Low and Mid sites had a thin shell hash layer at the surface, but the High site lacked shells.

The stratigraphic diagram for DBI shows alternating layers of silt and sandy silt at the Low site, and sandy silt and silty sand at the Mid and High sites (Figure 3.3). There was a small shell hash layer at the surface of the Low core, but shells were sparse in the Mid and High cores. Roots were prevalent at the Low site, but there was little visible macro-organic matter. The Mid and High sites had larger quantities of organic matter, as well as roots.

BJ was characterized at all sites by alternating layers of silt and sandy silt, with a small amount of mud at the High site (Figure 3.3). Plant material and other organic matter were prevalent in all cores. The shell hash layer present at the Chandeleur sites (KBP and DBI), however, is totally absent at BJ.

Every core illustrated the layering of episodic sedimentation that is typical of a salt marsh setting.

3.3 Bulk Density

Bulk density was calculated for the entirety of each core (Appendix 4). At RIG, values increased with movement toward the seaward edge, ranging from 0.378 to 0.801 g cm^{-3} at the High site, 0.465 to 1.060 g cm^{-3} at the Mid site, and 0.642 to 1.143 g cm^{-3} at the Low site. When plotted against depth, each core showed a similar trend; generally, there were mid-range values at the surface, followed by a rapid decline, and then a gradual increase to a maximum bulk density near the bottom of the core (Figure 3.4). None of the other sites showed any obvious significant trends with respect to depth (Fig. 3.4). At KBP and DBI, the Low and Mid sites were generally denser than the High sites, with values ranging from 0.261 to 1.403 g cm^{-3}, and 0.187 to 1.081 g cm^{-3}, respectively. Bulk density values at BJ were lower than at the Chandeleur sites. Bulk density ranged from 0.210 to 0.521 g cm^{-3} at the High site, 0.318 to 0.933 g cm^{-3} at the Mid site, and 0.145 to 0.462 g cm^{-3} at the Low site. The cores were apparently highly mixed and, again, no trend with depth was visible.

3.4 Sedimentary Organic Carbon

SOC was determined at each sample interval to a depth of 30 cm (Appendix 3). Depth profiles for each site are found in Figure 3.5. At RIG, SOC varied from 1 to 3% at the Low site, 0.4 to 21% at the Mid site, and 1 to 9% at the High site. Under steady-state conditions, an ideal SOC trend has a high at the surface, with exponential decline below (Burdige, 2007). None of the cores at RIG exhibit this trend, or any evident trends with depth. The Mid and High sites, in particular, illustrate pervasive mixing at this station.

SOC showed more variation with movement toward the drier end of the marsh at KBP. SOC varied from 0.3 to 4% at the Low site, 0.5 to 6% at the Mid site, and 0.2 to 27% at the High site. When graphed, none of the cores show trends with depth. In the High core, there were peaks from 2.5-3 cm, 9-11 cm, and 18-21 cm depth, corresponding to peat facies. The High site at KBP was the only core of any station that showed a well-defined peat-like zone. Peat was described as any unit containing semi-carbonized plant remains with a moisture content of at least 75%.

At DBI, SOC again showed more variation with movement toward the drier end of the marsh, with variation from 1 to 6% at the Low site, 2 to 16% at the Mid site, and 1 to 19% at the High site. The Mid and High sites have the ideal trend for SOC. The Low site, however, shows no trend with depth.

At BJ, SOC varied from 4 to 25% at the Low site, 5 to 15% at the Mid site, and 8 to 23% at the High site. While the High site had generally higher SOC than the Mid or Low sites, unlike the Chandeleur sites, BJ showed no trend of increasing SOC variation with movement toward the drier (high) end of the marsh. In general, BJ had higher SOC concentrations than the Chandeleur sites at all zones, but especially at the Low site.

SOC inventories were also calculated. These values are reported in Appendix 3.

3.5 Carbonate

Like SOC, the carbonate percentage was calculated for every core at each sample interval to a depth of 30 cm (Appendix 4). At RIG, carbonate varied from 4-12%, with the High site showing the most variation. There were no apparent trends with depth.

At KBP, carbonate percentages varied from 1 to 7% at the Low site and 3 to 19% at the High site. At DBI, carbonate percentages varied from 5 to 11% at the Low site and

4 to 16% at the High site. Surprisingly, while there was a small shell layer at the surface of the Low core at DBI, this was not indicated in the carbonate values. The Mid cores at KBP and DBI exhibited very high percentages of carbonate at the surface (up to 59 and 60%, respectively), which decreased down-core (approximately 9 and 10%, respectively, at 30 cm depth).

At BJ, carbonate varied from 5 to 20%, with the Mid and Low sites being slightly skewed toward the lower end of the range.

3.6 Organic Geochemistry

After analyzing 320 sites along the Louisiana coast, Iqbal et al. (2007) found 1,500 ng g^{-1} (ppb) to be the upper limit [TPAH] baseline for marsh sites in southeastern Louisiana. In the Iqbal study, the three-year average [TPAH] concentration for 95% of the sites was less than 7,500 ng g^{-1}, a defined limit of fivefold the baseline high concentration. It is important to note that *none* of the samples in the Iqbal et al. study had a concentration exceeding 9,600 ng g^{-1}.

The total and compound-specific results of all samples analyzed for TPAH and TPH are found in Appendices 6 and 7, respectively. Levels of [TPAH] are summarized in Figure 3.6. Values of [TPAH] are reported without perylene, which can be produced biogenically (Budzinski et al., 1997). At RIG, samples were bulked from 0-5 cm and 6-10 cm, for a total of two samples at each site. [TPH] was below 120 μg g^{-1} at all three RIG sites, and the [TPAH] levels at all sites were consistently below upper-level background for this area (263.1 to 1064.9 ng g^{-1}).

Samples were similarly bulked at KBP. [TPH] was below 100 μg g^{-1} at all KBP sites. The [TPAH] levels at KBP were also quite low, and well below the upper-level background (72.8 to 284.9 ng g^{-1}).

Because it was collected later and was expected to be a heavily impacted site, DBI was sampled at a higher resolution than the previous two sites. Samples were analyzed at 0-1, 1-2, 2-3, 3-4 and 4-5 cm intervals for each core. There was wide variation in both [TPH] and [TPAH] along transect at DBI. The High and Low sites had [TPH] near or below 100 μg g^{-1}. However, the Mid site revealed [TPH] up to 956 μg g^{-1} near the surface. At a depth of 3 cm, [TPH] dropped back down to approximately 50 μg g^{-1}. With regard to [TPAH], the Low and Mid sites ranged between 96 and 467 ng g^{-1}. These values are well below the upper limit background for the area. However, the High site revealed [TPAH] up to 5,420 ng g^{-1}. All five compounds listed by the DHHS as animal carcinogens (benz(a)anthracene, benzo(b)fluoranthene, benzo(a)pyrene, dibenz(a,h)anthracene, and ideno(1,2,3-c,d)pyrene) were detected at the High site.

Seven samples were analyzed from the BJ cores at one cm intervals to a depth of 3 cm at the High site and 2 cm at the Mid and Low sites. The High site had [TPAH] ranging from 4,345 to 18,279 ng g^{-1}. The Mid site had [TPAH] ranging from 19,356 to 21,913 ng g^{-1}. The Low site had [TPAH] ranging from 7,768 to 7,775 ng g^{-1}. Every sample analyzed from BJ had a value above the level at which biological effects can be seen (4,022 ng g^{-1}). In addition, all five compounds listed by the DHHS as animal carcinogens were detected in every BJ sample analyzed. [TPH] was likewise extremely high at the BJ Mid and High sites (1,705 to 6,937 μg g^{-1}).

3.7 Lead-210

Not all sites were suitable for the determination of sediment mass accumulation rates (g cm^{-2} y^{-1}) using $^{210}Pb_{xs}$ due to sediment mixing. However, sites at RIG, KBP and BJ were appropriate for the CRS model. Average rates are summarized in Table 3.1 (see Appendix 5 for all data).

All three sites at RIG were able to be modeled (Figure 3.7). Each site showed the same general trend: a very slow steady increase in accumulation rate over the last 100 years, until approximately 10 years before sampling (in 2010) when rates began quickly increasing. This trend is most convincing at the High site ($R^2 = 0.76$, $p < 0.01$).

The Low and Mid sites at KBP were modeled (Figure 3.7). The Mid site showed a similar general as those exhibited by the RIG sites, steady accumulation rates over the last 90 years, generally fluctuating between ~0.1 and 0.4 g cm^{-2} y^{-1} (Figure 3.7). Then, approximately 10 years before sampling (in 2010), rates began to increase. It is interesting that while the general trend of increase over the last 10 years is apparent at the Mid site, it is strongly influenced by a short period several years before sampling, when accumulation rates were nearly tenfold higher than the average.

The Low and High sites at BJ were also appropriate for modeling (Figure 3.7). At these sites, there was a steady increase in sedimentation rate over the last 100 years.

3.8 Beryllium-7

Beryllium-7 was present to a depth of 0.25 cm at the Mid site and 2.75 cm at the High site at RIG. Beryllium-7 was not detected at the Low site. At KBP, ^{7}Be was only present at the High site. At this location, ^{7}Be was present to a depth of 2.5 cm.

Beryllium-7 was not detected in any of the cores at DBI or BJ. All tabular ^{7}Be data can be found in Appendix 5.

3.9 Cesium-137

Like ^{7}Be, ^{137}Cs was only sporadically present (Appendix 5). At RIG, ^{137}Cs was only detected at the Mid and High sites. The absence of significant ^{137}Cs at the Low site precluded its use to assess sediment accumulation rates. However, the Mid and High sites were suitable for determination of sediment accumulation rates, which are summarized in Table 3.1. The rate at the High site is a minimum rate, as the full profile has not been constrained to date. The profile for the Mid site illustrating the first instance of ^{137}Cs (corresponding to the year 1953) and the maximum of ^{137}Cs (corresponding to the year 1963) is shown in Figure 3.8. Because of mixing in the top of the core, the first instance of ^{137}Cs yielded a sedimentation accumulation rate that was in better agreement with the $^{210}Pb_{xs}$ rate than when using the 1963 peak.

At KBP, ^{137}Cs was detected in the Mid and Low cores, but full profiles have not been constrained to date.

At DBI, ^{137}Cs was only detected at the Mid site below a depth of 13.5 cm. However, there is no discernible peak usable for calculating an age for the sediment.

Cesium-137 was detected in all cores at BJ, but full profiles have not been constrained to date.

3.10 Thorium-234

The depth of penetration of $^{234}Th_{xs}$ for each core is illustrated in Figures 3.9 and 3.10 and is summarized in Table 3.2. The mixing depth is defined as the maximum penetration depth of $^{234}Th_{xs}$ in the sediment column. Given the half-life of 24.1 days,

these values can be considered minimum mixing depths over the ~60 day (2.5 half-lives) memory of ^{234}Th.

3.11 Foraminifera

All foraminiferal data are from Brunner et al. (2013). A total of eight sites were used in the Brunner et al. study, including the four stations focused on in this thesis. It is important to note that only cores from intertidal sites were used for the foraminifera study. At RIG and BJ, the highest (High) marsh core was used to describe the intertidal zone, and at KBP and DBI the Mid core was used. The standing stock and depth of habitation (DOH) for each site are summarized in Table 3.3.

Brunner et al. (2013) determined a normal, regional condition for middle marsh foraminifera based on two control sites. These control sites were located along the north shore of the western Mississippi Sound in Pearl and Jourdan River marshes, and were sampled seasonally from 2004 to 2005, prior to the DWH spill. At these sites, the DOH varied, but was consistently deeper than 7.5 cm. During the summer months, the standing stocks at the control sites were 1,200 to 1,500 specimens/10 cm^2.

At RIG, a lightly oiled site, the standing stock was highly elevated (6,676 specimens/10 cm^2) as compared to the control sites. The DOH was unaffected when compared to the summer DOH at the control sites. The moderately oiled DBI site had a shallower DOH and reduced standing stock compared to RIG and the control sites. KBP also had a shallow DOH and reduced standing stock, although the reasoning behind this is not yet resolved. At BJ, the most heavily oiled site, not only was the standing stock well below that of the control sites and RIG (400 to 800 specimens/10 cm^2), but the DOH

was several centimeters shallower as well. Brunner et al. (2013) attributed this to a nearly abiotic zone created by heavy contamination by PAHs.

Both BJ cores contained specimens that were highly deformed (Figure 3.11). These deformities occurred at frequencies from 4 to 8%. The deformities observed include reversals in coiling direction, changes in the axis of coiling, misshapen chambers, multiple apertures, and extreme chamber inflation, among other characteristics. None of the deformed specimens observed were stained by rose Bengal, which means that they were dead at the time of collection. It is significant, however, that no grossly deformed specimens (dead or alive) were seen at any other site from this thesis.

Table 3.1. Sediment accumulation rates for all sites. Dashed lines indicate that the profile was not sufficiently resolved for modeling. Uncertainties reported at 1-sigma.

Station	Core Label	$^{210}Pb_{xs}$ Average Accumulation Rate (g cm^{-2} y^{-1})	$^{210}Pb_{xs}$ Average Linear Accumulation Rate (cm y^{-1})	^{137}Cs Average Accumulation Rate (cm y^{-1})
RIG	Low	0.42 ± 0.23	0.58 ± 0.34	--
	Mid	0.31 ± 0.07	0.56 ± 0.12	0.14 ± 0.02
	High	0.30 ± 0.22	0.56 ± 0.33	0.31 ± 0.02
KBP	Low	0.20 ± 0.10	0.27 ± 0.14	--
	Mid	0.58 ± 0.78	0.71 ± 0.85	--
	High	--	--	--
BJ	Low	0.09 ± 0.04	0.28 ± 0.12	--
	Mid	--	--	--
	High	0.18 ± 0.10	0.58 ± 0.37	--

Table 3.2. Mixing depths derived from ^{234}Th profiles. Asterisks indicate minimum depths, as the full profiles were not resolved.

Station	Core Label	Minimum Mixing Depth (cm)
RIG	Low	1.75
	Mid	3.5
	High	4.5
KBP	Low	2.25
	Mid	2.25
	High	3.5
DBI	Low	2.25
	Mid	3.5*
	High	3.5
BJ	Low	4.5
	Mid	3.5*
	High	4.5*

Table 3.3. Standing stock and depth of habitation for all sites. Full dataset available in Brunner et al. (2013).

Station	Standing Stock (live specimens/10 cm^2)	Depth of Habitation (cm)
RIG	6,676	> 10
KBP	157	6
DBI	461	6
BJ (1)	843	3
BJ (2)	406	4

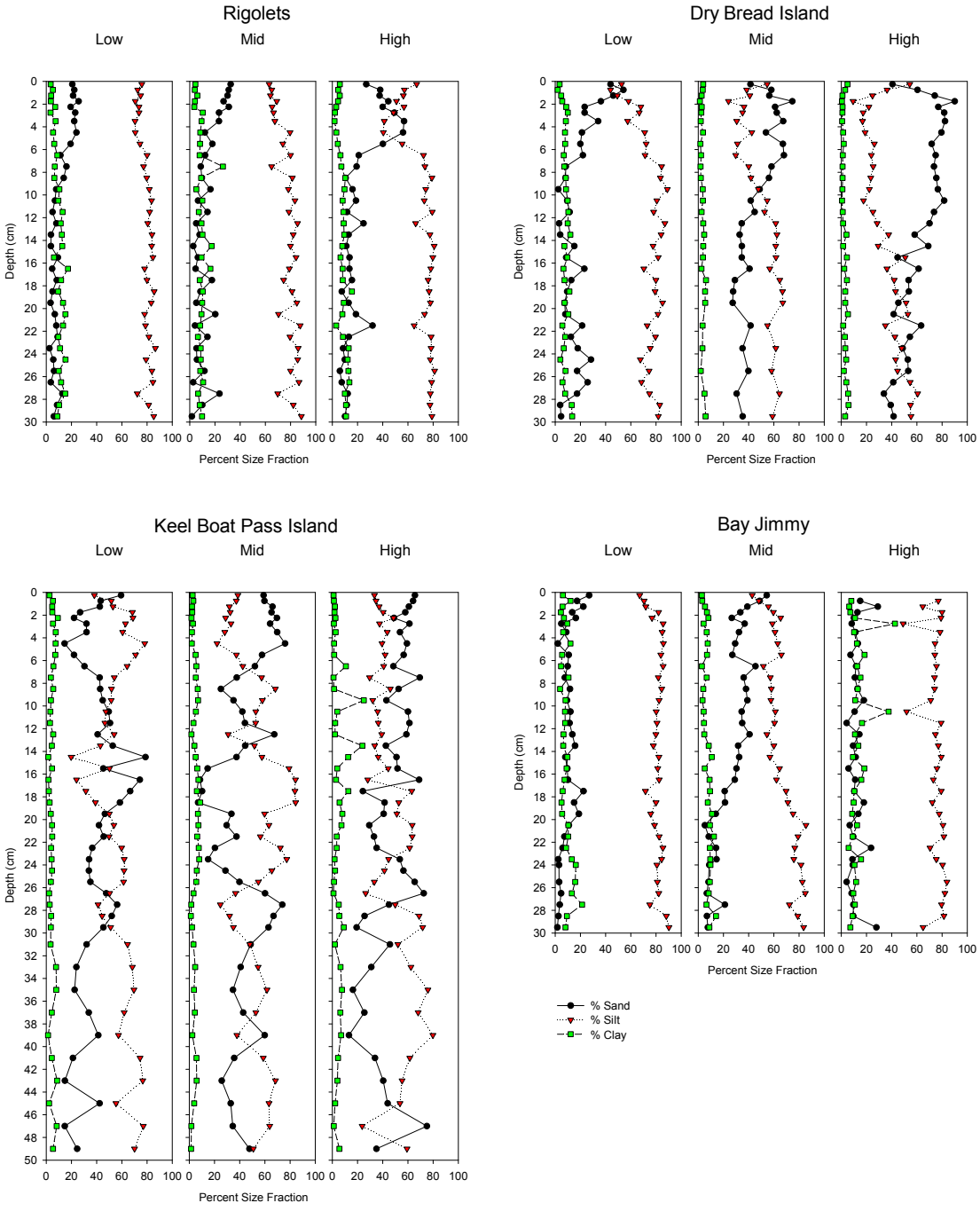

Figure 3.1. Grain size distributions for all sites.

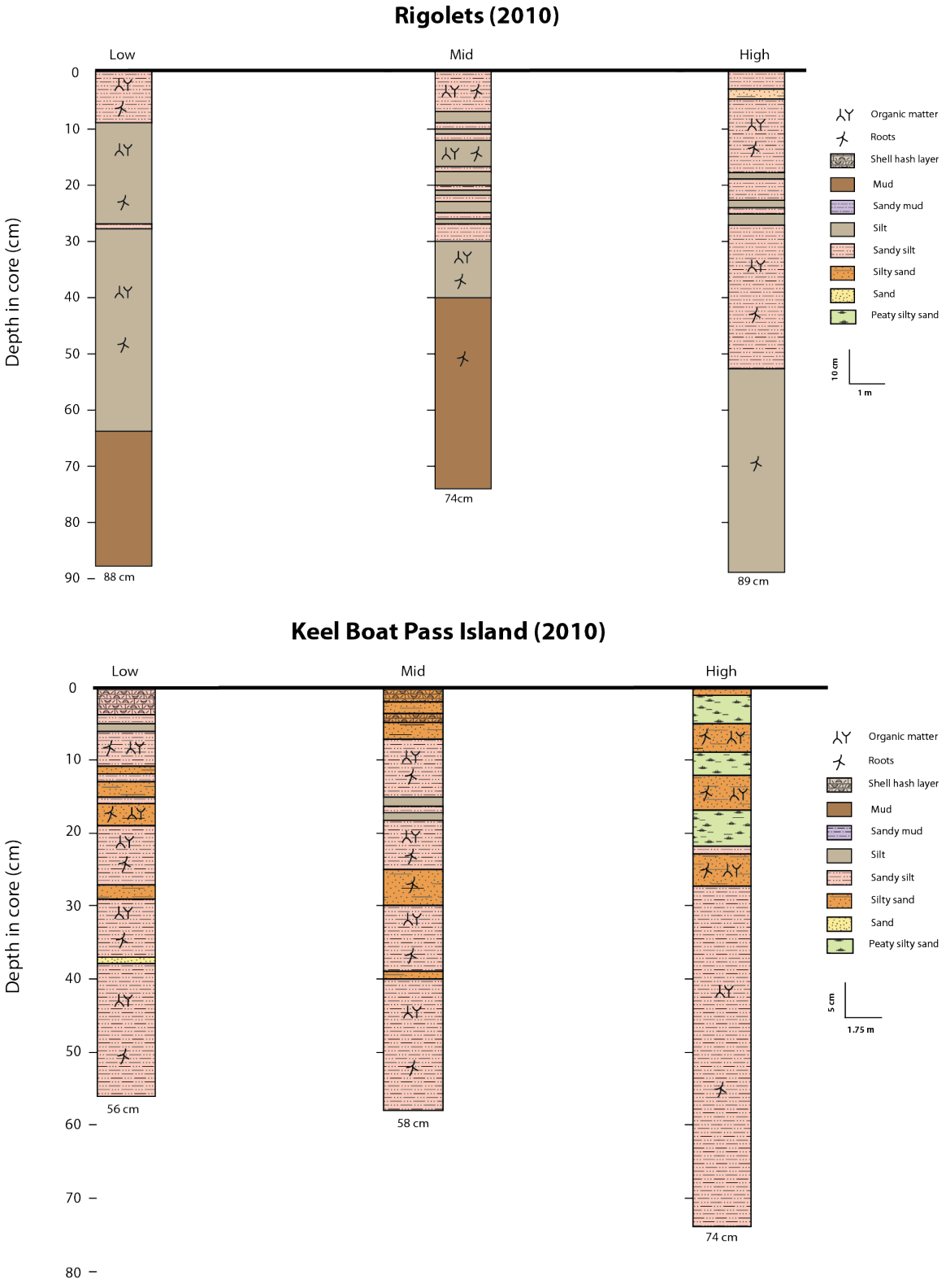

Figure 3.2. Stratigraphic diagrams for RIG and KBP.

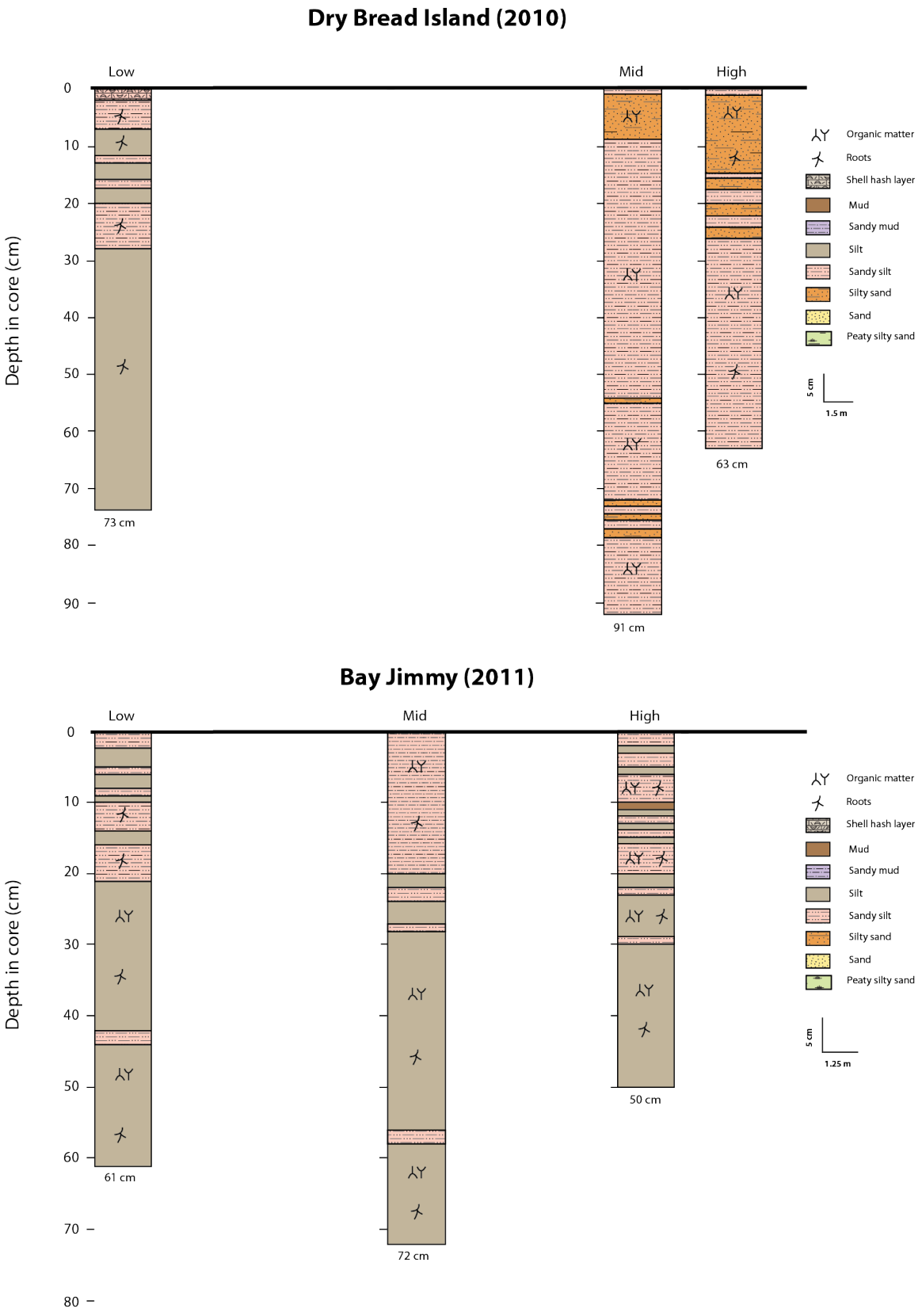

Figure 3.3. Stratigraphic diagrams for DBI and BJ.

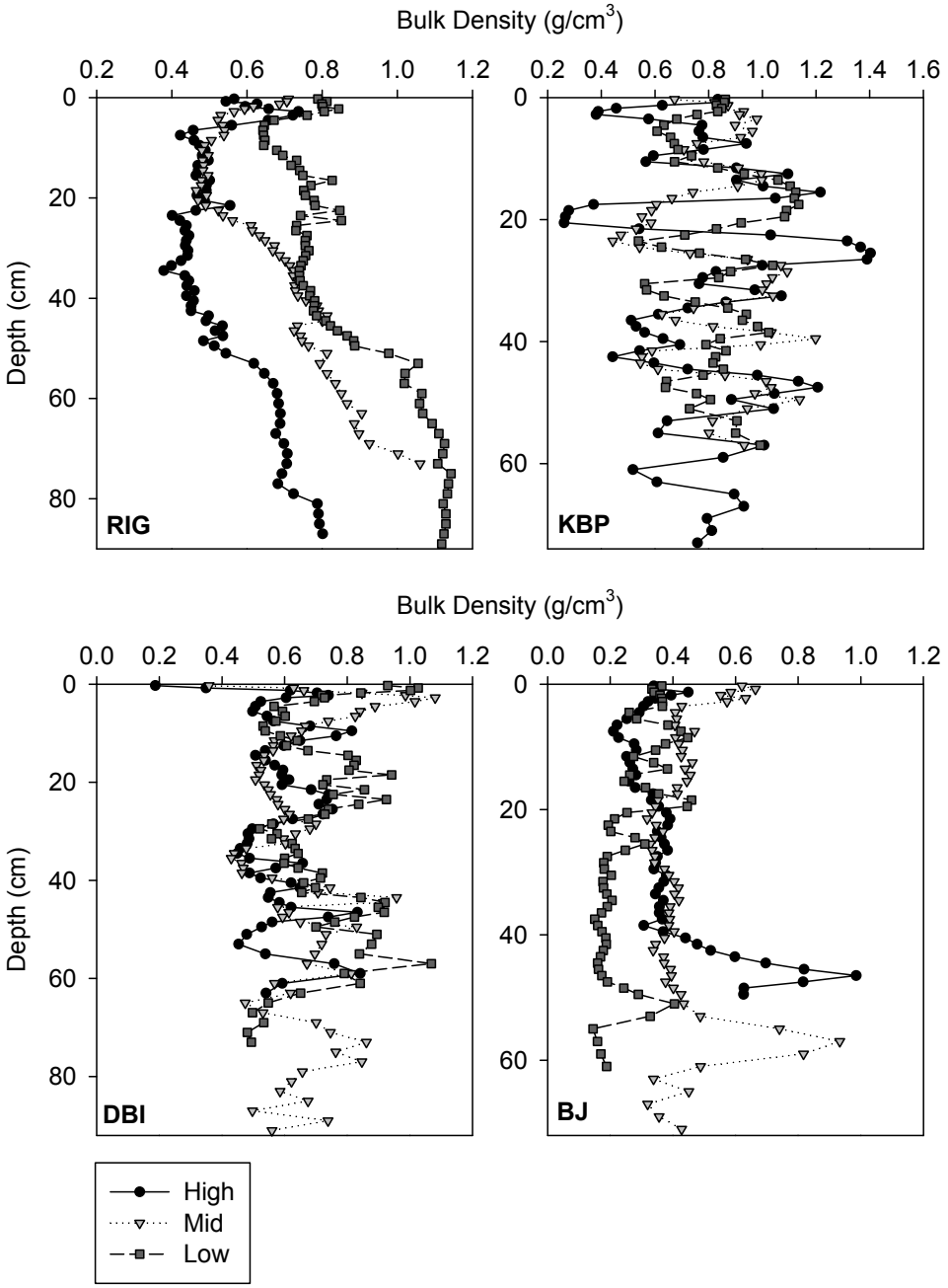

Figure 3.4. Bulk density plots for all sites.

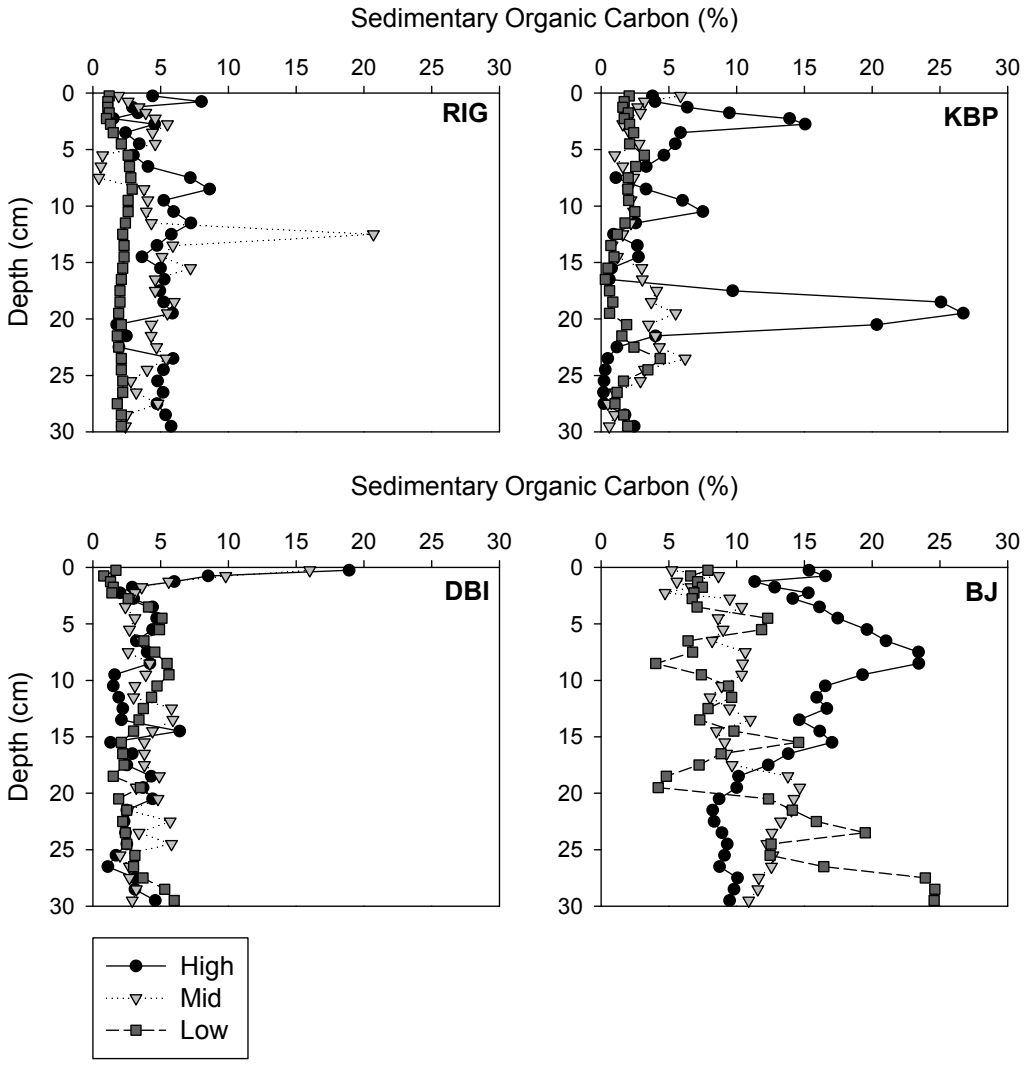

Figure 3.5. Percentages of sedimentary organic carbon (SOC) versus depth for all sites.

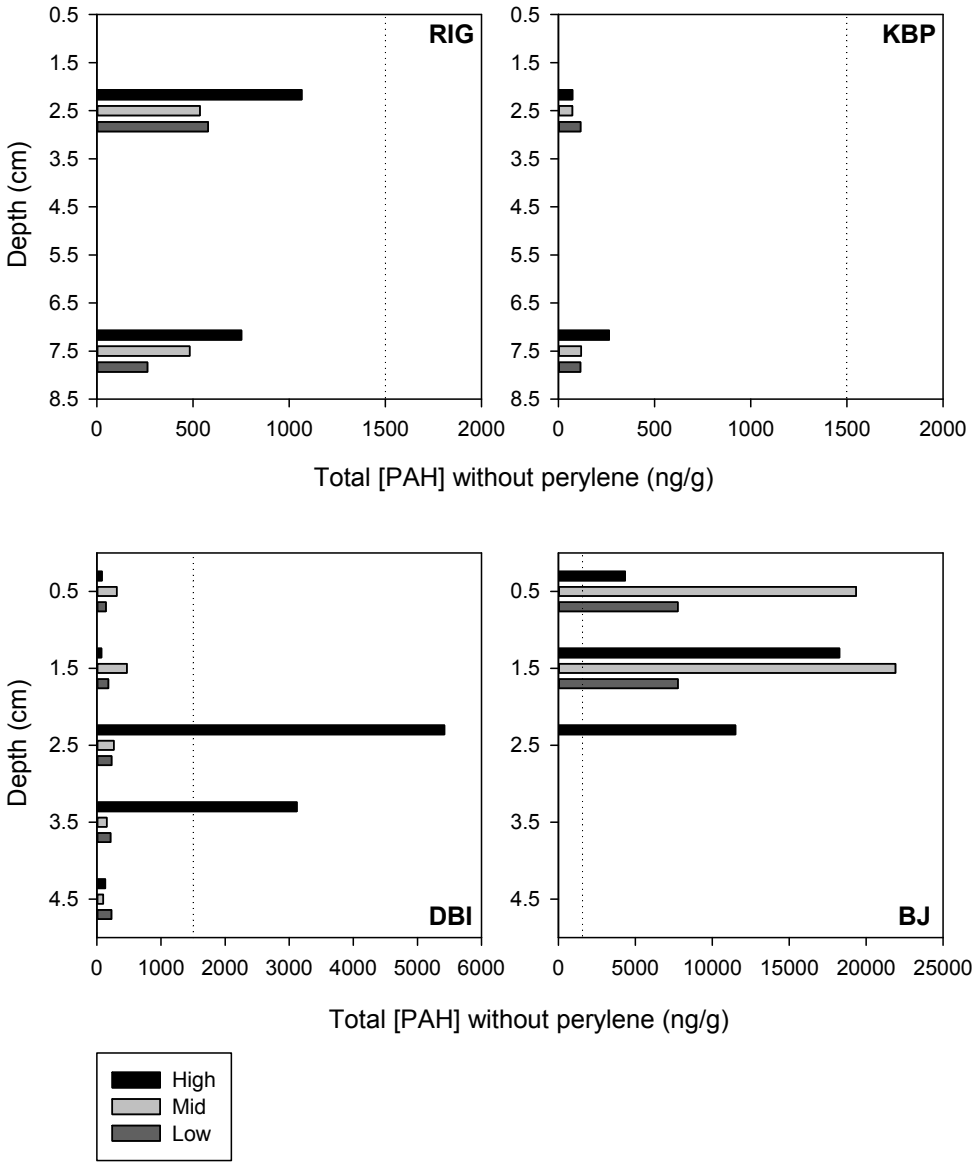

Figure 3.6. Total PAH concentrations (without perylene) for all sites. The dotted line indicates the upper limit background level (1,500 ng g^{-1}).

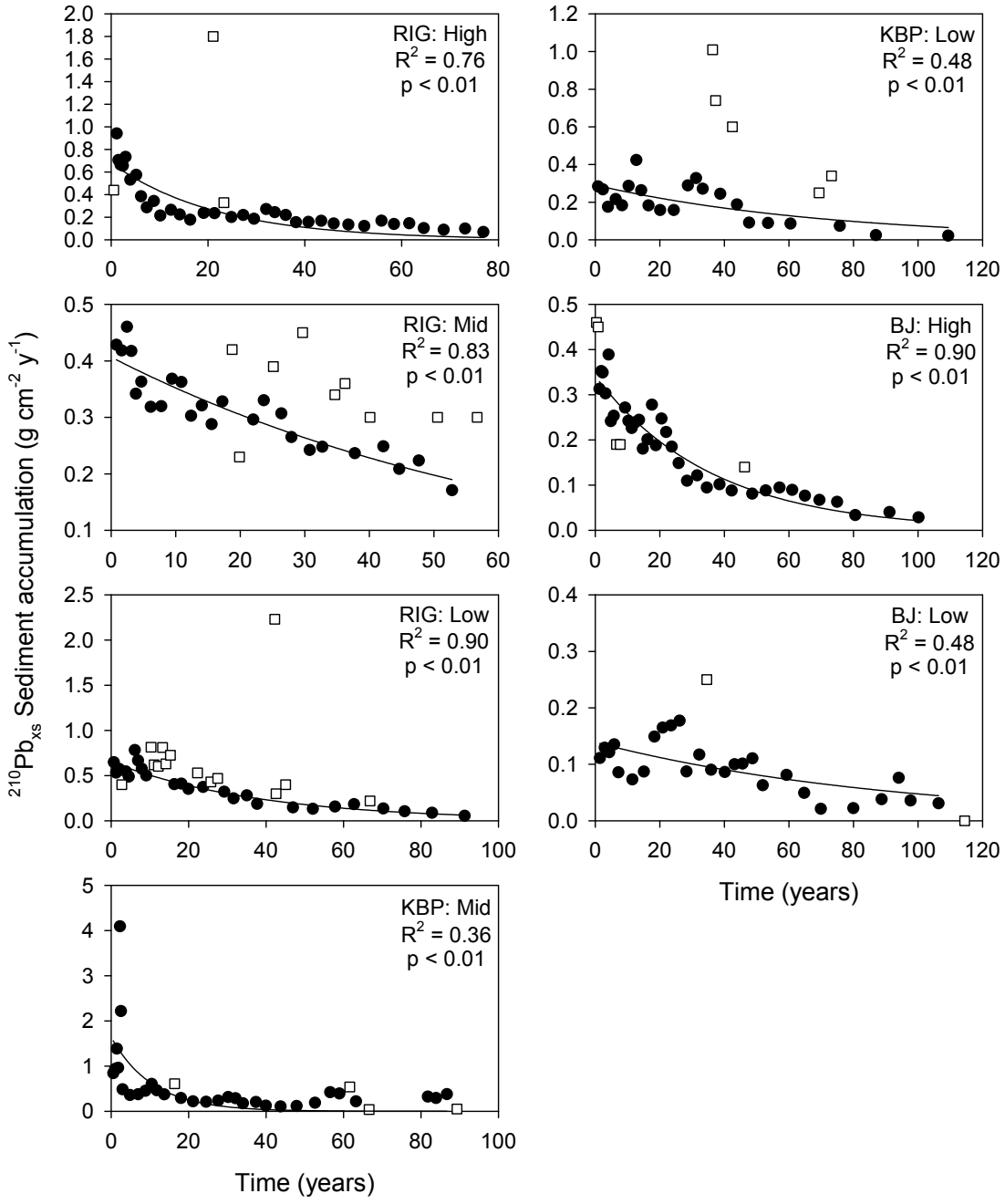

Figure 3.7. $^{210}Pb_{xs}$-based mass accumulation rates over time. All trends are best fit by an exponential regression. In addition, several points that fell well outside the general trend were also excluded based on the concept of nonlocal mixing (e.g., worm burrows). However, all points are plotted on the graph (points excluded from trends are represented by unfilled squares), and all data can be found in Appendix 5.

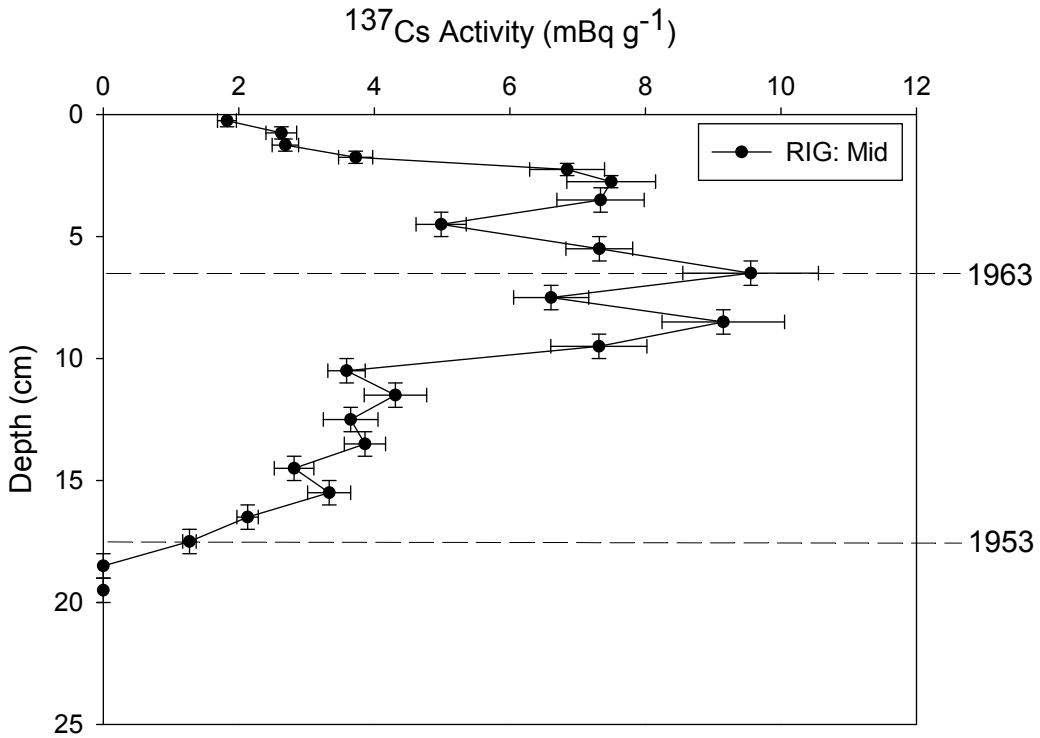

Figure 3.8. ^{137}Cs radionuclide profile for RIG Mid site. The first instance of activity and peak in activity, corresponding to the years 1953 and 1963, respectively, are indicated with dotted lines.

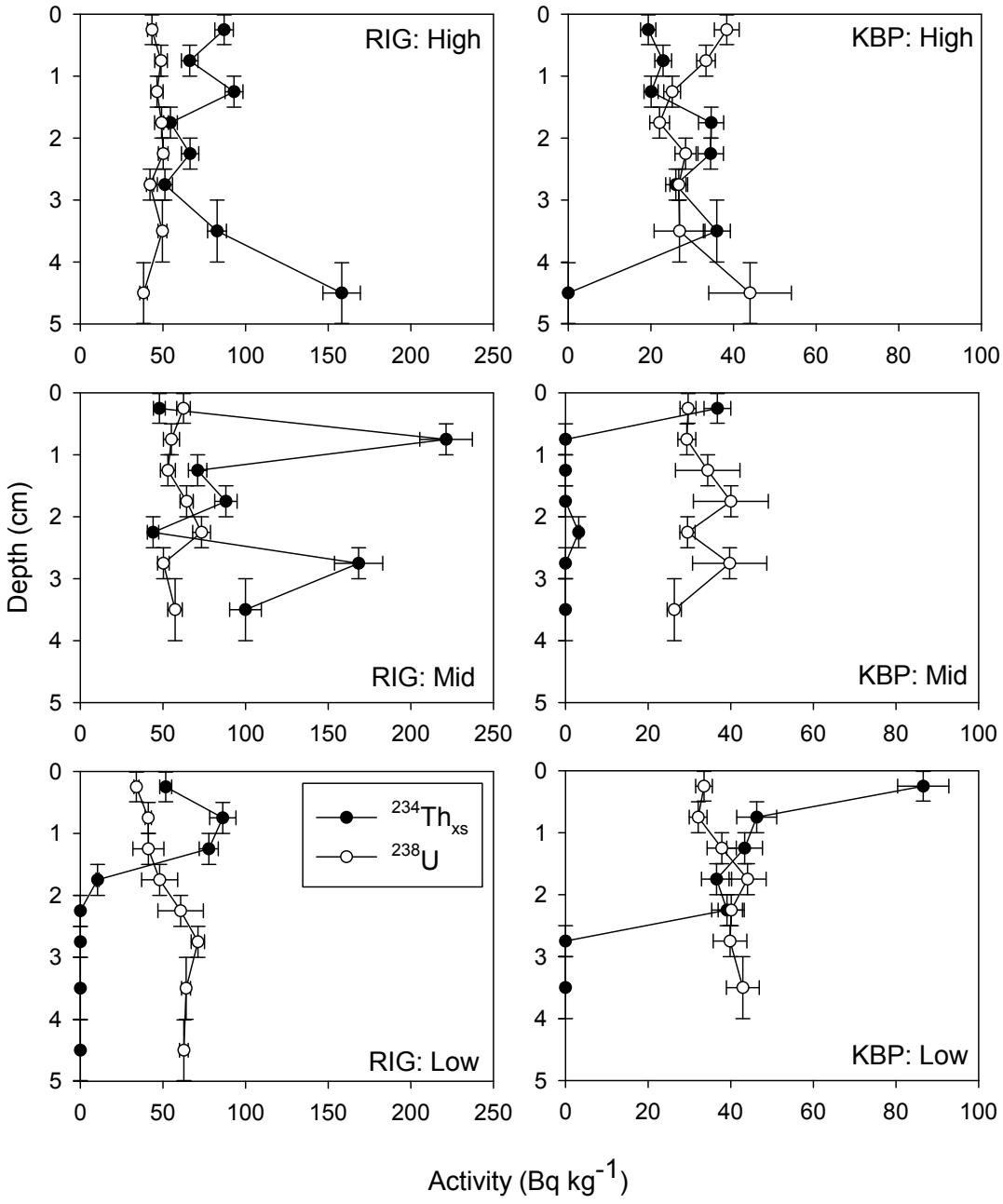

Figure 3.9. $^{234}Th_{xs}$ and ^{238}U activities versus depth for RIG and KBP sites.

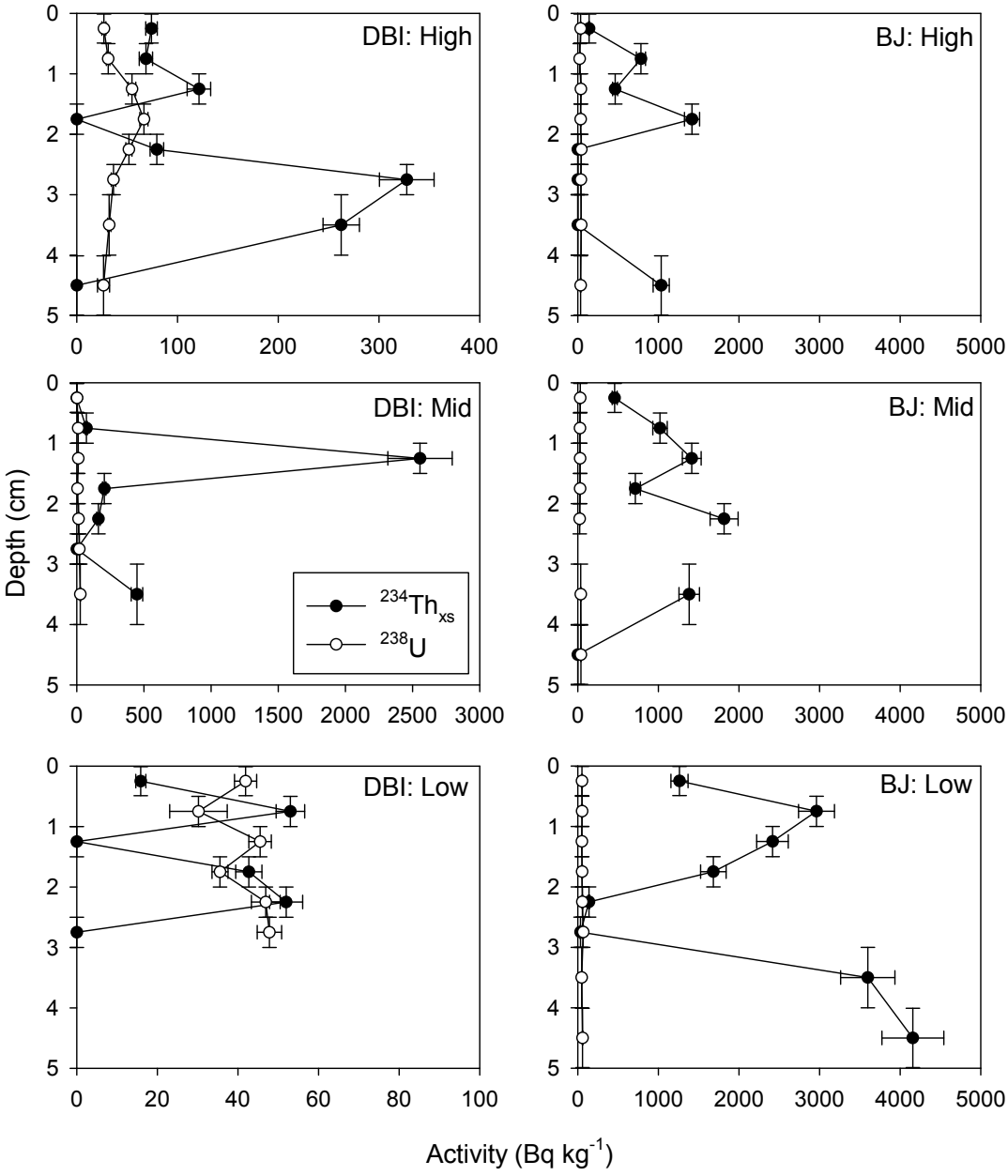

Figure 3.10. $^{234}Th_{xs}$ and ^{238}U activities versus depth for DBI and BJ sites.

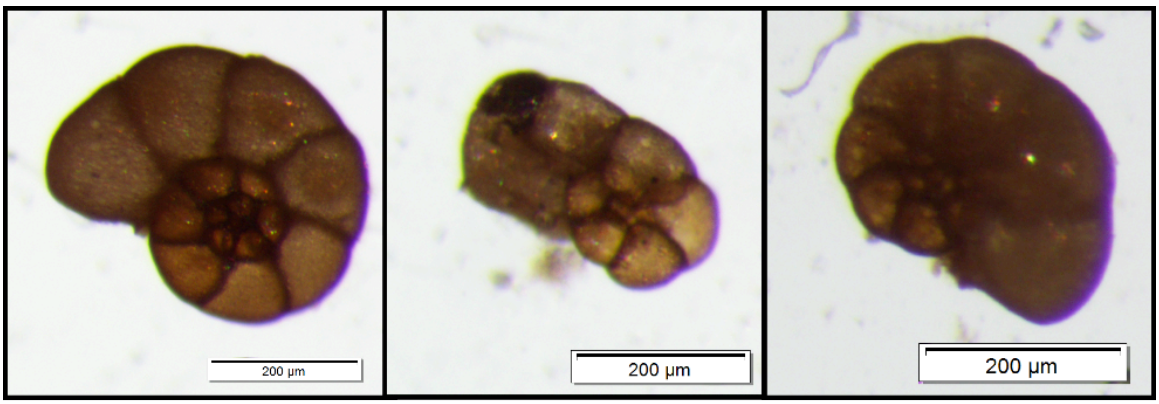

Figure 3.11. Specimens of *Balticammina pseudomacrescens*. Left: normal form; middle: specimen with deformed chambers; right: chamber inflation. All samples were identified and photographed by the author using an Olympus SZX16 microscope.

CHAPTER FOUR: DISCUSSION

4.1 Physical Property Constraints on Oil Deposition

Oil is relatively water insoluble, and thus is subject to sedimentary deposition. Because fine-grained sediments have a highly adsorptive nature, hydrocarbons easily attach to them (Means and McMillin, 1993). This can allow for the concentration of oil in marsh sediments to levels far above that of the originally polluted water column. BJ was dominated by silt with a high clay content, making it susceptible to retaining contaminants in its sediment. Indeed, PAH levels at BJ were quite high, even at the Low site.

4.2 Sedimentary Organic Carbon as an Indicator of Pollution

In addition to fine-grained sediments, hydrocarbons have been shown to be preferentially associated with the organic component of solid phase matrices (Schlautman and Morgan, 1993; Kim et al., 1999). Following the DWH spill, Natter et al. (2012) investigated the degradation of oil in salt marsh sediments and pore waters on the Gulf Coast, including Bay Jimmy and The Rigolets. They demonstrated that very high levels of SOC in marsh sediments were associated with heavily oiled sites following the DWH spill. Other studies, such as Polymenakou et al. (2006) and Burdige (2007), have also concluded that organic carbon should positively correlate with [TPAH] because PAHs are an organic contaminant. However, these studies were conducted in deep ocean environments where sediment accumulation rates are relatively low, as are the depths and intensities of sediment mixing.

It was still expected that with such high [TPAH] at the BJ sites (up to 21,913 ng g^{-1}), the SOC profiles would reflect these peaks at the surface. In fact, this is not evident.

The lack of any obvious trend with depth in most cores revealed these sites were highly mixed. It is important to note here that significant spatial heterogeneity, or "patchiness", of oil was seen at BJ and other sites. Spatial heterogeneity of oil may result from several factors, including bioturbation of sediment by benthic organisms, movement of larger organisms (birds, crabs, etc.) on the marsh surface, or small-scale variations in tidal advancement of water up the marsh interface. When revisited in June 2012, patches of oil were still found on the marsh surface at BJ (Figure 4.1). In addition, the cores used for foraminiferal analyses at BJ support this, as they had different standing stocks. It is therefore plausible that, even though they were intended to be replicates, the core used for hydrocarbon analyses was more heavily oiled than the cores used for sedimentology.

When looking at a salt marsh, though, it is prudent to consider the high amount of ambient terrestrial organic carbon. Terrestrial organic matter is delivered to the marsh via rivers and tidal inundation, or is produced *in situ*, and consists of living biomass, plant litter, and soil organic matter. In this study, anomalously high peaks in the SOC profile most closely corresponded with changes in stratigraphy. Areas with large quantities of roots and decaying plant matter (terrestrial organic matter) revealed peaks in the SOC profile. The correlation between SOC peaks and stratigraphy is most obvious at the KBP High site, where there were defined zones containing peat (Figures 3.2 and 3.5).

While terrestrial organic matter and patchiness may play a role, there is a better way to investigate relationships with SOC than concentration over depth profiles. An inventory-based approach allows for SOC concentrations to be integrated over a common depth. By looking at changes in overall carbon stocks, we can reduce uncertainties due to site-specific differences in biomass. While individual SOC profiles did not correlate with

hydrocarbon levels, SOC inventories demonstrated exponential relationships with TPH and PAH inventories (Table 4.1, Figure 4.2). These relationships were most pronounced at BJ. Since SOC was not part of the original oil, this indicates that either SOC was associated with hydrocarbons during transport or upon deposition in the marsh.

4.3 Source and Weathering of Hydrocarbons

Parent and alkyl-substituted PAHs are excellent forensic tracers due to their thermodynamic stability (Yunker et al., 2002). Because of this stability, it is possible to utilize parent and alkyl homologue PAHs for source characterization. Those PAHs derived from the Macondo oil may be of pyrogenic (combustion) or petrogenic (i.e., petroleum) origin, depending on whether or not they have been burned prior to reaching the marsh. Following an oil spill like this one, one expects to find large quantities of TPH, and low molecular weight (LWM) and alkylated PAHs (Lima et al., 2003; White et al., 2005; Wang et al., 2007). During and after the DWH event, a large amount of oil was burned inefficiently at the sea surface, and so we expected a higher proportion of combustion-derived PAHs contributing to the overall hydrocarbon distribution. This will be discussed later in more depth.

For all molecular ratio analyses, only those samples with [TPAH] above background values were used. To provide a greater sampling distribution, data collected by the Operational Science Advisory Team (OSAT) were plotted as well (NOAA, 2013) (Appendix 7e-f). All OSAT samples included were taken from marsh sediments between September 20 and 22, 2011, and were less than 3 km away from the stations sampled in this thesis. In order to be consistent with the OSAT data, only those ratios from the uppermost 2 cm of sediment collected for this thesis were used. The only samples from

this thesis that had above background PAH values in the uppermost 2 cm were those from BJ.

It was reported by Yunker et al. (2002) that PAHs of molecular masses 178 and 202 are most frequently used as parent PAH source indicators. For mass 178, an anthracene to anthracene plus phenanthrene (An/An+Phen) ratio < 0.10 is usually taken as an indication of petrogenic sources, while a ratio > 0.10 indicates a dominance of pyrogenic sources (Yunker et al., 2002). For mass 202, a fluoranthene to fluoranthene plus pyrene (Fl/Fl+Py) ratio < 0.50 is usually taken as an indication of petrogenic sources, while a ratio > 0.50 indicates a dominance of pyrogenic sources (Yunker et al., 2002). The Macondo-252 well oil sample plots clearly in the zone of petrogenic (petroleum) sourcing based on both ratios (Figure 4.3). Most of the marsh samples plot in the zone of petrogenic sourcing based on Fl/Fl+Py, but in the zone of pyrogenic (combustion) sourcing based on An/An+Phen. Both molecular ratios have been used with great success in many studies, but mass 202 may be more definitive because it has a larger difference in thermodynamic stability between the isomers. PAHs with smaller energy differences, like mass 178, may be less responsive to source identification.

Many studies have also successfully used ratios of C_0 to C_1 alkyl PAH homologues for source characterization (e.g., Gogou et al., 1996; Budzinski et al., 1997). The literature indicates that ratios of C_0/C_0+C_1 for the fluoranthene/pyrene (F/P) series are < 0.50 for petrogenic sources, and > 0.50 for pyrogenic sources. Ratios of C_0/C_0+C_1 for the phenanthrene/anthracene (P/A) series are similar, but more variable. Low C_0/C_0+C_1 P/A ratios (less than ~ 0.40) generally indicate petrogenic sources, but many of the ratios from pyrogenic sources are also < 0.40 (Yunker et al., 2002). From Figures 4.4, 4.5, and

4.6, it can clearly be seen that the Macondo Oil plots firmly within the petrogenic source area. In addition to all of the OSAT data points, many of the BJ samples from this thesis plot within the petrogenic source zone as well.

Unsurprisingly, however, the preceding plots do show that PAH ratios indicate mixed sources. PAHs in the northern GOMx are derived from a variety of sources, including Macondo well oil, natural oil seeps, the burning of fossil fuels, atmospheric transport, and other oil spills. Several processes may have modified these PAH assemblages, confounding the initial interpretation as to the sources of the PAHs. These processes include burning of oil slicks, biodegradation, phase partitioning, and physical transport. It is known that extensive burning took place at the sea surface during efforts to stop the flow of oil from the well to the shore. *In situ* burning of oil is utilized to remove fairly fresh oil before it emulsifies. The burning process generally consumes the majority of the oil, but it does leave a viscous and dense residue behind, and also generates considerable quantities of particulate matter (including pyrogenic PAHs) which can then either sink to the sea floor, be transported in the water column, or be atmospherically transported and deposited elsewhere (Brock et al., 2011) (Figure 4.7). The National Incident Command's Flow Rate Technical Group estimated that 5% (245,000 barrels, or 1.03 million gallons) of the oil released during the spill was burned during response efforts (Federal Interagency Solutions Group, 2010). More specifically, it has been verified that at least 409 controlled burns occurred between late April and mid July, 2010, with up to 26 burns taking place in one day (Allen, et al., 2011). Allen et al. (2011) estimated the total volume of oil burned at sea to be between 220,400 and 310,300 barrels (9.3 to 13.0 million gallons). These burns were typically carried out within 15

miles of the DWH spill source. From a review of the Navy Operational Global Atmospheric Prediction System (NOGAPS) data set, Hénaff et al. (2012) showed that the prevailing wind direction in the GOMx from April to July 2010 was generally northward from the Gulf. With so many burns occurring during this period, it is entirely possible that some quantity of combusted PAHs would be transported as aerosols and deposited along the coastline.

The burning of oil at the sea surface is certainly one cause as to why some homologue signatures are skewed toward the pyrogenic source zone, but weathering is definitely a contributing factor as well. It is well known that some PAHs react faster than others in chemical processes such as photodegradation (Federal Interagency Solutions Group, 2010). Therefore, it is unsurprising that PAH ratios in these samples would depart from those seen in the source oil.

One way to assess the importance of weathering is to examine a double-ratio plot for the PAHs C2-phenanthrenes/C2-chrysenes versus C3-phenanthrenes/C3-chrysenes (e.g., Sauer et al., 1998). Chrysenes tend to weather more slowly than phenanthrenes, so as the oil weathers these ratios become smaller (Wang and Fingas, 2003). Samples from this project and others follow a general linear trend of weathering with distance and time from the well (Figure 4.8). The Macondo oil has the highest ratios, followed by deep-water sediment samples collected in 2010 (Appendix 7c-d). Samples collected in 2011 from Bay Jimmy generally have the lowest ratios, indicating that they have been heavily weathered compared to the source oil. Surface sediment samples from the other marsh sites with comparatively lower [TPAH] did not even register both of these compounds.

Alkanes have also been used to evaluate the source and weathering of oils. The carbon preference index (CPI) of a sample is the weighted ratio of odd to even long-chain n-alkanes, and was calculated using the following equation (Bray and Evans, 1961):

$$CPI = 0.5[(\Sigma(C_{25} - C_{33})_{odd} / \Sigma(C_{24} - C_{32})_{even}) + (\Sigma(C_{25} - C_{33})_{odd} / \Sigma(C_{26} - C_{34})_{even})]$$

The n-alkanes in crude oil usually have an even distribution of odd and even carbon numbers (CPI = 1). In contrast, in plant waxes, odd-chain n-alkanes generally have a CPI greater than 4 (and up to 10) times more abundant than even-chain n-alkanes (Hong et al., 1995). Where there is a mixture of high terrigenous inputs as well as fossil fuels, it can be expected that the CPI will be slightly elevated. In this study, Macondo-252 oil had the expected CPI of 1, and all sampled locations have a CPI below 4, consistent with the incorporation of oil (Table 4.2).

The unresolved complex mixture (UCM) is the portion of petroleum hydrocarbons that cannot be resolved by gas chromatography. Because the molecules that make up the UCM are structurally complex, they are resistant to biological degradation (Hong et al., 1995). The accumulation of high concentrations of the UCM fraction in sediments provides evidence for long-term petroleum contamination (Reddy et al., 2002). Excluding the KBP High site at which no UCM was detected, UCM concentrations ranged from 9.88 to 4219.7 $\mu g\ g^{-1}$, which accounted for 45 to 97% of the non-aromatic hydrocarbons (Table 4.2). The relative importance of the UCM can be determined by expressing the ratio of unresolved to resolved compounds (U/R). U/R ratios of greater than 4 indicate petroleum contamination (Mazurek and Simoneit, 1984). At the Mid and High sites of BJ, the U/R reached values greater than 30 (Table 4.2). In addition, the isoprenoid hydrocarbons phytane and pristane are not primary constituents

of terrestrial biota (Simoneit et al., 1980). Their persistent presence in BJ Mid and High hydrocarbon fractions, combined with high U/R values, indicates petroleum contamination.

LMW n-alkanes ($C_{16} - C_{26}$) have short chains and are preferentially lost in microbial degradation, evaporation, and dissolution (Wang et al., 1995a; Wang et al., 1995b). The loss of LMW n-alkanes (Figure 4.9), combined with CPIs below 4 and high amounts of UCM, confirms that oil was degraded before being deposited in the marshes, and further indicates that the oil residues found at BJ are the least degraded of the collected samples. This may simply be due to the magnitude of oiling at this site.

4.4 Sensitivity of Radioisotope Tracers

It was anticipated at the outset of this project that the intense physical and biological mixing, coupled with erosion, might hinder the resolution and interpretation of the radioisotope data. Indeed, this was the case; vertical mixing rendered nearly all of the ^{137}Cs and some of the ^{210}Pb data (discussed later) inconclusive.

Beryllium-7 was particularly troubling. The constant fallout radionuclide ^{7}Be was measured to determine short-term sediment mixing depths. Where ^{7}Be was detected, it was confined to the near surface (0-2.75 cm). This suggests there was little mixing in the short-term memory of ^{7}Be (< 1 year). However, in most cases, there was a conspicuous absence of ^{7}Be. This is most likely due to one of three scenarios. First, sediment composition at some sites likely constrained ^{7}Be sorption. Beryllium-7 does not have an affinity for coarse-grained sediment or organic matter (Bloom and Crecelius, 1983). All sites were characterized by large quantities of macro-organic matter, and the Chandeleur sites were quite sandy. Second, it is well documented that many Louisiana marshes along

the GOMx are rapidly retreating. Therefore, the absence of ^{7}Be could be due to rapid erosion of the marsh surface. A third option is related to the cleanup of marshes following the DWH spill. In addition to the water flushing methods mentioned earlier, raking, skimming, and even vacuuming (Figure 4.10) were all approved, and utilized methods of removing oil from the marsh surface. Any one of these methods has the potential to remove sediment or scour the marsh surface. In particular, the vacuuming was controversial, with reports of effectiveness ranging from "large volumes of recovered oil" to simply "removal of marsh sediments and gouging of the marsh substrate" (Zengel and Michel, 2013). BJ was subjected to both flushing and vacuuming during cleanup activities. While there are no confirmed reports of flushing or vacuuming at KBP or DBI, these methods were approved for the two islands and may have taken place (Zengel and Michel, 2013).

It is also possible that a combination of these factors may have led to the absence and/or shallow penetration depth of ^{7}Be in near surface sediments. Unfortunately, there are too many factors complicating interpretation, and the question of the missing ^{7}Be remains unresolved.

It may have been beneficial to assess sediment accumulation rates by using additional short-term dating techniques (i.e., feldspar or glitter marker horizons, pollen analysis, rod sediment elevation tables (RSETs)). However, in addition to the fact that marker horizons or RSETs would need to have been in place prior to the unexpected DWH spill to be useful, mixing may still have been problematic.

It was originally anticipated that a bioturbation coefficient would be calculated from $^{234}Th_{xs}$. However, the ^{210}Pb profiles revealed such a large amount of physical

mixing that it was not prudent to attempt to assign a certain amount of that mixing as biological. Regardless, $^{234}Th_{xs}$ allowed for the determination of minimum mixing depths. At many stations, $^{234}Th_{xs}$ was still present in the deepest samples counted.

As expected, there does not appear to be any correlation between the $^{234}Th_{xs}$ mixing depths and DOH for foraminifera, as foraminifera are not major bioturbators. However, the DOH does indirectly indicate how deeply the sediment is bioturbated. Macrofauna, such as polychaetes and oligochaetes, constantly rework sediments as they burrow into them. It has been suggested by many that the bioirrigation and sediment oxidation capacity of macrofauna has a large impact on the vertical distribution of foraminifera (e.g., Goldstein et al., 1995; Jorissen et al., 1995; Gross, 2000; Bouchet et al., 2009). If this is the case, then it can be assumed that the DOH can also be interpreted as a minimum bioturbation depth for macrofauna.

4.5 Implications of Sediment Mixing on Hydrocarbon Transport and Fate

As indicated in section 1.4, the barge *Florida* ran aground in Buzzards Bay, Massachusetts in September, 1969, spilling 700,000 L of No. 2 fuel oil (Reddy et al., 2002; Peacock et al., 2005). Despite the use of oil booms, both subtidal and intertidal areas of nearby marshes were heavily contaminated with oil. Unoiled sediments accreted at a rate of 0.35 cm yr^{-1} now overlay sediments oiled during the spill (White et al., 2005). Nearly forty years later, researchers found that a substantial residue of the oil was still present 8-20 cm below the surface (Reddy et al., 2002; Peacock et al., 2005). While most of the volatile and water-soluble compounds have been removed, concentrations of PAHs remain nearly identical to those measured several years after the spill (Reddy et al., 2002;

Peacock et al., 2005). This suggests that PAHs may persist indefinitely in the sediment record at the Buzzards Bay marsh.

Given short-term mixing depths of 4.5 cm or deeper, it is plausible that oil delivered to GOMx marshes could be mixed deeply into the sediment substrate. High [TPAH] from 3-4 cm at the DBI High site and very high [TPAH] from 2-3 cm at the BJ High site shows that oil has effectively been mixed into sediments. Sediment accumulation rates of up to 0.55 g cm^{-2} y^{-1} (0.71 cm yr^{-1}) suggest that PAHs mixed into the substrate could be quickly buried. Once PAHs are buried in the sediment profile, it becomes very difficult for them to be further broken down. Bauer and Capone (1985) demonstrated that microbes in intertidal sediments rapidly degrade anthracenes and naphthalene in oxic environments. While oxygen is much less available once PAHs are buried, macrofaunal bioturbation, physical mixing and benthic photosynthesis periodically oxidize sediments. It is obvious from $^{234}Th_{xs}$ profiles that the sediments in Louisiana salt marshes are well mixed, and this may lend a hand to remediating buried oil.

4.6 Lead-210 Sediment Accumulation Rates and Implications for Survival of Marshes

Due to vertical mixing in the sediment column, many of the cores were unsuitable for CRS modeling. However, all of the RIG and KBP cores that were modeled showed an increase in sediment accumulation over approximately the last decade prior to sampling in 2010. On August 29, 2005, Hurricane Katrina made landfall in Louisiana and Mississippi as a category 3 hurricane with sustained winds of 125 mph (NOAA, 2005a). Less than one month later, Hurricane Rita, the most intense cyclone ever

recorded in the Gulf of Mexico, passed close by Louisiana with wind gusts of 180 mph (NOAA, 2005b). Turner et al. (2006) found that these two storms resulted in more than 131,106 metric tons of inorganic sediments accumulating in Louisianan coastal wetlands. It is important to note, however, that even where Hurricanes Katrina and Rita increased average sedimentation rates, there is no measurement of how much sediment was first scoured from marsh surfaces, and $^{210}Pb_{xs}$-based accumulation rates do not take into account sediment that is removed. At KBP, it is obvious from satellite images that significant erosion took place following the hurricanes (Figure 4.11). This point is further exhibited in the $^{210}Pb_{xs}$ inventories. Based on Appleby and Oldfield (1992), the expected fallout inventory for southern North America is 495 mBq cm^{-2}. Inventories are far less than this at four of the six sites modeled, meaning that they are in a net erosional state. Cesium-137 inventories too are below the expected value (98 mBq cm^{-2}) at all sites.

Both the emergence and continued survival of tidal salt marshes are related to the rate of relative sea level (RSL) rise (Mudd, 2011). One component of RSL change is land subsidence, such as that occurring in the Mississippi River delta. Shinkle and Dokka (2004) performed a geodetic survey with first-order leveling data based on U.S. National Geodetic Survey benchmarks, and found that large sections of the Mississippi River delta were subsiding at rates of 10-15 mm yr^{-1}. Several recent studies have attributed the rapid subsidence of marsh surfaces in the Gulf of Mexico to compaction of sediments and down-warping of the underlying crust (Meckel et al., 2006; Nicholls et al., 2007; Törnqvist et al., 2008).

There are several mechanisms that cause changes in eustatic sea level through geologic time, but the effects of global warming have resulted in a more rapid sea level rise in the last century (IPCC, 2007). Penland and Ramsey (1990) analyzed National Ocean Survey and U.S. Army Corps of Engineers tidal gauge databases along the Gulf Coast, and found that Louisiana is experiencing higher rates of RSL rise than any other Gulf Coast state (maxima of 1.04 and 1.19 $cm\ yr^{-1}$). Considering that the average sediment accumulation rates measured in this thesis are likely elevated over the short-term by the effects of Hurricanes Katrina and Rita, and considering current subsidence rates in the Mississippi River delta, the rate at which RSL is rising in Louisiana well exceeds sediment accumulation in these marshes.

Where Louisiana salt marshes were once naturally sustained by inputs of inorganic mineral matter from the Mississippi River, controlled modifications to the hydrology of the river have diminished this sediment supply. Now, marshes that would have helped to buffer the Louisiana coastline against sea-level rise are becoming more dependent on below-ground plant productivity to sustain marsh surface elevation (Langley et al., 2009). Unfortunately, the DWH spill exacerbated this problem by devastating plant communities in heavily-oiled areas. Lin and Mendelssohn (2012) investigated the effects of DWH oiling on *Spartina alterniflora* and *Juncus roemerianus*, two of the species common in the marshes studied in this thesis. At moderately oiled sites, *Juncus roemerianus* showed reduced above-ground biomass and shoot density, while *Spartina alterniflora* appeared to be unaffected. Heavy oiling in Barataria Bay (including Bay Jimmy) resulted in nearly complete mortality of both species. Given the concerns with rising sea level along the GOMx coast, this is particularly troubling.

Should these marshes experience long-term submergence, erosion will likely remobilize and redistribute buried PAHs back into GOMx waters.

Additionally, edge erosion of the marsh platform has the potential for remobilizing PAHs. Wilson and Allison (2008) analyzed transects of marsh and adjacent bay sediments in areas of Louisiana where the subaerial marsh platform had disappeared over the last ~80 years. The vibracores taken in Barataria Bay revealed an obvious ravinement surface at the marsh edge. They found that, on average, 1.5 m^3 of sediment per m shore-length is eroded from Barataria Bay marshes every year. They also determined that, while subsidence plays a role in the loss of elevation of a marsh, wave erosion caused 48 to 75% of that loss at Barataria Bay. This illustrates another way that PAHs may be released back into the aqueous environment.

4.7 Effects to Benthos (Meiofauna) Represented by Foraminifera

There are five PAH compounds listed by the U.S. Department of Health and Human Services as being carcinogenic to animals (benz(a)anthracene, benzo(b)fluoranthene, benzo(a)pyrene, dibenz(a,h)anthracene, and ideno(1,2,3-c,d)pyrene). Table 4.3 shows the percentage of these compounds over the [TPAH] for the four most polluted sites. While BJ is 11% and below, these compounds comprise up to 32% of the oil residues at DBI. This is an important factor when considering the possible impacts to the benthos, and ecosystem in general.

Brunner et al. (2013) suggested that the highly elevated standing stock at RIG could be attributed to a hypertrophic zone created by the small amount of oiling. In contrast, the shallow DOH and reduced standing stock at BJ and DBI are consistent with ill effects caused by oil pollution (Alve, 1995; Martinez-Colon, 2008). However, the

shallow DOH and low standing stock at KBP remain unexplained. Brunner et al. (2013) note that it (and DBI) had a distinctly different sedimentological environment than all other sites (carbonate-rich and sandy versus organic-rich and silty). This difference in lithology at KBP may be the cause for the low density and shallow DOH of foraminifera at this site. Another factor could be that the site is a rookery, and rookeries are known for eutrophication from bird excrement (Ellis et al., 2006).

Perhaps a more dramatic indication of severe ecological effects is demonstrated by foraminiferal deformities. Alve (1995) indicated that heavy exposure to pollution could manifest as test abnormalities in foraminifera. As discussed in Chapter One, rapid changes in variables such as temperature, pH, salinity, and turbidity can also induce deformities in foraminifera. River diversions in the summer of 2010 did cause reductions to salinity. However, the only site that showed deformities was BJ, while KBP and DBI were also subjected to reduced salinities. In addition, BJ was sampled in June 2011, nearly a year after salinities had returned to normal. While it is true that none of the deformed specimens found in the BJ cores were alive at the time of sampling, it seems that if the culprit was salinity, the Chandeleur sites would have been affected as well. Brunner et al. (2013) thus cautiously attributed the deformities to effects of the DWH spill.

Table 4.1. Inventories for ^{7}Be, ^{137}Cs, $^{210}Pb_{xs}$, and SOC. Inventories for radionuclides are provided in mBq cm^{-2} and inventories for SOC are given in mg cm^{-2}. The expected $^{210}Pb_{xs}$ inventory from atmospheric deposition alone is 495 mBq cm^{-2} based on southern North America (Appleby and Oldfield, 1992). The expected ^{137}Cs inventory from atmospheric deposition alone is 98 mBq cm^{-2} based on average coastal Louisiana (Milan et al., 1995).

Station	Core Label	^{7}Be	^{137}Cs	$^{210}Pb_{xs}$	SOC
RIG	Low	0	0	325.17	461.020
	Mid	1.71	47.23	332.26	708.769
	High	14.20	38.35	566.61	692.092
KBP	Low	0	--	174.24	405.374
	Mid	0	--	386.87	545.313
	High	19.17	0	--	797.468
DBI	Low	0	0	--	677.737
	Mid	0	9.69	--	738.747
	High	0	0	--	571.023
BJ	Low	0	--	101.00	916.119
	Mid	0	--	--	1261.842
	High	0	--	652.61	1246.922

Table 4.2. Petroleum hydrocarbon data for all stations. All values are averages over the top 5 cm of sediment. TPH = total petroleum hydrocarbons; UCM = unresolved complex mixture; U/R = ratio of unresolved to resolved compounds; CPI = carbon preference index.

Station	Core Label	TPH	UCM	U/R	CPI
RIG	Low	38.94	29.04	2.93	2.1
	Mid	111.23	65.29	1.42	3.4
	High	63.54	44.01	2.25	2.1
KBP	Low	47.65	30.58	1.79	1.0
	Mid	22.20	9.88	0.80	1.9
	High	19.19	0	0	2.8
DBI	Low	78.32	37.07	0.95	1.1
	Mid	464.15	346.44	2.81	0.9
	High	68.32	40.32	1.40	2.5
BJ	Low	333.85	292.06	6.97	3.0
	Mid	3806.51	3,689.33	31.36	2.0
	High	4351.80	4,219.70	30.45	2.6

Table 4.3. Percentages of known PAH compound carcinogens composing [TPAH] in oil residues. Only those samples with [TPAH] above background level are shown.

Station	Core Label	Depth (cm)	[TPAH] w/o perylene (ng/g)	% of known carcinogens
DBI	High	2 - 3	5,420.30	28%
	High	3 - 4	3,118.2	32%
BJ	High	0 - 1	4,345.48	11%
	High	1 - 2	18,279.4	1.7%
	High	2 - 3	11,510.8	1.7%
	Mid	0 - 1	19,356.2	0.65%
	Mid	1 - 2	21,913.3	0.54%
	Low	0 - 1	7,768.2	0.46%
	Low	1 - 2	7,774.6	0.34%

Figure 4.1. Photograph of oil patch at Bay Jimmy in June, 2012.

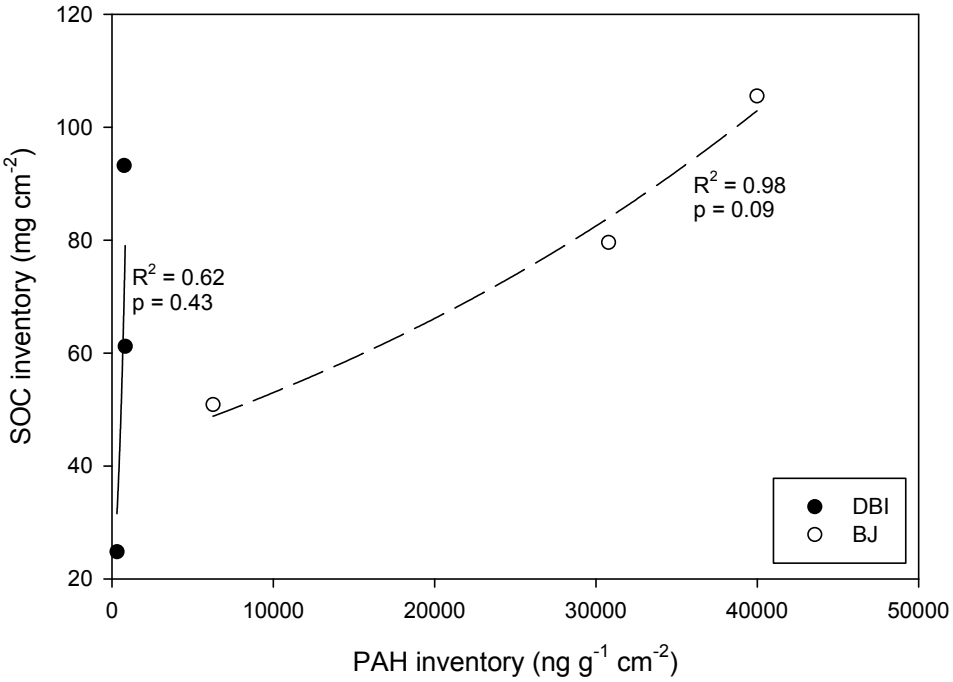

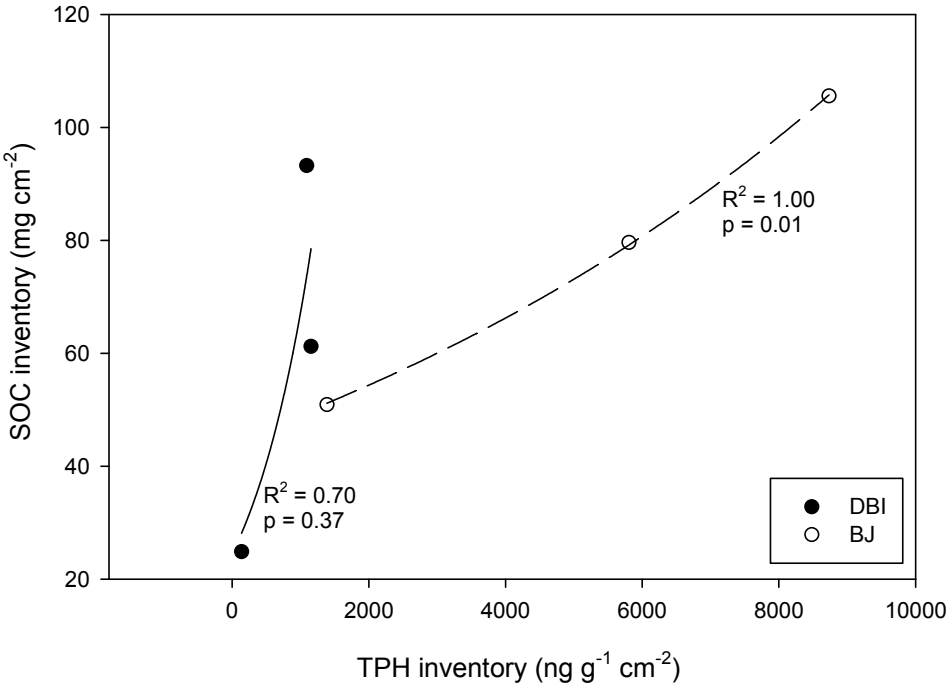

Figure 4.2. Plots of SOC inventories versus PAH and TPH inventories. All inventories were calculated over the uppermost 2 cm of sediment for each core. Because the sampling intervals at the lightly oiled sites (RIG and KBP) were bulked from 0 to 5 cm, it was not possible to explore PAH and TPH inventories at these sites.

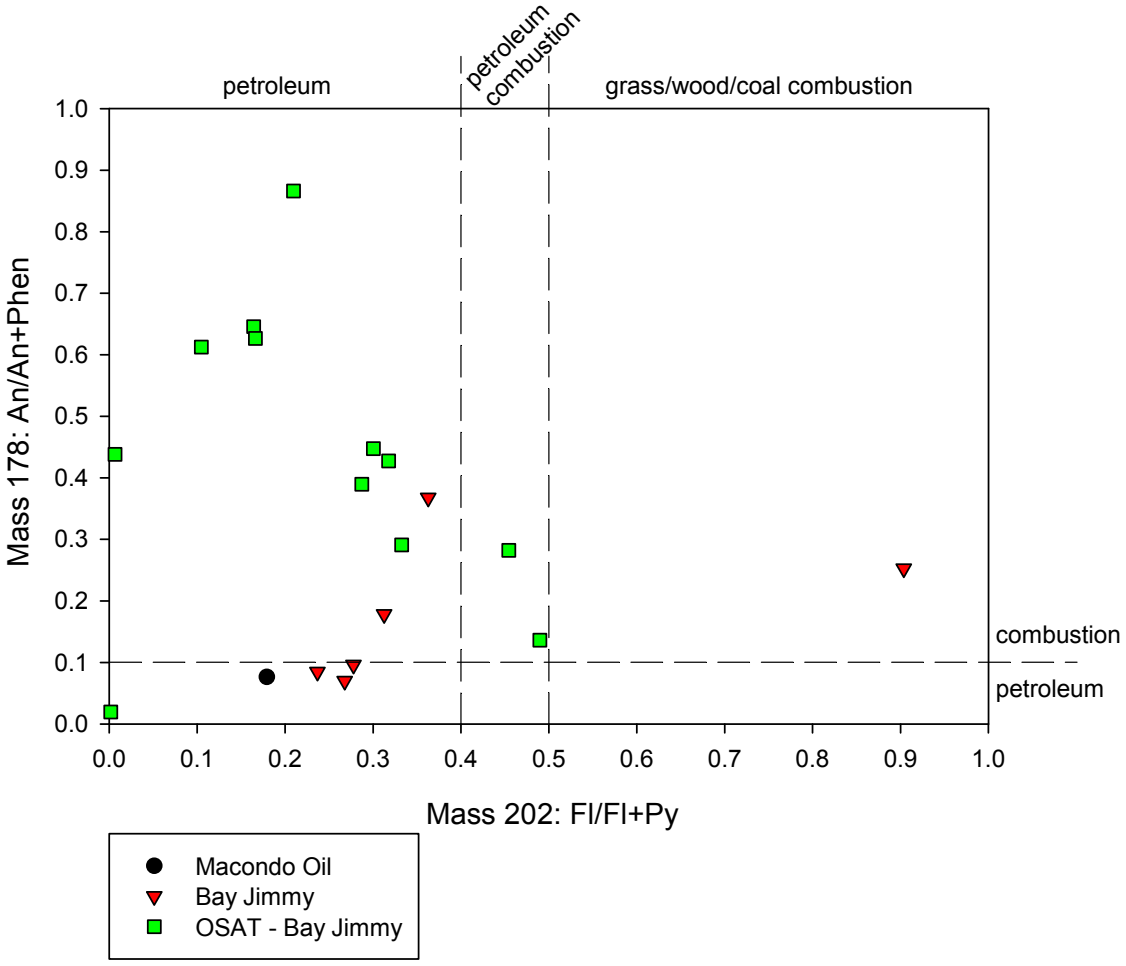

Figure 4.3. PAH compound cross plot for the ratios of Fl/Fl+Py versus An/An+Phen.

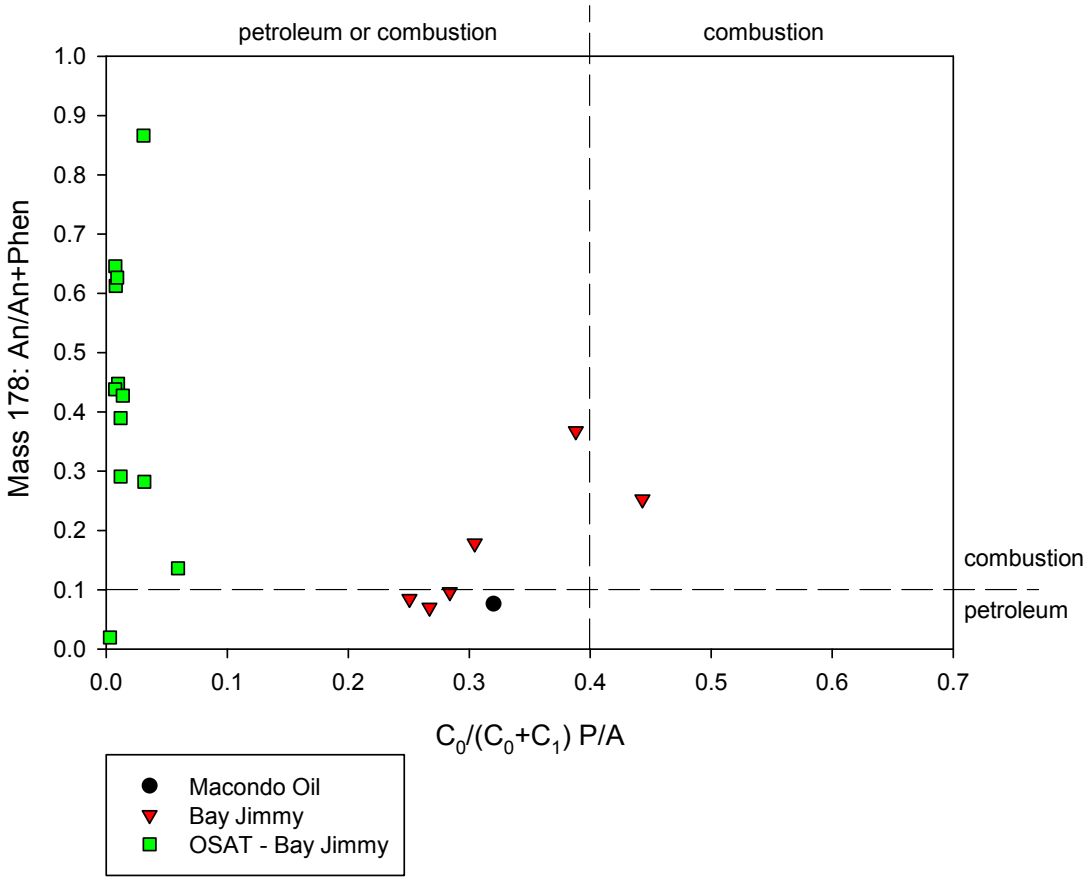

Figure 4.4. PAH compound cross plot for the ratios of $C_0/(C_0+C_1)$ P/A versus An/An+Phen. Note that the tentative petroleum/combustion boundaries provided for C_0/C_0+C_1 P/A are based on fewer literature data points than the boundaries given for the parent PAH ratios and accordingly are less certain (Yunker et al., 2002).

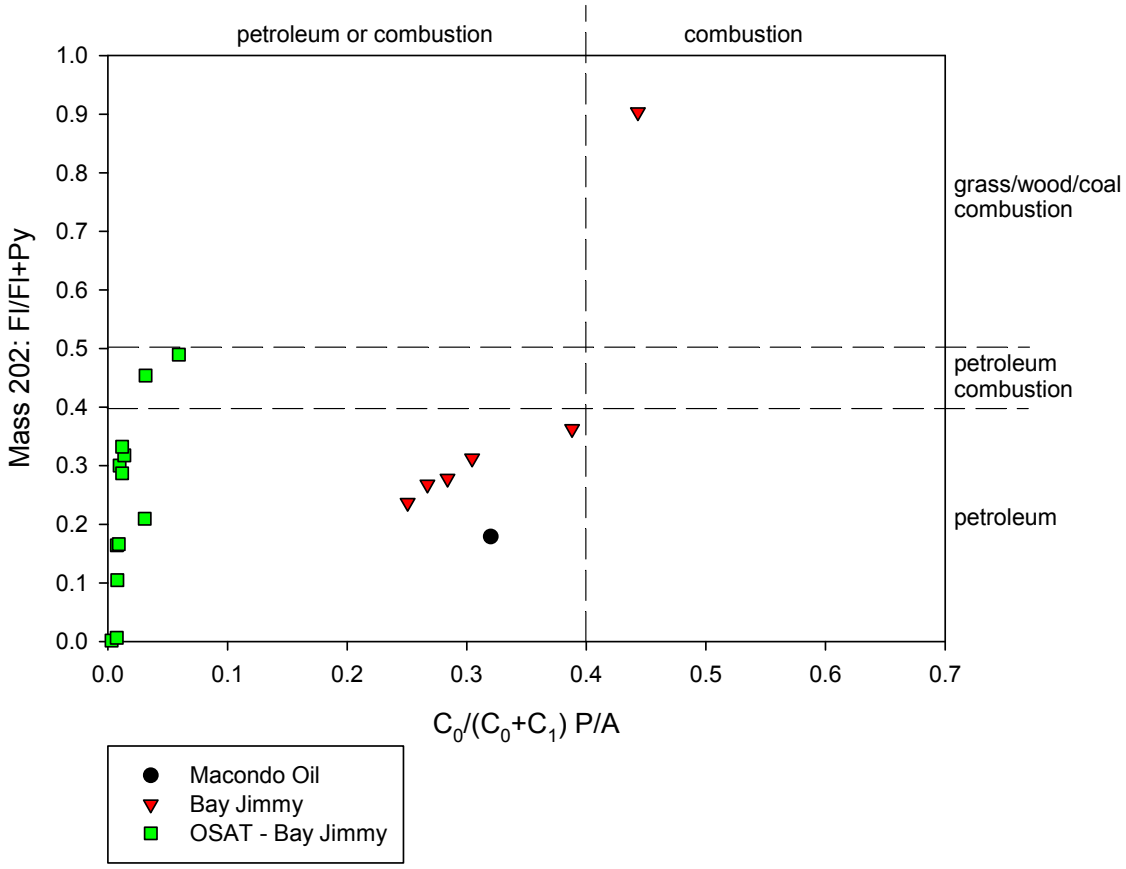

Figure 4.5. PAH compound cross plot for the ratios of $C_0/(C_0+C_1)$ P/A versus Fl/Fl+Py. Note that the tentative petroleum/combustion boundaries provided for C_0/C_0+C_1 P/A are based on fewer literature data points than the boundaries given for the parent PAH ratios and accordingly are less certain (Yunker et al., 2002).

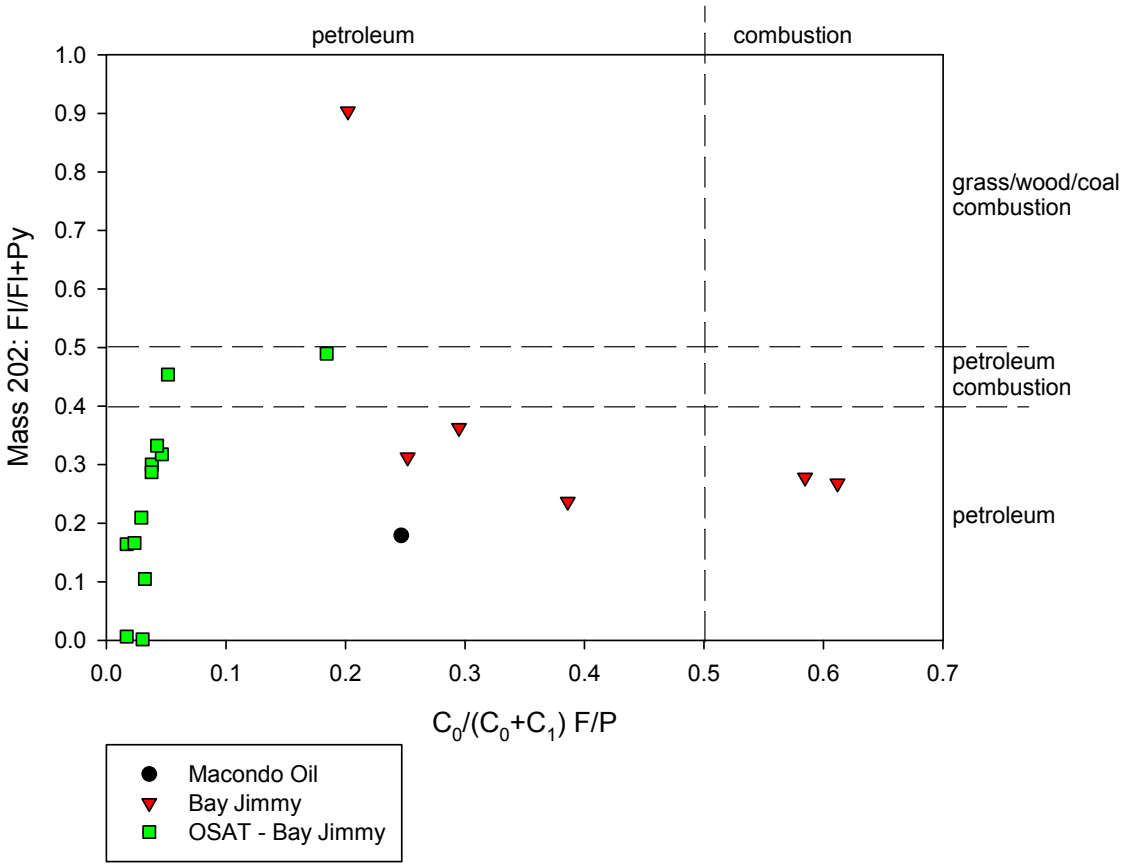

Figure 4.6. PAH compound cross plot for the ratios of $C_0/(C_0+C_1)$ F/P versus Fl/Fl+Py. Note that the tentative petroleum/combustion boundaries provided for C_0/C_0+C_1 F/P are based on fewer literature data points than the boundaries given for the parent PAH ratios and accordingly are less certain (Yunker et al., 2002).

Figure 4.7. Photograph of an at sea controlled burn operation following the DWH spill. In this method, pairs of shrimp boats approximately 50 m apart would collect oil in their booms in a U-shaped configuration. A small boat would then position itself upwind of the contained oil and use a handheld igniter to activate the burn. Burns were monitored from the water and air. Imagery courtesy of Allen et al. (2011).

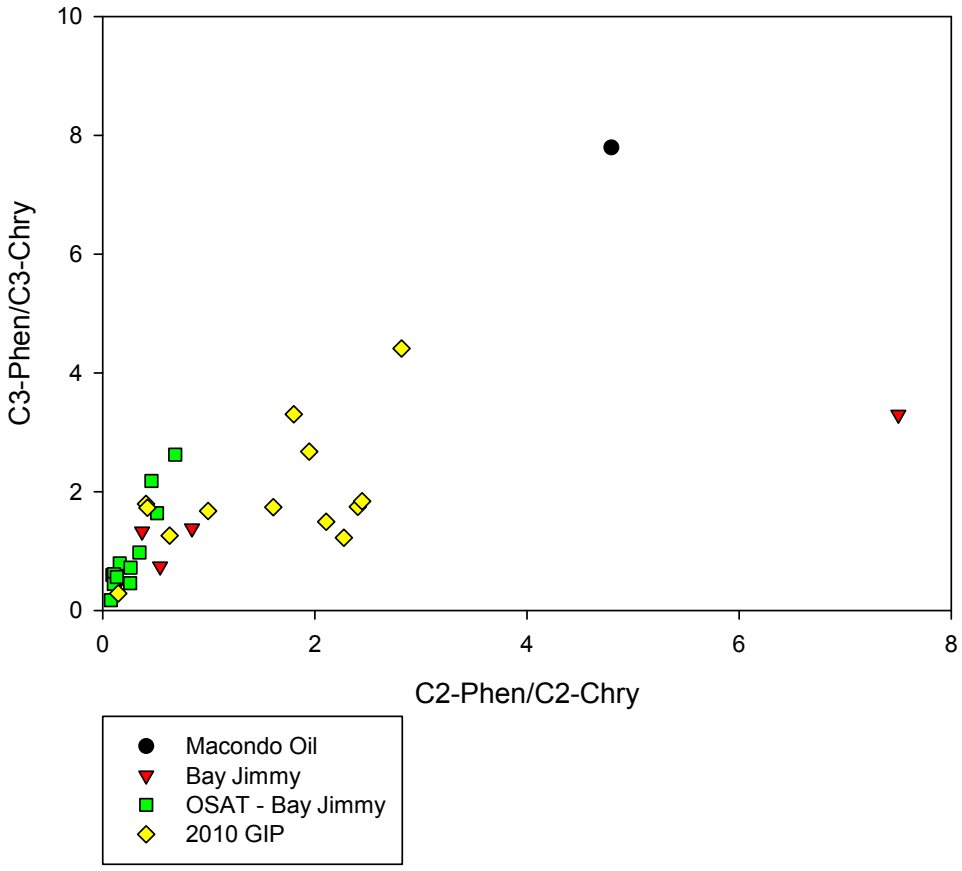

Figure 4.8. PAH compound cross plot for the ratios of C_2 phenanthrene/chrysene versus C_3 phenanthrene/chrysene. The GIP samples were collected on an October, 2010 oceanographic cruise led by Dr. Kevin Yeager in the northern GOMx. These station locations were selected to provide a general radial coverage surrounding the Macondo Well.

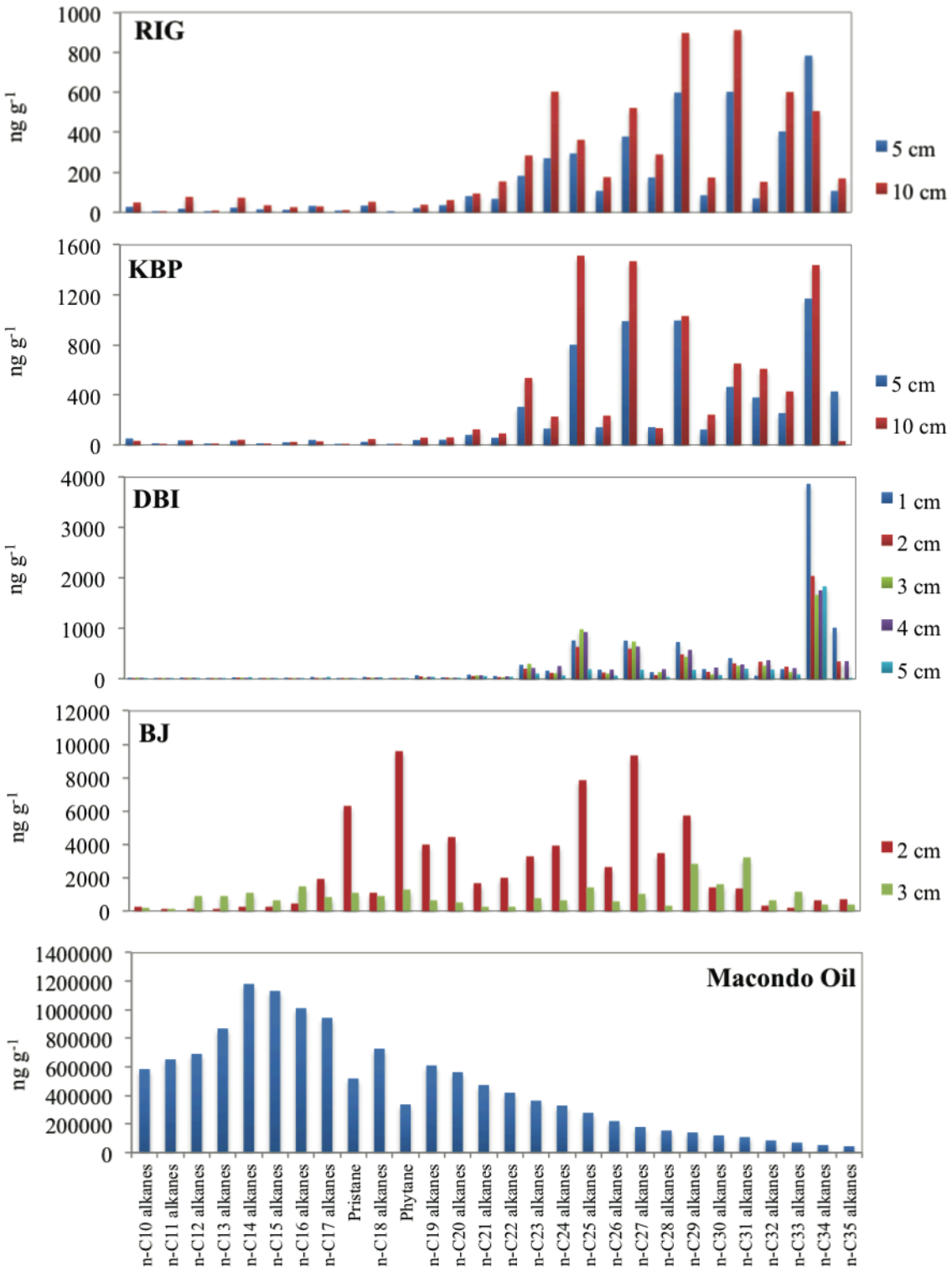

Figure 4.9. Levels of n-alkanes for Macondo-252 oil and representative cores from each site.

Figure 4.10. Photograph of vessel-based marsh vacuuming being performed as part of approved cleanup activities. Photo courtesy of U.S. Coast Guard.

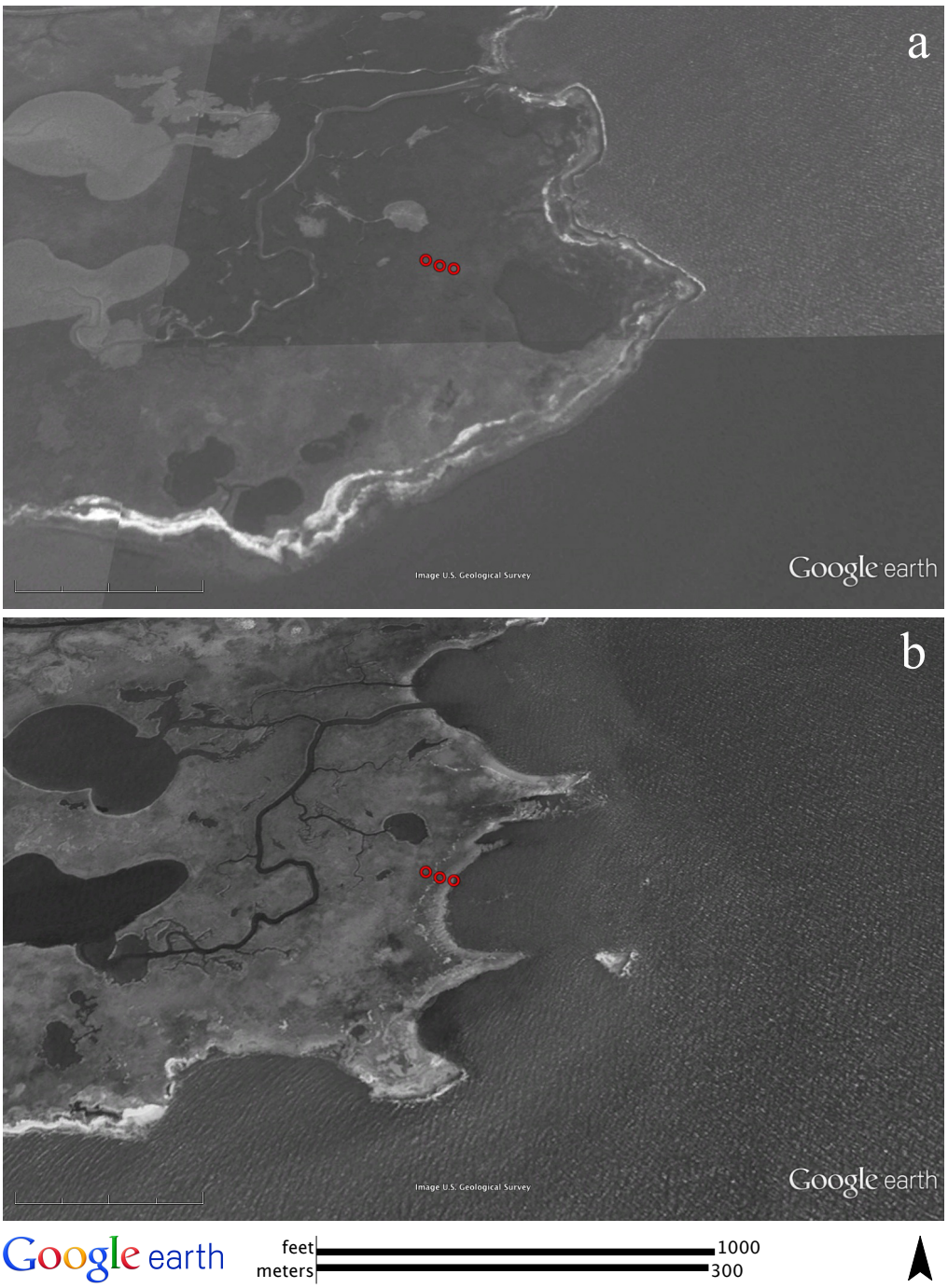

Figure 4.11. Effect of 2005 hurricane season on eastern edge of KBP. Image (a) was taken prior to Hurricanes Katrina and Rita on January 19, 2004, and image (b) was taken following the hurricanes on October 28, 2005. 2010 sampling sites are indicated with red circles. Imagery courtesy of U.S. Geological Survey.

CHAPTER FIVE: SUMMARY AND CONCLUSIONS

This thesis is part of a larger research effort examining conditions following the DWH spill from baseline to maximum exposure in a complete time series. The primary goal of this thesis was to determine how deeply oil from the 2010 Deepwater Horizon (DWH) spill has penetrated sediments in marshes along the Gulf Coast, and whether oil has quantifiably affected benthic ecosystems at these sites. This thesis focused on four field sites in Louisiana. Of the over 7,000 km of shoreline surveyed two years post-release, Louisiana was the only state to still have surface oiling conditions characterized as "heavy" (Michel et al., 2013).

The two hypotheses that were to be evaluated in this thesis were as follows:

H_1: Salt marsh sediments of Dry Bread Island and Bay Jimmy, Louisiana were significantly impacted by the DWH oil spill, as indicated by TPAH concentrations well above what is considered upper limit background for these areas (1.5 $\mu g\ g^{-1}$) (Iqbal et al., 2007).

H_2: These moderately to heavily DWH-oiled marsh sediments would be discernible from pristine to lightly DWH-oiled marsh sediments by exhibiting (a) high concentrations of SOC, (b) shallower bioturbation depths, and (c) low abundance and depth of habitation of meiofauna, as indicated by foraminifera.

Regarding H_1, BJ was the only site with [TPAH] consistently above the upper limit background. DBI did have one sample at the High site with [TPAH] above this limit as well, but the majority of samples were below the limit. Because of this, BJ was the only site considered "significantly impacted".

Molecular ratios of PAH parent and alkyl homologs indicate that the oil delivered to Louisiana marshes was highly weathered. However, the prevalence of LMW n-alkanes in samples from Bay Jimmy suggests that this oil was not as heavily weathered as at other sites. Very high [TPAH] of over 11,000 ng g^{-1} at a depth of 3 cm at the Bay Jimmy High site shows that oil has been mixed into sediments. Once PAHs are buried in the sediment profile, it becomes very difficult for them to be further broken down.

Regarding H_2, anomalously high peaks of SOC were associated with changes in the amount of terrestrial organic material (i.e., roots, plant debris) with depth. However, SOC inventories demonstrated strong positive relationships with TPH and PAH inventories in the uppermost 3 cm of sediment at DBI and BJ. This relationship can be explained by the influx of oil attached to organic matter. Short-term (< 1 year) bioturbation depths were not adequately quantified because of the strong overprint of physical mixing, in addition to the absence of ^{7}Be. The cause of the absence of ^{7}Be at most sites is unresolved, but could be due to sediment composition constraints on ^{7}Be sorption (coarse-grained sediment, high organic matter contents), rapid erosion of the marsh surface, or oil clean up activities. Minimum mixing depths were instead derived from $^{234}Th_{xs}$ profiles. Penetration depths of $^{234}Th_{xs}$ ranged between 0.25 and 4.5 cm. Sediment accumulation rates were determined using ^{210}Pb, with verification from an independent tracer, ^{137}Cs, in selected cores. Accumulation rates ranged from 0.19 to 0.55 g cm^{-2} y^{-1} (0.27 to 0.71 cm y^{-1}) and were highly affected by the 2005 hurricane season. As expected given their locations, $^{210}Pb_{xs}$ profiles reveal thorough, long-term (decadal) sediment mixing at all sites.

The U.S. government has estimated that 23% (1.1 million barrels or 47.3 million U.S. gallons) of the oil released in DWH remains in the environment (Federal Interagency Solutions Group, 2010). The fate of this oil was considered unknown, but possibilities suggested were that the oil remained in the water column, settled to the seafloor, mixed with sediment, was ingested by microbes, or was collected during shore cleanup activities. While it may be impossible to ascertain the fate of all the oil, the data in this thesis suggest that some of the oil was most definitely mixed into the sediment. Radioisotope inventories indicate that most of the sampled sites are, unsurprisingly, in a net erosional state. This means that oil trapped in salt marsh sediments poses an ongoing threat to the environment. As marshes containing trapped DWH oil continue to be eroded by wave action, or be submerged by rising sea level, there is a great potential for the remobilization of oil.

While it is unclear whether the benthos at DBI were detrimentally affected by the deposition of oil in Louisiana salt marshes, there were demonstrable impacts at BJ. Benthic foraminifera responded to the heavy oiling at Bay Jimmy by developing deformities and by showing decreases to both standing stock and DOH. These results are troubling, and long-term monitoring of oil in Barataria Bay and other coastal locations is warranted.

Appendix 1a
Folk ternary diagrams for all RIG cores. Points are shown for all grain size data 0.5 to 30 cm. Plotted using SEDPLOT (Poppe and Eliason, 2008).

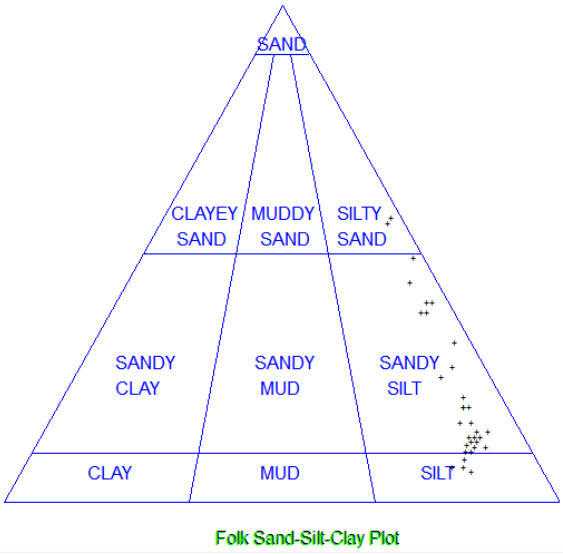

High

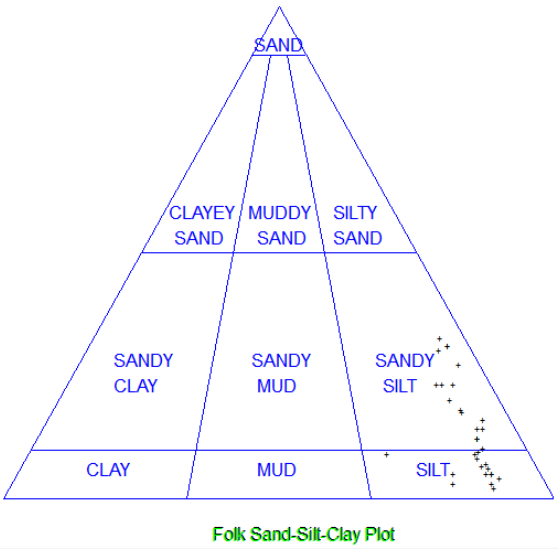

Mid

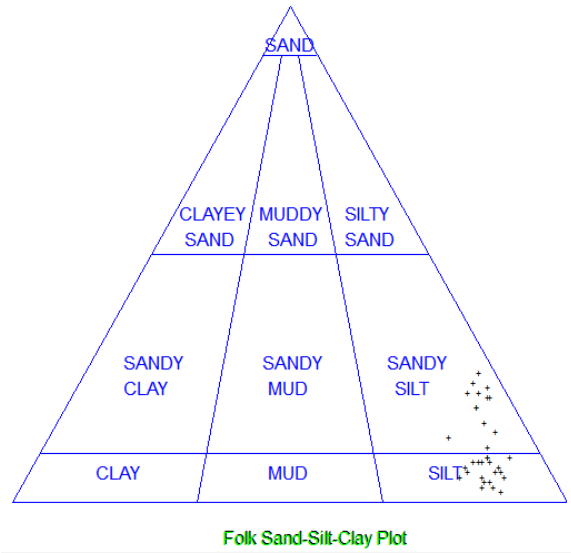

Low

Appendix 1b

Folk ternary diagrams for all KBP cores. Points are shown for all grain size data 0.5 to 50 cm. Plotted using SEDPLOT (Poppe and Eliason, 2008).

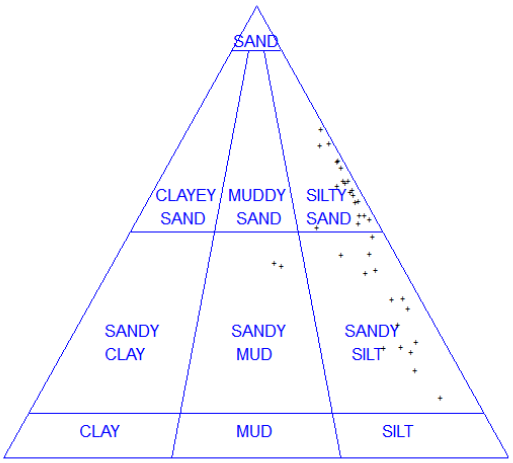

High

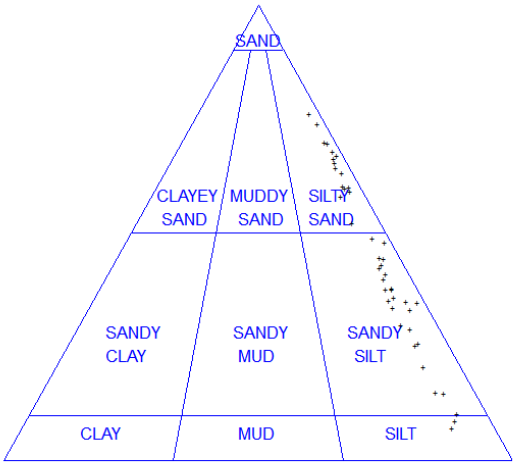

Mid

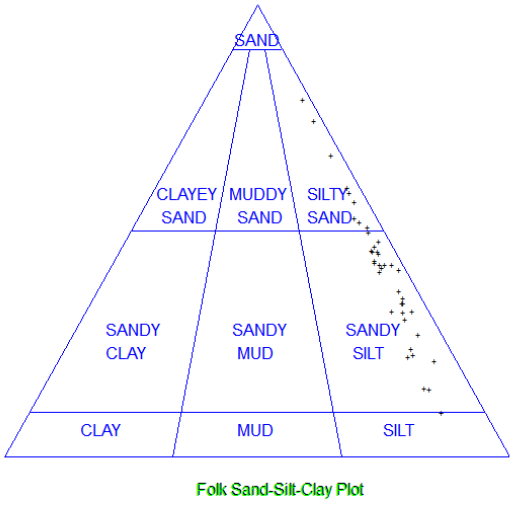

Low

Appendix 1c

Folk ternary diagrams for all DBI cores. Points are shown for all grain size data 0.5 to 30 cm. Plotted using SEDPLOT (Poppe and Eliason, 2008).

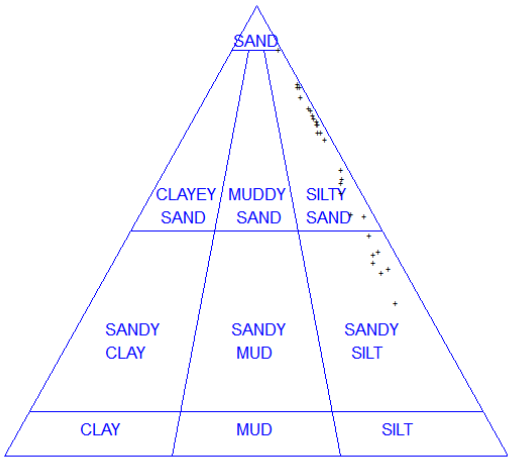

High

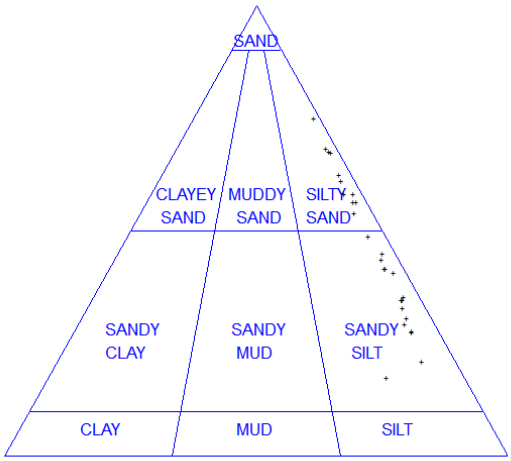

Mid

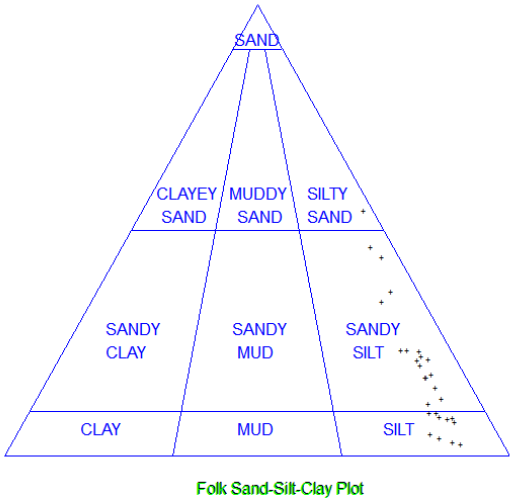

Low

Appendix 1d

Folk ternary diagrams for all BJ cores. Points are shown for all grain size data 0.5 to 30 cm. Plotted using SEDPLOT (Poppe and Eliason, 2008).

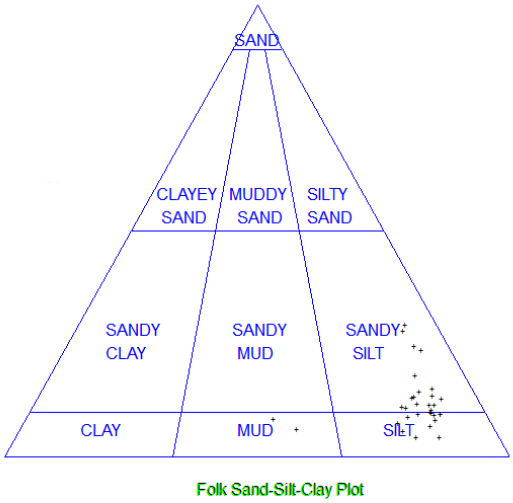

High

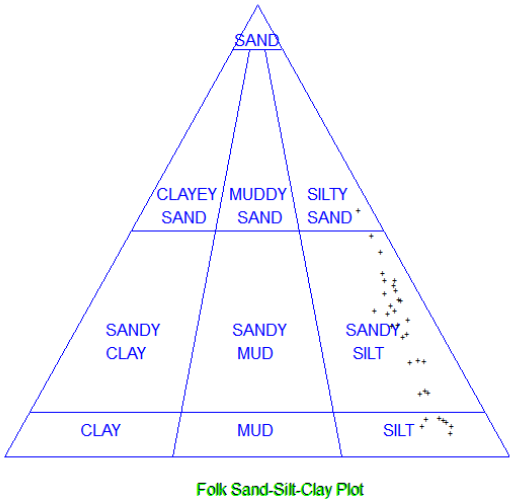

Mid

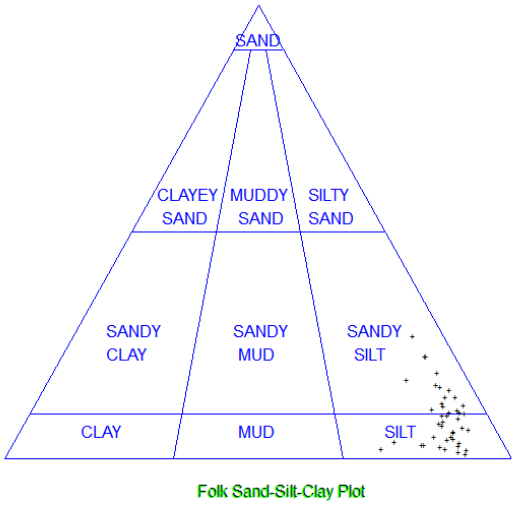

Low

APPENDIX 2

Haversine formula calculations to determine distance between two latitude/longitude points.

Site		Lat 1 (rad)	Lon 1 (rad)	Lat 2 (rad)	Lon 2 (rad)	Dist (rad)	Dist (m)
RIG	Low/ Mid	0.5265	1.5650	0.5265	1.5650	0.00000	7.980
	Mid/ High	0.5265	1.5650	0.5265	1.5650	0.00000	6.784
KBP	Low/ Mid	0.5215	1.5576	0.5215	1.5576	0.00000	13.758
	Mid/ High	0.5215	1.5576	0.5215	1.5576	0.00000	14.778
DBI	Low/ Mid	0.5208	1.5586	0.5208	1.5587	0.00000	21.412
	Mid/ High	0.5208	1.5587	0.5208	1.5587	0.00000	4.122
BJ	Low/ Mid	0.5139	1.5690	0.5139	1.5690	0.00000	10.244
	Mid/ High	0.5139	1.5690	0.5139	1.5690	0.00000	8.110

APPENDIX 3

Appendix 3a
Elemental analysis and grain size data for Rigolets High site.

Sample interval (cm)	Plot depth (cm)	SOC (%)	SOC Inventory (mg cm^{-2})	C/N Ratio	% Sand	% Silt	% Clay	Folk classification
0-0.5	0.25	4.400	12.435	24.900	26.97	66.95	5.98	sandy silt
0.5-1	0.75	8.009	21.754	25.563	38.03	57.21	4.66	sandy silt
1-1.5	1.25	2.902	9.084	19.000	37.53	56.43	5.93	sandy silt
1.5-2	1.75	3.318	9.872	24.429	44.43	50.91	4.55	sandy silt
2-2.5	2.25	1.499	4.928	19.000	39.96	56.90	3.04	sandy silt
2.5-3	2.75	4.544	16.731	20.909	49.26	48.55	2.07	sandy silt
3-4	3.5	2.399	17.318	17.714	56.93	41.22	1.75	silty sand
4-5	4.5	3.415	22.400	19.444	56.13	40.54	3.23	silty sand
5-6	5.5	2.981	16.670	16.667	40.12	55.44	4.34	sandy silt
6-7	6.5	4.057	18.526	17.000	21.01	72.43	6.48	sandy silt
7-8	7.5	7.183	30.322	22.750	19.26	73.49	7.16	sandy silt
8-9	8.5	8.605	39.447	21.850	10.56	79.06	10.30	sandy silt
9-10	9.5	5.221	24.702	16.625	16.04	74.16	9.72	sandy silt
10-11	10.5	5.947	29.047	17.706	18.77	72.96	8.20	sandy silt
11-12	11.5	7.228	34.729	22.938	11.74	79.31	8.88	sandy silt
12-13	12.5	5.788	28.755	17.176	24.80	66.15	8.98	sandy silt
13-14	13.5	4.725	22.160	17.071	12.93	77.48	9.51	sandy silt
14-15	14.5	3.614	16.980	18.200	11.11	80.85	7.97	sandy silt
15-16	15.5	4.981	23.109	17.067	13.64	79.78	6.50	sandy silt
16-17	16.5	5.255	26.294	17.667	13.54	78.18	8.19	sandy silt
17-18	17.5	4.938	24.279	16.867	15.62	76.02	8.27	sandy silt
18-19	18.5	5.218	25.637	17.733	7.52	76.85	15.54	silt
19-20	19.5	5.868	27.372	18.625	12.94	77.86	9.11	sandy silt
20-21	20.5	1.744	8.485	22.000	18.71	73.22	7.97	sandy silt
21-22	21.5	2.462	13.657	17.857	31.90	64.93	3.04	sandy silt
22-23	22.5	1.912	8.863	19.400	13.08	78.40	8.43	sandy silt
23-24	23.5	5.903	23.655	18.813	8.53	78.40	12.99	silt
24-25	24.5	5.191	21.862	18.133	9.93	77.80	12.19	sandy silt
25-26	25.5	4.767	20.894	17.357	5.98	81.19	12.76	silt
26-27	26.5	5.178	22.513	17.267	7.49	78.86	13.56	silt
27-28	27.5	4.729	21.062	16.929	12.17	77.79	9.97	sandy silt
28-29	28.5	5.351	23.456	17.933	11.52	77.53	10.87	sandy silt
29-30	29.5	5.763	25.099	18.063	10.02	79.03	10.87	sandy silt
			Total Inventory 692.092					

Appendix 3b
Elemental analysis and grain size data for Rigolets Mid site.

Sample interval (cm)	Plot depth (cm)	SOC (%)	SOC Inventory (mg cm^{-2})	C/N Ratio	% Sand	% Silt	% Clay	Folk classification
0-0.5	0.25	1.900	6.748	19.600	32.42	63.03	4.44	sandy silt
0.5-1	0.75	2.600	9.173	16.500	30.89	65.09	3.92	sandy silt
1-1.5	1.25	3.400	11.667	16.091	29.90	64.04	5.97	sandy silt
1.5-2	1.75	3.900	12.034	15.077	26.80	69.07	4.03	sandy silt
2-2.5	2.25	4.600	13.646	19.250	30.93	65.37	3.60	sandy silt
2.5-3	2.75	5.500	15.551	19.786	23.15	66.53	10.22	sandy silt
3-4	3.5	4.400	23.310	16.214	23.09	67.52	9.30	sandy silt
4-5	4.5	4.600	24.015	16.714	11.99	79.62	8.31	sandy silt
5-6	5.5	0.710	3.801	17.917	17.95	73.88	8.09	sandy silt
6-7	6.5	0.588	3.177	17.727	12.15	79.99	7.79	sandy silt
7-8	7.5	0.435	2.342	17.444	8.66	64.96	26.31	silt
8-9	8.5	3.765	19.018	17.818	9.52	81.42	8.98	silt
9-10	9.5	4.049	19.718	16.833	16.38	78.31	5.22	sandy silt
10-11	10.5	3.937	18.880	17.636	6.51	83.51	9.90	silt
11-12	11.5	4.314	21.445	18.083	14.04	78.72	7.15	sandy silt
12-13	12.5	20.700	99.643	6.766	5.07	85.56	9.29	silt
13-14	13.5	5.900	28.597	20.133	7.74	82.11	10.07	silt
14-15	14.5	5.100	24.606	19.846	2.73	79.91	17.28	silt
15-16	15.5	7.200	35.715	22.750	6.33	84.33	9.27	silt
16-17	16.5	4.600	21.995	19.250	4.55	79.03	16.33	silt
17-18	17.5	4.600	21.973	18.077	17.53	74.52	7.90	sandy silt
18-19	18.5	6.000	27.881	20.200	8.48	81.19	10.27	silt
19-20	19.5	5.500	27.074	20.214	5.14	84.99	9.80	silt
20-21	20.5	4.300	20.208	18.583	20.24	70.44	9.26	sandy silt
21-22	21.5	4.300	21.068	16.000	4.11	87.64	8.19	silt
22-23	22.5	4.700	24.613	21.909	13.96	79.52	6.45	sandy silt
23-24	23.5	5.400	28.938	19.500	5.28	86.05	8.60	silt
24-25	24.5	4.000	22.453	17.083	5.66	85.62	8.65	silt
25-26	25.5	2.800	17.083	17.875	11.64	79.97	8.31	sandy silt
26-27	26.5	3.200	19.648	18.000	2.65	86.69	10.59	silt
27-28	27.5	4.800	30.404	20.500	23.52	69.81	6.61	sandy silt
28-29	28.5	2.500	16.192	16.250	9.84	82.19	7.91	sandy silt
29-30	29.5	2.400	16.152	17.143	1.67	88.55	9.71	silt
			Total Inventory 708.769					

Appendix 3c
Elemental analysis and grain size data for Rigolets Low site.

Sample interval (cm)	Plot depth (cm)	SOC (%)	SOC Inventory (mg cm^{-2})	C/N Ratio	% Sand	% Silt	% Clay	Folk classification
0-0.5	0.25	1.2	4.729	21.667	20.61	75.80	3.50	sandy silt
0.5-1	0.75	1.1	4.468	14.000	22.18	72.51	5.22	sandy silt
1-1.5	1.25	1.1	4.396	11.600	21.27	74.85	3.79	sandy silt
1.5-2	1.75	1.2	4.807	12.600	25.65	70.61	3.65	sandy silt
2-2.5	2.25	1	4.219	13.000	19.31	73.54	7.05	sandy silt
2.5-3	2.75	1.3	5.235	13.200	22.93	73.59	3.39	sandy silt
3-4	3.5	1.5	11.399	12.833	22.14	70.38	7.38	sandy silt
4-5	4.5	2.1	14.105	17.833	23.90	70.62	5.39	sandy silt
5-6	5.5	2.6	16.795	14.667	19.29	74.33	6.29	sandy silt
6-7	6.5	2.7	17.335	17.250	11.21	79.97	8.74	sandy silt
7-8	7.5	2.8	18.027	17.250	15.97	77.22	6.74	sandy silt
8-9	8.5	2.9	18.779	14.800	13.80	79.71	6.41	sandy silt
9-10	9.5	2.6	16.745	16.875	7.83	81.74	10.36	silt
10-11	10.5	2.6	17.652	16.750	6.84	83.57	9.52	silt
11-12	11.5	2.4	16.681	17.857	4.95	82.04	12.93	silt
12-13	12.5	2.2	16.100	16.000	7.98	80.49	11.45	silt
13-14	13.5	2.3	16.499	16.714	3.70	83.85	12.37	silt
14-15	14.5	2.3	17.018	14.250	3.64	83.58	12.70	silt
15-16	15.5	2.2	16.464	15.714	9.19	84.63	6.11	silt
16-17	16.5	2.1	17.348	15.286	4.67	78.03	17.21	silt
17-18	17.5	2	15.395	16.500	8.29	79.92	11.71	silt
18-19	18.5	2	15.015	14.571	4.97	85.60	9.36	silt
19-20	19.5	1.9	14.347	14.286	3.37	83.28	13.29	silt
20-21	20.5	2.1	16.341	15.286	6.75	78.02	15.14	silt
21-22	21.5	1.8	14.053	15.000	7.92	78.74	13.26	silt
22-23	22.5	1.9	16.086	15.833	8.94	81.46	9.53	silt
23-24	23.5	2.1	15.588	13.500	2.48	86.58	10.87	silt
24-25	24.5	2.1	17.867	15.714	5.53	79.18	15.21	silt
25-26	25.5	2.2	16.100	16.000	6.13	83.82	9.97	silt
26-27	26.5	2.2	16.054	18.667	3.53	84.62	11.77	silt
27-28	27.5	1.8	13.670	15.000	12.74	72.19	14.99	sandy silt
28-29	28.5	2.1	15.851	18.500	8.57	81.21	10.15	silt
29-30	29.5	2.1	15.851	15.857	5.96	85.25	8.72	silt
			Total Inventory 461.020					

Appendix 3d
Elemental analysis and grain size data for Keel Boat Pass High site.

Sample interval (cm)	Plot depth (cm)	SOC (%)	SOC Inventory (mg cm^{-2})	C/N Ratio	% Sand	% Silt	% Clay	Folk classification
0-0.5	0.25	3.790	15.807	28.500	65.58	33.44	0.98	silty sand
0.5-1	0.75	3.980	16.814	34.000	64.06	34.67	1.27	silty sand
1-1.5	1.25	6.352	19.905	32.200	60.76	37.18	2.06	silty sand
1.5-2	1.75	9.465	21.552	34.071	57.93	40.33	1.74	silty sand
2-2.5	2.25	13.902	27.006	30.522	48.92	48.58	2.50	sandy silt
2.5-3	2.75	15.050	28.641	30.160	61.23	37.50	1.27	silty sand
3-4	3.5	5.855	33.732	33.000	53.69	43.61	2.70	silty sand
4-5	4.5	5.477	42.434	30.889	59.20	39.44	1.36	silty sand
5-6	5.5	4.632	35.365	29.000	56.62	41.93	1.45	silty sand
6-7	6.5	3.337	25.971	23.556	44.84	44.41	10.75	sandy silt
7-8	7.5	1.096	10.301	18.667	69.44	29.59	0.97	silty sand
8-9	8.5	3.316	25.879	27.667	52.63	45.99	1.38	silty sand
9-10	9.5	6.004	35.663	38.375	42.92	32.07	25.01	sandy mud
10-11	10.5	7.502	42.442	29.231	60.02	35.99	3.99	silty sand
11-12	11.5	2.555	23.074	26.000	61.22	36.52	2.26	silty sand
12-13	12.5	0.918	10.055	15.667	58.76	39.12	2.12	silty sand
13-14	13.5	2.670	24.105	22.667	42.48	33.66	23.86	sandy mud
14-15	14.5	2.750	27.583	22.667	50.96	36.45	12.59	silty sand
15-16	15.5	0.770	9.362	13.000	51.68	44.39	3.93	silty sand
16-17	16.5	0.600	6.287	14.000	68.90	28.16	2.94	silty sand
17-18	17.5	9.705	36.018	27.333	24.22	63.05	12.73	sandy silt
18-19	18.5	25.077	69.819	23.463	41.47	52.79	5.74	sandy silt
19-20	19.5	26.729	71.162	23.328	40.79	51.23	7.98	sandy silt
20-21	20.5	20.348	53.174	22.622	29.32	63.42	7.26	sandy silt
21-22	21.5	4.012	21.692	20.100	33.05	63.43	3.52	sandy silt
22-23	22.5	1.163	11.985	14.750	35.14	61.39	3.47	sandy silt
23-24	23.5	0.493	6.487	12.500	53.54	44.67	1.79	silty sand
24-25	24.5	0.301	4.110	7.500	56.45	41.35	2.20	silty sand
25-26	25.5	0.219	3.072	-	65.36	33.30	1.34	silty sand
26-27	26.5	0.172	2.390	-	72.57	26.46	0.97	silty sand
27-28	27.5	0.200	1.999	-	44.95	49.94	5.11	sandy silt
28-29	28.5	1.766	14.600	14.833	25.57	68.90	5.53	sandy silt
29-30	29.5	2.441	18.981	17.714	19.25	71.71	9.04	sandy silt
30-31	30.5	-	-	-	-	-	-	-
31-32	31.5	-	-	-	45.72	52.23	2.05	sandy silt
32-33	32.5	-	-	-	-	-	-	-
33-34	33.5	-	-	-	30.94	62.54	6.52	-

Sample interval (cm)	Plot depth (cm)	SOC (%)	SOC Inventory (mg cm^{-2})	C/N Ratio	% Sand	% Silt	% Clay	Folk classification
34-35	34.5	-	-	-	23.31	68.93	7.76	sandy silt
35-36	35.5	-	-	-	16.37	75.98	7.65	-
36-37	36.5	-	-	-	-	-	-	-
37-38	37.5	-	-	-	25.45	68.22	6.33	-
38-39	38.5	-	-	-	-	-	-	-
39-40	39.5	-	-	-	13.21	79.8	6.99	sandy silt
40-41	40.5	-	-	-	-	-	-	-
41-42	41.5	-	-	-	33.86	61.59	4.55	-
42-43	42.5	-	-	-	-	-	-	-
43-44	43.5	-	-	-	40.41	55.48	4.11	-
44-45	44.5	-	-	-	24.34	66.35	9.31	sandy silt
45-46	45.5	-	-	-	43.89	53.84	2.27	-
46-47	46.5	-	-	-	-	-	-	-
47-48	47.5	-	-	-	75.03	23.81	1.16	-
48-49	48.5	-	-	-	-	-	-	-
49-50	49.5	-	-	-	35.07	59.26	5.67	sandy silt
			Total Inventory 797.468					

Appendix 3e
Elemental analysis and grain size data for Keel Boat Pass Mid site.

Sample interval (cm)	Plot depth (cm)	SOC (%)	SOC Inventory (mg cm^{-2})	C/N Ratio	% Sand	% Silt	% Clay	Folk classification
0-0.5	0.25	5.860	19.718	21.200	58.87	38.51	2.62	silty sand
0.5-1	0.75	3.200	13.151	23.143	59.61	37.25	3.14	silty sand
1-1.5	1.25	2.700	11.778	23.167	66.05	31.82	2.13	silty sand
1.5-2	1.75	2.900	12.249	21.000	65.27	32.44	2.29	silty sand
2-2.5	2.25	2.000	9.305	20.600	69.53	28.78	1.69	silty sand
2.5-3	2.75	1.600	7.317	20.250	64.13	33.04	2.83	silty sand
3-4	3.5	2.100	20.569	21.000	69.78	28.15	2.07	silty sand
4-5	4.5	2.800	25.140	20.143	76.01	22	1.99	silty sand
5-6	5.5	1.000	9.622	16.333	57.71	37.35	4.94	silty sand
6-7	6.5	1.600	14.711	19.500	52.05	42.38	5.57	silty sand
7-8	7.5	2.400	18.155	20.500	37.6	57.31	5.09	sandy silt
8-9	8.5	2.000	14.152	19.800	25.03	68.28	6.69	sandy silt
9-10	9.5	2.200	16.190	16.000	35.06	57.97	6.97	sandy silt
10-11	10.5	2.400	18.766	17.429	42.08	52.75	5.17	sandy silt
11-12	11.5	2.200	20.041	18.500	44.09	52.62	3.29	sandy silt
12-13	12.5	1.600	15.934	20.000	67.51	30.85	1.64	silty sand
13-14	13.5	0.800	7.984	13.333	44.3	51.67	4.03	sandy silt
14-15	14.5	1.200	10.900	15.000	37.41	57.59	5	sandy silt
15-16	15.5	3.000	22.229	15.200	14.53	79.16	6.31	sandy silt
16-17	16.5	3.043	20.169	14.667	8.47	84.29	7.24	silt
17-18	17.5	4.100	24.804	15.923	10.12	83.87	6.01	sandy silt
18-19	18.5	3.700	21.723	15.750	6.96	84.43	8.61	silt
19-20	19.5	5.500	30.342	19.786	33.44	59.72	6.84	sandy silt
20-21	20.5	3.500	20.492	16.091	29.57	63.22	7.21	sandy silt
21-22	21.5	4.000	21.212	15.385	37.43	56.35	6.22	sandy silt
22-23	22.5	4.300	20.340	16.846	20.3	72.22	7.48	sandy silt
23-24	23.5	6.200	27.465	15.650	14.88	77.31	7.81	sandy silt
24-25	24.5	3.200	17.378	16.000	28.6	65.49	5.91	sandy silt
25-26	25.5	2.900	21.193	16.111	39.74	54.77	5.49	sandy silt
26-27	26.5	1.036	9.789	20.500	60.08	36.6	3.32	silty sand
27-28	27.5	0.500	5.347	-	73.79	24.64	1.57	silty sand
28-29	28.5	1.000	10.924	16.000	66.86	31.93	1.21	silty sand
29-30	29.5	0.600	6.224	16.000	62.88	34.96	2.16	silty sand
30-31	30.5	-	-	-	-	-	-	-
31-32	31.5	-	-	-	48.6	48.12	3.28	sandy silt
32-33	32.5	-	-	-	-	-	-	-
33-34	33.5	-	-	-	40.73	54.65	4.62	sandy silt

Sample interval (cm)	Plot depth (cm)	SOC (%)	SOC Inventory (mg cm^{-2})	C/N Ratio	% Sand	% Silt	% Clay	Folk classification
34-35	34.5	-	-	-	-	-	-	-
35-36	35.5	-	-	-	34.61	61.72	3.67	sandy silt
36-37	36.5	-	-	-	-	-	-	-
37-38	37.5	-	-	-	42.74	52.89	4.37	sandy silt
38-39	38.5	-	-	-	-	-	-	-
39-40	39.5	-	-	-	59.79	37.86	2.35	silty sand
40-41	40.5	-	-	-	-	-	-	-
41-42	41.5	-	-	-	35.58	58.79	5.63	sandy silt
42-43	42.5	-	-	-	-	-	-	-
43-44	43.5	-	-	-	25.69	68.52	5.79	sandy silt
44-45	44.5	-	-	-	-	-	-	-
45-46	45.5	-	-	-	32.84	63.37	3.79	sandy silt
46-47	46.5	-	-	-	-	-	-	-
47-48	47.5	-	-	-	34.46	63.93	1.61	sandy silt
48-49	48.5	-	-	-	-	-	-	-
49-50	49.5	-	-	-	47.71	50.91	1.38	sandy silt
			Total Inventory 545.313					

Appendix 3f
Elemental analysis and grain size data for Keel Boat Pass Low site.

Sample interval (cm)	Plot depth (cm)	SOC (%)	SOC Inventory (mg cm^{-2})	C/N Ratio	% Sand	% Silt	% Clay	Folk classification
0-0.5	0.25	2.075	8.946	17.667	59.31	38.16	2.53	silty sand
0.5-1	0.75	1.700	7.296	21.000	43.14	51.58	5.28	sandy silt
1-1.5	1.25	1.600	6.634	20.000	42.44	52.88	4.68	sandy silt
1.5-2	1.75	2.000	8.487	20.600	26.85	68.34	4.81	sandy silt
2-2.5	2.25	1.700	7.085	21.250	22.05	68.77	9.18	sandy silt
2.5-3	2.75	2.100	7.948	17.667	31.85	62.83	5.32	sandy silt
3-4	3.5	2.400	16.348	20.333	31.91	60.59	7.50	sandy silt
4-5	4.5	2.100	13.297	15.429	9.67	81.66	8.67	silt
5-6	5.5	3.196	19.423	18.333	14.92	75.56	9.52	sandy silt
6-7	6.5	2.559	16.826	17.778	30.25	64.11	5.64	sandy silt
7-8	7.5	2.003	13.456	17.000	42.37	53.97	3.66	sandy silt
8-9	8.5	1.976	13.548	16.500	42.74	51.75	5.51	sandy silt
9-10	9.5	2.034	14.973	17.333	44.76	51.55	3.69	sandy silt
10-11	10.5	2.494	16.789	17.857	49.52	47.26	3.22	sandy silt
11-12	11.5	1.762	14.685	18.200	50.56	46.52	2.92	silty sand
12-13	12.5	1.190	11.095	20.000	40.71	53.81	5.48	sandy silt
13-14	13.5	0.721	7.629	18.000	52.68	42.90	4.42	silty sand
14-15	14.5	0.951	10.494	25.000	78.72	19.69	1.59	silty sand
15-16	15.5	0.509	5.723	13.000	45.27	50.14	4.59	sandy silt
16-17	16.5	0.317	3.548	9.000	74.24	24.00	1.76	silty sand
17-18	17.5	0.621	7.050	15.500	66.59	31.40	2.01	silty sand
18-19	18.5	0.860	9.375	14.667	58.39	39.00	2.61	silty sand
19-20	19.5	0.621	6.723	10.333	46.48	50.00	3.52	sandy silt
20-21	20.5	1.885	17.364	23.500	41.79	53.64	4.57	sandy silt
21-22	21.5	1.534	12.722	15.000	45.56	49.79	4.65	sandy silt
22-23	22.5	2.422	17.223	15.375	36.48	59.78	3.74	sandy silt
23-24	23.5	4.369	23.534	19.909	33.99	61.81	4.20	sandy silt
24-25	24.5	3.459	21.591	19.778	33.73	61.71	4.56	sandy silt
25-26	25.5	1.659	12.708	16.600	35.01	61.33	3.66	sandy silt
26-27	26.5	1.183	11.088	24.000	47.52	50.25	2.23	sandy silt
27-28	27.5	1.025	10.647	17.333	56.20	41.12	2.68	silty sand
28-29	28.5	1.667	14.695	17.000	51.89	44.28	3.83	silty sand
29-30	29.5	1.961	16.424	16.500	45.31	51.07	3.62	sandy silt
30-31	30.5	-	-	-	-	-	-	-
31-32	31.5	-	-	-	32.00	64.60	3.40	sandy silt
32-33	32.5	-	-	-	-	-	-	-
33-34	33.5	-	-	-	23.85	68.38	7.77	sandy silt

Sample interval (cm)	Plot depth (cm)	SOC (%)	SOC Inventory (mg cm^{-2})	C/N Ratio	% Sand	% Silt	% Clay	Folk classification
34-35	34.5	-	-	-	-	-	-	-
35-36	35.5	-	-	-	22.47	69.63	7.90	sandy silt
36-37	36.5	-	-	-	-	-	-	-
37-38	37.5	-	-	-	33.70	61.94	4.36	sandy silt
38-39	38.5	-	-	-	-	-	-	-
39-40	39.5	-	-	-	41.26	57.38	1.36	sandy silt
40-41	40.5	-	-	-	-	-	-	-
41-42	41.5	-	-	-	21.13	74.52	4.35	sandy silt
42-43	42.5	-	-	-	-	-	-	-
43-44	43.5	-	-	-	14.75	76.64	8.61	sandy silt
44-45	44.5	-	-	-	-	-	-	-
45-46	45.5	-	-	-	42.31	55.44	2.25	sandy silt
46-47	46.5	-	-	-	-	-	-	-
47-48	47.5	-	-	-	14.64	77.10	8.26	sandy silt
48-49	48.5	-	-	-	-	-	-	-
49-50	49.5	-	-	-	24.53	70.12	5.35	sandy silt
			Total Inventory 405.374					

Appendix 3g
Elemental analysis and grain size data for Dry Bread Island High site.

Sample interval (cm)	Plot depth (cm)	SOC (%)	SOC Inventory (mg cm^{-2})	C/N Ratio	% Sand	% Silt	% Clay	Folk classification
0-0.5	0.25	18.900	17.655	27.882	40.61	54.46	4.93	sandy silt
0.5-1	0.75	8.500	14.824	24.722	60.52	36.44	3.04	silty sand
1-1.5	1.25	6.000	18.543	26.917	74.18	24.85	0.97	silty sand
1.5-2	1.75	2.900	10.199	24.500	90.00	9.42	0.58	sand
2-2.5	2.25	2.000	7.395	26.250	76.98	21.97	1.05	silty sand
2.5-3	2.75	3.000	9.066	30.200	81.71	17.41	0.88	silty sand
3-4	3.5	4.400	23.024	20.818	82.36	16.96	0.69	silty sand
4-5	4.5	4.700	23.819	27.000	79.51	19.00	1.49	silty sand
5-6	5.5	4.400	21.897	27.125	71.75	26.30	1.96	silty sand
6-7	6.5	3.200	17.389	21.857	74.87	23.92	1.21	silty sand
7-8	7.5	4.000	22.559	20.400	73.54	25.39	1.07	silty sand
8-9	8.5	4.200	28.595	23.667	75.41	23.53	1.06	silty sand
9-10	9.5	1.600	13.032	16.800	76.69	22.40	0.91	silty sand
10-11	10.5	1.500	11.466	24.667	81.68	17.72	0.61	silty sand
11-12	11.5	1.900	12.330	24.250	73.59	25.26	1.15	silty sand
12-13	12.5	2.200	13.127	22.600	70.03	28.54	1.43	silty sand
13-14	13.5	2.100	11.293	21.600	58.26	37.58	4.16	silty sand
14-15	14.5	6.400	32.412	22.786	69.06	29.43	1.51	silty sand
15-16	15.5	1.300	7.002	22.667	44.66	50.85	4.48	sandy silt
16-17	16.5	2.900	16.470	20.857	61.35	36.30	2.34	silty sand
17-18	17.5	2.500	14.868	20.667	53.44	42.04	4.52	silty sand
18-19	18.5	4.300	25.389	19.545	42.70	51.83	5.47	sandy silt
19-20	19.5	3.700	22.704	21.333	45.31	51.53	3.15	sandy silt
20-21	20.5	4.400	26.029	20.364	41.62	52.97	5.32	-
21-22	21.5	2.500	17.107	20.667	63.37	35.11	1.53	silty sand
22-23	22.5	2.300	17.026	23.000	54.46	42.59	2.85	-
23-24	23.5	2.400	17.617	17.714	48.70	48.07	3.22	sandy silt
24-25	24.5	2.500	17.731	18.714	52.8	43.17	3.93	-
25-26	25.5	1.700	12.794	18.000	53.16	44.80	2.04	silty sand
26-27	26.5	1.100	7.937	23.667	41.28	54.60	4.02	-
27-28	27.5	3.100	19.379	22.429	33.79	60.74	5.47	sandy silt
28-29	28.5	3.100	17.499	20.000	39.22	54.92	5.75	-
29-30	29.5	4.600	22.846	20.000	41.54	55.41	3.05	sandy silt
			Total Inventory 571.023					

Appendix 3h
Elemental analysis and grain size data for Dry Bread Island Mid site.

Sample interval (cm)	Plot depth (cm)	SOC (%)	SOC Inventory (mg cm^{-2})	C/N Ratio	% Sand	% Silt	% Clay	Folk classification
0-0.5	0.25	16.000	28.696	29.033	41.39	54.72	3.89	sandy silt
0.5-1	0.75	9.800	30.795	25.450	57.99	38.47	3.54	silty sand
1-1.5	1.25	5.600	18.516	20.857	56.38	40.96	2.67	silty sand
1.5-2	1.75	3.600	15.246	22.875	74.70	24.03	1.27	silty sand
2-2.5	2.25	3.100	15.279	20.750	60.95	36.31	2.74	silty sand
2.5-3	2.75	2.700	14.587	22.833	62.34	35.26	2.41	silty sand
3-4	3.5	2.400	24.383	18.857	67.45	30.58	1.97	silty sand
4-5	4.5	3.100	27.553	23.286	53.71	42.55	3.74	silty sand
5-6	5.5	2.700	22.695	17.625	67.21	31.12	1.67	silty sand
6-7	6.5	3.600	29.720	19.300	68.01	29.80	2.19	silty sand
7-8	7.5	2.600	19.220	19.714	58.07	40.11	1.82	silty sand
8-9	8.5	4.200	27.975	19.636	56.10	41.85	2.05	silty sand
9-10	9.5	3.900	25.505	20.400	48.65	47.81	3.54	sandy silt
10-11	10.5	3.100	19.249	20.125	41.58	54.77	3.65	sandy silt
11-12	11.5	3.000	16.999	19.375	44.72	52.67	2.61	sandy silt
12-13	12.5	5.800	32.696	20.333	34.46	61.60	3.94	sandy silt
13-14	13.5	5.900	33.216	19.933	32.76	62.55	4.69	sandy silt
14-15	14.5	4.400	23.537	18.583	34.57	61.53	3.90	sandy silt
15-16	15.5	3.800	20.267	19.100	34.54	61.77	3.70	sandy silt
16-17	16.5	3.800	19.403	19.200	40.66	56.84	2.50	sandy silt
17-18	17.5	3.800	19.894	17.778	29.08	64.77	6.15	sandy silt
18-19	18.5	4.900	25.457	17.714	27.67	66.96	5.37	sandy silt
19-20	19.5	3.200	16.290	16.400	27.28	67.21	5.51	sandy silt
20-21	20.5	4.800	25.733	20.083	41.77	54.96	3.45	-
21-22	21.5	2.600	14.244	18.571	35.11	61.63	3.26	sandy silt
22-23	22.5	5.700	31.627	22.231	39.74	58.18	1.99	-
23-24	23.5	3.400	19.546	18.778	30.49	64.56	4.96	sandy silt
24-25	24.5	5.800	33.558	20.786	35.19	58.92	5.78	-
25-26	25.5	2.000	12.010	20.400	20.96	72.29	6.75	sandy silt
26-27	26.5	2.700	16.608	22.091	44.37	52.19	3.06	-
27-28	27.5	2.700	16.122	20.000	17.23	67.12	15.65	sandy silt
28-29	28.5	3.200	22.383	22.857	32.97	60.78	6.14	-
29-30	29.5	2.900	19.735	18.375	43.45	52.98	3.57	sandy silt
			Total Inventory 738.747					

Appendix 3i
Elemental analysis and grain size data for Dry Bread Island Low site.

Sample interval (cm)	Plot depth (cm)	SOC (%)	SOC Inventory (mg cm^{-2})	C/N Ratio	% Sand	% Silt	% Clay	Folk classification
0-0.5	0.25	1.700	7.895	18.400	43.86	52.73	3.41	sandy silt
0.5-1	0.75	0.800	4.105	20.000	54.10	43.99	1.91	silty sand
1-1.5	1.25	1.300	6.511	21.333	46.10	49.25	4.65	sandy silt
1.5-2	1.75	1.500	6.322	19.250	36.21	58.23	5.56	sandy silt
2-2.5	2.25	1.400	5.030	18.500	23.31	67.94	8.75	sandy silt
2.5-3	2.75	2.600	9.453	19.286	23.26	66.76	9.98	sandy silt
3-4	3.5	4.100	28.489	17.333	34.02	57.56	8.42	sandy silt
4-5	4.5	5.100	28.872	18.643	21.18	71.07	7.75	sandy silt
5-6	5.5	4.910	29.127	16.600	19.93	72.23	7.84	sandy silt
6-7	6.5	3.759	22.616	16.643	21.92	71.35	6.73	sandy silt
7-8	7.5	4.556	26.057	16.714	8.37	84.48	7.15	silt
8-9	8.5	5.468	29.029	18.467	8.13	83.54	8.33	silt
9-10	9.5	5.603	30.126	17.625	2.41	89.02	8.57	silt
10-11	10.5	4.730	27.725	17.143	9.49	80.69	9.82	silt
11-12	11.5	4.330	27.722	16.769	11.45	78.14	10.41	sandy silt
12-13	12.5	3.711	22.465	17.000	3.04	87.05	9.91	silt
13-14	13.5	3.400	22.917	14.250	3.94	84.11	11.95	silt
14-15	14.5	3.000	24.076	13.818	15.09	77.65	7.26	sandy silt
15-16	15.5	2.100	17.395	13.125	8.64	81.76	9.60	silt
16-17	16.5	2.200	18.073	14.625	23.09	70.39	6.52	sandy silt
17-18	17.5	2.300	18.536	13.000	12.68	79.97	7.35	sandy silt
18-19	18.5	1.500	14.121	12.667	9.44	79.32	11.24	silt
19-20	19.5	3.500	25.692	15.417	7.48	85.21	7.31	silt
20-21	20.5	1.900	13.717	15.833	8.00	81.55	10.35	-
21-22	21.5	2.500	21.364	16.125	21.34	73.03	5.63	sandy silt
22-23	22.5	2.200	16.603	14.000	12.43	79.55	7.93	-
23-24	23.5	2.400	22.196	17.714	17.83	75.46	6.71	sandy silt
24-25	24.5	2.500	20.913	18.714	28.33	67.55	4.01	-
25-26	25.5	3.100	22.902	14.727	17.30	74.57	8.13	sandy silt
26-27	26.5	3.000	21.858	15.500	25.72	68.44	5.74	-
27-28	27.5	3.700	24.998	16.545	17.26	74.86	7.88	sandy silt
28-29	28.5	5.300	29.620	16.353	3.94	82.91	13.06	-
29-30	29.5	6.000	31.214	15.400	4.64	81.90	13.46	silt
			Total Inventory 677.737					

Appendix 3j
Elemental analysis and grain size data for Bay Jimmy High site.

Sample interval (cm)	Plot depth (cm)	SOC (%)	SOC Inventory (mg cm^{-2})	C/N Ratio	% Sand	% Silt	% Clay	Folk classification
0-0.5	0.25	15.340	25.641	15.653	na	na	na	na
0.5-1	0.75	16.550	29.259	19.857	15.02	76.99	7.99	sandy silt
1-1.5	1.25	11.330	25.434	20.571	29.02	64.68	6.30	sandy silt
1.5-2	1.75	12.803	25.229	20.406	12.86	79.95	7.19	sandy silt
2-2.5	2.25	15.298	26.267	18.256	9.96	79.17	10.87	silt
2.5-3	2.75	14.148	22.703	19.297	8.32	49.05	42.63	mud
3-4	3.5	16.116	49.403	16.160	11.32	78.42	10.26	sandy silt
4-5	4.5	17.457	51.068	19.500	13.14	74.42	12.44	sandy silt
5-6	5.5	19.615	49.610	22.455	7.32	74.24	18.44	silt
6-7	6.5	21.027	46.613	21.192	11.76	75.62	12.62	sandy silt
7-8	7.5	23.423	49.221	19.650	10.79	74.00	15.21	sandy silt
8-9	8.5	23.447	53.010	20.167	12.90	74.07	13.03	sandy silt
9-10	9.5	19.291	53.296	20.102	24.59	68.78	6.63	sandy silt
10-11	10.5	16.545	46.848	19.349	6.10	54.83	39.07	mud
11-12	11.5	15.909	40.032	18.767	4.32	79.22	16.46	silt
12-13	12.5	16.654	43.677	17.633	14.36	74.75	10.89	sandy silt
13-14	13.5	14.624	39.761	15.220	9.39	77.06	13.55	silt
14-15	14.5	16.132	45.504	20.268	11.41	79.39	9.20	sandy silt
15-16	15.5	17.047	44.345	20.738	5.74	75.94	18.32	silt
16-17	16.5	13.805	38.624	18.100	11.04	73.04	15.92	sandy silt
17-18	17.5	12.334	41.539	15.634	10.28	79.35	10.37	sandy silt
18-19	18.5	10.149	33.580	16.677	17.92	72.25	9.83	sandy silt
19-20	19.5	10.004	35.444	17.552	13.52	77.78	8.70	sandy silt
20-21	20.5	8.706	33.007	19.217	6.75	80.75	12.50	silt
21-22	21.5	8.236	32.192	18.304	9.49	81.45	9.06	silt
22-23	22.5	8.344	31.962	18.304	23.66	70.47	5.87	sandy silt
23-24	23.5	8.917	31.231	18.240	8.89	75.42	15.69	silt
24-25	24.5	9.303	33.725	18.192	9.10	80.41	10.49	silt
25-26	25.5	9.106	33.936	10.386	4.28	83.89	11.83	silt
26-27	26.5	8.749	33.502	16.148	8.19	81.03	10.78	silt
27-28	27.5	10.067	35.283	19.074	9.60	79.62	10.78	silt
28-29	28.5	9.805	33.816	15.906	9.55	81.47	8.98	silt
29-30	29.5	9.486	32.163	19.400	27.87	64.92	7.21	sandy silt
			Total Inventory 1246.922					

Appendix 3k
Elemental analysis and grain size data for Bay Jimmy Mid site.

Sample interval (cm)	Plot depth (cm)	SOC (%)	SOC Inventory (mg cm^{-2})	C/N Ratio	% Sand	% Silt	% Clay	Folk classification
0-0.5	0.25	5.215	16.179	20.846	54.31	42.79	2.90	silty sand
0.5-1	0.75	8.663	28.746	19.174	48.75	48.14	3.11	sandy silt
1-1.5	1.25	5.592	16.366	20.786	38.96	55.74	5.30	sandy silt
1.5-2	1.75	6.637	18.333	21.000	33.40	59.70	6.90	sandy silt
2-2.5	2.25	4.725	14.937	22.273	26.55	65.45	8.00	sandy silt
2.5-3	2.75	9.497	27.195	18.538	36.81	58.95	4.24	sandy silt
3-4	3.5	10.372	44.412	20.840	32.32	60.98	6.70	sandy silt
4-5	4.5	8.632	35.180	18.000	29.28	63.22	7.50	sandy silt
5-6	5.5	9.006	37.100	19.870	27.01	66.07	6.92	sandy silt
6-7	6.5	8.194	33.285	20.367	45.36	51.76	2.88	sandy silt
7-8	7.5	10.648	49.945	22.417	36.04	57.26	6.70	sandy silt
8-9	8.5	10.447	42.644	21.200	37.87	58.13	4.00	sandy silt
9-10	9.5	10.371	43.448	20.115	38.94	57.67	3.39	sandy silt
10-11	10.5	8.897	38.305	20.409	34.42	61.28	4.30	sandy silt
11-12	11.5	8.049	34.314	16.120	34.85	60.63	4.52	sandy silt
12-13	12.5	9.482	43.785	20.167	40.66	54.55	4.79	sandy silt
13-14	13.5	11.010	48.304	20.036	31.61	60.08	8.31	sandy silt
14-15	14.5	8.519	38.844	19.217	32.39	56.96	10.65	sandy silt
15-16	15.5	9.123	40.553	18.038	30.31	64.60	5.09	sandy silt
16-17	16.5	9.255	38.254	19.625	28.93	62.15	8.92	sandy silt
17-18	17.5	9.665	40.080	19.346	20.92	69.80	9.28	sandy silt
18-19	18.5	13.782	48.527	15.977	21.21	71.27	7.52	sandy silt
19-20	19.5	14.658	50.517	18.846	13.85	75.33	10.82	sandy silt
20-21	20.5	14.221	47.423	17.976	5.22	85.56	9.22	silt
21-22	21.5	14.046	44.687	19.432	8.31	79.29	12.40	silt
22-23	22.5	13.243	45.898	19.000	14.06	76.72	9.22	sandy silt
23-24	23.5	12.601	46.433	20.063	14.54	75.96	9.50	sandy silt
24-25	24.5	12.235	41.925	19.063	8.67	81.68	9.65	silt
25-26	25.5	12.685	41.651	16.974	8.06	82.76	9.18	silt
26-27	26.5	12.572	41.995	19.636	6.73	85.04	8.23	silt
27-28	27.5	11.632	39.884	17.676	21.09	72.46	6.45	sandy silt
28-29	28.5	11.560	39.475	16.886	6.86	79.07	14.07	silt
29-30	29.5	10.891	43.221	13.600	7.52	83.72	8.76	silt
			Total Inventory 1261.842					

Appendix 3l
Elemental analysis and grain size data for Bay Jimmy Low site.

Sample interval (cm)	Plot depth (cm)	SOC (%)	SOC Inventory (mg cm^{-2})	C/N Ratio	% Sand	% Silt	% Clay	Folk classification
0-0.5	0.25	7.881	14.363	17.826	26.89	67.04	6.07	sandy silt
0.5-1	0.75	6.603	10.998	19.529	17.29	70.55	12.16	sandy silt
1-1.5	1.25	7.127	12.120	17.476	22.30	71.90	5.80	sandy silt
1.5-2	1.75	7.475	13.410	17.500	13.44	82.03	4.53	sandy silt
2-2.5	2.25	6.859	12.463	16.524	16.29	76.84	6.87	sandy silt
2.5-3	2.75	6.729	12.328	13.640	4.83	85.64	9.53	silt
3-4	3.5	7.084	25.946	17.800	8.71	84.97	6.32	silt
4-5	4.5	12.293	32.018	19.273	2.02	85.88	12.10	silt
5-6	5.5	11.843	33.698	16.472	10.66	83.89	5.45	sandy silt
6-7	6.5	6.417	24.663	18.556	9.80	85.65	4.55	silt
7-8	7.5	6.755	28.737	20.412	7.59	81.89	10.52	silt
8-9	8.5	4.038	18.063	18.818	11.65	84.56	3.79	sandy silt
9-10	9.5	7.409	27.894	19.842	9.34	82.51	8.15	silt
10-11	10.5	9.404	32.452	12.231	12.01	80.24	7.75	sandy silt
11-12	11.5	9.636	26.431	18.407	11.32	80.82	7.86	sandy silt
12-13	12.5	7.895	26.719	20.000	13.52	79.94	6.54	sandy silt
13-14	13.5	7.289	27.880	18.800	15.70	77.97	6.33	sandy silt
14-15	14.5	9.806	25.719	17.643	8.02	82.32	9.66	silt
15-16	15.5	14.579	35.625	16.636	9.57	81.43	9.00	silt
16-17	16.5	8.855	27.693	20.500	10.06	82.56	7.38	sandy silt
17-18	17.5	7.233	25.642	20.611	22.39	71.68	5.93	sandy silt
18-19	18.5	4.814	22.132	20.250	14.94	80.08	4.98	sandy silt
19-20	19.5	4.219	18.802	18.000	18.74	75.85	5.41	sandy silt
20-21	20.5	12.355	31.367	17.914	10.72	78.89	10.39	sandy silt
21-22	21.5	14.116	30.193	18.789	7.29	82.49	10.22	silt
22-23	22.5	15.885	30.788	18.721	5.89	85.49	8.62	silt
23-24	23.5	19.499	39.380	21.370	2.41	84.50	13.09	silt
24-25	24.5	12.548	35.008	21.759	2.97	80.75	16.28	silt
25-26	25.5	12.478	38.720	17.972	3.07	81.13	15.80	silt
26-27	26.5	16.439	40.748	18.435	4.62	82.20	13.18	silt
27-28	27.5	23.920	45.539	19.355	3.55	75.10	21.35	silt
28-29	28.5	24.620	44.182	20.097	2.50	88.15	9.35	silt
29-30	29.5	24.577	44.401	18.191	1.70	90.20	8.10	silt
			Total Inventory 916.119					

APPENDIX 4

Appendix 4a
Carbonate values for all RIG sites.

Sample interval (cm)	Plot depth (cm)	Carbonate (%)		
		HIGH	MID	LOW
0-0.5	0.25	7.133	5.796	6.213
0.5-1	0.75	6.721	5.162	4.826
1-1.5	1.25	5.083	5.170	4.508
1.5-2	1.75	5.336	5.670	5.226
2-2.5	2.25	5.788	5.873	5.904
2.5-3	2.75	6.045	5.393	4.381
3-4	3.5	5.462	5.859	5.098
4-5	4.5	5.083	6.515	5.267
5-6	5.5	8.093	6.242	6.420
6-7	6.5	8.443	6.053	5.429
7-8	7.5	10.993	6.114	5.000
8-9	8.5	12.356	6.902	5.209
9-10	9.5	10.328	6.858	5.603
10-11	10.5	11.664	10.323	6.664
11-12	11.5	9.833	8.383	5.956
12-13	12.5	10.321	11.638	5.240
13-14	13.5	9.700	9.336	5.179
14-15	14.5	8.355	12.767	5.473
15-16	15.5	7.543	10.781	6.140
16-17	16.5	8.633	13.311	7.664
17-18	17.5	9.585	11.635	8.000
18-19	18.5	11.243	9.816	6.808
19-20	19.5	9.106	13.967	7.148
20-21	20.5	3.695	9.990	8.414
21-22	21.5	6.929	9.220	7.470
22-23	22.5	7.448	10.657	8.890
23-24	23.5	9.678	9.574	7.206
24-25	24.5	10.294	7.171	10.272
25-26	25.5	8.475	7.963	6.594
26-27	26.5	11.905	8.154	6.532
27-28	27.5	10.023	8.417	5.683
28-29	28.5	10.692	7.982	6.083
29-30	29.5	12.392	7.532	5.627

Appendix 4b
Carbonate values for all KBP sites.

Sample interval (cm)	Plot depth (cm)	Carbonate (%)		
		HIGH	MID	LOW
0-0.5	0.25	6.680	17.444	1.385
0.5-1	0.75	5.693	11.416	5.682
1-1.5	1.25	7.317	11.262	4.853
1.5-2	1.75	9.573	11.152	4.495
2-2.5	2.25	10.460	8.575	4.469
2.5-3	2.75	11.233	8.563	4.771
3-4	3.5	9.378	7.583	4.538
4-5	4.5	7.193	8.831	5.311
5-6	5.5	9.064	5.347	5.452
6-7	6.5	6.504	5.948	5.717
7-8	7.5	4.065	6.517	4.286
8-9	8.5	6.486	6.801	4.322
9-10	9.5	9.546	6.565	4.443
10-11	10.5	13.481	7.072	5.229
11-12	11.5	5.964	6.379	4.957
12-13	12.5	4.850	5.389	5.036
13-14	13.5	7.369	5.781	4.371
14-15	14.5	6.974	7.183	5.499
15-16	15.5	4.011	7.784	4.186
16-17	16.5	3.498	8.424	3.550
17-18	17.5	9.993	9.166	4.565
18-19	18.5	18.708	9.103	4.965
19-20	19.5	18.787	15.995	3.851
20-21	20.5	16.628	1.526	4.730
21-22	21.5	10.997	9.374	4.926
22-23	22.5	6.748	9.973	5.423
23-24	23.5	6.645	10.925	7.418
24-25	24.5	5.838	8.756	6.820
25-26	25.5	5.665	8.419	6.476
26-27	26.5	5.204	6.533	4.876
27-28	27.5	4.771	5.167	3.951
28-29	28.5	7.270	6.019	4.477
29-30	29.5	7.931	5.948	4.599

Appendix 4c
Carbonate values for all DBI sites.

Sample interval (cm)	Plot depth (cm)	Carbonate (%)		
		HIGH	MID	LOW
0-0.5	0.25	15.772	59.533	5.675
0.5-1	0.75	9.273	47.635	5.199
1-1.5	1.25	6.088	48.168	6.072
1.5-2	1.75	5.229	40.920	6.348
2-2.5	2.25	5.289	35.122	7.859
2.5-3	2.75	5.179	29.743	8.286
3-4	3.5	7.240	16.777	8.361
4-5	4.5	6.973	12.541	9.026
5-6	5.5	7.859	18.882	9.427
6-7	6.5	7.236	16.844	8.085
7-8	7.5	7.195	12.529	7.897
8-9	8.5	5.519	12.600	8.775
9-10	9.5	4.064	12.210	9.630
10-11	10.5	4.025	21.265	9.657
11-12	11.5	4.559	11.565	9.266
12-13	12.5	4.292	11.093	8.553
13-14	13.5	5.413	10.633	8.225
14-15	14.5	6.113	10.213	7.461
15-16	15.5	5.066	11.451	7.261
16-17	16.5	6.330	11.155	8.403
17-18	17.5	6.045	11.421	8.640
18-19	18.5	9.566	14.919	8.179
19-20	19.5	7.314	12.719	8.920
20-21	20.5	8.447	10.622	7.726
21-22	21.5	6.758	9.844	6.326
22-23	22.5	7.451	16.229	7.288
23-24	23.5	6.504	12.327	5.515
24-25	24.5	7.155	11.640	6.213
25-26	25.5	7.209	11.089	8.667
26-27	26.5	4.053	10.407	6.957
27-28	27.5	7.302	9.496	8.425
28-29	28.5	9.364	9.262	10.649
29-30	29.5	10.719	9.599	11.011

Appendix 4d
Carbonate values for all BJ sites.

Sample interval (cm)	Plot depth (cm)	Carbonate (%)		
		HIGH	MID	LOW
0-0.5	0.25	-	6.956	12.087
0.5-1	0.75	16.552	8.923	12.368
1-1.5	1.25	12.976	5.561	12.156
1.5-2	1.75	14.817	8.163	12.028
2-2.5	2.25	16.184	7.011	10.835
2.5-3	2.75	15.728	8.684	11.537
3-4	3.5	16.513	10.010	12.832
4-5	4.5	15.547	9.361	15.099
5-6	5.5	19.021	7.958	13.246
6-7	6.5	19.722	8.717	10.148
7-8	7.5	20.389	10.425	9.082
8-9	8.5	18.233	9.426	10.325
9-10	9.5	15.481	10.422	11.834
10-11	10.5	16.792	9.720	13.132
11-12	11.5	16.909	9.082	6.314
12-13	12.5	16.904	7.499	12.223
13-14	13.5	16.451	9.109	10.521
14-15	14.5	17.038	8.583	13.160
15-16	15.5	16.804	8.601	14.546
16-17	16.5	16.026	7.917	11.436
17-18	17.5	15.846	8.557	10.993
18-19	18.5	15.031	12.314	8.991
19-20	19.5	13.109	12.244	8.281
20-21	20.5	13.054	11.663	12.815
21-22	21.5	11.130	12.000	16.037
22-23	22.5	12.846	9.997	18.802
23-24	23.5	12.085	9.454	17.992
24-25	24.5	12.421	8.433	14.681
25-26	25.5	12.504	10.979	13.741
26-27	26.5	11.695	10.672	15.955
27-28	27.5	12.373	10.238	20.335
28-29	28.5	13.145	12.900	19.354
29-30	29.5	12.938	10.509	20.488

APPENDIX 5

Appendix 5a
Calculated porosity and bulk density values for all RIG sites.

Sample interval (cm)	Plot depth (cm)	Porosity (%)	Bulk density (g cm^{-3})	Porosity (%)	Bulk density (g cm^{-3})	Porosity (%)	Bulk density (g cm^{-3})
		HIGH		MID		LOW	
0-0.5	0.25	0.767	0.565	0.712	0.710	0.682	0.788
0.5-1	0.75	0.771	0.543	0.713	0.706	0.673	0.812
1-1.5	1.25	0.745	0.626	0.719	0.686	0.678	0.799
1.5-2	1.75	0.757	0.595	0.747	0.617	0.677	0.801
2-2.5	2.25	0.734	0.657	0.755	0.593	0.660	0.844
2.5-3	2.75	0.697	0.736	0.766	0.565	0.675	0.805
3-4	3.5	0.707	0.722	0.782	0.530	0.693	0.760
4-5	4.5	0.732	0.656	0.785	0.522	0.728	0.672
5-6	5.5	0.772	0.559	0.785	0.535	0.737	0.646
6-7	6.5	0.812	0.457	0.783	0.540	0.739	0.642
7-8	7.5	0.823	0.422	0.784	0.538	0.738	0.644
8-9	8.5	0.806	0.458	0.793	0.505	0.736	0.648
9-10	9.5	0.804	0.473	0.800	0.487	0.738	0.644
10-11	10.5	0.797	0.488	0.803	0.480	0.724	0.679
11-12	11.5	0.798	0.480	0.796	0.497	0.718	0.695
12-13	12.5	0.794	0.497	0.778	0.481	0.703	0.732
13-14	13.5	0.807	0.469	0.799	0.485	0.709	0.717
14-15	14.5	0.808	0.470	0.801	0.482	0.700	0.740
15-16	15.5	0.808	0.464	0.792	0.496	0.696	0.748
16-17	16.5	0.793	0.500	0.803	0.478	0.665	0.826
17-18	17.5	0.797	0.492	0.803	0.478	0.688	0.770
18-19	18.5	0.797	0.491	0.807	0.465	0.696	0.751
19-20	19.5	0.806	0.466	0.796	0.492	0.694	0.755
20-21	20.5	0.803	0.487	0.807	0.470	0.685	0.778
21-22	21.5	0.775	0.555	0.798	0.490	0.684	0.781
22-23	22.5	0.812	0.464	0.784	0.524	0.657	0.847
23-24	23.5	0.833	0.401	0.778	0.536	0.699	0.742
24-25	24.5	0.826	0.421	0.770	0.561	0.655	0.851
25-26	25.5	0.819	0.438	0.752	0.610	0.703	0.732
26-27	26.5	0.820	0.435	0.749	0.614	0.704	0.730
27-28	27.5	0.816	0.445	0.739	0.633	0.693	0.759
28-29	28.5	0.818	0.438	0.737	0.648	0.694	0.755
29-30	29.5	0.819	0.436	0.727	0.673	0.694	0.755
30-31	30.5	0.823	0.443	0.733	0.668	0.694	0.764
31-32	31.5	0.823	0.441	0.725	0.687	0.698	0.756

Sample interval (cm)	Plot depth (cm)	Porosity (%)	Bulk density (g cm^{-3})	Porosity (%)	Bulk density (g cm^{-3})	Porosity (%)	Bulk density (g cm^{-3})
		HIGH		MID		LOW	
32-33	32.5	0.830	0.424	0.719	0.702	0.700	0.749
33-34	33.5	0.841	0.398	0.714	0.714	0.703	0.743
34-35	34.5	0.849	0.378	0.710	0.724	0.704	0.739
35-36	35.5	0.826	0.434	0.711	0.723	0.704	0.739
36-37	36.5	0.822	0.445	0.706	0.735	0.704	0.741
37-38	37.5	0.824	0.439	0.709	0.727	0.700	0.749
38-39	38.5	0.816	0.460	0.708	0.729	0.693	0.769
39-40	39.5	0.825	0.439	0.706	0.735	0.693	0.766
40-41	40.5	0.817	0.458	0.697	0.756	0.688	0.780
41-42	41.5	0.820	0.451	0.686	0.786	0.689	0.779
42-43	42.5	0.820	0.451	0.684	0.790	0.689	0.777
43-44	43.5	0.801	0.497	0.675	0.813	0.686	0.785
44-45	44.5	0.804	0.491	0.680	0.800	0.676	0.809
45-46	45.5	0.786	0.534	0.706	0.734	0.671	0.822
46-47	46.5	0.794	0.515	0.710	0.725	0.664	0.840
47-48	47.5	0.786	0.535	0.703	0.742	0.654	0.866
48-49	48.5	0.806	0.484	0.702	0.746	0.647	0.884
49-50	49.5	0.795	0.513	0.695	0.763	0.645	0.886
50-52	51	0.783	0.543	0.675	0.812	0.609	0.977
52-54	53	0.753	0.618	0.682	0.794	0.578	1.055
54-56	55	0.742	0.646	0.675	0.812	0.592	1.020
56-58	57	0.732	0.670	0.666	0.835	0.593	1.018
58-60	59	0.728	0.680	0.660	0.851	0.574	1.065
60-62	61	0.727	0.684	0.654	0.866	0.576	1.059
62-64	63	0.725	0.689	0.638	0.905	0.573	1.067
64-66	65	0.725	0.688	0.646	0.886	0.563	1.092
66-68	67	0.730	0.676	0.641	0.898	0.556	1.110
68-70	69	0.721	0.698	0.630	0.926	0.550	1.125
70-72	71	0.717	0.707	0.599	1.001	0.552	1.121
72-74	73	0.718	0.706	0.576	1.060	0.557	1.107
74-76	75	0.723	0.693	-	-	0.543	1.143
76-78	77	0.727	0.682	-	-	0.546	1.136
78-80	79	0.711	0.723	-	-	0.547	1.133
80-82	81	0.685	0.787	-	-	0.551	1.122
82-84	83	0.684	0.790	-	-	0.548	1.129
84-86	85	0.683	0.792	-	-	0.548	1.129
86-88	87	0.680	0.801	-	-	0.551	1.124
88-89	88.5	-	-	-	-	0.553	1.118

Appendix 5b
Calculated porosity and bulk density values for all KBP sites.

Sample interval (cm)	Plot depth (cm)	Porosity (%)	Bulk density (g cm^{-3})	Porosity (%)	Bulk density (g cm^{-3})	Porosity (%)	Bulk density (g cm^{-3})
		HIGH		MID		LOW	
0-0.5	0.25	0.658	0.834	0.720	0.673	0.650	0.862
0.5-1	0.75	0.653	0.845	0.664	0.822	0.653	0.858
1-1.5	1.25	0.739	0.627	0.645	0.872	0.665	0.829
1.5-2	1.75	0.806	0.455	0.656	0.845	0.656	0.849
2-2.5	2.25	0.829	0.389	0.623	0.931	0.663	0.834
2.5-3	2.75	0.832	0.381	0.630	0.915	0.693	0.757
3-4	3.5	0.761	0.576	0.603	0.979	0.723	0.681
4-5	4.5	0.679	0.775	0.634	0.898	0.743	0.633
5-6	5.5	0.685	0.764	0.613	0.962	0.752	0.608
6-7	6.5	0.682	0.778	0.628	0.919	0.733	0.658
7-8	7.5	0.621	0.940	0.693	0.756	0.728	0.672
8-9	8.5	0.681	0.780	0.713	0.708	0.722	0.686
9-10	9.5	0.753	0.594	0.701	0.736	0.702	0.736
10-11	10.5	0.762	0.566	0.682	0.782	0.726	0.673
11-12	11.5	0.633	0.903	0.630	0.911	0.663	0.833
12-13	12.5	0.559	1.095	0.598	0.996	0.624	0.932
13-14	13.5	0.633	0.903	0.599	0.998	0.575	1.058
14-15	14.5	0.592	1.003	0.634	0.908	0.556	1.103
15-16	15.5	0.511	1.216	0.698	0.741	0.549	1.124
16-17	16.5	0.579	1.048	0.730	0.663	0.551	1.119
17-18	17.5	0.842	0.371	0.751	0.605	0.544	1.135
18-19	18.5	0.867	0.278	0.759	0.587	0.562	1.090
19-20	19.5	0.872	0.266	0.771	0.552	0.565	1.083
20-21	20.5	0.880	0.261	0.760	0.585	0.627	0.921
21-22	21.5	0.778	0.541	0.782	0.530	0.665	0.829
22-23	22.5	0.585	1.031	0.805	0.473	0.711	0.711
23-24	23.5	0.472	1.316	0.815	0.443	0.778	0.539
24-25	24.5	0.453	1.366	0.778	0.543	0.745	0.624
25-26	25.5	0.438	1.403	0.702	0.731	0.690	0.766
26-27	26.5	0.444	1.389	0.620	0.945	0.622	0.937
27-28	27.5	0.600	0.999	0.571	1.069	0.582	1.039
28-29	28.5	0.666	0.827	0.560	1.092	0.644	0.882
29-30	29.5	0.684	0.778	0.583	1.037	0.661	0.838
30-31	30.5	0.694	0.764	0.594	1.015	0.775	0.561
31-32	31.5	0.611	0.972	0.600	1.000	0.773	0.569
32-33	32.5	0.572	1.071	0.584	1.039	0.747	0.633

Sample interval (cm)	Plot depth (cm)	Porosity (%)	Bulk density (g cm^{-3})	Porosity (%)	Bulk density (g cm^{-3})	Porosity (%)	Bulk density (g cm^{-3})
		HIGH		MID		LOW	
33-34	33.5	0.654	0.864	0.653	0.866	0.700	0.749
34-35	34.5	0.711	0.722	0.703	0.743	0.652	0.871
35-36	35.5	0.755	0.613	0.750	0.626	0.624	0.940
36-37	36.5	0.796	0.511	0.730	0.676	0.630	0.925
37-38	37.5	0.788	0.530	0.673	0.816	0.607	0.982
38-39	38.5	0.775	0.561	0.587	1.034	0.591	1.023
39-40	39.5	0.748	0.630	0.521	1.198	0.663	0.843
40-41	40.5	0.723	0.693	0.603	0.993	0.684	0.790
41-42	41.5	0.783	0.543	0.764	0.589	0.654	0.865
42-43	42.5	0.823	0.442	0.780	0.551	0.670	0.826
43-44	43.5	0.762	0.596	0.782	0.546	0.673	0.816
44-45	44.5	0.711	0.722	0.756	0.611	0.658	0.855
45-46	45.5	0.608	0.981	0.656	0.861	0.688	0.779
46-47	46.5	0.547	1.134	0.594	1.014	0.743	0.643
47-48	47.5	0.518	1.206	0.587	1.033	0.744	0.639
48-49	48.5	0.582	1.044	0.611	0.972	0.698	0.755
49-50	49.5	0.646	0.884	0.544	1.139	0.677	0.807
50-52	51	0.583	1.042	0.622	0.944	0.709	0.729
52-54	53	0.742	0.645	0.674	0.815	0.638	0.905
54-56	55	0.756	0.611	0.680	0.801	0.640	0.900
56-58	57	0.598	1.006	0.627	0.932	0.603	0.992
58-60	59	0.659	0.854	-	-	-	-
60-62	61	0.793	0.518	-	-	-	-
62-64	63	0.757	0.607	-	-	-	-
64-66	65	0.642	0.895	-	-	-	-
66-68	67	0.628	0.930	-	-	-	-
68-70	69	0.682	0.794	-	-	-	-
70-72	71	0.676	0.811	-	-	-	-
72-74	73	0.697	0.758	-	-	-	-

Appendix 5c
Calculated porosity and bulk density values for all DBI sites.

Sample interval (cm)	Plot depth (cm)	Porosity (%)	Bulk density (g cm^{-3})	Porosity (%)	Bulk density (g cm^{-3})	Porosity (%)	Bulk density (g cm^{-3})
		HIGH		MID		LOW	
0-0.5	0.25	0.915	0.187	0.840	0.359	0.624	0.359
0.5-1	0.75	0.187	0.349	0.732	0.628	0.587	0.628
1-1.5	1.25	0.852	0.618	0.726	0.661	0.596	0.661
1.5-2	1.75	0.349	0.703	0.653	0.847	0.660	0.847
2-2.5	2.25	0.743	0.739	0.598	0.986	0.710	0.986
2.5-3	2.75	0.618	0.604	0.560	1.081	0.704	1.081
3-4	3.5	0.713	0.523	0.587	1.016	0.715	1.016
4-5	4.5	0.703	0.507	0.637	0.889	0.766	0.889
5-6	5.5	0.700	0.498	0.658	0.841	0.755	0.841
6-7	6.5	0.739	0.543	0.662	0.826	0.753	0.826
7-8	7.5	0.754	0.564	0.699	0.739	0.764	0.739
8-9	8.5	0.604	0.681	0.726	0.666	0.780	0.666
9-10	9.5	0.785	0.815	0.732	0.654	0.777	0.654
10-11	10.5	0.523	0.764	0.747	0.621	0.758	0.621
11-12	11.5	0.791	0.649	0.769	0.567	0.737	0.567
12-13	12.5	0.507	0.597	0.766	0.564	0.752	0.564
13-14	13.5	0.795	0.538	0.766	0.563	0.724	0.563
14-15	14.5	0.498	0.506	0.780	0.535	0.673	0.535
15-16	15.5	0.778	0.539	0.781	0.533	0.664	0.533
16-17	16.5	0.543	0.568	0.791	0.511	0.667	0.511
17-18	17.5	0.768	0.595	0.785	0.524	0.673	0.524
18-19	18.5	0.564	0.590	0.785	0.520	0.620	0.520
19-20	19.5	0.749	0.614	0.792	0.509	0.700	0.509
20-21	20.5	0.757	0.592	0.779	0.536	0.708	0.536
21-22	21.5	0.722	0.684	0.777	0.548	0.653	0.548
22-23	22.5	0.699	0.740	0.770	0.555	0.694	0.555
23-24	23.5	0.702	0.734	0.765	0.575	0.624	0.575
24-25	24.5	0.712	0.709	0.760	0.579	0.660	0.579
25-26	25.5	0.696	0.753	0.757	0.601	0.699	0.601
26-27	26.5	0.709	0.722	0.750	0.615	0.703	0.615
27-28	27.5	0.745	0.625	0.757	0.597	0.723	0.597
28-29	28.5	0.770	0.564	0.714	0.699	0.769	0.699
29-30	29.5	0.795	0.497	0.723	0.681	0.784	0.681
30-31	30.5	0.807	0.483	0.746	0.634	0.770	0.634
31-32	31.5	0.806	0.486	0.761	0.596	0.777	0.596
32-33	32.5	0.808	0.480	0.759	0.603	0.750	0.603

Sample interval (cm)	Plot depth (cm)	Porosity (%)	Bulk density (g cm^{-3})	Porosity (%)	Bulk density (g cm^{-3})	Porosity (%)	Bulk density (g cm^{-3})
		HIGH		MID		LOW	
33-34	33.5	0.817	0.458	0.809	0.477	0.747	0.477
34-35	34.5	0.821	0.449	0.824	0.439	0.743	0.439
35-36	35.5	0.805	0.488	0.828	0.429	0.760	0.429
36-37	36.5	0.737	0.657	0.815	0.462	0.761	0.462
37-38	37.5	0.771	0.572	0.813	0.468	0.743	0.468
38-39	38.5	0.805	0.487	0.815	0.463	0.712	0.463
39-40	39.5	0.791	0.523	0.776	0.560	0.714	0.560
40-41	40.5	0.752	0.620	0.737	0.658	0.736	0.658
41-42	41.5	0.740	0.649	0.702	0.745	0.721	0.745
42-43	42.5	0.778	0.554	0.717	0.706	0.738	0.706
43-44	43.5	0.781	0.547	0.617	0.958	0.663	0.958
44-45	44.5	0.767	0.583	0.634	0.915	0.632	0.915
45-46	45.5	0.752	0.620	0.769	0.578	0.640	0.578
46-47	46.5	0.667	0.832	0.755	0.614	0.633	0.614
47-48	47.5	0.704	0.739	0.763	0.593	0.671	0.593
48-49	48.5	0.776	0.560	0.740	0.650	0.696	0.650
49-50	49.5	0.789	0.526	0.668	0.830	0.720	0.830
50-52	51	0.808	0.479	0.707	0.732	0.642	0.732
52-54	53	0.819	0.453	0.713	0.718	0.649	0.718
54-56	55	0.785	0.539	0.722	0.696	0.664	0.696
56-58	57	0.697	0.758	0.731	0.671	0.573	0.671
58-60	59	0.664	0.841	0.675	0.813	0.684	0.813
60-62	61	0.763	0.592	0.773	0.567	0.664	0.567
62-64	63	0.784	0.540	0.752	0.619	0.740	0.619
64-66	65	-	-	0.810	0.474	0.781	0.474
66-68	67	-	-	0.788	0.531	0.801	0.531
68-70	69	-	-	0.720	0.701	0.787	0.701
70-72	71	-	-	0.702	0.746	0.808	0.746
72-74	73	-	-	0.656	0.861	0.802	0.861
74-76	75	-	-	0.695	0.763	-	-
76-78	77	-	-	0.661	0.846	-	-
78-80	79	-	-	0.737	0.656	-	-
80-82	81	-	-	0.751	0.622	-	-
82-84	83	-	-	0.766	0.585	-	-
84-86	85	-	-	0.730	0.675	-	-
86-88	87	-	-	0.801	0.497	-	-
88-90	89	-	-	0.705	0.739	-	-
90-91	90.5	-	-	0.776	0.560	-	-

Appendix 5d
Calculated porosity and bulk density values for all BJ sites.

Sample interval (cm)	Plot depth (cm)	Porosity (%)	Bulk density (g cm^{-3})	Porosity (%)	Bulk density (g cm^{-3})	Porosity (%)	Bulk density (g cm^{-3})
		HIGH		MID		LOW	
0-0.5	0.25	0.852	0.339	0.743	0.620	0.846	0.364
0.5-1	0.75	0.842	0.354	0.719	0.664	0.861	0.333
1-1.5	1.25	0.806	0.449	0.757	0.585	0.857	0.340
1.5-2	1.75	0.828	0.394	0.769	0.552	0.849	0.359
2-2.5	2.25	0.848	0.343	0.739	0.632	0.848	0.363
2.5-3	2.75	0.859	0.321	0.756	0.573	0.847	0.366
3-4	3.5	0.863	0.307	0.817	0.428	0.847	0.366
4-5	4.5	0.868	0.293	0.827	0.408	0.887	0.260
5-6	5.5	0.884	0.253	0.825	0.412	0.877	0.285
6-7	6.5	0.898	0.222	0.829	0.406	0.840	0.384
7-8	7.5	0.901	0.210	0.799	0.469	0.822	0.425
8-9	8.5	0.894	0.226	0.825	0.408	0.816	0.447
9-10	9.5	0.874	0.276	0.821	0.419	0.842	0.376
10-11	10.5	0.873	0.283	0.817	0.431	0.853	0.345
11-12	11.5	0.888	0.252	0.820	0.426	0.883	0.274
12-13	12.5	0.883	0.262	0.803	0.462	0.857	0.338
13-14	13.5	0.880	0.272	0.811	0.439	0.840	0.382
14-15	14.5	0.874	0.282	0.807	0.456	0.888	0.262
15-16	15.5	0.883	0.260	0.811	0.445	0.892	0.244
16-17	16.5	0.877	0.280	0.824	0.413	0.867	0.313
17-18	17.5	0.854	0.337	0.823	0.415	0.851	0.355
18-19	18.5	0.858	0.331	0.846	0.352	0.810	0.460
19-20	19.5	0.849	0.354	0.848	0.345	0.817	0.446
20-21	20.5	0.839	0.379	0.853	0.333	0.890	0.254
21-22	21.5	0.835	0.391	0.860	0.318	0.906	0.214
22-23	22.5	0.838	0.383	0.849	0.347	0.914	0.194
23-24	23.5	0.851	0.350	0.840	0.368	0.908	0.202
24-25	24.5	0.846	0.363	0.851	0.343	0.879	0.279
25-26	25.5	0.842	0.373	0.857	0.328	0.865	0.310
26-27	26.5	0.838	0.383	0.855	0.334	0.889	0.248
27-28	27.5	0.850	0.350	0.852	0.343	0.910	0.190
28-29	28.5	0.853	0.345	0.852	0.341	0.915	0.179
29-30	29.5	0.856	0.339	0.851	0.373	0.914	0.181
30-31	30.5	0.848	0.379	0.845	0.387	0.919	0.203
31-32	31.5	0.852	0.371	0.839	0.404	0.929	0.177
32-33	32.5	0.858	0.355	0.833	0.418	0.929	0.178

Sample interval (cm)	Plot depth (cm)	Porosity (%)	Bulk density (g cm^{-3})	Porosity (%)	Bulk density (g cm^{-3})	Porosity (%)	Bulk density (g cm^{-3})
		HIGH		MID		LOW	
33-34	33.5	0.862	0.344	0.838	0.405	0.924	0.189
34-35	34.5	0.852	0.369	0.832	0.419	0.918	0.206
35-36	35.5	0.857	0.357	0.843	0.391	0.924	0.191
36-37	36.5	0.857	0.356	0.845	0.387	0.931	0.172
37-38	37.5	0.854	0.366	0.844	0.390	0.940	0.150
38-39	38.5	0.877	0.307	0.845	0.387	0.936	0.160
39-40	39.5	0.852	0.369	0.839	0.404	0.931	0.173
40-41	40.5	0.824	0.440	0.851	0.373	0.926	0.186
41-42	41.5	0.809	0.477	0.862	0.345	0.925	0.188
42-43	42.5	0.792	0.521	0.865	0.337	0.929	0.178
43-44	43.5	0.761	0.598	0.852	0.371	0.932	0.169
44-45	44.5	0.722	0.696	0.851	0.372	0.936	0.160
45-46	45.5	0.673	0.819	0.843	0.392	0.935	0.163
46-47	46.5	0.606	0.985	0.842	0.395	0.931	0.173
47-48	47.5	0.674	0.816	0.849	0.377	0.924	0.191
48-49	48.5	0.749	0.627	0.839	0.401	0.903	0.243
49-50	49.5	0.750	0.626	0.830	0.426	0.884	0.290
50-52	51	-	-	0.826	0.435	0.838	0.405
52-54	53	-	-	0.805	0.487	0.869	0.328
54-56	55	-	-	0.704	0.740	0.942	0.145
56-58	57	-	-	0.627	0.933	0.936	0.159
58-60	59	-	-	0.673	0.817	0.932	0.170
60-62	61	-	-	0.805	0.488	0.925	0.188
62-64	63	-	-	0.865	0.338	-	-
64-66	65	-	-	0.820	0.451	-	-
66-68	67	-	-	0.872	0.320	-	-
68-70	69	-	-	0.858	0.356	-	-
70-72	71	-	-	0.829	0.428	-	-

APPENDIX 6

Appendix 6a
^{7}Be, ^{137}Cs, and ^{210}Pb values for Rigolets High site.

Sample interval (cm)	Plot depth (cm)	^{7}Be (mBq/g)	^{7}Be error (mBq/g)	^{137}Cs (Bq/kg)	^{137}Cs error (Bq/kg)	^{210}Pb (Bq/kg)	^{210}Pb error (Bq/kg)	$^{210}Pb_{xs}$ (Bq/kg)	$^{210}Pb_{xs}$ error (Bq/kg)
0-0.5	0.25	26.20	2.33	0.92	0.10	46.72	2.67	32.37	1.65
0.5-1	0.75	11.36	0.80	1.58	0.13	53.36	3.25	39.01	2.23
1-1.5	1.25	6.48	0.57	1.52	0.15	32.26	1.87	17.91	0.86
1.5-2	1.75	2.00	0.15	1.15	0.11	37.92	2.27	23.56	1.25
2-2.5	2.25	0.00	0.00	0.00	0.00	39.03	2.16	24.68	1.14
2.5-3	2.75	2.94	0.21	0.00	0.00	38.99	2.11	24.63	1.09
3-4	3.5	0.00	0.00	0.00	0.00	35.85	2.15	21.50	1.13
4-5	4.5	0.00	0.00	1.13	0.09	43.01	2.47	28.65	1.46
5-6	5.5	0.00	0.00	0.00	0.00	39.97	2.52	25.62	1.50
6-7	6.5	0.00	0.00	1.87	0.18	51.27	3.38	36.91	2.36
7-8	7.5	0.00	0.00	3.34	0.39	61.98	3.70	47.62	2.69
8-9	8.5	0.00	0.00	2.88	0.26	52.49	3.29	38.13	2.27
9-10	9.5	0.00	0.00	4.71	0.29	72.00	4.86	57.65	3.85
10-11	10.5	0.00	0.00	2.48	0.16	58.18	4.01	43.83	2.99
11-12	11.5	0.00	0.00	3.88	0.34	63.13	3.99	48.78	2.97
12-13	12.5	0.00	0.00	4.16	0.30	71.47	4.69	57.12	3.67
13-14	13.5	0.00	0.00	2.00	0.19	53.90	3.37	39.55	2.35
14-15	14.5	0.00	0.00	4.54	0.37	19.41	1.16	5.06	0.15
15-16	15.5	0.00	0.00	5.30	0.55	51.56	3.18	37.21	2.16
16-17	16.5	0.00	0.00	5.73	0.61	39.95	2.38	25.60	1.37
17-18	17.5	0.00	0.00	4.77	0.33	53.26	3.07	38.90	2.05
18-19	18.5	0.00	0.00	4.07	0.38	47.46	3.01	33.10	1.99
19-20	19.5	0.00	0.00	4.78	0.30	50.70	3.03	36.35	2.01
20-21	20.5	-	-	2.69	0.21	37.59	2.33	23.24	1.32
21-22	21.5	-	-	3.34	0.38	38.66	2.26	24.31	1.25
22-23	22.5	-	-	6.88	0.63	39.70	2.42	25.35	1.40
23-24	23.5	-	-	9.55	0.88	47.48	2.75	33.13	1.74
24-25	24.5	-	-	-	-	44.29	2.55	29.93	1.53
25-26	25.5	-	-	-	-	40.48	2.30	26.13	1.28
26-27	26.5	-	-	-	-	42.17	2.33	27.82	1.31
27-28	27.5	-	-	-	-	41.45	2.47	27.10	1.45
28-29	28.5	-	-	-	-	41.08	2.30	26.73	1.28
29-30	29.5	-	-	-	-	31.94	1.78	17.59	0.76
30-31	30.5	-	-	-	-	33.95	2.11	19.59	1.10
31-32	31.5	-	-	-	-	31.26	1.81	16.91	0.80
32-33	32.5	-	-	-	-	35.88	2.41	21.53	1.40

Sample interval (cm)	Plot depth (cm)	^{7}Be (mBq/g)	^{7}Be error (mBq/g)	^{137}Cs (Bq/kg)	^{137}Cs error (Bq/kg)	^{210}Pb (Bq/kg)	^{210}Pb error (Bq/kg)	^{210}Pb$_{xs}$ (Bq/kg)	^{210}Pb$_{xs}$ error (Bq/kg)
33-34	33.5	-	-	-	-	36.11	2.08	21.75	1.07
34-35	34.5	-	-	-	-	31.60	2.07	17.24	1.05
35-36	35.5	-	-	-	-	35.54	2.31	21.19	1.29
36-37	36.5	-	-	-	-	34.55	1.55	20.20	0.53
37-38	37.5	-	-	-	-	-	-	-	-
38-39	38.5	-	-	-	-	32.77	2.04	18.42	1.02
39-40	39.5	-	-	-	-	32.16	2.09	17.81	1.08
40-41	40.5	-	-	-	-	28.18	1.63	13.83	0.61
41-42	41.5	-	-	-	-	25.34	1.59	10.99	0.57
42-43	42.5	-	-	-	-	22.81	1.25	8.45	0.23
43-44	43.5	-	-	-	-	15.80	0.99	1.45	-0.03
44-45	44.5	-	-	-	-	15.70	0.97	1.35	-0.05
45-46	45.5	-	-	-	-	15.98	1.01	1.63	-0.01
46-47	46.5	-	-	-	-	12.29	1.03	-2.06	0.02
47-48	47.5	-	-	-	-	14.55	0.89	0.20	-0.12
48-49	48.5	-	-	-	-	15.31	0.87	0.96	-0.14
49-50	49.5	-	-	-	-	13.19	1.28	-1.16	0.27

Appendix 6b
Radioisotope values for Rigolets Mid site.

Sample interval (cm)	Plot depth (cm)	^{7}Be (mBq/g)	^{7}Be error (mBq/g)	^{137}Cs (Bq/kg)	^{137}Cs error (Bq/kg)	^{210}Pb (Bq/kg)	^{210}Pb error (Bq/kg)	$^{210}Pb_{xs}$ (Bq/kg)	$^{210}Pb_{xs}$ error (Bq/kg)
0-0.5	0.25	4.81	0.41	1.82	0.14	36.37	2.26	22.71	1.33
0.5-1	0.75	0.00	0.00	2.63	0.23	36.81	2.13	23.15	1.21
1-1.5	1.25	0.00	0.00	2.69	0.19	36.77	1.97	23.11	1.05
1.5-2	1.75	0.00	0.00	3.72	0.25	34.19	1.95	20.53	1.02
2-2.5	2.25	0.00	0.00	6.84	0.55	35.82	1.68	22.16	0.75
2.5-3	2.75	0.00	0.00	7.50	0.65	40.08	2.09	26.42	1.17
3-4	3.5	0.00	0.00	7.34	0.64	37.67	2.25	24.01	1.33
4-5	4.5	0.00	0.00	4.98	0.37	39.74	2.51	26.08	1.59
5-6	5.5	0.00	0.00	7.32	0.49	38.35	2.50	24.69	1.57
6-7	6.5	0.00	0.00	9.55	1.00	34.08	1.96	20.42	1.04
7-8	7.5	0.00	0.00	6.61	0.55	33.46	2.05	19.80	1.12
8-9	8.5	0.00	0.00	9.15	0.90	36.26	2.31	22.60	1.39
9-10	9.5	0.00	0.00	7.31	0.71	33.94	1.92	20.28	1.00
10-11	10.5	0.00	0.00	3.59	0.28	35.19	2.16	21.53	1.24
11-12	11.5	0.00	0.00	4.31	0.46	31.64	2.04	17.98	1.12
12-13	12.5	0.00	0.00	3.65	0.40	27.06	1.62	13.40	0.70
13-14	13.5	0.00	0.00	3.86	0.30	37.26	2.52	23.60	1.60
14-15	14.5	0.00	0.00	2.81	0.29	30.80	1.77	17.14	0.84
15-16	15.5	0.00	0.00	3.33	0.32	28.31	1.57	14.65	0.65
16-17	16.5	0.00	0.00	2.13	0.16	25.62	1.65	11.96	0.72
17-18	17.5	0.00	0.00	1.27	0.10	28.13	1.79	14.47	0.87
18-19	18.5	0.00	0.00	0.00	0.00	29.57	1.82	15.91	0.89
19-20	19.5	0.00	0.00	0.00	0.00	22.56	1.38	8.90	0.46
20-21	20.5	-	-	-	-	29.56	1.97	15.90	1.04
21-22	21.5	-	-	-	-	28.28	1.84	14.62	0.92
22-23	22.5	-	-	-	-	23.89	1.49	10.23	0.56
23-24	23.5	-	-	-	-	22.87	1.40	9.21	0.47
24-25	24.5	-	-	-	-	26.69	1.69	13.03	0.76
25-26	25.5	-	-	-	-	23.31	1.54	9.65	0.62
26-27	26.5	-	-	-	-	24.46	1.43	10.80	0.50
27-28	27.5	-	-	-	-	25.48	1.60	11.82	0.68
28-29	28.5	-	-	-	-	23.72	1.37	10.06	0.44
29-30	29.5	-	-	-	-	20.56	1.21	6.90	0.28
30-31	30.5	-	-	-	-	24.70	1.36	11.04	0.44
31-32	31.5	-	-	-	-	19.43	1.23	5.77	0.30
32-33	32.5	-	-	-	-	18.59	1.16	4.93	0.24
33-34	33.5	-	-	-	-	24.41	1.38	10.75	0.45
34-35	34.5	-	-	-	-	20.61	1.34	6.95	0.41

Sample interval (cm)	Plot depth (cm)	^{7}Be (mBq/g)	^{7}Be error (mBq/g)	^{137}Cs (Bq/kg)	^{137}Cs error (Bq/kg)	^{210}Pb (Bq/kg)	^{210}Pb error (Bq/kg)	$^{210}Pb_{xs}$ (Bq/kg)	$^{210}Pb_{xs}$ error (Bq/kg)
35-36	35.5	-	-	-	-	26.31	1.69	12.65	0.77
36-37	36.5	-	-	-	-	21.25	1.24	7.59	0.32
37-38	37.5	-	-	-	-	22.44	1.23	8.78	0.30
38-39	38.5	-	-	-	-	23.05	1.38	9.39	0.46
39-40	39.5	-	-	-	-	22.07	1.28	8.41	0.36
40-41	40.5	-	-	-	-	12.41	1.05	-1.25	0.12
41-42	41.5	-	-	-	-	14.68	0.81	1.02	-0.11
42-43	42.5	-	-	-	-	-	-	-	-
43-44	43.5	-	-	-	-	12.89	0.87	-0.77	-0.06
44-45	44.5	-	-	-	-	14.42	0.89	0.76	-0.04
45-46	45.5	-	-	-	-	-	-	-	-
46-47	46.5	-	-	-	-	15.39	0.99	1.73	0.06
47-48	47.5	-	-	-	-	15.01	0.94	1.35	0.02
48-49	48.5	-	-	-	-	12.15	0.93	-1.51	0.01
49-50	49.5	-	-	-	-	13.82	0.90	0.16	-0.02

Appendix 6c
Radioisotope values for Rigolets Low site.

Sample interval (cm)	Plot depth (cm)	^{7}Be (mBq/g)	^{7}Be error (mBq/g)	^{137}Cs (Bq/kg)	^{137}Cs error (Bq/kg)	^{210}Pb (Bq/kg)	^{210}Pb error (Bq/kg)	$^{210}Pb_{xs}$ (Bq/kg)	$^{210}Pb_{xs}$ error (Bq/kg)
0-0.5	0.25	0.00	0.00	0.00	0.00	32.88	1.76	16.07	0.72
0.5-1	0.75	0.00	0.00	0.00	0.00	31.93	1.53	15.11	0.49
1-1.5	1.25	0.00	0.00	0.00	0.00	34.84	2.25	18.03	1.21
1.5-2	1.75	0.00	0.00	0.00	0.00	33.16	2.18	16.35	1.14
2-2.5	2.25	0.00	0.00	0.00	0.00	39.75	2.30	22.93	1.26
2.5-3	2.75	0.00	0.00	0.00	0.00	33.07	1.94	16.26	0.90
3-4	3.5	0.00	0.00	0.00	0.00	34.34	2.04	17.53	1.00
4-5	4.5	0.00	0.00	0.00	0.00	27.34	1.63	10.53	0.59
5-6	5.5	0.00	0.00	0.00	0.00	28.84	1.86	12.03	0.82
6-7	6.5	0.00	0.00	0.00	0.00	30.30	2.02	13.49	0.98
7-8	7.5	0.00	0.00	0.00	0.00	31.73	1.95	14.92	0.91
8-9	8.5	0.00	0.00	0.00	0.00	25.70	1.52	8.89	0.49
9-10	9.5	0.00	0.00	0.00	0.00	28.18	1.42	11.36	0.38
10-11	10.5	0.00	0.00	0.00	0.00	28.11	1.69	11.30	0.65
11-12	11.5	0.00	0.00	0.00	0.00	24.95	1.48	8.14	0.44
12-13	12.5	0.00	0.00	0.00	0.00	26.96	1.78	10.15	0.74
13-14	13.5	0.00	0.00	0.00	0.00	25.34	1.59	8.53	0.55
14-15	14.5	0.00	0.00	0.00	0.00	31.41	2.02	14.60	0.98
15-16	15.5	0.00	0.00	0.00	0.00	30.41	1.94	13.60	0.90
16-17	16.5	-	-	-	-	31.70	1.87	14.89	0.83
17-18	17.5	-	-	-	-	26.15	1.62	9.33	0.58
18-19	18.5	-	-	-	-	29.36	1.71	12.54	0.68
19-20	19.5	0.00	0.00	0.00	0.00	27.13	1.58	10.32	0.55
20-21	20.5	-	-	-	-	25.76	1.53	8.95	0.49
21-22	21.5	-	-	-	-	29.05	1.74	12.24	0.70
22-23	22.5	-	-	-	-	31.29	1.78	14.48	0.74
23-24	23.5	-	-	-	-	28.49	1.77	11.68	0.73
24-25	24.5	0.00	0.00	0.00	0.00	32.49	2.22	15.68	1.19
25-26	25.5	-	-	-	-	18.03	1.21	1.21	0.17
26-27	26.5	-	-	-	-	25.61	1.48	8.79	0.44
27-28	27.5	-	-	-	-	22.94	1.29	6.13	0.25
28-29	28.5	-	-	-	-	31.55	2.15	14.74	1.11
29-30	29.5	0.00	0.00	0.00	0.00	30.79	2.11	13.98	1.07
30-31	30.5	-	-	-	-	26.80	1.71	9.99	0.67
31-32	31.5	-	-	-	-	24.22	1.43	7.41	0.39
32-33	32.5	-	-	-	-	22.34	1.31	5.53	0.27
33-34	33.5	-	-	-	-	24.61	1.58	7.80	0.54
34-35	34.5	-	-	-	-	25.09	1.60	8.27	0.56

Sample interval (cm)	Plot depth (cm)	^{7}Be (mBq/g)	^{7}Be error (mBq/g)	^{137}Cs (Bq/kg)	^{137}Cs error (Bq/kg)	^{210}Pb (Bq/kg)	^{210}Pb error (Bq/kg)	$^{210}Pb_{xs}$ (Bq/kg)	$^{210}Pb_{xs}$ error (Bq/kg)
35-36	35.5	-	-	-	-	24.56	1.47	7.75	0.43
36-37	36.5	-	-	-	-	25.60	1.40	8.79	0.36
37-38	37.5	-	-	-	-	26.53	1.49	9.72	0.45
38-39	38.5	-	-	-	-	17.98	1.08	1.17	0.04
39-40	39.5	-	-	-	-	23.88	1.49	7.07	0.45
40-41	40.5	-	-	-	-	16.55	0.98	-0.26	-0.06
41-42	41.5	-	-	-	-	16.02	0.97	-0.79	-0.07
42-43	42.5	-	-	-	-	14.95	0.95	-1.86	-0.09
43-44	43.5	-	-	-	-	14.80	0.93	-2.01	-0.11
44-45	44.5	-	-	-	-	18.00	1.07	1.19	0.03
45-46	45.5	-	-	-	-	16.87	1.11	0.06	0.07
46-47	46.5	-	-	-	-	-	-	-	-
47-48	47.5	-	-	-	-	15.56	0.94	-1.25	-0.10

Appendix 6d
Radioisotope values for Keel Boat Pass Island High site.

Sample interval (cm)	Plot depth (cm)	^{7}Be (mBq/g)	^{7}Be error (mBq/g)	^{137}Cs (Bq/kg)	^{137}Cs error (Bq/kg)	^{210}Pb (Bq/kg)	^{210}Pb error (Bq/kg)
0-0.5	0.25	33.99	2.87	0.00	0.00	56.29	3.19
0.5-1	0.75	11.82	1.27	0.00	0.00	34.47	2.14
1-1.5	1.25	13.35	1.33	0.00	0.00	38.82	2.27
1.5-2	1.75	7.54	0.80	0.00	0.00	49.03	2.79
2-2.5	2.25	0.00	0.00	0.00	0.00	56.56	3.91
2.5-3	2.75	0.00	0.00	0.00	0.00	49.19	2.97
3-4	3.5	0.00	0.00	0.00	0.00	44.38	2.57
4-5	4.5	0.00	0.00	0.00	0.00	-	-
5-6	5.5	-	-	-	-	54.40	3.24
6-7	6.5	-	-	-	-	42.78	2.81
7-8	7.5	-	-	-	-	28.43	1.80
8-9	8.5	-	-	-	-	41.29	2.63
9-10	9.5	-	-	-	-	40.32	2.43
10-11	10.5	-	-	-	-	43.30	2.20
11-12	11.5	-	-	-	-	31.53	1.85
12-13	12.5	-	-	-	-	24.81	1.27
13-14	13.5	-	-	-	-	30.25	1.79
14-15	14.5	-	-	-	-	30.21	1.51
15-16	15.5	-	-	-	-	26.39	1.54
16-17	16.5	-	-	-	-	19.83	1.17
17-18	17.5	-	-	-	-	39.66	2.36
18-19	18.5	-	-	-	-	49.97	3.08
19-20	19.5	-	-	-	-	62.06	4.71
20-21	20.5	-	-	-	-	76.35	3.96
21-22	21.5	-	-	-	-	47.14	2.81
22-23	22.5	-	-	-	-	31.04	1.87
23-24	23.5	-	-	-	-	25.40	1.50
24-25	24.5	-	-	-	-	25.20	1.47
25-26	25.5	-	-	-	-	23.41	1.42
26-27	26.5	-	-	-	-	21.40	1.23
27-28	27.5	-	-	-	-	29.15	1.63
28-29	28.5	-	-	-	-	49.61	2.87
29-30	29.5	-	-	-	-	51.35	2.86
30-31	30.5	-	-	-	-	52.94	3.46
31-32	31.5	-	-	-	-	49.60	3.13
32-33	32.5	-	-	-	-	47.75	3.33
33-34	33.5	-	-	-	-	51.48	3.25
34-35	34.5	-	-	-	-	49.12	3.03

Sample interval (cm)	Plot depth (cm)	^{7}Be (mBq/g)	^{7}Be error (mBq/g)	^{137}Cs (Bq/kg)	^{137}Cs error (Bq/kg)	^{210}Pb (Bq/kg)	^{210}Pb error (Bq/kg)
35-36	35.5	-	-	-	-	52.65	3.35
36-37	36.5	-	-	-	-	51.90	3.24
37-38	37.5	-	-	-	-	40.69	2.68
38-39	38.5	-	-	-	-	41.83	2.72
39-40	39.5	-	-	-	-	46.15	3.25

Appendix 6e
Radioisotope values for Keel Boat Pass Island Mid site.

Sample interval (cm)	Plot depth (cm)	^{7}Be (mBq/g)	^{7}Be error (mBq/g)	^{137}Cs (Bq/kg)	^{137}Cs error (Bq/kg)	^{210}Pb (Bq/kg)	^{210}Pb error (Bq/kg)	^{210}Pb$_{xs}$ (Bq/kg)	^{210}Pb$_{xs}$ error (Bq/kg)
0-0.5	0.25	0.00	0.00	0.00	0.00	41.30	2.40	18.06	1.01
0.5-1	0.75	0.00	0.00	0.00	0.00	37.16	2.19	13.92	0.79
1-1.5	1.25	0.00	0.00	0.00	0.00	35.57	1.96	12.33	0.57
1.5-2	1.75	0.00	0.00	0.00	0.00	31.48	1.74	8.24	0.34
2-2.5	2.25	0.00	0.00	0.51	0.04	34.94	2.07	11.70	0.67
2.5-3	2.75	0.00	0.00	0.00	0.00	20.47	1.23	-2.77	-0.16
3-4	3.5	0.00	0.00	0.00	0.00	25.96	1.52	2.72	0.13
4-5	4.5	-	-	-	-	-	-	-	-
5-6	5.5	-	-	-	-	28.22	1.56	4.98	0.17
6-7	6.5	-	-	-	-	45.22	2.57	21.98	1.18
7-8	7.5	-	-	-	-	51.12	3.25	27.88	1.85
8-9	8.5	-	-	-	-	48.16	2.67	24.92	1.28
9-10	9.5	-	-	-	-	42.91	2.97	19.67	1.58
10-11	10.5	-	-	-	-	37.31	2.34	14.07	0.94
11-12	11.5	-	-	-	-	40.63	2.53	17.40	1.14
12-13	12.5	-	-	-	-	43.37	2.94	20.13	1.54
13-14	13.5	-	-	-	-	34.85	2.16	11.61	0.76
14-15	14.5	-	-	-	-	45.66	2.95	22.42	1.56
15-16	15.5	-	-	-	-	50.16	3.03	26.92	1.63
16-17	16.5	-	-	-	-	48.58	2.85	25.34	1.45
17-18	17.5	-	-	-	-	44.08	2.68	20.84	1.28
18-19	18.5	-	-	-	-	37.83	2.17	14.59	0.78
19-20	19.5	-	-	-	-	38.25	2.29	15.01	0.89
20-21	20.5	-	-	-	-	45.91	2.84	22.68	1.44
21-22	21.5	-	-	-	-	40.91	2.50	17.67	1.11
22-23	22.5	-	-	-	-	49.59	2.93	26.35	1.54
23-24	23.5	-	-	-	-	50.37	3.16	27.13	1.76
24-25	24.5	-	-	-	-	45.34	2.73	22.10	1.33
25-26	25.5	-	-	-	-	35.09	2.21	11.85	0.81
26-27	26.5	-	-	-	-	23.08	1.30	-0.16	-0.09
27-28	27.5	-	-	-	-	22.10	1.30	-1.14	-0.09
28-29	28.5	-	-	-	-	22.82	1.28	-0.42	-0.11
29-30	29.5	-	-	-	-	20.96	1.21	-2.28	-0.19
30-31	30.5	-	-	-	-	27.98	1.82	4.74	0.42
31-32	31.5	-	-	-	-	20.29	1.13	-2.95	-0.27
32-33	32.5	-	-	-	-	27.96	1.57	4.73	0.18
33-34	33.5	-	-	-	-	26.43	1.50	3.19	0.10
34-35	34.5	-	-	-	-	30.58	1.82	7.34	0.43

Sample interval (cm)	Plot depth (cm)	^{7}Be (mBq/g)	^{7}Be error (mBq/g)	^{137}Cs (Bq/kg)	^{137}Cs error (Bq/kg)	^{210}Pb (Bq/kg)	^{210}Pb error (Bq/kg)	$^{210}Pb_{xs}$ (Bq/kg)	$^{210}Pb_{xs}$ error (Bq/kg)
35-36	35.5	-	-	-	-	52.71	3.09	29.47	1.70
36-37	36.5	-	-	-	-	26.09	1.42	2.85	0.02
37-38	37.5	-	-	-	-	26.16	1.71	2.92	0.31
38-39	38.5	-	-	-	-	22.38	1.41	-0.86	0.02
39-40	39.5	-	-	-	-	20.76	1.22	-2.48	-0.18
40-41	40.5	-	-	-	-	25.32	1.47	2.08	0.08
41-42	41.5	-	-	-	-	35.68	2.33	12.44	0.93
42-43	42.5	-	-	-	-	34.44	2.18	11.20	0.78
43-44	43.5	-	-	-	-	31.38	1.65	8.14	0.26
44-45	44.5	-	-	-	-	31.51	1.86	8.27	0.46
45-46	45.5	-	-	-	-	24.76	1.61	1.52	0.22
46-47	46.5	-	-	-	-	23.57	1.50	0.33	0.10
47-48	47.5	-	-	-	-	24.24	1.41	1.00	0.01
48-49	48.5	-	-	-	-	23.08	1.33	-0.16	-0.06
49-50	49.5	-	-	-	-	22.40	1.45	-0.84	0.05

Appendix 6f
Radioisotope values for Keel Boat Pass Island Low site.

Sample interval (cm)	Plot depth (cm)	^{7}Be (mBq/g)	^{7}Be error (mBq/g)	^{137}Cs (Bq/kg)	^{137}Cs error (Bq/kg)	^{210}Pb (Bq/kg)	^{210}Pb error (Bq/kg)	^{210}Pb$_{xs}$ (Bq/kg)	^{210}Pb$_{xs}$ error (Bq/kg)
0-0.5	0.25	0.00	0.00	0.00	0.00	37.53	2.03	10.81	0.47
0.5-1	0.75	0.00	0.00	0.00	0.00	44.80	2.65	18.08	1.10
1-1.5	1.25	0.00	0.00	0.00	0.00	45.01	2.47	18.29	0.91
1.5-2	1.75	0.00	0.00	0.84	0.11	53.03	3.30	26.31	1.75
2-2.5	2.25	0.00	0.00	0.00	0.00	46.64	2.78	19.92	1.23
2.5-3	2.75	0.00	0.00	0.00	0.00	48.80	2.87	22.08	1.31
3-4	3.5	0.00	0.00	1.71	0.17	39.87	2.15	13.15	0.60
4-5	4.5	-	-	-	-	35.11	2.16	8.38	0.60
5-6	5.5	-	-	-	-	39.44	2.83	12.72	1.27
6-7	6.5	-	-	-	-	43.47	2.42	16.75	0.86
7-8	7.5	-	-	-	-	43.86	2.46	17.14	0.90
8-9	8.5	-	-	-	-	41.74	2.45	15.02	0.89
9-10	9.5	-	-	-	-	34.10	2.06	7.38	0.50
10-11	10.5	-	-	-	-	32.78	1.82	6.06	0.26
11-12	11.5	-	-	-	-	33.49	2.01	6.77	0.45
12-13	12.5	-	-	-	-	28.43	1.62	1.71	0.06
13-14	13.5	-	-	-	-	22.83	1.34	-3.89	-0.22
14-15	14.5	-	-	-	-	25.04	1.42	-1.69	-0.13
15-16	15.5	-	-	-	-	23.10	1.39	-3.62	-0.16
16-17	16.5	-	-	-	-	18.58	1.10	-8.15	-0.46
17-18	17.5	-	-	-	-	20.97	1.19	-5.75	-0.37
18-19	18.5	-	-	-	-	25.92	1.58	-0.81	0.02
19-20	19.5	-	-	-	-	28.96	1.49	2.24	-0.07
20-21	20.5	-	-	-	-	32.99	2.10	6.27	0.55
21-22	21.5	-	-	-	-	29.07	1.88	2.35	0.32
22-23	22.5	-	-	-	-	33.66	2.27	6.94	0.71
23-24	23.5	-	-	-	-	39.01	2.40	12.29	0.85
24-25	24.5	-	-	-	-	37.05	2.18	10.33	0.63
25-26	25.5	-	-	-	-	35.12	2.29	8.40	0.74
26-27	26.5	-	-	-	-	29.13	1.84	2.41	0.28
27-28	27.5	-	-	-	-	24.61	1.59	-2.11	0.04
28-29	28.5	-	-	-	-	28.28	1.75	1.56	0.19
29-30	29.5	-	-	-	-	32.56	1.86	5.83	0.30
30-31	30.5	-	-	-	-	37.21	2.42	10.49	0.86
31-32	31.5	-	-	-	-	32.34	1.71	5.61	0.15
32-33	32.5	-	-	-	-	28.90	1.70	2.18	0.15
33-34	33.5	-	-	-	-	27.66	1.80	0.94	0.24
34-35	34.5	-	-	-	-	25.37	1.41	-1.36	-0.14

Sample interval (cm)	Plot depth (cm)	^{7}Be (mBq/g)	^{7}Be error (mBq/g)	^{137}Cs (Bq/kg)	^{137}Cs error (Bq/kg)	^{210}Pb (Bq/kg)	^{210}Pb error (Bq/kg)	$^{210}Pb_{xs}$ (Bq/kg)	$^{210}Pb_{xs}$ error (Bq/kg)
35-36	35.5	-	-	-	-	26.57	1.51	-0.15	-0.05
36-37	36.5	-	-	-	-	24.56	1.27	-2.16	-0.29
37-38	37.5	-	-	-	-	25.72	1.45	-1.00	-0.11
38-39	38.5	-	-	-	-	26.19	1.55	-0.53	-0.01
39-40	39.5	-	-	-	-	28.25	1.67	1.53	0.11

Appendix 6g
Radioisotope values for Dry Bread Island High site.

Sample interval (cm)	Plot depth (cm)	^{7}Be (mBq/g)	^{7}Be error (mBq/g)	^{137}Cs (Bq/kg)	^{137}Cs error (Bq/kg)	^{210}Pb (Bq/kg)	^{210}Pb error (Bq/kg)
0-0.5	0.25	0.00	0.00	0.00	0.00	36.43	2.29
0.5-1	0.75	0.00	0.00	0.00	0.00	37.37	2.40
1-1.5	1.25	0.00	0.00	0.00	0.00	31.71	1.83
1.5-2	1.75	0.00	0.00	0.00	0.00	28.38	1.66
2-2.5	2.25	0.00	0.00	0.00	0.00	23.56	1.38
2.5-3	2.75	0.00	0.00	0.00	0.00	22.57	1.42
3-4	3.5	0.00	0.00	0.00	0.00	19.73	0.98
4-5	4.5	0.00	0.00	0.00	0.00	20.47	0.89
5-6	5.5	-	-	-	-	22.05	0.98
6-7	6.5	-	-	-	-	22.38	1.14
7-8	7.5	-	-	-	-	31.62	1.85
8-9	8.5	-	-	-	-	25.09	1.49
9-10	9.5	0.00	0.00	0.00	0.00	21.08	1.22
10-11	10.5	-	-	-	-	20.21	1.17
11-12	11.5	-	-	-	-	22.28	1.27
12-13	12.5	-	-	-	-	24.52	1.45
13-14	13.5	-	-	-	-	23.33	1.30
14-15	14.5	0.00	0.00	0.00	0.00	27.17	1.65
15-16	15.5	-	-	-	-	25.03	1.44
16-17	16.5	-	-	-	-	26.10	1.51
17-18	17.5	-	-	-	-	30.52	1.83
18-19	18.5	-	-	-	-	36.03	2.23
19-20	19.5	0.00	0.00	0.00	0.00	34.30	1.87
20-21	20.5	-	-	-	-	33.40	2.07
21-22	21.5	-	-	-	-	29.37	1.97
22-23	22.5	-	-	-	-	29.66	1.87
23-24	23.5	-	-	-	-	-	-
24-25	24.5	0.00	0.00	0.00	0.00	32.59	1.99
25-26	25.5	-	-	-	-	21.69	1.30
26-27	26.5	-	-	-	-	20.46	1.23
27-28	27.5	-	-	-	-	28.37	1.86
28-29	28.5	-	-	-	-	32.90	1.91
29-30	29.5	0.00	0.00	0.00	0.00	37.82	2.69
30-31	30.5	-	-	-	-	45.86	2.13
31-32	31.5	-	-	-	-	39.82	2.38
32-33	32.5	-	-	-	-	41.96	2.58
33-34	33.5	-	-	-	-	34.06	2.19
34-35	34.5	-	-	-	-	32.56	1.88

Sample interval (cm)	Plot depth (cm)	^{7}Be (mBq/g)	^{7}Be error (mBq/g)	^{137}Cs (Bq/kg)	^{137}Cs error (Bq/kg)	^{210}Pb (Bq/kg)	^{210}Pb error (Bq/kg)
35-36	35.5	-	-	-	-	34.28	2.08
36-37	36.5	-	-	-	-	31.40	1.87
37-38	37.5	-	-	-	-	30.80	1.97
38-39	38.5	-	-	-	-	22.33	1.35
39-40	39.5	-	-	-	-	29.88	1.94
40-41	40.5	-	-	-	-	44.21	3.05
41-42	41.5	-	-	-	-	34.83	1.92
42-43	42.5	-	-	-	-	39.44	2.49
43-44	43.5	-	-	-	-	55.01	3.46
44-45	44.5	-	-	-	-	46.44	2.82
45-46	45.5	-	-	-	-	37.69	2.30
46-47	46.5	-	-	-	-	31.35	1.81
47-48	47.5	-	-	-	-	34.00	2.05
48-49	48.5	-	-	-	-	38.28	2.12
49-50	49.5	-	-	-	-	50.53	3.09

Appendix 6h
Radioisotope values for Dry Bread Island Mid site.

Sample interval (cm)	Plot depth (cm)	^{7}Be (mBq/g)	^{7}Be error (mBq/g)	^{137}Cs (Bq/kg)	^{137}Cs error (Bq/kg)	^{210}Pb (Bq/kg)	^{210}Pb error (Bq/kg)
0-0.5	0.25	0.00	0.00	0.00	0.00	15.54	0.97
0.5-1	0.75	0.00	0.00	0.00	0.00	19.24	1.16
1-1.5	1.25	0.00	0.00	0.00	0.00	15.06	0.88
1.5-2	1.75	0.00	0.00	0.00	0.00	17.59	1.10
2-2.5	2.25	0.00	0.00	0.00	0.00	24.53	1.70
2.5-3	2.75	0.00	0.00	0.00	0.00	18.17	1.05
3-4	3.5	0.00	0.00	0.00	0.00	27.84	1.55
4-5	4.5	0.00	0.00	0.00	0.00	37.77	2.20
5-6	5.5	0.00	0.00	0.00	0.00	31.81	1.79
6-7	6.5	0.00	0.00	0.00	0.00	33.33	2.02
7-8	7.5	0.00	0.00	0.00	0.00	33.09	1.97
8-9	8.5	0.00	0.00	0.00	0.00	36.40	2.25
9-10	9.5	0.00	0.00	0.00	0.00	35.35	1.77
10-11	10.5	0.00	0.00	0.00	0.00	33.84	1.99
11-12	11.5	0.00	0.00	0.00	0.00	38.70	2.36
12-13	12.5	0.00	0.00	0.00	0.00	36.23	1.98
13-14	13.5	0.00	0.00	1.16	0.12	36.83	2.31
14-15	14.5	0.00	0.00	1.04	0.09	39.80	2.35
15-16	15.5	0.00	0.00	0.00	0.00	34.61	2.05
16-17	16.5	0.00	0.00	0.00	0.00	37.92	2.09
17-18	17.5	0.00	0.00	0.00	0.00	36.04	2.03
18-19	18.5	0.00	0.00	1.21	0.12	30.80	1.36
19-20	19.5	0.00	0.00	1.22	0.12	37.75	1.94
20-21	20.5	0.00	0.00	1.23	0.14	32.09	1.69
21-22	21.5	0.00	0.00	2.29	0.30	38.16	2.37
22-23	22.5	0.00	0.00	0.00	0.00	34.05	2.04
23-24	23.5	0.00	0.00	1.54	0.21	32.72	2.09
24-25	24.5	0.00	0.00	1.43	0.16	-	-
25-26	25.5	0.00	0.00	1.13	0.12	31.69	2.02
26-27	26.5	0.00	0.00	1.94	0.18	34.59	2.10
27-28	27.5	0.00	0.00	1.01	0.07	30.32	1.78
28-29	28.5	0.00	0.00	0.00	0.00	28.51	1.50
29-30	29.5	0.00	0.00	0.00	0.00	32.22	1.54
30-31	30.5	0.00	0.00	0.000	0.000	42.07	2.54
31-32	31.5	0.00	0.00	1.905	0.187	36.44	2.35
32-33	32.5	-	-	-	-	34.74	2.02
33-34	33.5	-	-	-	-	39.49	2.51
34-35	34.5	-	-	-	-	45.12	2.92

Sample interval (cm)	Plot depth (cm)	^{7}Be (mBq/g)	^{7}Be error (mBq/g)	^{137}Cs (Bq/kg)	^{137}Cs error (Bq/kg)	^{210}Pb (Bq/kg)	^{210}Pb error (Bq/kg)
35-36	35.5	-	-	-	-	41.69	2.55
36-37	36.5	-	-	-	-	39.14	2.30
37-38	37.5	-	-	-	-	41.17	2.67
38-39	38.5	-	-	-	-	28.67	1.79
39-40	39.5	-	-	-	-	38.76	2.51
40-41	40.5	-	-	-	-	45.41	3.08
41-42	41.5	-	-	-	-	38.58	2.22
42-43	42.5	-	-	-	-	35.94	2.24
43-44	43.5	-	-	-	-	37.51	2.34
44-45	44.5	-	-	-	-	34.57	1.86
45-46	45.5	-	-	-	-	35.77	2.04
46-47	46.5	-	-	-	-	36.03	2.02
47-48	47.5	-	-	-	-	35.23	2.56
48-49	48.5	-	-	-	-	35.38	2.49
49-50	49.5	-	-	-	-	37.89	2.45

Appendix 6i
Radioisotope values for Dry Bread Island Low site.

Sample interval (cm)	Plot depth (cm)	^{7}Be (mBq/g)	^{7}Be error (mBq/g)	^{137}Cs (Bq/kg)	^{137}Cs error (Bq/kg)	^{210}Pb (Bq/kg)	^{210}Pb error (Bq/kg)
0-0.5	0.25	0.00	0.00	0.00	0.00	19.15	1.11
0.5-1	0.75	0.00	0.00	0.00	0.00	25.69	1.48
1-1.5	1.25	0.00	0.00	0.00	0.00	23.62	1.30
1.5-2	1.75	0.00	0.00	0.00	0.00	24.03	1.40
2-2.5	2.25	0.00	0.00	0.00	0.00	20.63	1.16
2.5-3	2.75	0.00	0.00	0.00	0.00	25.69	1.44
3-4	3.5	0.00	0.00	0.00	0.00	22.89	1.36
4-5	4.5	0.00	0.00	0.00	0.00	23.66	1.38
5-6	5.5	0.00	0.00	0.00	0.00	9.15	0.51
6-7	6.5	0.00	0.00	0.00	0.00	28.39	1.50
7-8	7.5	0.00	0.00	0.00	0.00	25.53	1.49
8-9	8.5	0.00	0.00	0.00	0.00	24.58	1.44
9-10	9.5	0.00	0.00	0.00	0.00	26.56	1.53
10-11	10.5	0.00	0.00	0.00	0.00	31.80	1.90
11-12	11.5	0.00	0.00	0.00	0.00	27.78	1.53
12-13	12.5	0.00	0.00	0.00	0.00	24.96	1.42
13-14	13.5	0.00	0.00	0.00	0.00	23.25	1.23
14-15	14.5	0.00	0.00	0.00	0.00	23.42	1.35
15-16	15.5	-	-	-	-	22.74	1.30
16-17	16.5	-	-	-	-	24.63	1.43
17-18	17.5	-	-	-	-	23.97	1.25
18-19	18.5	-	-	-	-	21.84	1.04
19-20	19.5	0.00	0.00	0.00	0.00	23.15	1.24
20-21	20.5	-	-	-	-	23.82	1.30
21-22	21.5	-	-	-	-	23.19	1.28
22-23	22.5	-	-	-	-	21.12	1.09
23-24	23.5	-	-	-	-	18.85	0.92
24-25	24.5	0.00	0.00	0.00	0.00	21.18	1.24
25-26	25.5	-	-	-	-	21.30	1.22
26-27	26.5	-	-	-	-	24.41	1.47
27-28	27.5	-	-	-	-	19.32	1.15
28-29	28.5	-	-	-	-	21.75	1.27
29-30	29.5	-	-	-	-	22.77	1.32
30-31	30.5	-	-	-	-	19.54	1.23
31-32	31.5	-	-	-	-	22.56	1.35
32-33	32.5	-	-	-	-	22.35	1.38
33-34	33.5	-	-	-	-	23.88	1.50
34-35	34.5	-	-	-	-	24.21	1.34

Sample interval (cm)	Plot depth (cm)	^{7}Be (mBq/g)	^{7}Be error (mBq/g)	^{137}Cs (Bq/kg)	^{137}Cs error (Bq/kg)	^{210}Pb (Bq/kg)	^{210}Pb error (Bq/kg)
35-36	35.5	-	-	-	-	24.57	1.54
36-37	36.5	-	-	-	-	26.26	1.66
37-38	37.5	-	-	-	-	22.73	1.43
38-39	38.5	-	-	-	-	20.68	1.12
39-40	39.5	-	-	-	-	16.09	1.00
40-41	40.5	-	-	-	-	23.75	1.52
41-42	41.5	-	-	-	-	20.37	1.32
42-43	42.5	-	-	-	-	26.21	1.61
43-44	43.5	-	-	-	-	22.95	1.29
44-45	44.5	-	-	-	-	24.50	1.53
45-46	45.5	-	-	-	-	27.02	1.73
46-47	46.5	-	-	-	-	23.89	1.64
47-48	47.5	-	-	-	-	26.44	1.54
48-49	48.5	-	-	-	-	25.41	1.72
49-50	49.5	-	-	-	-	22.99	1.60

Appendix 6j
Radioisotope values for Bay Jimmy High site.

Sample interval (cm)	Plot depth (cm)	^{7}Be (mBq/g)	^{7}Be error (mBq/g)	^{137}Cs (Bq/kg)	^{137}Cs error (Bq/kg)	^{210}Pb (Bq/kg)	^{210}Pb error (Bq/kg)	$^{210}Pb_{xs}$ (Bq/kg)	$^{210}Pb_{xs}$ error (Bq/kg)
0-0.5	0.25	0.00	0.00	2.03	0.17	-	-	-	-
0.5-1	0.75	0.00	0.00	0.00	0.00	75.95	4.58	43.60	2.52
1-1.5	1.25	0.00	0.00	1.79	0.24	75.93	4.65	43.57	2.59
1.5-2	1.75	0.00	0.00	1.64	0.20	75.58	4.85	43.23	2.79
2-2.5	2.25	0.00	0.00	1.72	0.14	93.88	6.01	61.53	3.95
2.5-3	2.75	0.00	0.00	-	-	86.18	6.36	53.82	4.30
3-4	3.5	0.00	0.00	2.04	0.23	85.55	5.52	53.20	3.46
4-5	4.5	0.00	0.00	2.21	0.21	91.93	6.27	59.58	4.21
5-6	5.5	-	-	-	-	77.60	5.53	45.25	3.47
6-7	6.5	-	-	-	-	103.49	6.18	71.14	4.11
7-8	7.5	-	-	-	-	98.31	6.95	65.96	4.89
8-9	8.5	-	-	-	-	116.47	6.92	84.12	4.86
9-10	9.5	-	-	-	-	116.03	6.67	83.68	4.61
10-11	10.5	-	-	-	-	87.43	5.66	55.07	3.60
11-12	11.5	-	-	-	-	92.08	6.13	59.73	4.07
12-13	12.5	-	-	-	-	94.23	5.18	61.87	3.12
13-14	13.5	-	-	-	-	88.80	4.36	56.45	2.30
14-15	14.5	-	-	-	-	85.69	4.54	53.34	2.47
15-16	15.5	-	-	-	-	101.68	6.34	69.33	4.28
16-17	16.5	-	-	-	-	91.89	5.85	59.54	3.79
17-18	17.5	-	-	-	-	73.77	5.54	41.42	3.48
18-19	18.5	-	-	-	-	90.72	6.17	58.36	4.11
19-20	19.5	-	-	-	-	74.68	5.64	42.32	3.58
20-21	20.5	-	-	-	-	78.19	5.06	45.84	3.00
21-22	21.5	-	-	-	-	83.03	4.53	50.67	2.47
22-23	22.5	-	-	-	-	91.12	5.24	58.77	3.18
23-24	23.5	-	-	-	-	105.02	7.44	72.67	5.38
24-25	24.5	-	-	-	-	92.04	7.00	59.69	4.94
25-26	25.5	-	-	-	-	101.25	6.02	68.89	3.96
26-27	26.5	-	-	-	-	89.25	6.18	56.90	4.12
27-28	27.5	-	-	-	-	90.54	6.95	58.19	4.89
28-29	28.5	-	-	-	-	64.61	4.01	32.25	1.95
29-30	29.5	-	-	-	-	84.02	4.92	51.66	2.86
30-31	30.5	-	-	-	-	74.01	4.96	41.66	2.90
31-32	31.5	-	-	-	-	66.64	4.60	34.29	2.54
32-33	32.5	-	-	-	-	64.45	4.08	32.09	2.01
33-34	33.5	-	-	-	-	65.15	4.37	32.80	2.31
34-35	34.5	-	-	-	-	64.46	3.57	32.10	1.50

Sample interval (cm)	Plot depth (cm)	^{7}Be (mBq/g)	^{7}Be error (mBq/g)	^{137}Cs (Bq/kg)	^{137}Cs error (Bq/kg)	^{210}Pb (Bq/kg)	^{210}Pb error (Bq/kg)	^{210}Pb$_{xs}$ (Bq/kg)	^{210}Pb$_{xs}$ error (Bq/kg)
35-36	35.5	-	-	-	-	61.16	4.28	28.81	2.22
36-37	36.5	-	-	-	-	74.42	6.05	42.07	3.99
37-38	37.5	-	-	-	-	58.15	4.22	25.80	2.16
38-39	38.5	-	-	-	-	59.27	3.19	26.92	1.13
39-40	39.5	-	-	-	-	62.22	3.77	29.87	1.71
40-41	40.5	-	-	-	-	-	-	-	-
41-42	41.5	-	-	-	-	45.35	2.61	12.99	0.55
42-43	42.5	-	-	-	-	36.84	2.26	4.49	0.20
43-44	43.5	-	-	-	-	34.70	2.05	2.35	-0.01
44-45	44.5	-	-	-	-	32.03	2.13	-0.32	0.07
45-46	45.5	-	-	-	-	30.33	2.00	-2.02	-0.06

Appendix 6k
Radioisotope values for Bay Jimmy Mid site.

Sample interval (cm)	Plot depth (cm)	^{7}Be (mBq/g)	^{7}Be error (mBq/g)	^{137}Cs (Bq/kg)	^{137}Cs error (Bq/kg)	^{210}Pb (Bq/kg)	^{210}Pb error (Bq/kg)
0-0.5	0.25	0.00	0.00	0.00	0.00	51.87	3.37
0.5-1	0.75	0.00	0.00	0.57	0.07	52.48	2.82
1-1.5	1.25	0.00	0.00	1.56	0.23	54.93	2.59
1.5-2	1.75	0.00	0.00	1.44	0.11	64.31	4.56
2-2.5	2.25	0.00	0.00	0.96	0.11	47.25	3.06
2.5-3	2.75	0.00	0.00	1.47	0.16	63.65	4.07
3-4	3.5	0.00	0.00	1.57	0.19	73.34	4.78
4-5	4.5	0.00	0.00	1.35	0.15	67.40	3.93
5-6	5.5	-	-	-	-	65.03	4.48
6-7	6.5	-	-	-	-	76.61	5.28
7-8	7.5	-	-	-	-	72.48	4.17
8-9	8.5	-	-	-	-	75.35	4.28
9-10	9.5	-	-	-	-	74.90	4.35
10-11	10.5	-	-	-	-	79.76	5.28
11-12	11.5	-	-	-	-	55.01	3.38
12-13	12.5	-	-	-	-	55.98	3.60
13-14	13.5	-	-	-	-	-	-
14-15	14.5	-	-	-	-	59.14	3.83
15-16	15.5	-	-	-	-	65.38	3.98
16-17	16.5	-	-	-	-	62.32	3.83
17-18	17.5	-	-	-	-	60.45	3.89
18-19	18.5	-	-	-	-	75.25	5.20
19-20	19.5	-	-	-	-	70.71	3.97
20-21	20.5	-	-	-	-	72.74	5.00
21-22	21.5	-	-	-	-	54.78	3.81
22-23	22.5	-	-	-	-	71.40	4.28
23-24	23.5	-	-	-	-	62.26	4.00
24-25	24.5	-	-	-	-	61.72	3.54
25-26	25.5	-	-	-	-	55.84	3.73
26-27	26.5	-	-	-	-	67.09	3.63
27-28	27.5	-	-	-	-	67.58	4.97
28-29	28.5	-	-	-	-	69.50	4.67
29-30	29.5	-	-	-	-	72.88	5.37
30-31	30.5	-	-	-	-	94.03	5.51
31-32	31.5	-	-	-	-	98.43	5.63
32-33	32.5	-	-	-	-	100.96	7.00
33-34	33.5	-	-	-	-	85.37	6.69
34-35	34.5	-	-	-	-	90.46	6.74

Sample interval (cm)	Plot depth (cm)	^{7}Be (mBq/g)	^{7}Be error (mBq/g)	^{137}Cs (Bq/kg)	^{137}Cs error (Bq/kg)	^{210}Pb (Bq/kg)	^{210}Pb error (Bq/kg)
35-36	35.5	-	-	-	-	86.98	5.09
36-37	36.5	-	-	-	-	84.18	5.84
37-38	37.5	-	-	-	-	85.35	5.71
38-39	38.5	-	-	-	-	78.69	5.32
39-40	39.5	-	-	-	-	80.58	5.28
40-41	40.5	-	-	-	-	89.38	5.11
41-42	41.5	-	-	-	-	66.68	4.26
42-43	42.5	-	-	-	-	68.46	4.28
43-44	43.5	-	-	-	-	72.83	4.57
44-45	44.5	-	-	-	-	63.68	4.13
45-46	45.5	-	-	-	-	70.65	4.05
46-47	46.5	-	-	-	-	58.47	3.47
47-48	47.5	-	-	-	-	60.40	2.94
48-49	48.5	-	-	-	-	60.17	4.38
49-50	49.5	-	-	-	-	61.79	4.09

Appendix 6l
Radioisotope values for Bay Jimmy Low site.

Sample interval (cm)	Plot depth (cm)	^{7}Be (mBq/g)	^{7}Be error (mBq/g)	^{137}Cs (Bq/kg)	^{137}Cs error (Bq/kg)	^{210}Pb (Bq/kg)	^{210}Pb error (Bq/kg)	$^{210}Pb_{xs}$ (Bq/kg)	$^{210}Pb_{xs}$ error (Bq/kg)
0-0.5	0.25	0.00	0.00	16.72	1.24	40.42	2.45	24.00	1.30
0.5-1	0.75	0.00	0.00	21.25	1.37	-	-	-	-
1-1.5	1.25	0.00	0.00	18.95	1.24	42.76	2.47	26.34	1.31
1.5-2	1.75	0.00	0.00	17.70	1.16	38.05	2.74	21.63	1.59
2-2.5	2.25	0.00	0.00	12.26	0.79	38.45	2.31	22.03	1.16
2.5-3	2.75	0.00	0.00	7.40	0.55	35.34	2.42	18.92	1.26
3-4	3.5	0.00	0.00	5.90	0.37	43.84	2.50	27.42	1.34
4-5	4.5	0.00	0.00	3.07	0.20	44.87	2.95	28.45	1.79
5-6	5.5	-	-	-	-	37.91	2.54	21.49	1.39
6-7	6.5	-	-	-	-	27.86	1.78	11.44	0.63
7-8	7.5	-	-	-	-	25.97	1.69	9.55	0.53
8-9	8.5	-	-	-	-	25.02	1.63	8.60	0.47
9-10	9.5	-	-	-	-	24.04	1.63	7.62	0.47
10-11	10.5	-	-	-	-	30.51	2.18	14.09	1.02
11-12	11.5	-	-	-	-	25.91	1.85	9.49	0.69
12-13	12.5	-	-	-	-	20.57	1.45	4.15	0.29
13-14	13.5	-	-	-	-	27.10	1.74	10.68	0.58
14-15	14.5	-	-	-	-	26.39	1.75	9.98	0.59
15-16	15.5	-	-	-	-	24.33	1.69	7.91	0.53
16-17	16.5	-	-	-	-	23.59	1.50	7.17	0.34
17-18	17.5	-	-	-	-	22.37	1.41	5.95	0.25
18-19	18.5	-	-	-	-	25.35	1.65	8.93	0.49
19-20	19.5	-	-	-	-	22.08	1.35	5.66	0.19
20-21	20.5	-	-	-	-	24.33	1.37	7.91	0.21
21-22	21.5	-	-	-	-	30.93	1.97	14.51	0.81
22-23	22.5	-	-	-	-	26.77	1.60	10.35	0.45
23-24	23.5	-	-	-	-	21.27	1.40	4.85	0.24
24-25	24.5	-	-	-	-	18.53	1.20	2.11	0.04
25-26	25.5	-	-	-	-	20.13	1.41	3.71	0.25
26-27	26.5	-	-	-	-	19.76	1.19	3.34	0.03
27-28	27.5	-	-	-	-	20.47	1.28	4.05	0.12
28-29	28.5	-	-	-	-	17.86	1.13	1.44	-0.02
29-30	29.5	-	-	-	-	20.75	1.41	4.33	0.25
30-31	30.5	-	-	-	-	20.35	1.18	3.93	0.02
31-32	31.5	-	-	-	-	18.09	1.15	1.67	-0.01
32-33	32.5	-	-	-	-	17.04	1.07	0.62	-0.09
33-34	33.5	-	-	-	-	15.77	1.27	-0.65	0.11
34-35	34.5	-	-	-	-	16.45	1.14	0.03	-0.02

APPENDIX 7

^{234}Th and ^{238}U data for all sites.

Station	Core Label	Plot depth (cm)	Decay-corrected $^{234}Th_{xs}$ (Bq kg^{-1})	Decay-corrected $^{234}Th_{xs}$ error	^{238}U (Bq kg^{-1})	^{238}U error
RIG	High	0.25	86.95	5.60	43.25	2.61
		0.75	66.12	4.98	48.80	3.86
		1.25	92.95	5.43	46.34	3.69
		1.75	54.48	4.12	49.08	4.22
		2.25	66.38	5.22	50.16	2.93
		2.75	51.13	4.61	42.12	2.18
		3.5	82.68	5.70	49.62	2.66
		4.5	158.11	11.28	38.25	2.28
	Mid	0.25	47.79	3.58	62.37	4.05
		0.75	221.31	15.90	55.05	4.87
		1.25	70.92	5.54	52.95	4.48
		1.75	88.05	6.77	64.29	4.00
		2.25	43.97	3.43	73.32	5.38
		2.75	168.34	14.58	50.20	3.52
		3.5	99.87	9.61	57.25	4.37
	Low	0.25	51.65	3.57	33.88	1.54
		0.75	86.16	7.95	41.05	1.91
		1.25	77.69	5.81	41.16	9.34
		1.75	10.40	0.95	47.98	10.93
		2.25	0.00	0.00	60.62	13.73
		2.75	0.00	0.00	71.09	4.01
		3.5	0.00	0.00	63.92	2.71
		4.5	0.00	0.00	62.60	2.62
KBP	High	0.25	19.38	1.85	38.38	3.00
		0.75	23.00	2.02	33.36	2.24
		1.25	20.07	1.70	25.18	2.02
		1.75	34.60	3.05	22.13	2.37
		2.25	34.49	3.07	28.40	2.57
		2.75	26.06	2.45	26.77	2.14
		3.5	35.98	3.28	26.97	6.15
		4.5	0.00	0.00	44.03	10.00
	Mid	0.25	36.78	3.25	29.68	1.95
		0.75	0.00	0.00	29.39	2.16
		1.25	0.00	0.00	34.45	7.80
		1.75	0.00	0.00	40.05	9.08
		2.25	3.20	0.33	29.54	1.85
		2.75	0.00	0.00	39.77	8.98
		3.5	0.00	0.00	26.35	1.70

Station	Core Label	Plot depth (cm)	Decay-corrected $^{234}Th_{xs}$ (Bq kg^{-1})	Decay-corrected $^{234}Th_{xs}$ error	^{238}U (Bq kg^{-1})	^{238}U error
KBP	Low	0.25	86.62	6.20	33.54	2.01
		0.75	46.32	4.83	32.14	2.15
		1.25	43.37	4.33	37.83	3.51
		1.75	36.58	3.63	44.10	4.49
		2.25	39.13	3.71	40.14	3.16
		2.75	0.00	0.00	39.84	4.06
		3.5	0.00	0.00	42.95	3.96
DBI	High	0.25	74.09	5.72	26.91	2.01
		0.75	68.55	6.60	31.08	1.79
		1.25	121.23	11.67	54.73	3.75
		1.75	0.00	0.00	66.55	4.03
		2.25	79.44	6.74	51.68	3.08
		2.75	327.51	27.14	36.37	2.19
		3.5	262.37	18.05	32.12	1.62
		4.5	0.00	0.00	26.43	5.98
	Mid	0.25	0.00	0.00	1.37	0.11
		0.75	71.28	6.29	9.86	0.75
		1.25	2554.97	239.55	10.50	0.57
		1.75	204.03	12.38	4.71	0.37
		2.25	160.20	13.12	12.54	0.90
		2.75	0.00	0.00	18.50	1.06
		3.5	447.63	43.36	25.96	1.78
	Low	0.25	15.86	1.25	41.87	2.76
		0.75	53.00	3.56	30.17	7.13
		1.25	0.00	0.00	45.47	2.78
		1.75	42.67	3.26	35.53	1.98
		2.25	51.94	4.11	46.87	3.56
		2.75	0.00	0.00	47.79	3.03
BJ	High	0.25	140.64	7.23	35.57	2.17
		0.75	784.14	56.23	24.78	1.02
		1.25	464.16	30.94	39.40	3.36
		1.75	1418.13	94.31	36.06	2.47
		2.25	0.00	0.00	44.16	2.38
		2.75	0.00	0.00	39.35	1.95
		3.5	0.00	0.00	41.89	3.72
		4.5	1035.30	100.22	35.60	2.86
	Mid	0.25	458.20	30.65	30.77	2.63
		0.75	1020.65	89.75	28.16	1.96
		1.25	1414.10	117.13	29.27	1.54
		1.75	714.84	63.47	28.61	2.45
		2.25	1816.42	173.29	24.13	1.28
		2.75	-	-	-	-

Station	Core Label	Plot depth (cm)	Decay-corrected $^{234}Th_{xs}$ (Bq kg^{-1})	Decay-corrected $^{234}Th_{xs}$ error	^{238}U (Bq kg^{-1})	^{238}U error
BJ	Mid	3.5	1383.01	126.99	37.68	2.40
		4.5	0.00	0.00	39.86	2.55
	Low	0.25	1262.31	106.42	53.22	3.64
		0.75	2962.32	222.88	53.81	4.08
		1.25	2416.81	196.27	50.23	3.27
		1.75	1682.46	158.01	54.93	3.85
		2.25	139.97	9.80	58.15	3.64
		2.75	33.45	3.00	66.93	3.51
		3.5	3598.91	336.27	49.71	2.62
		4.5	4157.80	384.15	59.82	4.60

APPENDIX 8

Appendix 8a
Compound-specific polycyclic aromatic hydrocarbon data. All units are ng/g. A label of "nd" indicates that the compound was below detection limits.

Station	Core Label	Sampling Interval	TPAH w/ perylene	TPAH w/o perylene	Naphthalene	C1-Naphthalenes	C2-Naphthalenes	C3-Naphthalenes	C4-Naphthalenes
RIG	High	5 cm	1106.9	1064.9	15.2	10.7	19.1	16.3	nd
		10 cm	780.0	751.8	22.3	18.5	39.5	31.8	nd
	Mid	5 cm	565.9	535.3	12.7	9.2	27.9	20.9	nd
		10 cm	506.4	482.0	13.8	9.3	17.7	15.2	nd
	Low	5 cm	611.1	577.9	14.3	13.6	17.2	25.8	nd
		10 cm	274.3	263.1	15.7	10.1	11.9	8.8	nd
KBP	High	5 cm	93.4	74.2	12.2	10.1	10.6	8.4	nd
		10 cm	284.9	264.5	32.6	26.3	27.8	15.9	nd
	Mid	5 cm	95.9	72.8	10.8	10.6	9.1	7.0	nd
		10 cm	148.7	118.9	6.1	5.9	6.9	7.7	nd
	Low	5 cm	144.1	115.5	6.3	6.3	10.3	6.4	nd
		10 cm	154.9	114.8	5.4	4.9	7.2	5.2	nd
DBI	High	1 cm	107.2	78.6	17.7	16.0	nd	nd	nd
		2 cm	92.7	71.6	15.5	14.5	15.3	nd	nd
		3 cm	5503.2	5420.3	12.4	9.9	12.0	nd	nd
		4 cm	3183.6	3118.2	23.3	20.6	20.6	nd	nd
		5 cm	142.9	131.9	17.8	15.7	16.3	nd	nd
	Mid	1 cm	375.2	309.3	35.1	39.3	58.1	nd	nd
		2 cm	511.7	467.3	33.2	24.8	40.3	51.1	nd
		3 cm	292.6	261.8	23.6	14.6	22.2	15.4	nd
		4 cm	169.3	153.6	14.3	13.7	14.5	8.9	nd
		5 cm	112.2	99.5	8.8	6.5	8.6	4.5	nd
	Low	1 cm	170.3	141.4	6.4	6.7	11.3	8.4	nd
		2 cm	225.6	178.6	6.8	6.2	12.4	7.9	nd
		3 cm	265.1	228.7	8.2	6.3	10.6	8.0	nd
		4 cm	246.4	211.9	9.8	9.1	11.6	8.2	nd
		5 cm	268.2	227.5	8.9	7.1	10.1	7.1	nd
BJ	High	1 cm	4357.6	4345.5	18.0	14.1	12.2	13.1	14.0
		2 cm	18521.6	18279.4	332.1	191.1	220.1	258.9	305.4
		3 cm	11599.1	11510.8	337.7	164.2	155.3	197.7	244.4
	Mid	1 cm	19422.0	19356.2	152.2	96.3	101.6	155.3	297.4

Station	Core Label	Sampling Interval	TPAH w/ perylene	TPAH w/o perylene	Naphthalene	C1-Naphthalenes	C2-Naphthalenes	C3-Naphthalenes	C4-Naphthalenes
BJ	Mid	2 cm	21973.6	21913.3	96.1	57.1	56.8	87.1	130.4
	Low	1 cm	7779.5	7768.2	219.8	181.1	208.5	278.6	412.9
		2 cm	7802.7	7774.6	206.7	164.0	176.9	274.6	310.9

Station	Core Label	Sampling Interval	Biphenyl	Acenaphthylene	Acenaphthene	Fluorene	C1-Fluorenes	C2-Fluorenes	C3-Fluorenes
RIG	High	5 cm	3.3	17.1	4.1	8.8	11.7	nd	nd
		10 cm	5.9	26.0	nd	3.4	52.0	55.9	26.0
	Mid	5 cm	4.6	12.2	10.8	4.2	2.6	21.9	nd
		10 cm	3.4	8.5	16.8	3.9	37.2	35.5	nd
	Low	5 cm	4.1	9.0	1.8	4.1	1.5	nd	nd
		10 cm	3.2	2.8	0.6	2.2	33.6	36.6	nd
KBP	High	5 cm	3.1	nd	nd	nd	9.8	nd	nd
		10 cm	7.1	nd	nd	2.8	45.9	43.7	nd
	Mid	5 cm	2.7	nd	nd	1.3	6.8	nd	nd
		10 cm	1.8	0.5	nd	1.1	20.3	13.0	3.6
	Low	5 cm	3.3	nd	nd	1.5	15.5	22.1	nd
		10 cm	1.6	0.4	nd	1.4	17.1	13.6	nd
DBI	High	1 cm	5.9	nd	nd	nd	nd	nd	nd
		2 cm	4.7	nd	nd	nd	nd	nd	nd
		3 cm	5.0	100.0	nd	nd	nd	nd	nd
		4 cm	7.3	97.2	nd	nd	nd	nd	nd
		5 cm	3.5	1.6	nd	nd	nd	nd	nd
	Mid	1 cm	17.7	nd	nd	nd	nd	nd	nd
		2 cm	13.3	nd	nd	4.2	66.9	nd	nd
		3 cm	8.9	0.7	nd	3.2	38.8	nd	nd
		4 cm	3.5	1.8	nd	1.5	19.1	nd	nd
		5 cm	2.3	0.5	nd	1.4	16.1	7.6	nd
	Low	1 cm	2.3	0.6	0.7	2.9	28.6	nd	nd
		2 cm	2.4	0.7	nd	3.7	41.4	nd	nd
		3 cm	2.3	0.6	nd	3.9	36.9	32.4	nd
		4 cm	3.3	0.7	nd	4.2	48.0	31.0	nd
		5 cm	3.0	nd	nd	4.4	49.5	33.6	10.8
BJ	High	1 cm	nd	2.3	1.9	11.0	20.9	32.7	0.0
		2 cm	30.9	9.0	6.3	35.1	119.8	345.6	1262.6
		3 cm	1098.7	5.9	22.6	94.1	128.2	384.5	547.5
	Mid	1 cm	846.1	4.3	12.0	80.1	111.2	445.7	957.7
		2 cm	400.0	3.7	6.8	31.1	86.7	423.6	1136.8
	Low	1 cm	1231.4	6.6	21.5	118.8	142.1	418.8	605.7
		2 cm	1242.6	3.7	19.6	113.8	147.2	465.1	504.9

Station	Core Label	Sampling Interval	Phenanthrene	Anthracene	C1-Phenanthrenes/Anthracenes	C2-Phenanthrenes/Anthracenes	C3-Phenanthrenes/Anthracenes	C4-Phenanthrenes/Anthracenes	Dibenzothiophene
RIG	High	5 cm	68.7	29.2	34.8	32.0	nd	nd	3.2
		10 cm	14.3	18.3	18.5	18.7	14.3	6.4	nd
	Mid	5 cm	14.0	15.6	17.1	16.5	nd	nd	2.9
		10 cm	14.4	10.7	13.7	9.4	6.8	nd	3.7
	Low	5 cm	17.0	12.9	23.0	24.5	17.6	nd	nd
		10 cm	11.9	3.9	8.6	6.8	nd	nd	1.3
KBP	High	5 cm	8.2	1.6	nd	nd	nd	nd	nd
		10 cm	13.9	2.2	11.6	nd	nd	nd	nd
	Mid	5 cm	5.8	1.3	5.3	nd	nd	nd	nd
		10 cm	4.6	1.1	3.5	2.4	nd	nd	nd
	Low	5 cm	3.8	2.0	0.0	nd	nd	nd	nd
		10 cm	4.4	1.3	4.6	4.1	nd	nd	nd
DBI	High	1 cm	7.5	1.8	nd	nd	nd	nd	nd
		2 cm	5.7	1.0	nd	nd	nd	nd	nd
		3 cm	10.9	103.7	55.6	75.7	37.5	nd	nd
		4 cm	8.8	70.3	21.0	37.0	22.3	nd	nd
		5 cm	6.0	1.9	5.4	nd	nd	nd	nd
	Mid	1 cm	21.5	3.6	nd	34.9	nd	nd	nd
		2 cm	12.3	3.0	26.0	34.4	29.8	nd	nd
		3 cm	8.1	2.4	17.6	25.1	15.1	nd	nd
		4 cm	5.5	2.6	6.9	nd	nd	nd	nd
		5 cm	5.0	1.1	7.9	nd	nd	nd	0.7
	Low	1 cm	9.8	4.2	6.1	nd	nd	nd	nd
		2 cm	9.7	2.9	8.9	nd	nd	nd	2.0
		3 cm	9.9	3.0	6.9	3.8	nd	nd	
		4 cm	9.9	5.3	7.3	nd	nd	nd	nd
		5 cm	10.1	3.1	6.8	nd	nd	nd	nd
BJ	High	1 cm	45.1	15.2	75.7	160.1	275.7	543.1	6.0
		2 cm	103.0	59.9	256.7	588.2	1673.8	2078.6	13.3
		3 cm	186.6	28.3	472.6	696.9	543.6	337.3	32.5
	Mid	1 cm	211.9	19.6	692.4	992.6	721.2	1139.8	43.3
		2 cm	82.2	17.8	228.6	334.1	502.9	1441.5	22.6
	Low	1 cm	168.7	17.9	470.7	856.1	251.3	143.1	29.1
		2 cm	188.4	14.2	556.1	1006.8	378.7	96.1	35.1

Station	Core Label	Sampling Interval	C1-Dibenzothiophenes	C2-Dibenzothiophenes	C3-Dibenzothiophenes	Fluoranthene	Pyrene	C1-Fluoranthenes/Pyrenes	C2-Fluoranthenes/Pyrenes
RIG	High	5 cm	2.5	3.1	2.1	140.2	113.4	55.4	34.4
		10 cm	2.1	3.2	nd	52.7	41.7	25.7	21.6
	Mid	5 cm	2.2	3.0	2.3	46.2	36.4	22.4	25.2
		10 cm	2.4	2.9	2.1	36.1	24.5	14.2	31.0
	Low	5 cm	nd	nd	nd	49.1	46.0	24.8	26.6
		10 cm	1.2	nd	nd	22.0	15.1	8.9	nd
KBP	High	5 cm	nd	nd	nd	5.8	4.5	nd	nd
		10 cm	nd	nd	nd	11.5	10.4	nd	nd
	Mid	5 cm	nd	nd	nd	5.1	3.5	nd	nd
		10 cm	0.8	nd	nd	4.8	3.4	2.0	nd
	Low	5 cm	nd	nd	nd	5.3	4.2	3.1	6.2
		10 cm	1.0	1.6	nd	4.8	3.5	2.5	6.2
DBI	High	1 cm	nd	nd	nd	8.5	5.0	nd	nd
		2 cm	nd	nd	nd	6.2	4.0	nd	nd
		3 cm	nd	nd	nd	748.8	544.1	294.0	258.5
		4 cm	nd	nd	nd	209.5	183.2	138.8	113.1
		5 cm	1.3	nd	nd	7.1	5.2	4.4	11.3
	Mid	1 cm	nd	nd	nd	22.0	15.4	nd	nd
		2 cm	5.0	14.7	13.9	11.5	8.6	nd	nd
		3 cm	nd	8.3	7.0	8.0	5.7	3.9	nd
		4 cm	1.2	nd	nd	4.5	3.6	3.2	4.4
		5 cm	nd	nd	nd	5.4	3.6	2.5	nd
	Low	1 cm	nd	nd	nd	13.5	7.5	nd	nd
		2 cm	1.5	nd	nd	12.7	6.9	3.4	7.2
		3 cm	1.4	nd	nd	12.8	7.2	4.1	5.2
		4 cm	1.4	nd	nd	13.2	7.5	3.5	nd
		5 cm	1.4	nd	nd	14.4	7.8	3.3	nd
BJ	High	1 cm	23.7	56.1	144.4	82.5	8.8	360.5	356.4
		2 cm	108.1	377.5	912.8	116.8	205.3	770.2	1248.9
		3 cm	191.2	496.1	396.5	175.6	274.2	328.7	403.2
	Mid	1 cm	282.4	672.3	597.9	96.6	311.4	648.7	937.3
		2 cm	115.9	191.5	377.3	78.8	173.3	748.7	1569.5
	Low	1 cm	189.5	446.2	308.1	57.6	149.7	147.3	137.6
		2 cm	234.8	610.7	440.0	66.7	182.3	158.0	57.2

Station	Core Label	Sampling Interval	C3-Fluoranthenes/Pyrenes	Benz(a)anthracene	Chrysene	C1-Chrysenes	C2-Chrysenes	C3-Chrysenes	C4-Chrysenes
RIG	High	5 cm	13.6	51.3	59.7	25.2	10.1	nd	nd
		10 cm	8.3	19.6	35.6	14.9	8.5	nd	nd
	Mid	5 cm	nd	18.6	26.0	15.8	9.6	nd	nd
		10 cm	nd	11.8	17.9	11.4	8.0	nd	nd
	Low	5 cm	nd	21.5	32.1	25.4	11.3	nd	nd
		10 cm	nd	4.1	6.9	11.7	3.7	nd	nd
KBP	High	5 cm	nd	nd	nd	nd	nd	nd	nd
		10 cm	nd	1.9	2.8	nd	nd	nd	nd
	Mid	5 cm	nd	1.4	2.2	nd	nd	nd	nd
		10 cm	nd	1.8	3.0	2.6	nd	nd	nd
	Low	5 cm	nd	3.2	5.3	2.2	nd	nd	nd
		10 cm	3.4	2.0	3.3	3.1	3.5	nd	nd
DBI	High	1 cm	nd	2.2	6.6	nd	nd	nd	nd
		2 cm	nd	1.7	3.2	nd	nd	nd	nd
		3 cm	113.7	425.9	659.7	227.2	42.9	nd	nd
		4 cm	68.2	236.4	458.9	145.0	41.9	nd	nd
		5 cm	0.0	2.6	4.3	nd	nd	nd	nd
	Mid	1 cm	nd	7.6	42.5	nd	nd	nd	nd
		2 cm	nd	6.4	23.1	22.9	17.1	nd	nd
		3 cm	nd	1.8	5.0	16.4	5.3	nd	nd
		4 cm	nd	3.4	5.7	nd	nd	nd	nd
		5 cm	nd	1.8	3.0	2.4	nd	nd	nd
	Low	1 cm	nd	2.8	8.2	nd	nd	nd	nd
		2 cm	nd	3.2	6.6	4.2	nd	nd	nd
		3 cm	nd	3.3	6.6	5.5	nd	nd	nd
		4 cm	nd	3.5	7.1	nd	nd	nd	nd
		5 cm	nd	3.8	7.6	nd	nd	nd	nd
BJ	High	1 cm	454.8	385.4	305.8	0.0	431.6	207.1	64.1
		2 cm	2231.8	149.2	996.8	139.3	699.8	1212.7	595.1
		3 cm	361.0	40.6	541.6	848.9	820.0	473.0	146.8
	Mid	1 cm	1131.1	20.2	1707.0	2253.6	1837.0	972.4	249.0
		2 cm	1670.5	15.8	2456.7	3699.2	2856.6	1358.0	788.4
	Low	1 cm	115.1	6.5	25.5	92.5	114.1	76.3	73.6
		2 cm	16.5	5.5	17.7	20.4	6.3	7.5	10.2

Station	Core Label	Sampling Interval	Benzo(b)fluoranthene	Benzo(k)fluoranthene	Benzo(e)pyrene	Benzo(a)pyrene	Perylene	Indeno(1,2,3-c,d)pyrene	Dibenz(a,h)anthracene	Benzo(g,h,i)perylene
RIG	High	5 cm	86.7	31.8	44.9	41.1	42.0	39.1	5.3	31.0
		10 cm	48.3	16.0	23.3	18.8	28.2	20.4	4.1	15.4
	Mid	5 cm	45.7	15.8	21.6	15.4	30.6	17.3	2.8	15.7
		10 cm	35.2	11.8	15.6	10.0	24.4	14.0	2.5	10.8
	Low	5 cm	48.9	17.7	25.5	20.6	33.2	19.2	4.2	18.7
		10 cm	11.1	3.5	4.9	3.0	11.2	4.9	0.8	3.6
KBP	High	5 cm	nd	nd	nd	nd	19.2	nd	nd	nd
		10 cm	nd	nd	nd	nd	20.4	nd	4.3	3.9
	Mid	5 cm	nd	nd	nd	nd	23.1	nd	nd	nd
		10 cm	5.2	1.6	nd	1.8	29.8	2.1	9.5	2.0
	Low	5 cm	6.1	2.4	nd	nd	28.7	nd	nd	nd
		10 cm	4.3	1.1	nd	nd	40.1	1.8	nd	1.6
DBI	High	1 cm	4.9	2.6	nd	nd	28.6	nd	nd	nd
		2 cm	nd	nd	nd	nd	21.1	nd	nd	nd
		3 cm	642.6	229.5	240.4	205.4	82.9	205.0	41.3	118.8
		4 cm	474.8	161.8	169.6	142.8	65.4	134.8	32.1	85.9
		5 cm	5.6	1.9	5.3	1.8	11.1	2.6	6.8	3.7
	Mid	1 cm	11.7	nd	nd	nd	65.9	nd	nd	nd
		2 cm	4.9	nd	nd	nd	44.4	nd	nd	nd
		3 cm	3.2	nd	1.7	nd	30.8	nd	nd	nd
		4 cm	10.8	3.1	5.7	4.7	15.7	3.3	4.3	3.5
		5 cm	2.7	1.3	1.0	0.8	12.7	nd	3.5	0.7
	Low	1 cm	7.2	2.3	2.5	1.4	28.9	4.3	nd	3.8
		2 cm	8.2	2.5	2.8	2.2	46.9	4.1	5.0	3.3
		3 cm	10.5	2.7	2.7	3.3	36.4	6.2	16.4	4.5
		4 cm	9.4	2.8	nd	nd	34.5	4.7	7.2	3.3
		5 cm	10.5	2.8	nd	2.9	40.7	5.1	10.2	3.6
BJ	High	1 cm	44.9	15.9	92.3	22.2	12.1	8.8	4.4	14.9
		2 cm	113.7	25.3	389.5	15.0	242.2	29.7	0.9	50.5
		3 cm	73.2	18.0	127.7	38.6	88.4	31.2	14.6	32.2
	Mid	1 cm	66.2	10.1	403.4	12.4	65.7	12.5	14.2	39.8
		2 cm	40.4	13.7	494.7	31.5	60.3	17.6	13.0	56.2
	Low	1 cm	13.2	4.1	7.3	4.5	11.3	6.5	4.9	5.7
		2 cm	13.4	4.9	5.9	3.0	28.2	3.3	1.5	3.7

Appendix 8b
Calculated compound-specific polycyclic aromatic hydrocarbon data. All units are ng/g.

Station	Core Label	Sampling Interval	C1 and higher Fl/Py	C1 and higher Phen/An	Fl/Py	Phen/An	BaA/BaA+Chry	An/An+Phen	IP/IP+Bghi	Fl/Fl+Py
RIG	High	5 cm	103.4	66.8	1.2	2.4	0.5	0.3	0.6	0.6
		10 cm	55.6	57.8	1.3	0.8	0.4	0.6	0.6	0.6
	Mid	5 cm	47.6	33.6	1.3	0.9	0.4	0.5	0.5	0.6
		10 cm	45.2	29.8	1.5	1.4	0.4	0.4	0.6	0.6
	Low	5 cm	51.4	65.1	1.1	1.3	0.4	0.4	0.5	0.5
		10 cm	8.9	15.4	1.5	3.1	0.4	0.2	0.6	0.6
KBP	High	5 cm			1.3	5.2		0.2		0.6
		10 cm		11.6	1.1	6.3	0.4	0.1		0.5
	Mid	5 cm		5.3	1.5	4.6	0.4	0.2		0.6
		10 cm	2.0	5.9	1.4	4.2	0.4	0.2	0.5	0.6
	Low	5 cm	9.3		1.2	1.9	0.4	0.3		0.6
		10 cm	12.1	8.7	1.4	3.3	0.4	0.2	0.5	0.6
DBI	High	1 cm			1.7	4.1	0.2	0.2		0.6
		2 cm			1.6	5.7	0.3	0.1		0.6
		3 cm	666.2	168.8	1.4	0.1	0.4	0.9	0.6	0.6
		4 cm	320.1	80.3	1.1	0.1	0.3	0.9	0.6	0.5
		5 cm	15.7	5.4	1.4	3.1	0.4	0.2	0.4	0.6
	Mid	1 cm		34.9	1.4	5.9	0.2	0.1		0.6
		2 cm		90.2	1.3	4.2	0.2	0.2		0.6
		3 cm	3.9	57.8	1.4	3.4	0.3	0.2		0.6
		4 cm	7.5	6.9	1.2	2.1	0.4	0.3	0.5	0.6
		5 cm	2.5	7.9	1.5	4.5	0.4	0.2		0.6
	Low	1 cm		6.1	1.8	2.3	0.3	0.3	0.5	0.6
		2 cm	10.7	8.9	1.8	3.4	0.3	0.2	0.6	0.6
		3 cm	9.3	10.6	1.8	3.3	0.3	0.2	0.6	0.6
		4 cm	3.5	7.3	1.8	1.9	0.3	0.3	0.6	0.6
		5 cm	3.3	6.8	1.9	3.3	0.3	0.2	0.6	0.6
BJ	High	1 cm	1171.6	1054.7	9.4	3.0	0.6	0.3	0.4	0.9
		2 cm	4251.0	4597.4	0.6	1.7	0.1	0.4	0.4	0.4
		3 cm	1092.8	2050.2	0.6	6.6	0.1	0.1	0.5	0.4
	Mid	1 cm	2717.0	3546.1	0.3	10.8	0.0	0.1	0.2	0.2
		2 cm	3988.6	2507.0	0.5	4.6	0.0	0.2	0.2	0.3
	Low	1 cm	400.0	1721.2	0.4	9.4	0.2	0.1	0.5	0.3
		2 cm	231.6	2037.6	0.4	13.3	0.2	0.1	0.5	0.3

Station	Core Label	Sampling Interval	C2-Phen/C2-Chry	C3-Phen/C3-Chry	C2D/C2P	C3D/C3P	C3D/C3C	C0/(C0+C1) P/A	C0/(C0+C1) F/P
RIG	High	5 cm	3.2		0.1			0.7	0.8
		10 cm	2.2		0.2			0.6	0.8
	Mid	5 cm	1.7		0.2			0.6	0.8
		10 cm	1.2		0.3	0.3		0.6	0.8
	Low	5 cm	2.2					0.6	0.8
		10 cm	1.8					0.6	0.8
KBP	High	5 cm							
		10 cm						0.6	
	Mid	5 cm						0.6	
		10 cm						0.6	0.8
	Low	5 cm							0.8
		10 cm	1.2		0.4			0.6	0.8
DBI	High	1 cm							
		2 cm							
		3 cm	1.8					0.7	0.8
		4 cm	0.9					0.8	0.7
		5 cm						0.6	0.7
	Mid	1 cm							
		2 cm	2.0		0.4	0.5		0.4	
		3 cm	4.7		0.3	0.5		0.4	0.8
		4 cm						0.5	0.7
		5 cm						0.4	0.8
	Low	1 cm						0.7	
		2 cm						0.6	0.9
		3 cm						0.7	0.8
		4 cm						0.7	0.9
		5 cm						0.7	0.9
BJ	High	1 cm	0.4	1.3	0.4	0.5	0.7	0.4	0.2
		2 cm	0.8	1.4	0.6	0.5	0.8	0.4	0.3
		3 cm	0.8	1.1	0.7	0.7	0.8	0.3	0.6
	Mid	1 cm	0.5	0.7	0.7	0.8	0.6	0.3	0.4
		2 cm	0.1	0.4	0.6	0.8	0.3	0.3	0.3
	Low	1 cm	7.5	3.3	0.5	1.2	4.0	0.3	0.6
		2 cm	160.8	50.2	0.6	1.2	58.4	0.3	0.6

Appendix 8c
Compound-specific polycyclic aromatic hydrocarbon data for 2010 GIP samples. All units are ng/g. A label of "nd" indicates that the compound was below detection limits.

Station	Sampling Interval	TPAH w/ perylene	TPAH w/o perylene	Naphthalene	C1-Naphthalenes	C2-Naphthalenes	C3-Naphthalenes	C4-Naphthalenes
GIP_1_10MC	2 cm	-	231.9	8.4	7.5	11.6	7.8	4.5
GIP_2_10MC	2 cm	-	513.8	10.7	10.9	14.2	10.5	5.5
GIP_3_10MC	2 cm	-	477.3	11.2	14.1	32.3	10.5	8.4
GIP_12_10MC	2 cm	825.6	700.0	20.8	25.3	24.3	17.8	10.9
GIP_15_10MC	2 cm	6158.4	6133.2	19.0	23.6	41.6	160.2	292.6
GIP_16_10MC	1 cm	2512.2	2191.6	34.1	51.8	50.5	58.1	0.0
GIP_17_10MC	1 cm	3077.3	3077.3	19.7	32.0	27.8	36.0	0.0
GIP_17_10MC	2 cm	427.2	415.3	11.5	11.5	9.4	7.4	6.4
GIP_18_10MC	1 cm	1821.2	1821.2	18.3	31.8	115.0	205.1	0.0
GIP_19_10MC	2 cm	294.5	290.1	15.8	14.4	10.9	6.0	5.1
GIP_22_10MC	2 cm	155.8	152.9	13.8	10.5	5.8	3.3	2.5
GIP_23_10MC	1 cm	819.8	819.8	24.1	28.4	26.2	28.0	0.0
GIP_25_10MC	2 cm	-	1085.8	12.7	13.3	14.5	19.1	21.1

Station	Sampling Interval	Biphenyl	Acenaphthylene	Acenaphthene	Fluorene	C1-Fluorenes	C2-Fluorenes	C3-Fluorenes	Phenanthrene
GIP_1_10MC	2 cm	2.1	1.4	1.9	1.6	7.5	11.5	12.9	5.7
GIP_2_10MC	2 cm	2.8	1.9	2.1	2.0	5.1	17.9	13.8	2.6
GIP_3_10MC	2 cm	2.9	1.4	1.3	1.7	8.0	13.4	99.2	7.7
GIP_12_10MC	2 cm	9.0	6.1	2.1	3.3	15.2	23.7	29.4	20.6
GIP_15_10MC	2 cm	8.7	2.3	3.1	6.1	82.1	178.9	378.4	46.6
GIP_16_10MC	1 cm	10.5	10.3	0.0	6.7	4.2	0.0	0.0	38.6
GIP_17_10MC	1 cm	5.8	8.4	0.0	0.0	0.0	117.5	222.9	19.4
GIP_17_10MC	2 cm	3.2	2.7	1.8	1.5	8.8	14.0	20.5	9.3
GIP_18_10MC	1 cm	8.2	5.2	0.0	0.0	0.0	0.0	0.0	54.3
GIP_19_10MC	2 cm	3.6	3.3	1.1	1.4	5.7	6.1	5.5	12.9
GIP_22_10MC	2 cm	2.5	1.2	0.8	2.2	3.7	4.9	10.0	6.2
GIP_23_10MC	1 cm	6.6	0.0	0.0	3.6	39.4	50.4	61.6	13.2
GIP_25_10MC	2 cm	3.2	3.5	2.4	4.0	12.4	38.4	66.5	15.8

Station	Sampling Interval	Anthracene	C1-Phenanthrenes/Anthracenes	C2-Phenanthrenes/Anthracenes	C3-Phenanthrenes/Anthracenes	C4-Phenanthrenes/Anthracenes	Dibenzothiophene	C1-Dibenzothiophenes
GIP_1_10MC	2 cm	2.9	8.2	14.6	8.1	13.0	1.4	2.7
GIP_2_10MC	2 cm	2.9	11.5	18.2	11.6	10.0	1.1	3.3
GIP_3_10MC	2 cm	3.9	10.1	23.2	19.9	14.7	1.0	1.7
GIP_12_10MC	2 cm	12.9	27.1	33.1	36.4	20.6	2.4	7.0
GIP_15_10MC	2 cm	9.0	264.6	843.7	828.5	578.8	13.9	73.3
GIP_16_10MC	1 cm	16.3	60.1	136.4	184.9	109.3	5.4	0.0
GIP_17_10MC	1 cm	6.1	58.2	183.8	324.2	191.7	2.3	14.9
GIP_17_10MC	2 cm	3.3	12.3	19.6	22.6	23.0	2.0	3.1
GIP_18_10MC	1 cm	4.2	179.9	173.9	150.2	54.4	0.0	38.2
GIP_19_10MC	2 cm	10.0	14.1	12.5	7.1	7.0	1.2	2.6
GIP_22_10MC	2 cm	1.8	6.6	4.4	4.6	4.3	0.8	1.7
GIP_23_10MC	1 cm	4.9	15.4	37.5	73.3	0.0	1.2	3.1
GIP_25_10MC	2 cm	5.7	33.0	111.3	120.3	84.7	2.6	11.0

Station	Sampling Interval	C2-Dibenzothiophenes	C3-Dibenzothiophenes	Fluoranthene	Pyrene	C1-Fluoranthenes/Pyrenes	C2-Fluoranthenes/Pyrenes	C3-Fluoranthenes/Pyrenes	Benz(a)anthracene
GIP_1_10MC	2 cm	3.8	5.0	5.8	5.7	4.7	5.3	0.0	3.2
GIP_2_10MC	2 cm	4.6	7.5	9.9	10.1	9.7	7.4	4.4	4.4
GIP_3_10MC	2 cm	4.2	6.9	7.6	8.3	8.0	9.1	8.4	3.9
GIP_12_10MC	2 cm	11.3	14.4	24.0	28.5	25.7	18.4	16.0	14.6
GIP_15_10MC	2 cm	269.4	326.0	28.8	53.8	153.2	203.8	108.5	19.8
GIP_16_10MC	1 cm	44.5	70.1	48.6	62.8	53.6	97.2	0.0	32.8
GIP_17_10MC	1 cm	54.8	118.2	21.7	30.0	61.9	127.8	0.0	14.3
GIP_17_10MC	2 cm	7.5	9.4	9.2	8.5	10.4	10.8	12.5	4.5
GIP_18_10MC	1 cm	74.7	45.5	15.8	17.9	21.3	0.0	0.0	6.5
GIP_19_10MC	2 cm	2.6	3.2	11.7	12.0	8.8	6.0	3.5	4.4
GIP_22_10MC	2 cm	1.5	1.6	4.8	4.0	2.4	2.0	1.7	3.3
GIP_23_10MC	1 cm	11.1	23.6	12.5	12.9	19.7	30.9	0.0	4.3
GIP_25_10MC	2 cm	40.1	50.5	14.2	17.1	21.6	34.7	20.3	9.9

Station	Sampling Interval	Chrysene	C1-Chrysenes	C2-Chrysenes	C3-Chrysenes	C4-Chrysenes	Benzo(b)fluoranthene	Benzo(k)fluoranthene
GIP_1_10MC	2 cm	5.0	4.5	6.9	5.4	9.6	7.2	4.3
GIP_2_10MC	2 cm	7.8	8.1	11.3	6.7	4.7	13.2	7.9
GIP_3_10MC	2 cm	6.8	7.2	9.7	11.4	37.6	12.1	10.4
GIP_12_10MC	2 cm	18.0	19.2	17.0	13.6	12.6	29.6	13.3
GIP_15_10MC	2 cm	117.6	260.6	299.6	187.8	70.7	35.4	12.7
GIP_16_10MC	1 cm	106.6	169.2	203.5	126.9	0.0	71.2	25.0
GIP_17_10MC	1 cm	158.9	347.9	451.1	180.8	58.2	38.9	9.6
GIP_17_10MC	2 cm	17.0	21.9	31.1	17.9	12.0	12.1	6.1
GIP_18_10MC	1 cm	71.8	152.6	175.1	89.7	30.0	19.1	5.7
GIP_19_10MC	2 cm	9.2	5.3	5.5	5.8	5.4	13.4	6.7
GIP_22_10MC	2 cm	4.2	1.7	1.8	2.5	2.2	6.5	4.0
GIP_23_10MC	1 cm	35.5	68.5	89.2	42.4	0.0	14.5	3.2
GIP_25_10MC	2 cm	30.9	44.8	61.8	36.4	21.8	18.8	7.0

Station	Sampling Interval	Benzo(e)pyrene	Benzo(a)pyrene	Perylene	Indeno(1,2,3-c,d)pyrene	Dibenz(a,h)anthracene	Benzo(g,h,i)perylene
GIP_1_10MC	2 cm	4.1	2.3	61.1	6.5	2.3	5.2
GIP_2_10MC	2 cm	7.5	5.6	224.4	10.3	3.1	11.0
GIP_3_10MC	2 cm	6.8	4.3	190.6	9.3	3.6	10.2
GIP_12_10MC	2 cm	19.1	11.2	125.5	18.3	5.9	21.5
GIP_15_10MC	2 cm	53.0	19.9	25.2	22.2	13.3	22.2
GIP_16_10MC	1 cm	63.5	149.6	320.7	35.8	10.1	43.5
GIP_17_10MC	1 cm	89.8	0.0	0.0	15.2	15.7	12.2
GIP_17_10MC	2 cm	9.6	3.5	11.9	9.4	3.6	4.5
GIP_18_10MC	1 cm	36.3	0.0	0.0	9.4	6.0	5.4
GIP_19_10MC	2 cm	8.4	3.4	4.5	13.9	3.6	11.2
GIP_22_10MC	2 cm	3.2	1.0	2.9	5.4	4.5	3.0
GIP_23_10MC	1 cm	17.9	0.0	0.0	7.7	3.6	5.2
GIP_25_10MC	2 cm	17.9	6.0	14.7	17.3	5.6	13.7

Appendix 8d
Calculated compound-specific polycyclic aromatic hydrocarbon data for 2010 GIP samples. All units are ng/g.

Station	Sampling Interval	C1 and higher Fl/Py	C1 and higher Phen/An	Fl/Py	Phen/An	BaA/BaA+Chry	An/An+Phen	IP/IP+Bghi
GIP_1_10MC	2 cm	10.0	43.9	1.0	2.0	0.4	0.3	0.6
GIP_2_10MC	2 cm	21.5	51.2	1.0	0.9	0.4	0.5	0.5
GIP_3_10MC	2 cm	25.5	67.9	0.9	2.0	0.4	0.3	0.5
GIP_12_10MC	2 cm	60.1	117.2	0.8	1.6	0.4	0.4	0.5
GIP_15_10MC	2 cm	465.4	2515.6	0.5	5.2	0.1	0.2	0.5
GIP_16_10MC	1 cm	150.8	490.7	0.8	2.4	0.2	0.3	0.5
GIP_17_10MC	1 cm	189.7	757.9	0.7	3.2	0.1	0.2	0.6
GIP_17_10MC	2 cm	33.7	77.5	1.1	2.8	0.2	0.3	0.7
GIP_18_10MC	1 cm	21.3	558.3	0.9	13.0	0.1	0.1	0.6
GIP_19_10MC	2 cm	18.3	40.6	1.0	1.3	0.3	0.4	0.6
GIP_22_10MC	2 cm	6.1	19.8	1.2	3.4	0.4	0.2	0.6
GIP_23_10MC	1 cm	50.6	126.2	1.0	2.7	0.1	0.3	0.6
GIP_25_10MC	2 cm	76.5	349.2	0.8	2.8	0.2	0.3	0.6

Station	Sampling Interval	Fl/Fl+Py	C2-Phen/C2-Chry	C3-Phen/C3-Chry	C2D/C2P	C3D/C3P	C3D/C3C	C0/(C0+C1) P/A	C0/(C0+C1) F/P
GIP_1_10MC	2 cm	0.5	2.1	1.5	0.3	0.6	0.9	0.5	0.7
GIP_2_10MC	2 cm	0.5	1.6	1.7	0.3	0.6	1.1	0.3	0.7
GIP_3_10MC	2 cm	0.5	2.4	1.7	0.2	0.3	0.6	0.5	0.7
GIP_12_10MC	2 cm	0.5	1.9	2.7	0.3	0.4	1.1	0.6	0.7
GIP_15_10MC	2 cm	0.3	2.8	4.4	0.3	0.4	1.7	0.2	0.4
GIP_16_10MC	1 cm	0.4	0.7	1.5	0.3	0.4	0.6	0.5	0.7
GIP_17_10MC	1 cm	0.4	0.4	1.8	0.3	0.4	0.7	0.3	0.5
GIP_17_10MC	2 cm	0.5	0.6	1.3	0.4	0.4	0.5	0.5	0.6
GIP_18_10MC	1 cm	0.5	1.0	1.7	0.4	0.3	0.5	0.2	0.6
GIP_19_10MC	2 cm	0.5	2.3	1.2	0.2	0.4	0.5	0.6	0.7
GIP_22_10MC	2 cm	0.5	2.4	1.8	0.3	0.4	0.6	0.5	0.8
GIP_23_10MC	1 cm	0.5	0.4	1.7	0.3	0.3	0.6	0.5	0.6
GIP_25_10MC	2 cm	0.5	1.8	3.3	0.4	0.4	1.4	0.4	0.6

Appendix 8e
Compound-specific polycyclic aromatic hydrocarbon data for selected 2011 OSAT samples collected at Bay Jimmy. All samples were bulked from 0 to 2 cm depth. All units are ng/g.

Station	TPAH w/ perylene	TPAH w/o perylene	Naphthalene	C1-Naphthalenes	C2-Naphthalenes	C3-Naphthalenes	C4-Naphthalenes	Biphenyl
LAAP39323	190763.44	190613.44	12.6	24.7	75.7	380	2300	9.96
LAAP39325	25073.76	24967.76	8.8	5.97	12.5	23.9	194	1.76
LAAP39329	4657.113	4635.213	8.28	3.53	5.9	8.95	25.9	1.43
LAAP39347	209502.59	20494.09	20.4	44.4	130	563	3160	8.6
LAAP39349	22250.407	22204.907	6.79	5.67	11.4	11.5	75.2	2.3
LAAP39351	3402.562	3377.262	9.79	5.45	13.6	12.1	13.1	2.59
LAAP39353	126083.01	126022.81	24.2	34.7	90	304	2280	10.1
LAAP39356	10582.799	10581.419	6.16	4.72	11.7	9.67	37.3	2.07
LAAP39357	4757.58	4733.38	4.33	3.9	9.49	8.87	17.5	1.79
LAAP39362	721.85	706.35	7.13	5.36	11.9	9.33	8.76	2.39
LAAP39363	342.719	332.119	6.97	5	13.1	11.3	10.9	2.18
LAAP39364	1634.26	1614.56	7.78	5.68	15.4	12.4	11.5	2.73
LAAP39372	1514.639	1508.899	3.95	4.32	8.53	7.25	4.11	1.83
LAAP39374	1305.051	1293.651	4.25	3.41	6.4	4.85	4.44	1.73
LAAP39376	3398.227	3373.927	6.07	4.85	8.7	7.02	6.27	2.04

Station	Acenaphthylene	Acenaphthene	Fluorene	C1-Fluorenes	C2-Fluorenes	C3-Fluorenes	Phenanthrene	Anthracene	C1-Phenanthrenes/Anthracenes
LAAP39323	5.56	45.6	44.8	479	2250	8280	193	3.83	1890
LAAP39325	78.7	3.6	5.95	1.63	268	1190	21	136	127
LAAP39329	1.3	1.79	1.81	8.34	38.2	124	6.21	5.03	55.3
LAAP39347	8.99	4.9	56.2	868	3360	13800	251	196	2400
LAAP39349	2	0.935	3.82	1.54	154	1100	10.8	19.7	1.2
LAAP39351	1.05	1.04	2.74	1.73	1.73	1.73	6.3	4.7	24.5
LAAP39353	17.6	22.5	56.3	489	2400	11800	110	174	815
LAAP39356	0.938	0.793	2.7	1.33	102	498	6.91	11.6	1.04
LAAP39357	0.965	0.679	2.06	5.72	1.47	107	6.22	3.97	1.15
LAAP39362	3.9	1.48	1.82	2.71	1.41	1.41	5.29	2.34	12.1
LAAP39363	0.905	1.24	1.62	2.7	1.62	1.62	4.68	1.44	16
LAAP39364	1.04	2.44	3.03	4.34	1.62	1.62	18.6	2.93	25.2
LAAP39372	0.713	0.999	1.61	3.4	1.68	1.68	4.81	1.89	1.31
LAAP39374	0.857	0.858	1.17	1.5	7.56	1.44	4.76	1.84	10.9
LAAP39376	0.878	0.878	1.76	2.61	14.2	33.4	6.29	2.58	16.7

Station	C2-Phenanthrenes/Anthracenes	C3-Phenanthrenes/Anthracenes	C4-Phenanthrenes/Anthracenes	Dibenzothiophene	C1-Dibenzothiophenes	C2-Dibenzothiophenes	C3-Dibenzothiophenes	Fluoranthene
LAAP39323	8470	21300	33200	2.26	1520	6210	14400	2.78
LAAP39325	406	1480	2950	0.85	0.85	376	1140	37.1
LAAP39329	182	342	562	2.19	15.5	90.5	253	10.9
LAAP39347	8840	18500	30100	4.3	1140	6060	12500	5.3
LAAP39349	247	1100	2700	0.805	0.805	163	959	16.6
LAAP39351	106	206	456	1.58	12.2	34.6	232	10.8
LAAP39353	4470	12800	18500	5.88	514	4570	9860	91.3
LAAP39356	135	599	1310	0.696	0.696	113	532	10.3
LAAP39357	63.1	204	587	2.13	0.769	35.4	147	12
LAAP39362	31.7	30.1	77.6	1.25	2.89	7.23	12.3	10.7
LAAP39363	12	10.1	33.7	0.984	2.14	3.82	4.78	8.2
LAAP39364	47.6	59.1	210	1.97	5.01	13.8	28.2	33.6
LAAP39372	17.6	21.7	166	1.02	0.876	0.876	0.876	8.74
LAAP39374	28.3	34.6	173	0.84	0.753	0.753	8.05	10
LAAP39376	62.1	188	470	1.2	0.771	18.2	99	9.71

Station	Pyrene	C1-Fluoranthenes/Pyrenes	C2-Fluoranthenes/Pyrenes	C3-Fluoranthenes/Pyrenes	Benz(a)anthracene	Chrysene	C1-Chrysenes	C2-Chrysenes	C3-Chrysenes	C4-Chrysenes
LAAP39323	1670	6220	11800	16500	2.26	13200	13200	12400	8120	6530
LAAP39325	140	703	1260	1840	0.85	2770	2770	2540	1870	1690
LAAP39329	25.4	105	208	249	0.873	592	592	529	350	277
LAAP39347	821	5090	10600	15300	4.3	19100	19100	17300	11300	9420
LAAP39349	84.6	520	1140	1770	0.805	3020	3020	2710	1840	1760
LAAP39351	23.2	82.8	178	201	0.906	399	399	406	286	262
LAAP39353	781	3250	5630	8280	5.88	9390	9390	9740	5870	4570
LAAP39356	51.7	280	578	810	0.696	1290	1290	1290	979	756
LAAP39357	29.8	132	228	288	0.769	683	683	610	455	390
LAAP39362	13.1	19.6	29.7	30.6	6.73	71.8	71.8	69.3	51.5	60.9
LAAP39363	8.56	7.65	12.1	11	2.79	24.2	24.2	24.3	17.3	29.5
LAAP39364	35	38.7	63.4	72.7	11.2	193	193	185	129	144
LAAP39372	10.5	37.1	87.1	95.5	0.876	256	256	234	126	154
LAAP39374	13.5	30.7	55.1	68.2	4.02	177	177	175	126	125
LAAP39376	19.5	75.6	110	156	0.771	484	484	468	334	302

Station	Benzo(b)fluoranthene	Benzo(k)fluoranthene	Benzo(e)pyrene	Benzo(a)pyrene	Perylene	Indeno(1,2,3-c,d)pyrene	Dibenz(a,h)anthracene	Benzo(g,h,i)perylene
LAAP39323	719	1.79	2460	220	150	55.6	108	255
LAAP39325	438	92.3	665	234	106	152	56.7	152
LAAP39329	25.1	0.69	102	4.52	21.9	5.17	3.31	14.4
LAAP39347	1140	3.4	3620	387	8.5	80.3	139	307
LAAP39349	117	0.637	539	24.9	45.5	14.2	17.7	59.7
LAAP39351	24.7	0.716	65.1	3.94	25.3	4.72	2.67	9.85
LAAP39353	784	4.65	1540	151	60.2	59.7	121	198
LAAP39356	76.5	0.55	216	10.4	1.38	7.25	9.92	24.7
LAAP39357	40.7	0.608	123	6.19	24.2	6.7	4.86	17.1
LAAP39362	13	3.5	18	7.03	15.5	5.39	1.8	7.1
LAAP39363	4.92	1.65	6.87	2.66	10.6	1.97	0.905	3.05
LAAP39364	23	4.58	40.8	9.69	19.7	8	3.28	11.9
LAAP39372	7.33	0.693	61.7	2.63	5.74	3.3	1.47	10.4
LAAP39374	11.1	1.49	46.7	4.16	11.4	3.76	2.41	9.66
LAAP39376	32.4	0.609	74	3.96	24.3	6.16	3.71	14.7

Appendix 8f
Calculated compound-specific polycyclic aromatic hydrocarbon data for selected 2011 OSAT samples collected at Bay Jimmy. All samples were bulked from 0 to 2 cm depth. All units are ng/g.

Station	C1 and higher Fl/Py	C1 and higher Phen/An	Fl/Py	Phen/An	BaA/BaA+Chry	An/An+Phen	IP/IP+Bghi	Fl/Fl+Py
LAAP39323	34520.0	64860.0	0.0	50.4	0.0	0.0	0.2	0.0
LAAP39325	3803.0	4963.0	0.3	0.2	0.0	0.9	0.5	0.2
LAAP39329	562.0	1141.3	0.4	1.2	0.0	0.4	0.3	0.3
LAAP39347	30990.0	59840.0	0.0	1.3	0.0	0.4	0.2	0.0
LAAP39349	3430.0	4048.2	0.2	0.5	0.0	0.6	0.2	0.2
LAAP39351	461.8	792.5	0.5	1.3	0.0	0.4	0.3	0.3
LAAP39353	17160.0	36585.0	0.1	0.6	0.0	0.6	0.2	0.1
LAAP39356	1668.0	2045.0	0.2	0.6	0.0	0.6	0.2	0.2
LAAP39357	648.0	855.3	0.4	1.6	0.0	0.4	0.3	0.3
LAAP39362	79.9	151.5	0.8	2.3	0.1	0.3	0.4	0.4
LAAP39363	30.8	71.8	1.0	3.3	0.1	0.2	0.4	0.5
LAAP39364	174.8	341.9	1.0	6.3	0.1	0.1	0.4	0.5
LAAP39372	219.7	206.6	0.8	2.5	0.0	0.3	0.2	0.5
LAAP39374	154.0	246.8	0.7	2.6	0.0	0.3	0.3	0.4
LAAP39376	341.6	736.8	0.5	2.4	0.0	0.3	0.3	0.3

Station	C2-Phen/C2-Chry	C3-Phen/C3-Chry	C2D/C2P	C3D/C3P	C3D/C3C	C0/(C0+C1) P/A	C0/(C0+C1) F/P
LAAP39323	0.7	2.6	0.7	0.7	1.8	0.1	0.2
LAAP39325	0.2	0.8	0.9	0.8	0.6	0.6	0.2
LAAP39329	0.3	1.0	0.5	0.7	0.7	0.2	0.3
LAAP39347	0.5	1.6	0.7	0.7	1.1	0.2	0.1
LAAP39349	0.1	0.6	0.7	0.9	0.5	1.0	0.2
LAAP39351	0.3	0.7	0.3	1.1	0.8	0.3	0.3
LAAP39353	0.5	2.2	1.0	0.8	1.7	0.3	0.2
LAAP39356	0.1	0.6	0.8	0.9	0.5	0.9	0.2
LAAP39357	0.1	0.4	0.6	0.7	0.3	0.9	0.2
LAAP39362	0.5	0.6	0.2	0.4	0.2	0.4	0.5
LAAP39363	0.5	0.6	0.3	0.5	0.3	0.3	0.7
LAAP39364	0.3	0.5	0.3	0.5	0.2	0.5	0.6
LAAP39372	0.1	0.2	0.0	0.0	0.0	0.8	0.3
LAAP39374	0.2	0.3	0.0	0.2	0.1	0.4	0.4
LAAP39376	0.1	0.6	0.3	0.5	0.3	0.3	0.3

APPENDIX 9

Appendix 9a

Compound-specific petroleum hydrocarbon data. All units are μg/g.

Station	Core Label	Sampling Interval	n-C10 alkanes	n-C11 alkanes	n-C12 alkanes	n-C13 alkanes	n-C14 alkanes	n-C15 alkanes	n-C16 alkanes	n-C17 alkanes
RIG	High	5 cm	27.5	5.5	17.6	2.8	23.3	14.5	12.3	32.0
		10 cm	49.1	2.3	77.1	8.6	72.7	35.2	25.6	29.7
	Mid	5 cm	17.4	5.6	18.8	5.7	24.5	10.1	18.8	23.8
		10 cm	15.9	4.5	19.5	7.6	24.3	11.6	11.7	14.9
	Low	5 cm	18.3	3.6	16.1	8.7	25.3	17.7	18.2	36.5
		10 cm	25.4	7.6	22.2	9.7	39.8	15.2	18.8	25.7
KBP	High	5 cm	51.2	12.3	36.0	11.5	33.4	12.4	20.1	40.1
		10 cm	32.1	6.1	36.3	11.4	41.1	11.1	23.8	28.0
	Mid	5 cm	40.6	21.6	35.6	16.6	31.5	12.2	20.1	25.1
		10 cm	32.7	6.1	15.7	7.7	29.8	12.6	18.1	31.2
	Low	5 cm	160.4	6.1	11.9	5.7	20.6	18.0	17.2	66.8
		10 cm	32.4	6.4	20.6	10.9	33.8	15.9	18.1	86.4
DBI	High	1 cm	27.9	10.0	28.9	15.1	34.3	14.7	27.5	42.2
		2 cm	19.9	10.2	22.5	7.8	28.9	10.6	19.4	22.3
		3 cm	29.1	11.0	26.7	11.6	28.8	10.8	14.9	16.6
		4 cm	25.7	20.9	25.4	10.1	23.7	11.8	18.0	15.9
		5 cm	1.1	4.5	24.2	7.5	33.7	12.9	24.4	28.4
	Mid	1 cm	77.8	19.8	95.8	42.7	164.0	264.2	191.8	472.9
		2 cm	108.7	13.0	89.0	41.9	147.7	150.0	102.8	407.6
		3 cm	49.7	7.0	55.6	25.6	110.4	86.0	87.2	214.2
		4 cm	29.6	4.6	20.8	9.4	30.0	19.1	22.1	43.9
		5 cm	16.0	5.5	23.4	7.7	38.0	16.0	18.4	44.1
	Low	1 cm	16.9	2.9	13.9	7.9	29.1	16.9	26.2	29.0
		2 cm	7.4	4.6	16.6	7.8	28.5	9.4	22.1	31.3
		3 cm	22.0	7.9	18.3	11.6	31.0	11.2	18.4	28.8
		4 cm	37.7	11.6	29.5	15.0	50.2	18.5	29.4	27.8
		5 cm	35.8	10.9	34.1	15.0	48.9	19.1	31.2	30.4
BJ	High	2 cm	254.2	148.0	125.6	113.2	220.5	262.1	436.1	1923.7
		3 cm	154.5	124.2	923.5	923.2	1107	654.4	1450.6	809.2
	Mid	1 cm	84.3	129.9	370.8	473.7	706.6	536.8	1363.4	1125.1
		2 cm	106.6	140.3	310.2	333.9	476.0	392.7	970.1	1936.9

Station	Core Label	Sampling Interval	n-C10 alkanes	n-C11 alkanes	n-C12 alkanes	n-C13 alkanes	n-C14 alkanes	n-C15 alkanes	n-C16 alkanes	n-C17 alkanes
BJ	Low	1 cm	90.7	315.3	891.2	1182.8	1715.5	1040.3	2517.1	1336.1
		2 cm	83.9	366.7	966.5	1150.6	1438.0	931.9	2273.2	1297.7

Station	Core Label	Sampling Interval	Pristane	n-C18 alkanes	Phytane	n-C19 alkanes	n-C20 alkanes	n-C21 alkanes	n-C22 alkanes	n-C23 alkanes
RIG	High	5 cm	8.5	33.3	4.2	21.1	35.6	80.9	67.5	182.1
		10 cm	11.0	52.4	0.0	37.8	61.1	93.7	154.2	283.9
	Mid	5 cm	16.1	33.8	46.6	26.8	37.0	70.7	39.1	145.7
		10 cm	3.1	35.6	20.7	21.5	40.3	68.9	32.9	133.0
	Low	5 cm	17.7	26.5	7.3	31.9	32.8	55.0	29.4	92.8
		10 cm	3.9	46.6	2.2	27.1	60.8	73.4	64.9	158.1
KBP	High	5 cm	7.9	24.3	2.3	39.4	41.6	79.6	57.2	303.9
		10 cm	7.6	46.4	6.6	57.7	59.4	123.7	91.7	535.1
	Mid	5 cm	12.3	21.9	2.3	25.4	30.6	47.0	27.6	80.3
		10 cm	7.3	38.9	4.8	29.1	18.0	40.7	28.2	109.9
	Low	5 cm	25.8	28.6	2.6	30.3	21.4	51.0	29.7	135.3
		10 cm	16.0	32.0	4.8	40.8	28.1	40.8	35.1	201.3
DBI	High	1 cm	21.0	42.7	1.9	74.3	34.6	86.8	60.9	281.7
		2 cm	12.4	31.1	2.8	52.6	30.1	59.9	38.9	204.8
		3 cm	12.7	27.1	2.1	26.3	22.4	72.1	36.9	300.7
		4 cm	17.7	30.9	2.0	45.0	27.8	73.9	53.4	218.4
		5 cm	4.8	35.1	4.2	41.2	24.8	71.1	42.6	296.4
	Mid	1 cm	82.3	178.1	9.0	463.2	187.9	389.7	207.4	1614.8
		2 cm	49.6	131.0	9.0	355.3	77.5	309.3	215.0	1899.6
		3 cm	24.6	83.4	9.1	229.1	69.2	205.3	135.9	831.7
		4 cm	8.0	28.4	5.9	38.8	31.1	48.7	38.4	121.1
		5 cm	6.3	37.2	2.6	44.0	25.7	58.2	45.2	108.4
	Low	1 cm	5.2	46.9	4.9	67.9	30.3	71.3	54.8	213.0
		2 cm	6.9	53.3	3.6	20.7	28.0	46.5	39.3	182.6
		3 cm	10.2	68.6	3.7	32.0	21.8	50.4	38.9	196.7
		4 cm	4.0	69.8	14.5	35.0	39.2	62.6	58.6	242.8
		5 cm	10.3	71.2	2.0	76.3	44.3	83.7	78.9	282.1
BJ	High	2 cm	6323.2	1070.3	9602.3	3961.5	4413.2	1642.8	2010.5	3301.3
		3 cm	1077	899.4	1264.9	667.5	536.1	271.3	280.1	753.6
	Mid	1 cm	1202.4	1605.3	2263.1	793.1	988.4	960.2	391.9	903.1
		2 cm	6056.1	2063.6	8923.1	3679.1	2115.7	3055.4	358.8	1762.1
	Low	1 cm	1631.7	1702.7	1684.4	310.9	908.5	681.4	617.3	985.4
		2 cm	1268.8	1888.7	1723.5	1031.5	833.7	735.1	585.0	814.7

Station	Core Label	Sampling Interval	n-C24 alkanes	n-C25 alkanes	n-C26 alkanes	n-C27 alkanes	n-C28 alkanes	n-C29 alkanes	n-C30 alkanes	n-C31 alkanes
RIG	High	5 cm	270.4	294.1	106.8	378.7	174.4	599.0	85.1	602.5
		10 cm	603.2	362.5	176.0	521.9	289.2	896.5	173.9	910.8
	Mid	5 cm	28.2	451.0	197.7	901.0	242.7	1056.9	165.5	1243.0
		10 cm	129.4	562.0	307.2	1042.4	357.5	776.9	259.3	924.5
	Low	5 cm	89.0	151.1	83.9	333.0	96.8	273.9	33.1	177.5
		10 cm	225.2	314.1	182.5	716.8	179.6	313.9	112.9	390.0
KBP	High	5 cm	130.2	801.1	140.4	989.9	140.9	995.0	122.5	463.9
		10 cm	226.1	1513.6	233.6	1469.2	134.1	1030.8	241.4	651.2
	Mid	5 cm	46.5	206.0	102.5	327.6	103.9	544.6	62.0	383.3
		10 cm	40.3	212.4	69.0	390.0	138.6	1040.2	188.8	1018.6
	Low	5 cm	85.0	282.6	178.0	421.1	216.3	773.9	166.1	658.1
		10 cm	89.9	273.0	150.6	410.4	174.6	756.9	159.2	733.7
DBI	High	1 cm	165.8	764.8	186.5	761.1	136.9	733.8	197.3	415.3
		2 cm	123.5	636.9	129.0	598.4	77.3	487.3	141.9	308.6
		3 cm	114.6	985.9	110.6	743.5	136.7	439.4	90.5	263.9
		4 cm	258.6	931.5	188.1	644.0	196.3	578.2	227.2	289.0
		5 cm	167.5	966.7	175.6	1052.9	186.1	459.3	157.0	467.9
	Mid	1 cm	591.1	3471.9	678.0	3257.7	581.3	1472.5	878.8	1115.9
		2 cm	231.7	3587.7	624.1	3397.9	360.2	1605.6	1159.8	1777.9
		3 cm	256.3	1461.9	278.3	1248.9	240.4	793.6	708.1	807.5
		4 cm	62.0	179.3	61.2	259.3	51.2	175.0	92.0	280.6
		5 cm	70.6	194.6	68.2	185.4	41.3	182.6	78.2	205.1
	Low	1 cm	47.7	329.9	404.7	603.5	246.3	1834.9	395.4	1876.0
		2 cm	71.4	277.0	316.2	420.3	146.8	1074.8	250.5	1235.0
		3 cm	84.6	315.1	404.3	470.0	132.1	1122.0	244.9	1286.7
		4 cm	191.1	477.3	609.0	790.7	533.6	1524.8	638.3	1788.6
		5 cm	91.7	384.0	357.7	623.4	230.7	1716.8	588.5	2196.3
BJ	High	2 cm	3919.9	7837.2	2618.0	9316.2	3436.3	5728.8	1416.6	1345.4
		3 cm	608.1	1420.6	561.2	1013.2	287.6	2844.4	1582.3	3178.9
	Mid	1 cm	810	1625.7	337	822.5	506.8	1416.9	1894.6	2942.5
		2 cm	2531.0	3512.4	1301.6	3035.1	1007.5	3552.1	2832.7	3001.3
	Low	1 cm	1892.0	1420.2	490.6	1500.4	612.9	2490.0	822.6	2727.9
		2 cm	1531.6	1118.5	381.4	1197.4	487.6	1976.3	634.1	2146.9

Station	Core Label	Sampling Interval	n-C32 alkanes	n-C33 alkanes	n-C34 alkanes	n-C35 alkanes	Total Alkanes	Total TPH	Total UCM
RIG	High	5 cm	69.5	404.2	783.2	106.7	4442.9	63.54	44.01
		10 cm	152.3	601.6	506.2	169.3	6357.4	68.21	44.01
	Mid	5 cm	117.5	1086.1	9284.8	324.1	15638.9	111.23	65.29
		10 cm	119.1	665.0	701.9	164.0	6474.9	51.81	30.65
	Low	5 cm	46.1	120.7	672.7	35.2	2550.8	38.94	29.04
		10 cm	71.3	310.5	606.1	70.9	4095.0	47.91	27.3
KBP	High	5 cm	379.0	254.5	1170.3	427.3	6788.0	19.19	0
		10 cm	608.4	427.3	1438.9	30.2	9122.8	85.3	31.03
	Mid	5 cm	295.2	273.7	1296.0	76.2	4168.2	22.2	9.88
		10 cm	1076.5	564.8	2754.5	116.4	8040.4	36.29	14.46
	Low	5 cm	873.9	371.8	7857.8	84.9	12600.5	47.65	30.58
		10 cm	108.2	434.8	167.7	117.4	4199.5	32.92	17.11
DBI	High	1 cm	65.9	196.8	3868.9	1018.7	9316.2	102.82	68.78
		2 cm	343.7	245.0	2042.5	348.1	6056.2	58.08	32.57
		3 cm	262.6	136.8	1664.0	20.5	5618.7	50.25	26.48
		4 cm	372.0	216.2	1757.7	355.7	6634.7	61.07	32.26
		5 cm	26.4	122.7	80.7	22.1	4541.6	69.36	41.53
	Mid	1 cm	9105.3	1316.6	20831.1	298.8	48060.3	743.79	532.33
		2 cm	7168.1	1212.3	47434.8	7645.1	80312.1	514.11	296.82
		3 cm	2323.2	486.7	12278.1	244.4	23351.1	956.06	851.66
		4 cm	317.9	110.4	1823.3	20.2	3932.2	51.86	29.75
		5 cm	188.0	89.6	1837.0	23.6	3660.8	54.92	21.66
	Low	1 cm	2492.0	1050.8	3494.8	345.5	13758.4	80.46	49.44
		2 cm	1826.4	740.6	2461.3	192.4	9521.1	64.51	26.48
		3 cm	2171.0	764.9	2182.1	208.7	9957.7	72.95	35.57
		4 cm	1980.2	1079.6	3314.4	272.3	13946.0	75.16	32.79
		5 cm	2300.6	1385.6	5050.2	329.7	16129.5	98.5	41.07
BJ	High	2 cm	326.9	158.0	610.1	703.2	73225.1	6937.1	6734.5
		3 cm	612.7	1173.2	374.4	384.3	25937.2	1766.55	1704.9
	Mid	1 cm	645.7	717.6	214.8	223.6	26055.7	2414.18	2338.77
		2 cm	458.5	259.8	288.6	294.7	54755.4	5198.84	5039.89
	Low	1 cm	557.9	1469.4	190.5	438.4	32224.0	362.49	318.77
		2 cm	407.2	1215.2	143.3	375.2	29004.0	305.2	265.35

Appendix 9b
Calculated compound-specific petroleum hydrocarbon data.

Station	Core Label	Sampling Interval	CPI	n-C17/pristine (µg/g)	n-C18/phytane (µg/g)	UCM % of TPH	U/R	L/H
RIG	High	5 cm	2.5	3.8	7.9	69.3	2.3	0.4
		10 cm	2.4	2.7	--	64.5	1.8	0.4
	Mid	5 cm	3.4	1.5	0.7	58.7	1.4	0.1
		10 cm	2.8	4.8	1.7	59.2	1.4	0.3
	Low	5 cm	2.1	2.1	3.6	74.6	2.9	0.4
		10 cm	2.2	6.6	21.5	57.0	1.3	0.4
KBP	High	5 cm	2.8	5.1	10.4	0.0	0.0	0.3
		10 cm	2.7	3.7	7.0	36.4	0.6	0.5
	Mid	5 cm	1.9	2.0	9.4	44.5	0.8	0.2
		10 cm	1.4	4.3	8.2	39.8	0.7	0.1
	Low	5 cm	1.0	2.6	11.2	64.2	1.8	0.1
		10 cm	3.6	5.4	6.6	52.0	1.1	0.3
DBI	High	1 cm	2.2	2.0	22.7	66.9	2.0	0.2
		2 cm	1.8	1.8	11.3	56.1	1.3	0.3
		3 cm	2.4	1.3	13.2	52.7	1.1	0.5
		4 cm	1.6	0.9	15.3	52.8	1.1	0.4
		5 cm	4.6	5.9	8.4	59.9	1.5	0.7
	Mid	1 cm	0.6	5.7	19.8	71.6	2.5	0.2
		2 cm	0.7	8.2	14.6	57.7	1.4	0.1
		3 cm	0.8	8.7	9.2	89.1	8.2	0.2
		4 cm	1.1	5.5	4.8	57.4	1.3	0.2
		5 cm	1.2	7.1	14.1	39.4	0.7	0.3
	Low	1 cm	1.2	5.6	9.6	61.4	1.6	0.1
		2 cm	1.1	4.6	14.9	41.0	0.7	0.1
		3 cm	1.0	2.8	18.7	48.8	1.0	0.1
		4 cm	1.1	6.9	4.8	43.6	0.8	0.2
		5 cm	1.3	2.9	35.4	41.7	0.7	0.1
BJ	High	2 cm	2.5	0.3	0.1	97.1	33.2	2.1
		3 cm	2.7	0.8	0.7	96.5	27.7	0.9
	Mid	1 cm	1.9	0.9	0.7	96.9	31.0	1.5
		2 cm	2.0	0.3	0.2	96.9	31.7	2.6

Station	Core Label	Sampling Interval	CPI	n-C17/pristine (µg/g)	n-C18/phytane (µg/g)	UCM % of TPH	U/R	L/H
BJ	Low	1 cm	2.9	0.8	1.0	87.9	7.3	1.5
		2 cm	3.0	1.0	1.1	86.9	6.7	1.8

REFERENCES

Agency for Toxic Substances and Disease Registry (ATSDR), 1995. Toxicological profile for Polycyclic Aromatic Hydrocarbons (PAHs). Atlanta, GA: U.S. Department of Health and Human Services, Public Health Service, 458 p.

Allen, A.A., Jaeger, D., Mabile, N.J., Costanzo, D., 2011. The use of controlled burning during the Gulf of Mexico Deepwater Horizon MC-252 oil spill response. International Oil Spill Conference Proceedings: March 2011 (Abstract 194).

Alve, E., 1995. Benthic foraminiferal responses to estuarine pollution: a review. *Journal of Foraminiferal Research* 25(3): 190-203.

Appleby, P.G., Oldfield, F., 1978. The calculation of lead-210 dates assuming a constant rate of supply of unsupported ^{210}Pb to the sediment. *Catena* 5: 1-8.

Appleby, P.G., Oldfield, F., 1992. Application of ^{210}Pb to sedimentation studies. In: Ivanovich, M, Harmon, R.S. (Eds.), *Uranium series disequilibrium*. Oxford University Press, Oxford, p. 731-738.

Arnold, A.J., Parker, W.C., 1999. Biogeography of planktonic foraminifera. In: Sen Gupta, B.K. (Ed.), *Modern Foraminifera*. Kluwer Academic Publishers, UK, p. 37-55.

Batker, D., de la Torre, I., Costanza, R., Swedeen, P., Day, J., Boumans, R., Bagstad, K., 2010. Gaining ground: Wetlands, hurricanes and the economy: the value of restoring the Mississippi River delta. Earth Economics: Tacoma, WA. http://www.eartheconomics.org/FileLibrary/file/Reports/Louisiana/Earth_Economics_Report_on_the_Mississippi_River_Delta_compressed.pdf. Viewed 4 April 2012.

Bauer, J.E., Capone, D.G., 1985. Degradation and mineralization of the polycyclic aromatic hydrocarbons anthracene and naphthalene in Mid marine sediments. *Applied and Environmental Microbiology* 50(1): 81-90.

Beeftink, W.G., Rozema, J., 1988. The nature and functioning of salt marshes. In: Salomons, W., Bayne, B.L., Duvrsma, E.K., Forstner, U. (Eds.), *Pollution of the North Sea, an Assessment*. Springer, Berlin, p. 59-87.

Bilyard, G.R., 1987. The value of benthic infauna in marine pollution monitoring studies. *Marine Pollution Bulletin* 18: 581-585.

Bloom, N., Crecelius, E.A., 1983. Solubility behavior of atmospheric ^{7}Be in the marine environment. *Marine Chemistry* 12(4): 323-331.

Bouchet, V.M.P., Sauriau, P., Debenay, J., Mermillod-Blondin, F., Schmidt, S., Amiard, J., Dupas, B., 2009. Influence of the mode of macrofauna-mediated bioturbation on the vertical distribution of living benthic foraminifera: first insight from axial tomodensitometry. *Journal of Experimental Marine Biology and Ecology* 371(1): 20-33.

Bray, E.E., Evans, E.D., 1961. Distribution of n-paraffins as a clue to recognition of source beds. *Geochimica et Cosmochimica Acta* 22(1): 2-15

Brock, C.A., Murphy, D.M., Bahreini, R., Middlebrook, A.M., 2011. Formation and growth of organic aerosols downwind of the Deepwater Horizon oil spill. *Geophysical Research Letters* 38: L17805.

Brunner, C.A., Yeager, K.M., Hatch, R., Simpson, S., Keim, J., Briggs, K.B., Louchouarn, P., 2013. Effects of Oil from the 2010 Macondo Well Blowout on Marsh Foraminifera of Mississippi and Louisiana, USA. *Environmental Science & Technology* 47: 9115-9123.

Budzinski, H., Jones, I., Bellocq, J., Piérard, C., Garrigues, P., 1997. Evaluation of sediment contamination by polycyclic aromatic hydrocarbons in the Gironde estuary. *Marine Chemistry* 58: 85–97.

Burdige, D.J., 2007. Preservation of organic matter in marine sediments: controls, mechanisms, and an imbalance in sediment organic carbon budgets? *Chemical Reviews* 107: 467-485.

Burns, K.A., Ehrhardt, M.G., Howes, B.L., Taylor, C.D., 1993. Subtidal benthic community respiration and production near the heavily oiled Gulf Coast of Saudi Arabia. *Marine Pollution Bulletin* 27: 199-205.

Chang, R., 2007. *Chemistry, 9th Edition*. McGraw-Hill, New York, 1063 p.

Chmura, G.L., Anisfeld, S.C., Cahoon, D.R., Lynch, J.C., 2003. Global carbon sequestration in tidal, saline wetland soils. *Global Biogeochemical Cycles* 17(4): 1111.

Coleman, J.M., Robert, H.H., Stone, G.W., 1998. Mississippi River Delta: an overview. *Journal of Coastal Research* 14(3): 698-716.

Colombo, J.C., Cappelletti, N., Lasci, J., Migoya, M.C., Speranza, E., Skorupka, C.N., 2006. Sources, vertical fluxes, and equivalent toxicity of aromatic hydrocarbons in coastal sediments of the Río de la Plata Estuary, Argentina. *Environmental Science & Technology* 40(3): 734–740.

Costanza, R., Pérez-Maqueo, O., Martinez, M.L., Sutton, P., Anderson, S.J., Mulder, K., 2008. The value of coastal wetlands for hurricane protection. *AMBIO: A Journal*

of the Human Environment 37(4): 241-248.

Culbertson, J.B., Valiela, I., Pickart, M., Peacock, E.E., Reddy, C.M., 2008. Long-term consequences of residual petroleum on salt marsh grass. *Journal of Applied Ecology* 45: 1284-1292.

Day, P.R., 1965. Particle fractionation and particle-size analysis. In: Black, C.A. (Ed.), *Methods of Soil Analysis, Part 1*. American Society of Agronomy, Madison, WI, p. 545-567.

DeLaune, R.D., Patrick, W.H., Buresh, R.J., 1978. Sedimentation rates determined by ^{137}Cs dating in a rapidly accreting salt marsh. *Nature* 275: 532-533.

DeLaune, R.D., Patrick, W.H., Buresh, R.J., 1979. Effect of crude oil on a Louisiana *Spartina alterniflora* salt marsh. *Environmental Pollution* 20(1): 21-31.

DeLaune, R.D., Wright, A.L., 2011. Projected impact of Deepwater Horizon oil spill on U.S. Gulf Coast wetlands. *Soil Science Society of America Journal* 75: 1602-1612.

Ellis, J.C., Fariña, J.M., Witman, J.D., 2006. Nutrient transfer from sea to land: the case of gulls and cormorants in the Gulf of Maine source. *Journal of Animal Ecology* 75(2): 565-574.

Federal Interagency Solutions Group, 2010. *Oil Budget Calculator*. Interagency Solutions Group report to the National Incident Command, 49 p.

Fisk, H.N., 1944. *Geological investigation of the alluvial valley of the Lower Mississippi River*. U.S. Army Corps of Engineers, Mississippi River Commission, Vicksburg, Ms., 78 p.

Flow Rate Technical Group (FRTG), 2011. *Assessment of Flow Rate Estimates for the Deepwater Horizon / Macondo Well Oil Spill*. Report to the National Incident Command, Interagency Solutions Group, 22 p.

Frazier, D.E., 1967. Recent deltaic deposits of the Mississippi River: their development and chronology. *Transactions – Gulf Coast Association of Geological Societies* 17: 287-315.

Frere, M.H., Menzel, R.G., Larson, K.H., Overstreet, R., Reitemeier, R.F., 1963. *The behavior of radioactive fallout in soils and plants*. National Academy of Science-National Research Council, Washington, D.C., 32 p.

Frey, R.W., Basan, P.B., 1978. Coastal salt marshes. In: Davis, R.A. (Ed.), *Coastal Sedimentary Environments*. Springer-Verlag, New York, p. 101-169.

Gardner, W.S., Lee, R.F., Tenore, K.R., Smith, L.W., 1979. Degradation of selected polycyclic aromatic hydrocarbons in coastal sediments: importance of microbes and polychaete worms. *Water, Air, & Soil Pollution* 11: 339-347.

Gogou, A., Stratigakis, N., Kanakidou, M., Stephanou, E.G., 1996. Organic aerosols in Eastern Mediterranean: components source reconciliation by using molecular markers and atmospheric back trajectories. *Organic Geochemistry* 25: 79–96.

Goldberg, E.D., 1963. Geochronology with ^{210}Pb. In: *Proceedings, Radioactive Dating Symposium,* November 19-23, 1962. International Atomic Energy Agency, Vienna, p. 121-131.

Goldstein, S.T., 1999. Foraminifera: a biological overview. In: Sen Gupta, B.K. (Ed.), *Modern Foraminifera*. Kluwer Academic Publishers, UK, p. 37-55.

Goldstein, S.T., Watkins, G.T., Kuhn, R.M., 1995. Microhabitats of salt marsh foraminifera: St. Catherines Island, Georgia, USA. *Marine Micropaleontology* 26: 17-29.

Gosselink, J.G., 1984. *The ecology of delta marshes of coastal Louisiana: a community profile.* U.S. Fish and Wildlife Service FWS/OBS-84/09, 134 p.

Gross, O., 2000. Influence of temperature, oxygen and food availability on the migrational activity of bathyal benthic foraminifera: evidence by microcosm experiments. *Hydrobiologia* 426: 123-137.

Hartmann, P.C., Quinn, J.G., Cairns, R.W., King, J.W., 2004. The distribution and sources of polycyclic aromatic hydrocarbons in Narragansett Bay surface sediments. *Marine Pollution Bulletin* 48: 351−358.

Hénaff, M.L., Kourafalou, V.H., Paris, C.B., Helgers, J., Aman, Z.M., Hogan, P.J., Srinivasan, A., 2012. Surface evolution of the Deepwater Horizon oil spill patch: combined effects of circulation and wind-induced drift. *Environmental Science & Technology* 46: 7267-7273.

Hippensteel, S.P., 2005. Limiting the limits of bioturbation, or at least focusing on the positive. *PALAIOS* 20(4): 319-320.

Hong, H., Xu, L., Chen, J.C., Wong, Y.S., Wan, T.S.M., 1995. Environmental fate and chemistry of organic pollutants in the sediment of Xiamen and Victoria Harbours. *Marine Pollution Bulletin* 31(4-12): 229-236.

Hyland, J., Balthis, L., Karakassis, I., Magni, P., Petrov, A., Shine, J., Vestergaard, O., Warwick, R., 2005. Organic carbon content of sediments as an indicator of stress in the marine benthos. *Marine Ecology Progress Series* 295: 91-103.

Iqbal, J., Gisclair, D., McMillin, D.J., Portier, R.J., 2007. Aspects of petrochemical pollution in southeastern Louisiana (USA): pre-Katrina background and source characterization. *Environmental Toxicology and Chemistry* 26(9): 2001-2009.

Intergovernmental Panel on Climate Change (IPCC), 2007. Summary for Policymakers, In: Solomon, S., Qin, D., Manning, M., Chen, Z., Marquis, M., Avery, K.B., Tignor, M., Miller, H.L. (Eds.), *Climate Change 2007: The Physical Science Basis. Contribution of Working Group I to the Fourth Assessment Report of the Intergovernmental Panel on Climate Change*. Cambridge University Press, Cambridge, U.K. and New York, U.S.A., 18 p.

Jorissen, F.J., de Stigter, H.C., Widmark, J.G.V., 1995. A conceptual model explaining benthic foraminiferal microhabitats. *Marine Micropaleontology* 26: 3-15.

Kim, G.B., Maruya, K.A., Lee, R.F., Lee, J., Koh, C., Tanabe, S., 1999. Distribution and sources of polycyclic aromatic hydrocarbons in sediments from Kyeonggi Bay, Korea. *Marine Pollution Bulletin* 38(1): 7-15.

Kolb, C.R., Van Lopik, J.R., 1958. *Geology of the Mississippi deltaic plain, southeastern Louisiana*. Waterways Experiment Station, Vicksburg, Mississippi, Technical Report No. 3-483.

Krishnaswami, S., Benninger, L.K., Aller, R.C., Von Damm, K.L., 1980. Atmospherically derived radionuclides as tracers of sediment mixing and accumulation in near shore marine and lake sediments: evidence from ^{7}Be, ^{210}Pb, and ^{239,240}Pu. *Earth and Planetary Science Letters* 47: 307-318.

Lal, D., Peters, B., 1967. Cosmic-ray activity produced on the earth. In: *Handbuch der Physik* XLVI/2. Springer, Berlin, p. 551-612.

Langley, J.A., McKee, K.L., Cahoon, D.R., Cherry, J.A., Megonigal, J.P., 2009. Elevated CO_2 stimulates marsh elevation gain, counterbalancing sea-level rise. *Proceedings of the National Academy of Sciences* 106(15): 6182-6186.

Lima, A.L.C., Eglinton, T.I., and Reddy, C.M., 2003. High-resolution record of pyrogenic polycyclic aromatic hydrocarbon deposition during the 20th century. *Environmental Science & Technology* 37: 53–61.

Lin, Q., Mendelssohn, I.A., 2012. Impacts and recovery of the Deepwater Horizon oil spill on vegetation structure and function of coastal salt marshes in the Northern Gulf of Mexico. *Environmental Science & Technology* 46: 3737−3743.

Long, E.R., MacDonald, D.D., Smith, S.L., Calder, F.D., 1995. Incidence of adverse biological effects within ranges of chemical concentrations in marine and estuarine sediments. *Environmental Management* 19: 81-97.

Louisiana Department of Wildlife and Fisheries (LDWF), 2013. LDWF Commercial Fishing Closure. Retrieved from http://www.wlf.louisiana.gov/oilspill. Viewed 3 September 2013.

Mackay D., Shiu W.Y., 1975. Determination of the solubility of hydrocarbons in aqueous sodium chloride solutions. *The Canadian Journal of Chemical Engineering* 53: 239–242.

Martin, R.E., 2000. *Environmental micropaleontology: the application of microfossils to environmental geology*. Kluwer Academic/Plenum Publishers, New York, 481 p.

Martínez-Colón, M., Hallock, P., and Green-Ruiz, C., 2009. Strategies for using shallow-water benthic foraminifers as bioindicators of potentially toxic elements: a review. *Journal of Foraminiferal Research* 39(4): 278-299.

Mazurek, M.A., Simoneit, B.R.T., 1984. Characterization of biogenic and petroleum-derived organic matter in aerosols over remote, rural and urban areas. In: Keith, L.H. (Ed.), *Identification and Analysis of Organic Pollutants in Air.* Ann Arbor Science/Butterworth, Boston, p. 353-378.

Means, J.C., McMillin, D.J., 1993. Fate and transport of particle-reactive normal, alkylated and heterocyclic aromatic hydrocarbons in a sediment-water-colloid system: Gulf of Mexico Study/MMS 93-0018. U.S. Department of the Interior, Minerals Management Service, Gulf of Mexico OCS Regional Office, New Orleans, LA, 150 p.

Meckel, T.A., ten Brink, U.S., Williams, S.J., 2006. Current subsidence rates due to compaction of Holocene sediments in southern Louisiana. *Geophysical Research Letters* 33: L11403.

Michel, J., Owens, E.H., Zengel, S., Graham, A., Nixon, Z., Allard, T., Holton, W., Reimer, D., Lamarche, A., White, M., Rutherford, N., Childs, C., Mauseth, G., Challenger, G., Taylor, E., 2013. Extent and Degree of Shoreline Oiling: Deepwater Horizon Oil Spill, Gulf of Mexico, USA. *PLoS ONE* 8(6): e65087.

Milan, C.S., Swenson, E.M., Turner, R.E., Lee, J.M., 1995. Assessment of the ^{137}Cs method for estimating sediment accumulation rates: Louisiana salt marshes. *Journal of Coastal Research* 11(2): 296-307.

Möller, I., Spencer, T., French, J.R., Leggett, D.J., Dixon, M., 1999. Wave transformation over salt marshes: A Field and Numerical Modeling Study from North Norfolk, England. *Estuarine, Coastal and Shelf Science* 49: 411-426.

Molnia, B., 1974. A rapid and accurate method for the analysis of calcium carbonate in small samples. *Journal of Sedimentary Petrology* 44(2): 589-590.

Morvan, J., Le Cadre, V., Jorissen, F., Debenay, J., 2004. Foraminifera as potential bio-indicators of the "*Erika*" oil spill in the Bay of Bourgneuf: field and experimental studies. *Aquatic Living Resources* 17: 317-322.

Mudd, S.M., Howell, S.M., Morris, J.T., 2009. Impact of dynamic feedbacks between sedimentation, sea-level rise, and biomass production on near-surface marsh stratigraphy and carbon accumulation. *Estuarine, Coastal and Shelf Science* 82: 377-389.

Mudd, S.M., 2011. The life and death of salt marshes in response to anthropogenic disturbance of sediment supply. *Geology* 39, 511-512.

Murray, A.S., Olley, J.M., Wallbrink, P.J., 1992. Natural radionuclide behaviour in the fluvial environment. *Radiation Protection Dosimetry* 45: 285-288.

Murray, J.W., 2001. The niche of benthic foraminifera, critical thresholds and proxies. *Marine Micropaleontology* 41: 1-7.

Murray, J.W., 2006. *Ecology and Applications of Benthic Foraminifera*. Cambridge University Press, UK, 426 p.

National Oceanic and Atmospheric Administration (NOAA), 2005a. Hurricane Katrina. Retrieved from http://www.ncdc.noaa.gov. Accessed September 15, 2013.

National Oceanic and Atmospheric Administration (NOAA), 2005b. Hurricane Rita. Retrieved from http://www.ncdc.noaa.gov. Accessed September 15, 2013.

National Oceanic and Atmospheric Administration (NOAA), 2009. Tidal Station Locations and Ranges. Retrieved from http://tidesandcurrents.noaa.gov/tides10/tab2ec4.html. Accessed 7 April 2012.

National Oceanic and Atmospheric Administration (NOAA), 2010a. *Fishing industry in the Gulf of Mexico*. Retrieved from www.noaa.gov. Accessed 4 April 2012.

National Oceanic and Atmospheric Administration (NOAA), 2010b. *Shorelines and Coastal Habitats in the Gulf of Mexico*. Retrieved from www.noaa.gov. Accessed 4 April 2012

National Oceanic and Atmospheric Administration (NOAA), 2013. *Environmental Response Management Application*. Retrieved from http://response.restoration.noaa.gov/maps-and-spatial-data/environmental-response-management-application-erma. Accessed 22 October 2013.

Natter, M., Keevan, J., Wang, Y., Keimowitz, A.R., Okeke, B.C., Son, A., Lee, M., 2012. Level and Degradation of Deepwater Horizon Spilled Oil in Coastal Marsh Sediments and Pore-Water. *Environmental Science & Technology* 46: 5744−5755.

Nicholls, R.J., Wong, P.P., Burkett, V.R., Codignotto, J.O., Hay, J.E., McLean, R.F., Ragoonaden, S., Woodroffe, C.D., 2007. Coastal systems and low-lying areas. In: Parry, M.L., Canziani, O.F., Palutikof, J.P., van der Linden, P.J., Hanson, C.E. (Eds.), *Climate Change 2007: Impacts, Adaptation and Vulnerability. Contribution of Working Group II to the Fourth Assessment Report of the Intergovernmental Panel on Climate Change*. Cambridge University Press, Cambridge, UK, p. 315-356.

Noller, J.S., 2000. Lead-210 Geochronology. In: Noller, J.S., Sowers, J.M., Lettis, W.R. (Eds.), *Quaternary Geochronology: Methods and Applications*. American Geophysical Union, Washington, D.C., p. 115-120.

Peacock, E.E., Nelson, R.K., Solow, A.R., Warren, J.D., Baker, J.L., Reddy, C.M., 2005. The West Falmouth oil spill: ~100 kg of oil found to persist decades later. *Environmental Forensics* 6: 273–281.

Pearson, T.H., Rosenberg, R., 1978. Macrobenthic succession in relation to organic enrichment and pollution of the marine environment. *Oceanography and Marine Biology: Annual Review* 16: 229-311.

Penland, S., Ramsey, K.E., 1990. Relative sea-level rise in Louisiana and the Gulf of Mexico: 1908-1988. *Journal of Coastal Research* 6: 323-342.

Poag, W.C., 1981. *Ecologic Atlas of Benthic Foraminifera of the Gulf of Mexico*. Marine Science International: New York, 174 p.

Polovodova, I., and Schönfeld, J., 2008. Foraminiferal test abnormalities in the western Baltic Sea. *Journal of Foraminiferal Research*, 38(4): 318-336.

Polymenakou, P.N., Tselepides, A., Stephanou, E.G., Bertilsson, S., 2006. Carbon speciation and composition of natural microbial communities in polluted and pristine sediments of the Eastern Mediterranean. *Marine Pollution Bulletin* 52: 1396-1405.

Pope, R.H., Demaster, D.J., Smith, C.R., Seltmann, H. Jr., 1996. Rapid bioturbation in equatorial Pacific sediments: evidence from excess ^{234}Th measurements. *Deep Sea Research* II 43: 1339-1364.

Poppe, L.J., and Eliason, A.E., 2008. A Visual Basic program to plot sediment grain-size data on ternary diagrams. *Computers and Geosciences* 34: 561-565.

Reddy, C.M., Eglinton, T.I., Hounshell, A., White, H.K., Xu, L., Gaines, R.B., Frysinger, G.S., 2002. The West Falmouth oil spill after thirty years: the persistence of petroleum hydrocarbons in marsh sediments. *Environmental Science & Technology* 36: 4754-4760.

Reddy, C.M., Arey, J.S., Sewald, J.S., Sylva, S.P., Lemkau, K.L., Nelson, R.K., Carmichael, C.A., McIntyre, C.P., Fenwick, J., Ventura, G.T., Van Mooy, B.A.S., Camilli, R., 2011. Composition and fate of gas and oil released to the water column during the Deepwater Horizon oil spill. *Proceedings of the National Academy of Sciences* 109(50): 20229-20234.

Rosenbauer, R.J., Campbell, P.L., Lam, A., Lorenson, T.D., Hostettler, F.D., Thomas, B., Wong, F.L., 2010. *Reconnaissance of Macondo-1 well oil in sediment and tarballs from the Northern Gulf of Mexico Shoreline, Texas to Florida*. U.S. Geological Survey Open-File Report 2010-1290, 22 p.

Santschi, P.H., Presley, B.J., Wade, T.L., Garcia-Romero, B., Baskaran, M., 2001. Historical contamination of PAHs, PCBs, DDTs, and heavy metals in Mississippi River Delta, Galveston Bay and Tampa Bay sediment cores. *Marine Environmental Research* 52: 51-79.

Sauer, T.C., Michel, J., Hayes, M.O., Aurand, D.V., 1998. Hydrocarbon characterization and weathering of oiled intertidal sediments along the Saudi Arabian Coast two years after the Gulf war oil spill. *Environment International* 24: 43–60.

Schlautman, M.A., Morgan, J.J., 1993. Effects of aqueous chemistry on the binding of polycyclic aromatic hydrocarbons by dissolved humic materials. *Environmental Science & Technology* 27: 961-969.

Sen Gupta, B.K, 1999. Introduction to modern Foraminifera. In: Sen Gupta, B.K. (Ed.), *Modern Foraminifera*. Kluwer Academic Publishers, UK, p. 37-55.

Sharma, P., Gardner, L.R., Moore, W.S., Bollinger, M.S., 1987. Sedimentation and bioturbation in a salt marsh as revealed by ^{210}Pb, ^{137}Cs, and ^{7}Be studies. *Limnology and Oceanography* 32(2): 313-326.

Shinkle, K.D., Dokka, R.K., 2004. Rates of vertical displacement at benchmarks in the lower Mississippi Valley and the northern Gulf Coast. *NOAA Technical Report NOS/NGS 50*, 135 p.

Simoneit, B.R.T., Mazurek, M.A., Cahill, T.A., 1980. Contamination of the Lake Tahoe air basin by high molecular weight petroleum residues. *Journal of the Air Pollution Control Association* 30(4): 387-390.

Smith, J.G., 2011. *Organic Chemistry, Third Edition*. McGraw-Hill, New York, 1178 p.

Smoak, J.M., Patchineelam, S.R., 1999. Sediment mixing and accumulation in a mangrove ecosystem: evidence from ^{210}Pb, ^{234}Th and ^{7}Be. *Mangroves and Salt Marshes* 3: 17–27.

State of Louisiana, 2010. Office of Coastal Protection and Restoration officials open Davis Pond diversion to full capacity to help curb oil penetration into coastal marshes. Retrieved from http://coastal.louisiana.gov/index.cfm?md=newsroom&tmp=detail&articleID=1216. Viewed 3 September 2013.

Törnqvist, T.E., Wallace, D.J., Storms, J.E.A., Wallinga, J., Van Dam, R.L., Blaauw, M., Derksen, M.S., Klerks, C.J.W., Meijneken, C., Snijders, E.M.A., 2008. Mississippi Delta subsidence primarily caused by compaction of Holocene strata. *Nature Geoscience* 1(3): 173-176.

Turner, R.E., Baustian, J.J., Swenson, E.M., Spicer, J.S., 2006. Wetland sedimentation from Hurricanes Katrina and Rita. *Science* 314: 449-452.

United States Geological Survey (USGS), 2013. National Water Information System. Retrieved from http://waterdata.usgs.gov/la/nwis. Accessed 21 July 2013.

Valiela, I., Rutecki, D., Fox, S., 2004. Salt marshes: biological controls of food webs in a diminishing environment. *Journal of Experimental Marine Biology and Ecology* 300: 131-159.

Wang, L., Lee, F.S.C., Wang, X., Yin, Y., Li, J., 2007. Chemical characteristics and source implications of petroleum hydrocarbon contaminants in the sediments near major drainage outfalls along the coastal of Laizhou Bay, Bohai Sea, China. *Environmental Monitoring and Assessment* 125(1-3): 229-237.

Wang, Z.D., Fingas, M., Sergy, G., 1995a. Chemical characterization of crude oil residues from an Arctic beach by GC/MS and GC/FID. *Environmental Science & Technology* 29(10): 2622-2631.

Wang, Z.D., Fingas, M., Sergy, G., 1995b. Use of methyldibenzothiophenes as markers for differentiation and source identification of crude and weathered oils. *Environmental Science & Technology* 29(11): 2841-2849.

Wang, Z.D., Fingas, M., 2003. Development of oil hydrocarbon fingerprinting and identification techniques. *Marine Pollution Bulletin* 47: 423-452.

Wheatcroft, R.A., Martin, W.R., 1996. Spatial variability in short-term (^{234}Th) sediment bioturbation intensity along an organic-carbon gradient. *Journal of Marine Research* 54: 763-792.

Whitcomb, N.J., 1978. Effects of oil pollution upon selected species of benthic foraminiferids from the lower York River, Virginia. *Geological Society of America, Abstracts with Programs* 10: 515.

White, L.X., Lima, A.L.C., Eglington, T., Reddy, C.M., 2005. Abundance, composition, and vertical transport of PAHs in marsh sediments. *Environmental Science & Technology* 39(21): 8273-8280.

Williams, H.F.L., Hamilton, T.S., 1995. Sedimentary dynamics of an eroding tidal marsh derived from stratigraphic records of ^{137}Cs fallout, Fraser Delta, British Columbia, Canada. *Journal of Coastal Research* 11(4): 1145-1156.

Wilson, C.A., Allison, M.A., 2008. An equilibrium profile for retreating marsh shorelines in southeast Louisiana. *Estuarine, Coastal and Shelf Science* 80: 483-494.

Yan, B., Abrajano, T.A., Bopp, R.F., Chaky, D.A., Benedict, L.A., Chillrud, S.N., 2005. Molecular tracers of saturated and polycyclic aromatic hydrocarbon inputs into Central Park Lake, New York City. *Environmental Science & Technology* 39(18): 7012-7019.

Yanko, V., Ahmad, M., and Kaminski, M., 1998. Morphological deformities of benthic foraminiferal tests in response to pollution by heavy metals: implications for pollution monitoring. *Journal of Foraminiferal Research* 28(3): 177-200.

Yanko, V., Arnold, A.J., Parker, W.C., 1999. Effects of marine pollution on benthic Foraminifera. In: Sen Gupta, B.K. (Ed.), *Modern Foraminifera*. Kluwer Academic Publishers, UK, p. 37-55.

Yeager, K.M., Santschi, P.H., 2003. Invariance of isotope ratios of lithogenic radionuclides: more evidence for their use as sediment source tracers. *Journal of Environmental Radioactivity* 69(3): 159-176.

Yeager, K.M., Santschi, P.H., Rowe, G.T., 2004. Sediment accumulation and radionuclide inventories (^{239,240}Pu, ^{210}Pb and ^{234}Th) in the northern Gulf of Mexico, as influenced by organic matter and macrofaunal density. *Marine Chemistry* 91: 1-14.

Yeager, K.M., Santschi, P.H., Rifai, H.S., Suarez, M.P., Brinkmeyer, R., Hung, C., Schindler, K.J., Andres, M.J., Weaver, E.A., 2007. Dioxin Chronology and Fluxes in Sediments of the Houston Ship Channel, Texas: Influences of Non-Steady-State Sediment Transport and Total Organic Carbon. *Environmental Science & Technology* 41: 5291-5298.

Yunker, M.B., Snowdon, L.R., Macdonald, R.W., Smith, J.N., Fowler, M.G., Skibo, D.N., McLaughlin, F.A., Danyushevskaya, A.I., Petrova, V.I., Ivanov, G.I., 1996. Polycyclic aromatic hydrocarbon composition and potential sources for sediment samples from the Beaufort and Barents Seas. *Environmental Science & Technology* 30: 1310–1320.

Yunker, M.B., Macdonald, R.W., Vingarzan, R., Mitchell, R.H., Goyette, D., Sylvestre, S., 2002. PAHs in the Fraser River basin: a critical appraisal of PAH ratios as indicators of PAH source and composition. *Organic Geochemistry* 33: 489–515.

Zengel, S., Michel, J., 2013. Deepwater Horizon Oil Spill: Salt Marsh Oiling Conditions, Treatment Testing, and Treatment History in Northern Barataria Bay, Louisiana (Interim Report October 2011). *U.S. Dept. of Commerce, NOAA Technical Memorandum NOS OR&R* 42. Seattle, WA: Emergency Response Division, NOAA, 74 p.

VITA

Rachel S. Hatch
Lexington, Kentucky

Education:
B.S., Geology, University of Kentucky, 2010

Professional Positions:

08/11 – 12/13	Graduate Research and Teaching Assistant, University of Kentucky
08/09 – 12/10	Environmental and Coal Technologies Group Student Intern, Center for Applied Energy Research

Scholastic and Professional Honors:

Pioneer Natural Resources Fellowship (August 2013)
Brown-McFarlan Grant (April 2010, October 2010, November 2012, October 2013)
Pirtle Fellowship (May 2012, May 2013)
Outstanding Teaching Assistant Award (May 2013)
Gulf Coast Association of Geologists Student Research Grant (May 2013)
Geological Society of America Student Research Grant (Aril 2013)
Rice Scholarship (May 2009)
Kentucky AIPG Student Award (April 2009)

Peer-Reviewed Publications (listed in reverse chronology):

Brunner, C.A., Yeager, K.M., **Hatch, R.**, Simpson, S., Keim, J., Briggs, K.B., Louchouarn, P., 2013. Effects of Oil from the 2010 Macondo Well Blowout on Marsh Foraminifera of Mississippi and Louisiana, USA. *Environmental Science & Technology* 47: 9115-9123.

Green, U., Aizenshtat, Z., Hower, J.C., **Hatch, R.**, and Cohen, H., 2011. Modes of formation of carbon oxides [Co_x(x=1 or 2)] from coals during atmospheric storage. Part 2: effect of coal rank on the kinetics. *Energy Fuels* 25: 5626-5631.

O'Keefe, J., Neace, E., Lemley, E., Hower, J.C., Henke, K., Copley, G., **Hatch, R.**, Satterwhite, A., and Blake, D., 2011. Old Smokey coal fire, Floyd County, Kentucky: estimates of gaseous emission rates. *International Journal of Coal Geology* 87(2): 150-156.

Hower, J.C., O'Keefe, J., Eble, C., Volk, T., Richardson, A., Satterwhite, A., **Hatch, R.**, and Kostova, I., 2011. Notes on the origin of inertinite macerals in coals: Evidence for fungal and arthropod transformations of degraded minerals. *International Journal of Coal Geology* 86(2-3): 231-240.

Hower, J.C., O'Keefe, J., Eble, C., Volk, T., Richardson, A., Satterwhite, A., **Hatch, R.**, and Kostova, I., 2011. Notes on the origin of inertinite macerals in coals: Funginite associations with cutinite and suberinite. *International Journal of Coal Geology* 85(1): 186-190.

Silva, L.F.O., Ward, C.R., Hower, J.C., Izquierdo, M., Waanders, F., Oliveira, M.L.S., Li, Z., **Hatch, R.**, and Querol, X., 2010. Mineralogy and Leaching Characteristics of Coal Ash from a Major Brazilian Power Plant. *Coal Combustion and Gasification Products* 3: 51-65.

Professional Meeting Abstracts/Conference Proceedings:

Hatch, R., Yeager, K.M., Brunner, C.A., Wade, T., Briggs, K.B., Schindler, K.J., 2013. Salt Marsh Sediment Mixing Following Petroleum Hydrocarbon Exposure from the Deepwater Horizon Oil Spill. American Geophysical Union National Meeting, December 9-13, San Francisco, CA.

Brunner, C.A., Yeager, K.M., Briggs, K.B., Keim, J., Louchouarn, P., **Hatch, R.**, Schindler, K.J., 2013. Effect of oil contamination on infauna of Louisiana and Mississippi marshes with implications for marsh functioning. Gulf of Mexico Research Initiative, Gulf of Mexico Oil Spill and Ecosystem Science Conference, January 21-23, New Orleans, LA (invited).

Brunner, C.A., Yeager, K.M., Briggs, K.B., Keim, J., Louchouarn, P., **Hatch, R.**, Schindler, K.J., 2012. Effect of oil contamination on infauna of Louisiana and Mississippi marshes with implications for marsh functioning. American Geophysical Union National Meeting, December 3-7, San Francisco, CA (#B14A-05).

O'Keefe, J., Hower, J.C., **Hatch, R.**, Bartley, R.H., Bartley, S.E., 2011. Fungal forms in Miocene Eel River coals: correlating between reflected light petrography and palynology. Geological Society of America *Abstracts with Programs* 43(5): 501.

Eastridge, E.M., Mukherjee, A., **Hatch, R.**, and Fryar, A.E., 2011. Spatial variability in sediment arsenic concentrations, Murshidabad District, West Bengal, India. Geological Society of America *Abstracts with Programs* 43(5): 221.

Eastridge, E.M., **Hatch, R.**, Mukherjee, A., Fryar, A.E., and Scanlon, B., 2010. Arsenic speciation in aquifer sediments, West Bengal, India. Geological Society of America *Abstracts with Programs* 42(5): 437.